Synthesis and reactivity studies on oxo and sulphide compounds of the early transition metals

Alan Shaw

Synthesis and Reactivity Studies on Oxo and Sulphido Compounds of the Early Transition Metals

by

Alan Shaw, B.Sc. GRSC.
University of Durham

A thesis submitted in part fulfillment of the requirements for the degree of Doctor of Philosophy at the University of Durham.

October 1989

Statement of Copyright

Declaration

The work described in this thesis was carried out in the Department of Chemistry at the University of Durham between October 1986 and September 1989. All the work is my own, unless stated to the contrary, and it has not been submitted previously for a degree at this or any other University.

For my Mother

Acknowledgements

I would like primarily to express my sincere gratitude to my supervisor Dr. Vernon C. Gibson for his constant support throughout my period of study at Durham. His ability to inspire and stimulate the study of chemistry has meant the difference between a dream and reality.

To my colleagues, past and present, go my heartfelt thanks especially the other members of the group David, Peter and Jon for providing such a pleasant atmosphere in which to work. My thanks go also to Drs. Mark Briscoe, Terence Kee, Patrick Nicholson and Simon Wait for going before me and lighting the way.

I am especially indebted to Drs. W. Clegg (University of Newcastle-Upon-Tyne), M. Mc.Partlin and A.P.Bashall (Polytechnic of North London) for solving the crystal structures described herein and Dr. P.Bruce (Herriot Watt University) and Dr. Z.V. Hauptman for helping to uncomplicate the bronze work. Furthermore, without the help and co-operation of the Senior Experimental and Technical Staff at the Chemistry Department at Durham, none of this work would have been possible.

I am especially grateful to David for helping me to design this thesis. His expertise on the word processor and unselfish assistance during the latter stages has enabled me to complete the transition from handwritten manuscript to the final, typewritten product.

Finally, the award of an S.E.R.C. studentship is gratefully acknowledged and I would like to thank all my family for moral support.

Abstract

Synthesis and Reactivity Studies on Oxo and Sulphido Compounds of the Early Transition Metals.

This thesis describes studies directed towards the preparation of new oxo compounds of the early transition metals with a view to delineating some of the complex factors which govern their stability and reactivity. For a number of the types of compound studied, the work has also been extended to analogous sulphide systems in order to provide a contrast with another chalcogenide element and further aid an understanding of the bonding and reactivity of both of these elements in a transition metal enviroment.

Chapter 1 highlights the areas of transition metal oxo chemistry of relevance to the general theme of the thesis.

Chapter 2 describes the use of the commercially available reagents Me_3SiYR (R = alkyl, $SiMe_3$; Y = O, S), for rapid, convenient, solution syntheses of transition metal oxohalide and sulphidohalide compounds of molybdenum, tungsten, niobium and tantalum. In addition, this methodology allows the preparation of mixed oxosulphidohalide materials and, in certain cases, intermediate alkoxo(siloxo) halide compounds have been isolated.

Chapter 3 describes the synthesis, characterisation and reactivity of a series of mononuclear mono-oxo complexes of molybdenum and tungsten including $M(O)(OAr)_4$ [M=W, Ar=2,6-$Me_2C_6H_3$ (DMP), 2,4,6-$Me_3C_6H_2$ (TMP), 2,6-$Pr^iC_6H_3$ (DIPP); M=Mo, Ar=(DMP)], $M_2(O)_3(DMP)_6$ and $Mo(O)Cl_2(DMP)_2$. Attempts to synthesise related mononuclear complexes containing the cis di-oxo moeity are also discussed.

Chapter 4 describes the synthesis and reactivity of seven coordinate oxo and sulphidohalide derivatives of niobium and tantalum which exhibit the phenomenon of bond-stretch isomerism. Compounds prepared include $Nb(O)Br_3(PMe_3)_3$, $Nb(S)X_3(PMe_3)_3$ (X=Cl, Br) and $Ta(S)Cl_3(PMe_3)_3$. The latter three have been characterised by X-ray crystallography.

Chapter 5 describes the synthesis and reactivity of half-sandwich oxo compounds of niobium and tantalum. Some of the derivatives prepared include $[CpNbCl_3]_2(\mu_2\text{-}O)$, $[CpTaCl_3]_2(\mu_2\text{-}O)$ and $[Cp^*TaCl_3]_2(\mu_2O)$. The stability of $[Cp^*Ta(O)Cl_2]_2$ has been investigated and the X-ray structure of the trinuclear decomposition product $Cp^*_3Ta_3O_4Cl_4$ is described.

Chapter 6 describes the use of alkali metal aryloxides as intercalating agents and the preparation of a series of novel intercalation compounds, of the type $W(O)_2Cl_2 \cdot xM$ (M = Li, Na and K) which display the properties characteristic of tungsten bronzes.

Chapter 7 gives experimental details for chapters 2-6.

Alan Shaw (October 1989)

Abbreviations

NMR	Nuclear Magnetic Resonance
L	General 2-electron donor ligand
X	General 1-electron donor ligand
Cp	Cyclopentadienyl (C_5H_5)
Cp*	Pentamethylcyclopentadienyl (C_5Me_5)
Cp'	Generalised (C_5R_5) ligand
THF	Tetrahydrofuran
IR	Infrared
$t_{1/2}$	Half-life
Np	Neopentyl

Contents Page

Chapter One

Occurrence, Properties and Applications of Transition Metal Oxo Complexes.

1.1 Introduction.

Transition metal oxides play a crucial role in important hydrocarbon oxidation processes, both on an industrial scale using heterogeneous oxide catalysts and in the laboratory as selective oxygen atom transfer reagents. However, relatively little is understood about the fundamental factors which govern the reactivity of metal-bound oxygen atoms. This thesis describes studies directed towards the preparation of new oxide compounds of the early transition metals with a view to delineating some of the complex factors which govern their stability and reactivity. For a number of the types of compound studied, the work has also been extended to analogous sulphide systems in order to provide a contrast with another chalcogenide element and further aid an understanding of the bonding of both of these elements in a transition metal enviroment.

Initial studies were directed towards the development of a convenient route to oxo- and sulphido-halide starting materials. A suitable low temperature methodology is described in chapter 2 and the materials produced *via* this route provide the basis for the more highly derivatised oxo and sulphido compounds described in chapters 3, 4 and 5. Extended lattices are also exceedingly common in early transition metal oxide chemistry and the low temperature route to the little studied layered compound $W(O)_2Cl_2$ has allowed the preparation of a series of intercalation compounds which display the properties characteristic of the tungsten bronzes. These new 'Halide Bronzes' are described in chapter 6.

Since the primary objective of this thesis has been the study of the chemistry of metal-bound oxygen atoms rather than attempts to also encompass the many additional facets of metal sulphide chemistry, the remainder of this chapter is devoted to a review of the occurrence, properties and uses of transition metal oxo compounds. For economy of space, the extensive field of polyoxoanion chemistry is excluded from this review, most of the important aspects of oxo chemistry being illustrated with reference to low nuclearity species.

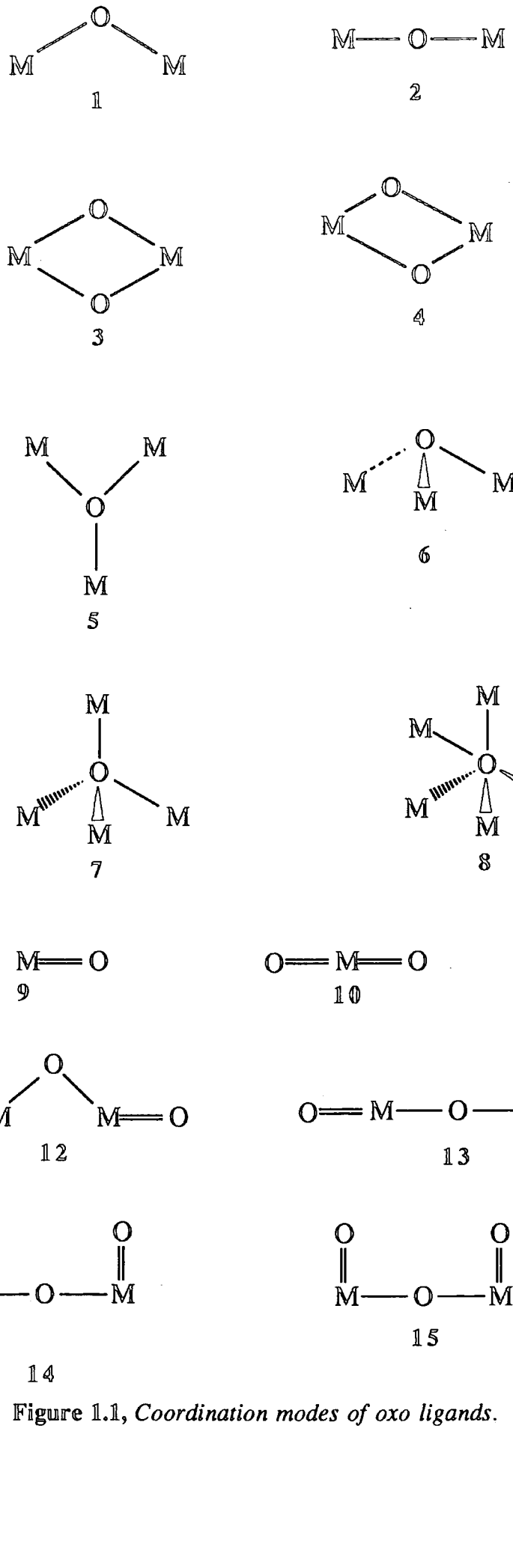

Figure 1.1, *Coordination modes of oxo ligands.*

1.2 Co-ordination Modes of Oxo Ligands.

Oxo ligands are found in a number of different enviroments as shown in figure 1.1 Singly bridged oxo complexes may have either bent (1) or linear bridges (2). The M-O-M angle can vary from *ca.* 140°C to 180°C and to a large extent the angle seems to be determined by the steric requirements of the other ligands attached to the metal. Two unusual examples of bent oxo bridges without other supporting bridging ligands are shown below.

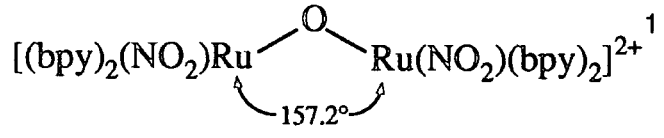

1

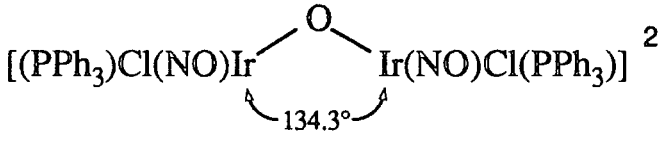

2

Figure 1.2

Linear M-O-M groups are found in some complexes of chromium[3], ruthenium and osmium[4]. Di-μ-oxo linkages are usually symmetrical (3) although there is one well-established example of an asymmetric form (4)[5].

Triply-bridging oxide ligands are found in a variety of complexes. The M_3O unit is generally symmetrical (5), ie. with essentially equal M-O distances, but may be flat or pyramidal (6) with the M-O-M angle as low as 90° when the oxide ligand forms a corner of a cube. Planar M_3O units occur in the basic carboxylates of such metals as iron, ruthenium, manganese, vanadium and chromium. Mixed metal units, eg. Fe_2CrO[6], and mixed oxidation states, eg. Cr^{II}, $Cr_2^{III}O$[7], and $Mn^{II}Mn_2^{III}O$[8] are also

known and there is a trinuclear Ru_3O-based unit in $[Ru_3O(CH_3CO_2)_6(L)_3]$[9] whose charge can be varied from +III to -II. Pyramidal M_3O units are commonly found where the M atoms are also linked by other bridges; examples include μ-OH in the $[Fe_8(O)_2(OH)_{12}(tacn)_6]^{VIII+}$,[10] μ-H in the $[Re_3(O)(H)_3(CO)_9]^{II-}$ anion[11] or another μ_3-O as in $[Mo_3O_2(OAc)_6(OH)_3]^{II+}$.[12]

A special case of pyramidal M_3O units involves the cubane framework (Figure 1.3) consisting of a tetrahedron of M atoms linked in threes by the four μ_3-O ligands comprising the interpenetrating tetrahedron of oxygens. It tends to occur in low oxidation state organometallic compounds for instance $[Os_4O_4(CO)_{12}]$[13] and $[Cr_4O_4(Cp)_4]$[14] and probably $[Mo_4O_8(Cp)_4]$[15]. Pyramidal μ_3-O ligands of this type are also found capping the triangular faces of octahedra and trigonal bypyramids, as in $[Ti_6O_8(Cp)_6]$[14] and $[V_5O_6(Cp)_5]$[14] respectively.

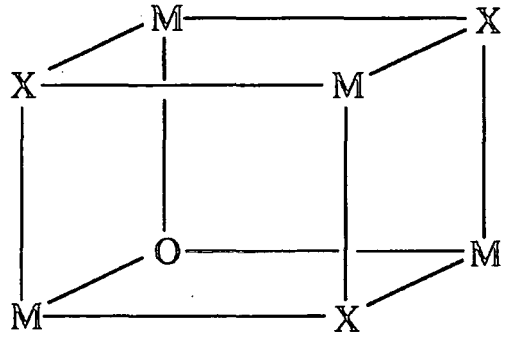

Figure 1.3

Four connected oxide ligands (7) are rare. Examples are shown below and include the well known basic beryllium acetate,[16] the analogous $[Cu_4OCl_6(Ph_3PO)_4]$[17] and the $[Pb_6O(OH)_6]^{IV+}$ cation[18]. A more recent and novel example is the 'butterfly' μ_4-oxide found in $Cp^*_4Ta_4(O)_7(OH)_2$[19].

μ_5-oxide (8) has been claimed, on the basis of infrared and mass spectrometric evidence in $[Fe_5O(OAc)_{12}]^+$ [20]. There seems, as yet, no established μ_6-oxide ligand. As μ_6-C and μ_6-N are both known, there seems a real possibility that μ_6-O may

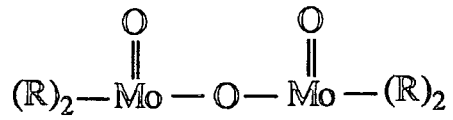

22

R=($EtOCS_2$)

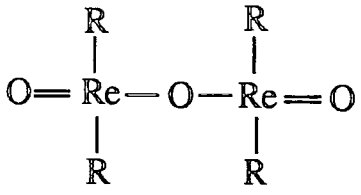

23

R=(Ph_2dtc)

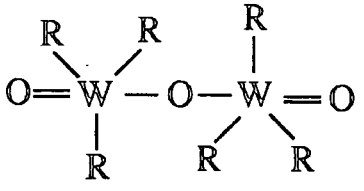

24

R=(CH_2CMe_3)

25

cis 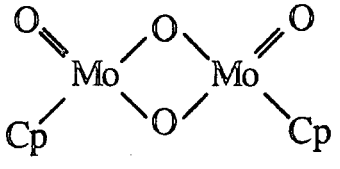

26

trans 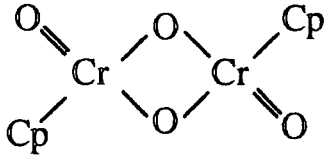

Figure 1.4

eventually be discovered in a polynuclear metal carbonyl oxide or related species. However the greater electronegativity of oxygen than of carbon or nitrogen may make incorporation of oxide into an appropriate metal cluster difficult. Of course, μ_6-O is well known in the solid state in, for instance, the alkaline earth oxides CaO, SrO and BaO.

The multiply bonded oxo group M=O is found not only in oxo compounds and oxo anions of non transition elements but also in a range of transition metal compounds.

Mono oxo compounds (9) occur for all transition metals through the vanadium to iron triads.

Di oxo compounds may be linear (trans) (10) as in $O=U=O^{II+}$ or angular (cis) (11) as in some molybdenum complexes and in ReO_2Me_3.[21]

Compounds that contain both multiple and singly bridging metal oxygen bonds exist in a variety of configurations (12-15) (Examples are shown in Figure 1.4).

1.3 Occurrence of Terminal Oxo Complexes.

Figure 1.5 summarises those complexes structurally characterised with metal oxo multiple bonds as a function of the position of the metal in the periodic table.
It can be seen that the majority of these compounds occur for metals in groups V,VI and VII, with a number of examples for iron, ruthenium and osmium, and a few examples in group IV. The distribution is concentrated along a diagonal from vanadium to rhenium as illustrated in figure 1.6. The distribution of compounds as a function of d electron count (or oxidation state) is also striking, as illustrated in figure 1.7. All of the titanium, niobium and tantalum structures are d^o. Vanadium readily forms oxo multiple bonds in both d^o and d^1 configurations, and Cr, Mo and W form strong multiple bonds even at d^2. There are very few examples of terminal oxo complexes with more than two d electrons (12 out of 633). A classic example is the unusual d^4 rhenium (III) complex $Re(O)I(MeC{\equiv}CMe)_2$ [27] (Figure 1.8).

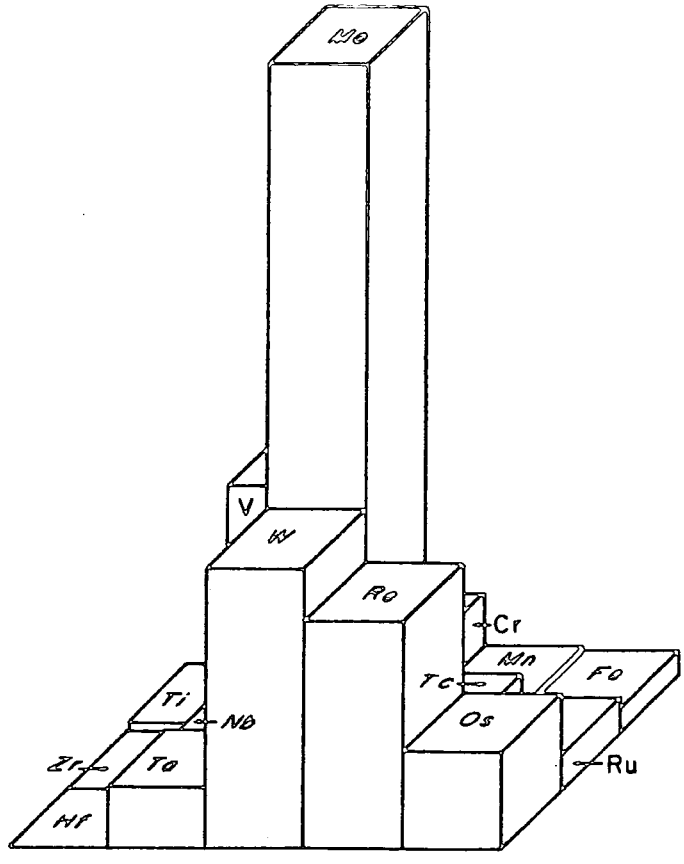

Figure 1.5, *Distribution of structurally characterised compounds with metal-ligand multiple bonds as a function of the position of the metal in the periodic table.*

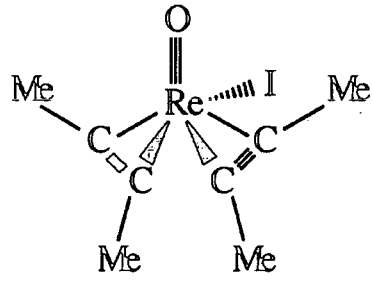

Figure 1.8, *Molecular structure of* $Re(O)I(MeC{\equiv}CMe)_2$.

It can be seen from these data, that the majority of oxo species are formed by elements in groups IVa-VIIa since these achieve high oxidation states fairly easily. In group VIII, only ruthenium and osmium have any extensive oxo chemistry, these being

Group	G Ia	G IIa	G IIIa	G IVa	G Va	G VIa	G VIIa	G VIII
	K	Ca	Sc	Ti 4	V 121	Cr 15	Mn 4	Fe 3
				Zr	Nb 17	Mo 294	Tc 26	Ru 10
				Hf	Ta 1	W 141	Re 75	Os 22

Figure 1.6, *Distribution of structurally characterised compounds with metal-oxo multiple bonds in groups IVa-VIII.*

Group	G Ia	G IIa	G IIIa	G IVa	G Va	G VIa	G VIIa	G VIII
	K	Ca	Sc	Ti d^0	V $d^{0,1}$	Cr $d^{0,1,2}$	Mn $d^{0,1}$	Fe d^4
				Zr	Nb d^0	Mo $d^{0,1,2}$	Tc $d^{1,2}$	Ru $d^{0,2,4}$
				Hf	Ta d^0	W $d^{0,1,2}$	Re $d^{0,1,2,4}$	Os $d^{0,2}$

Figure 1.7, *Distribution of structurally characterised compounds with metal-oxo multiple bonds in groups IVa-VIII as a function of d electron count.*

the only two elements of that group to form a number of high oxidation state species, eg. RuO_4, OsO_4 and $[OsO_4F_2]^{2-}$.

The origin of the diagonal trend of multiple bonds is not well understood, although it is undoubtedly related to the changes in energy and extension of the metal d orbitals across the periodic table. The very early transition metals have higher energy diffuse d orbitals, and therefore form more ionic, less covalent bonds than the later metals. The more polar the bond, it could be argued the greater the basicity of the ligand and the greater the tendency to bridge. To the right of the iron triad, the metal d orbitals become too contracted for good π bonding and bridged structures are again favoured. *Ab initio* calculations suggest that exchange and promotion energies also play an important role[28].

1.4 Stereochemistry.

Structural classification of oxo complexes recognises discrete molecular species and structures which are oligomeric in one or more dimensions leading to chains, layers and ultimately three dimensional networks. Some typical examples are shown in table 1.2.

Structure Type	Examples
Molecular structures	OsO_4[29], Tc_2O_7[30], $W(O)Cl_2(PMe_3)_3$[31]
Chain structures	CrO_3[32], $WOCl_4$[33], $NbOCl_3$[34]
Layer structures	MoO_3[35], Re_2O_7[36]
Three dimensional structures	WO_3[37], ReO_3[38]

Table 1.1, *Structural classification of oxo complexes.*

The type of structure adopted in any one particular case depends not only on the stoichiometry but also on the relative size of the atoms involved and the propensity to form pπ double bonds to oxygen. In the case of molecular structures of the type $[MO_xX_y]_{zn-}$ the use of sterically demanding substituents can have a marked effect on the type of geometry adopted and can force the formation of metal-oxo multiple bonds. Due to the tendency of titanium to form bridged rather than terminal oxo structures[39], coordinative saturation has been employed to force the terminal oxo bonding mode and several terminal oxo titanium complexes have been structurally characterised[40,41], an example being (α,γ- ımethyl-α,γ-dihydrooctaethylporphinato) oxotitanium (IV)[42] (Figure 1.9).

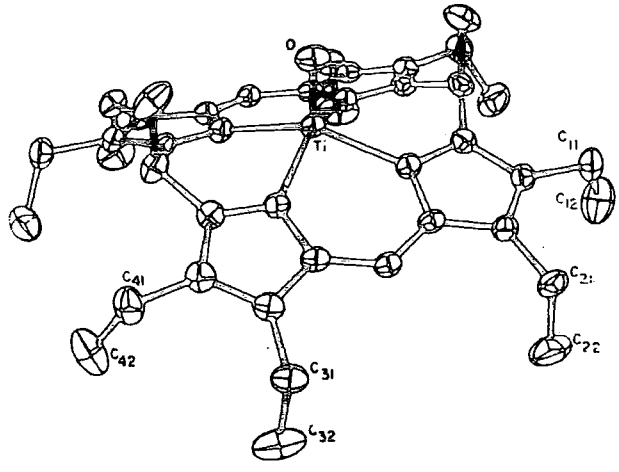

Figure 1.9, *Molecular structure of (α,γ-Dimethyl-α,γ-dihydrooctaethylporphinato) oxotitanium (IV).*

1.4.1 Coordination Compounds Containing Terminal Oxo Ligands.

The majority of compounds with metal-oxo multiple bonds are six coordinate and adopt distorted octahedral structures[43]. Octahedral coordination occurs in d^0,d^1,d^2 and d^4 electronic configurations and is the most common structure for compounds of the transition metals, with or without multiply bonded ligands, due to the excellent overlap possible for both σ and π bonding. The common oxo structures A and B

(Figure 1.10) are both six coordinate and contain terminal and bridging ligands.

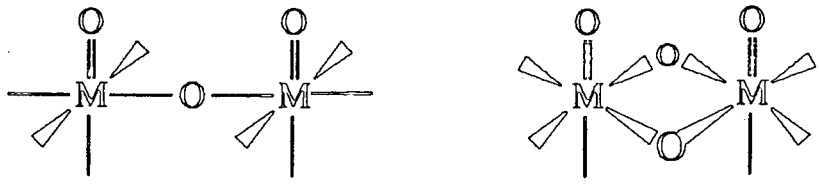

A B

Figure 1.10, *Common oxo structures.*

The next most common coordination number is 5 and these compounds are found predominantly in square pyramidal structures with the multiply bonded ligand at the apex. Thus all reported $[M(O)CL_4]^{n-}$ (n=0,1,2) molecules or ions have a C_4v geometry in the gas phase or in the solid state.

Tetrahedral structures are found primarily with a d^0 configuration, the most common examples being the tetra-oxo anions and their derivatives, [CrO_2Cl_2, MnO_4^-, ReO_4^-, RuO_4^-, OsO_4]. The reason for the prevalence of four, rather than higher coordination in the above complexes is probably a consequence of the extensive oxide to metal electron delocalisation; higher coordination numbers would place an excessive burden of negative charge on the central metal atom. Recently tetrahedral complexes have been isolated in d^1,d^2 and d^4 configurations; examples are $Re(O)_2(mesityl)_2$[44], $Os(O)_2(mesityl)_2$[44] and $Re(O)I(MeC{=}CMe)_2$[27]. The last seems to adopt this structure for electronic reasons, whereas the first two examples are four coordinate because of the steric bulk of the ligands.

It is noteworthy that some second and third row elements tend to give substituted oxo complexes of higher coordination numbers than their first row analogues, in line with the general tendency of heavier transition elements to expand their coordination spheres. Thus $[ReO_4]^-$ and OsO_4 react with alkali to give $[ReO_4(OH)_2]^{3-}$ and $[OsO_4(OH)_2]^{2-}$ while $[MnO_4]^-$ and $[RuO_4]^-$ do not.

The only other coordination number known is seven and these compounds are found predominantly with a d^0 configuration, the only exception being the d^2 complex

$Mo(O)(\eta^5\text{-}C_5H_4Me)_2$[45](Figure 1.11) if the $\eta^5\text{-}C_5H_4Me$ ligand is assumed to occupy three coordination sites..

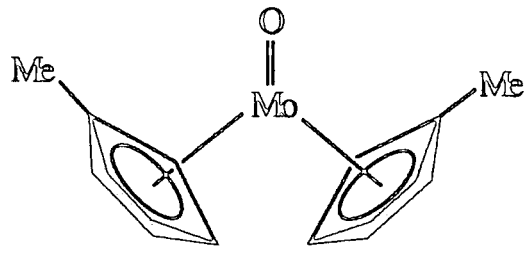

Figure 1.11, *Molecular structure of* $Mo(O)(\eta^5C_5H_4Me)_2$.

1.5 Structure and Bonding.

In this section, a simple outline of the bonding in metal-oxo complexes is given along with a section summarising known structural data on such species.

1.5.1 The Nature of the Metal-Ligand Multiple Bond.

Metal-oxo multiple bonds appear to have bond orders from three to possibly as low as one (Figure 1.12) and can be considered to consist of either a σ bond plus one or two π bonds.

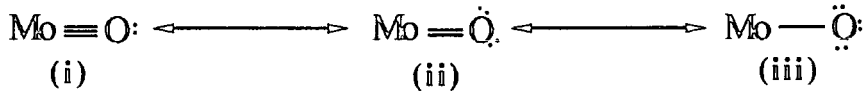

Figure 1.12

The π interactions involve overlap of metal d orbitals with p orbitals on the oxygen. If the z axis is taken as coincident with the metal-oxo multiple bond, overlap occurs between the d_{xz} and p_x orbitals and/or between d_{yz} and p_y (Figure 1.13).

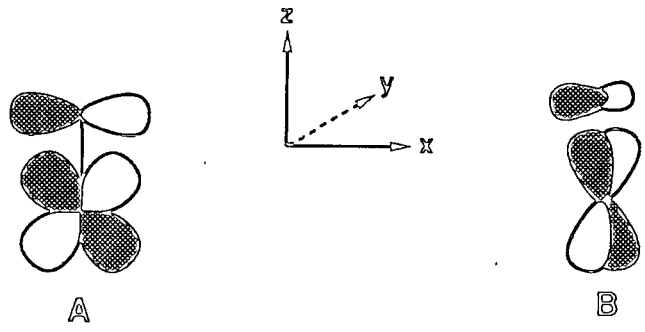

Figure 1.13

The p orbitals of the oxo ligand are lower in energy than the metal d orbitals due to the high electronegativity of oxygen. In an oxidation state formalism, the oxo ligand is best described as the closed shell anion O^{2-}, this description implying that the p_x,p_y and p_z orbitals are filled. In transition metal compounds, the π component is best regarded as arising from $O_{p\pi} \rightarrow Md_{\pi}$ electron flow, therefore productive π bonding requires the metal centre to be in a high oxidation state with a low d electron count. This is in part an explanation for the prevalence of d^0-d^2 configurations in the metal-oxo complexes discussed in section 1.2.

1.5.2 Ligand Field Description.

The majority of transition metal oxo complexes are six-coordinate (as discussed in section 1.2) and adopt a geometry best described as octahedral. Octahedral complexes are the easiest structures to analyse in molecular orbital terms because the σ and π orbitals are separate due to the high symmetry. All octahedral complexes have essentially the same σ bonding framework, regardless of π interactions. In a molecule assumed to have full O_h symmetry, the five metal d orbitals split into a degenerate e_g set ($d_x{}^2{}_{-y}{}^2$, $d_z{}^2$) of σ^* character and a nonbonding t_{2g}, set (d_{xy}, d_{xz}, d_{yz}). Introduction of an oxo, O^{2-} ligand lowers the symmetry to C_{4v} and splits the degeneracy of both the e_g and the t_{2g} orbitals (Figure 1.14).

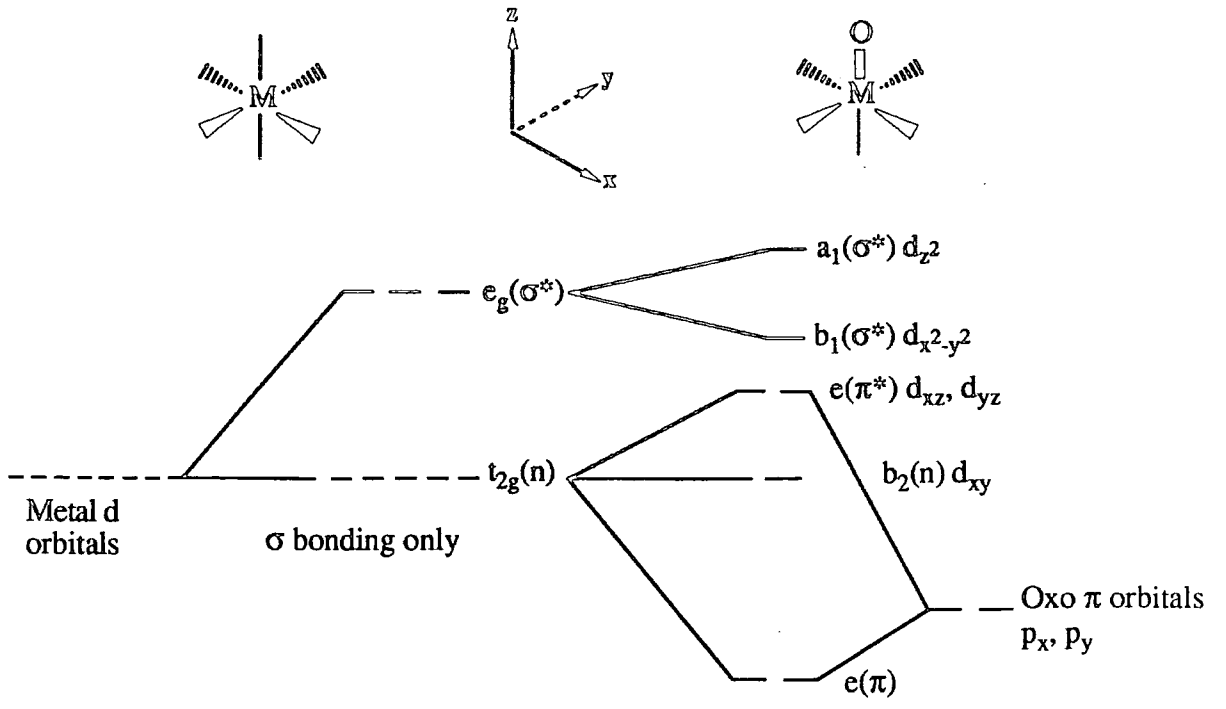

Figure 1.14

Qualitatively the e_g set is unchanged since both orbitals remain σ^*, the t_{2g} orbitals however are substantially split since two of them are now involved in π bonding (d_{xz} and d_{yz} if the z axis is taken as coincident with the metal-ligand bond axis). Thus the ligand field portion of the molecular orbital diagram consists of a non-bonding d_{xy} orbital, a π^*e set, and two σ^* levels.

1.5.3 Mono-Oxo Complexes.

In d^0, $d^1$and d^2 complexes, the metal-oxygen interaction is best described as a triple bond with one σ and two π bonds, the latter arising from overlap of the two oxygen p orbitals, p_x and p_y, with the two metal π^*e orbitals, d_{xz} and d_{yz}.[46,47,48] Up to two d electrons can be accommodated in the nonbonding d_{xy} orbital. In d^4 complexes, however, two electrons must occupy one of the metal π^*e orbitals, thus reducing the M-O bond order from three to two. This results in a formal double bond and a consequent lengthing of the M-O distance, as shown graphically in figure 1.15 for iron

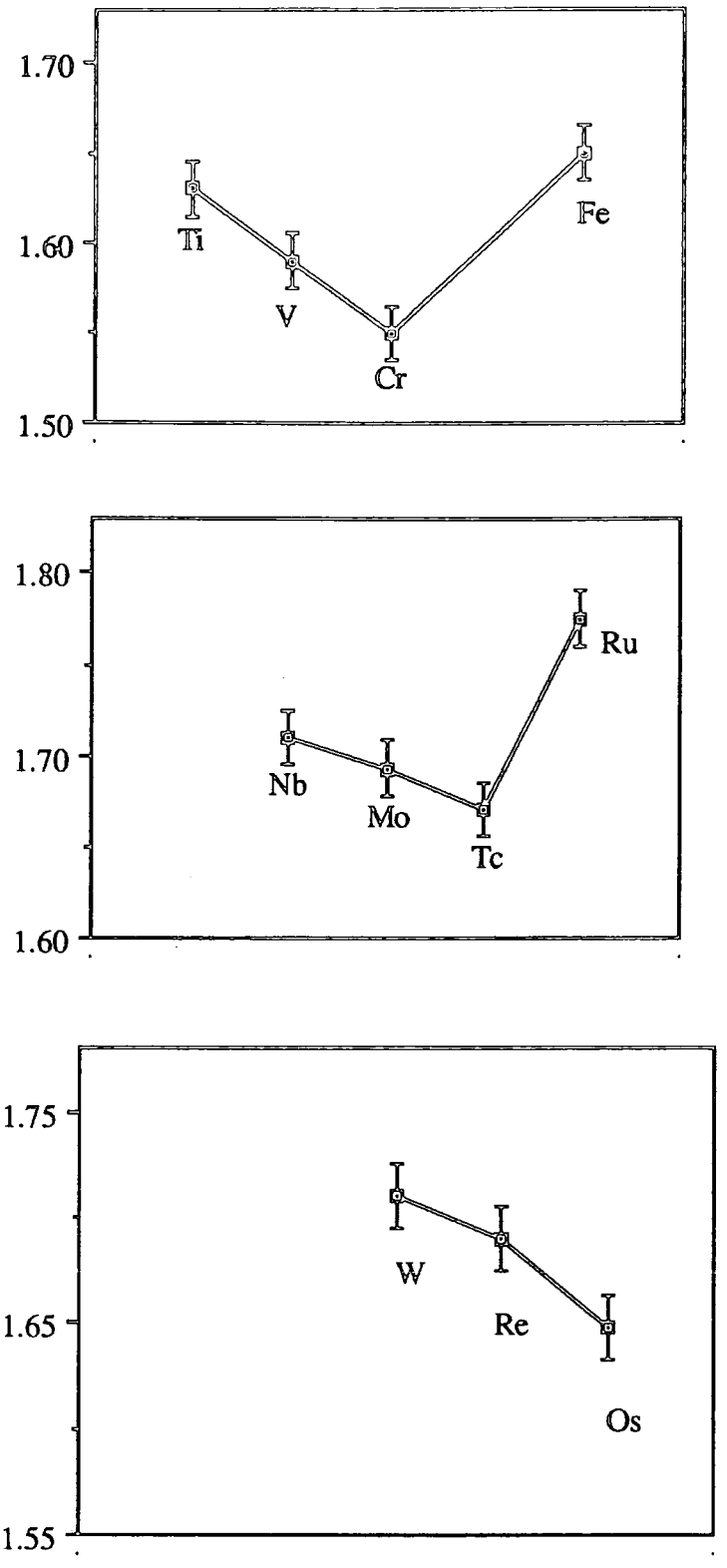

Figure 1.15, *Graphs showing average M-O distance for mono-oxo complexes of transition metals in the fourth , fifth and sixth periods. Bond lengths are in (Å), the error bars indicate the widths of the distributions.*

and ruthenium since the only structurally characterised iron and ruthenium mono-oxo structures are all d^4 octahedral.

All of the other structurally characterised oxo compounds have d^0, d^1 and d^2 electronic configurations and their average metal-oxygen bond distances follow a simple periodic trend in which M-O bond distances decrease on traversing a row from left to right and increase on descending a group. These trends are consistent with the changes in metal ionic radius[49].

1.5.4 Di- and Tri-Oxo Complexes.

In an octahedtral complex there are three metal d orbitals of π symmetry : d_{xy}, d_{xz} and d_{yz}. In a d^0 cis-dioxo complex, the three d orbitals must be shared among two oxo groups[50]. Thus, the net bond order is reduced from 3 to 2.5. Allison and Goddard[51] have suggested that this may be considered as a resonance hybrid of two forms containing one triple bond and one double bond. (Figure 1.16)

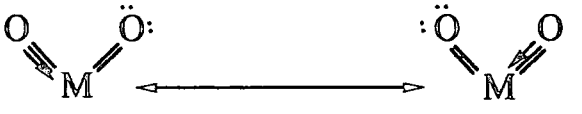

Figure 1.16, *Cis di-oxo resonance forms.*

Due to the reduced bond order, the mean metal oxygen bond lengths in di-oxo complexes must be longer than those in mono-oxo complexes and this is in fact the case (Tables 1.2 and 1.3).

In a d^2 dioxo compound one of the dπ orbitals is occupied by two d electrons; a trans geometry is almost invariably adopted[52] with two formal metal oxygen double bonds (Figure 1.17).

Complex	M=O (Å)	∠O-M-L	d^n	C.N.	Ref.
$[Cr(O)Cl_4]AsPh_4$	1.519(12)	104.5(1)	1	5	53
$[Mo(O)(O)_2(H_2O)_2$	1.647(5)		0	7	54
$WOCl_4$[a]	1.684(4)[a]	102.6(5)[a]	0	5	55
$Tc(O)Cl(sal_2en)$	1.626(11)	97.2±4.1	2	6	56
$OsOCl_4$[a]	1.663(5)[a]	108.3(2)[a]	2	5	57

Table 1.2

Complex	M=O (Å)	∠O-M-L	d^n	C.N.	Ref.
CrO_2Cl_2[a]	1.57±3[a]	105±4[a]	0	4	58
$Mo(O)_2Cl_2(H_2O)_2$	1.701(8)	103.0(5)	0	6	59
$WO_2Cl_2(acac)^-$	1.736(10)		0	6	60
$[Tc(O)_2(en)_2]Cl$	1.752(1)	178.6(3)	2	6	61
$Os(O)_2(C_6H_2Me_7)_2$	1.700(7)	136.1(3)	2	4	44

a Structure determined by electron difraction or microwavespectroscopy.
Measurement errors given in brackets are 99% confidence limits.

Table 1.3

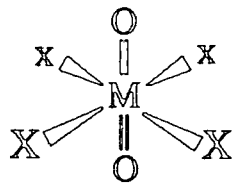

Figure 1.17, *d^2 trans dioxo complex.*

In a d^0 fac-trioxo complex[29] the three d_π orbitals interact with three oxo groups and the average bond order is two (one σ plus one π) and is a formal double bond.

1.5.5 Tetra-Oxo Complexes.

A list of the known structurally characterised tetra-oxo complexes is given in Table 1.4. It can be seen that all the compounds are four coordinate hence tetrahedral geometries are assumed as discussed in section 1.3. The ligand field description for mono-, di- and tri-oxo octahedral complexes is therefore not applicable and a different molecular orbital diagram is required (Figure 1.18)

The d orbitals in tetrahedral complexes split in the opposite way to those in an octahedral complex, that is in a " three above two pattern" (t_2 above e), σ and π bonding are not distinct in this symmetry. The upper t_2 set forms bonds of both σ and π symmetry complicating the assignment of bond orders in tetrahedral complexes, since from two to five π bonds can be formed.

The M-O bond lengths are however longer than similar bonds in mono-, di- or tri-oxo complexes of the same metal, indicating that the formal bond order is unlikely to be greater than two and in some cases could be less.

Complex	M=O (Å)	∠O-M-O	d e⁻	C.N.	Ref.
VO_4^{3-}	1.71 c		0	4	62
CrO_4^{2-} c	1.65 c		0	4	62
$[CrO_4]K_2$	1.636-1.651(3)		0	4	63
WO_4^{2-} c	1.78		0	4	62
MnO_4^- c	1.61 c		0	4	62
$[MnO_4]K$	1.600-1.612(5)	109.4±0.6	0	4	64
$[MnO_4]K_2$	1.633-1.660(5)	109.5±0.6	1	4	64
$[TcO_4]K$	1.711(3)		0	4	62
$[TcO_4]NH_4$	1.702(2)		0	4	65
ReO_4^-	1.721(4)		0	4	62
RuO_4 a	1.705(3) a		0	4	66
$Os(O)_4$ a	1.711(3) a		0	4	62

Table 1.4

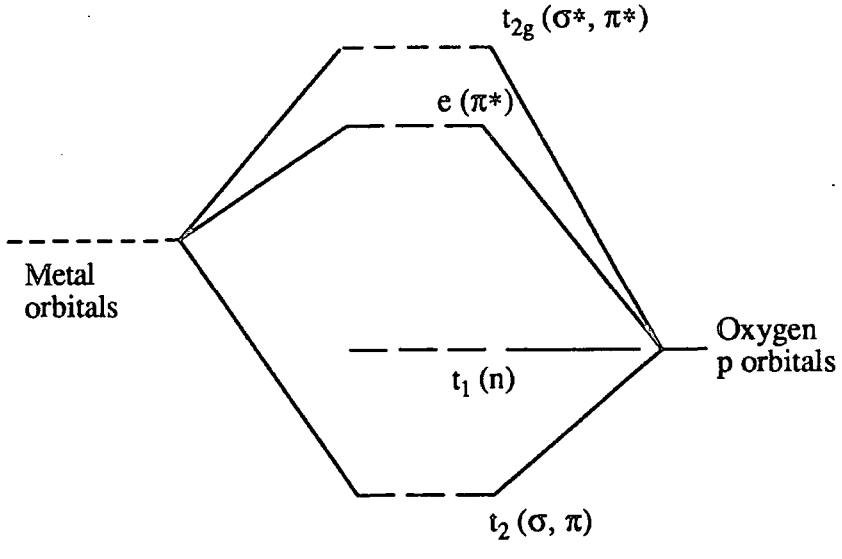

Figure 1.18, *Partial molecular orbital diagram for tetrahedral MO_4n-.*

1.6 Properties.

1.6.1 Infrared Spectroscopy of Oxo Complexes.

1.6.1.1 General Considerations.

The oxo group is an ideal chromophore for I.R. spectroscopy. Because of the large change in bond dipole for this ligand, absorbance bands due to M=O are generally intense. Moreover, since the stretching vibrations in the terminal ligand are not strongly coupled to other ligand oscillations, the bands are also often sharp. Observation of such a band at an appropriate frequency is commonly considered as diagnostic for the presence of a terminal oxo group. Bending bands have however, proven much less useful than the stretching modes and therefore any assignments must be based on stretching frequencies alone. In addition to the above, stretching frequencies for a whole range of transition metal oxo complexes are extremely well documented thus making an assignment by this technique relatively simple. Furthermore metal halogen modes occur at low frequencies (typically < 450cm^{-1} for Cl and Br) providing an unobstructed view of bands due to the multiply bonded oxo ligand.

1.6.1.2 Assignment of M-O Stretching Frequencies.

In 1959 Barraclough et al[67] proposed that bands in the region of 900-1100 cm^{-1} of oxo-metal species could be assigned as metal-oxygen stretching modes of terminal oxo ligands whilst bands due to bridging M-O-M systems occur at lower frequencies, 800-900 cm^{-1}. In his 1972 review, Griffith[39] proposed the range 900-1050 cm^{-1}, this being dependant on the oxidation state of the metal and the nature of the ancillary ligands. Although there have been one or two notable exceptions to this rule since, the basic proposals have stood up remarkably well.

In table 1.5 we show the range of reported values for the IR. stretching frequencies of mononuclear mono-oxo complexes for groups V-VIII. The indicated references are those containing the highest and lowest frequencies stated.

Metal	υ(M-O) cm^{-1}	References
V	875 - 1035	68, 69
Nb	835 - 1020	70, 71
Ta	905 - 935	72, 73
Cr	930 - 1028	74, 75
Mo	922 - 1050	76, 77
W	922 - 1058	77, 78
Mn	950 - 1060	79, 80
Tc	882 - 1020	81, 82
Re	945 - 1067	81, 83
Ru	a	84
Os	960 - 1040	85, 86

a Oxo ruthenium (IV) complexes show unusually low stretching frequencies (See Text).

Table 1.5, *Range of reported stretching frequencies for mono-oxo complexes.*

It can be seen in table 1.5 that some of the data lie somewhat below the 900-1100 range originally suggested by Barraclough[67]. Notably, the diamagnetic complexes $Cp_2M{=}O$, where M=Mo and W, have reported υ(M=O) values of 793-868 cm^{-1} for the molybdenum complex 793-868 cm^{-1} and 789-879 cm^{-1} for the tungsten analogue. This obviously raises the question as to whether they might in fact contain bridging oxo ligands. However, a recently reported[88] X-ray crystal structure has confirmed the

presence of a terminal oxo ligand for the analogue $(MeCp)_2Mo{=}O$. Since there is a rough inverse relationship between d(M=O) and υ(M=O) an unusually low stretching frequency should be the result of a long M-O bond, and this is in fact the case with the reported Mo-O bond length for $(MeCp)_2Mo{=}O$ being 1.721(2)Å which lies at the far end of the range for mono-oxo molybdenum complexes containing the M=O moeity. A tentative explanation for this unusually long bond length can be found by applying electron counting considerations. That is a M-O triple bond would result in a 20-electron complex and therefore the complex is restricted to a formal double bond.

1.6.1.3 Stretching Frequencies for Oxo Complexes.

The frequency ranges in table 1.5 seem at first glance to be independent of the nature of the metal that is present. This is in part due to the compensating trends in stretching force constants and the mass of the metal atoms. According to equation 1.1 which is derived from Hookes law[89], an increase in mass should lead to a decrease in frequency assuming the force constants remain unchanged. Therefore it is expected that the frequency will always decrease on proceeding down a given triad. This however is not the case and in the oxo complexes MOF_4 the reverse sequence is observed. Thus υ(M=O) increases $1028 < 1050 < 1058$ cm^{-1} along the series M=Cr, Mo, W.[74,77]

$$\nu = \frac{1}{2\Pi c}\left(\frac{f}{\frac{M_x My}{M_x + M_y}}\right)^{1/2}$$

Where m = the vibrational frequency (cm^{-1})
c = velocity of light (cm/sec)
f = force constant of bond (dyne/cm)
M_x and M_y = Mass (g) of atom x and atom y respectively .

Equation 1.1, *The relationship between vibrational frequency, force constant and the mass of the bonded atoms.*

Simply, the force constants do change and were predicted by Cotton and Wing[52] to increase not only across a period from left to right but also increase on descending a group. Table 1.6 includes the vibrational frequencies and stretching force constants for d^0 tetraoxo species of groups V-VIII as calculated by Müller[90] and shows a remarkable consistency with Cotton's prediction.

1.6.2 ^{17}O NMR of Oxo Complexes.

^{17}O NMR of transition metal-oxo compounds was first reported by Figgis, Kidd and Nyholm in 1962[91]. It was discovered that for the d^0 tetraoxometallates of V,Cr,Mo,W,Tc,Re,Ru and Os there is a linear relationship between the lowest energy ($t \rightarrow e$) electronic transition and the ^{17}O chemical shift. This observation was explained in terms of Ramsay's general equation for nuclear shielding[92]. Since this term results from the non-spherical distribution of electronic charge surrounding the oxygen nucleus it is therefore very sensitive to orbital mixing of the excited states in metal oxo species. Since such excited states involve placing an electron in an oxygen $p_x(\pi)$ or $p_y(\pi)$ orbital, this results in orbital angular momentum which is inversely proportional to the energy of the electronic transition, thus making ^{17}O NMR an excellent technique for studying the nature of bonding in oxo metal species.

^{17}O NMR has proven particularly useful for distinguishing between terminal and bridging oxygen atoms. This was first[93] demonstrated for a series of M_xO_y complexes (M=Cr,Mo) and the results are presented in table 1.7. As is generally the case, the chemical shift (relative to H_2O) is greater for terminal (typically greater than δ 700) than for the bridging oxo groups which usually occur below *ca.* δ 550.

Because ^{17}O chemical shifts derive from the paramagnetic term of the Ramsay equation, they are extremely sensitive to the π-bonding environment of the oxometal complexes (σ bonds, by definition have zero angular momentum about the direction of the bond axis and therefore are unimportant in this respect). Kidd in his 1967 review[94] states that "for a closely related series of compounds, the chemical shift does fall off monotonically with increased π bond order". For each series of compounds studied M_xO_y (M=Cr,Mo), a plot of the chemical shift versus π bond is fairly linear with a correlation coefficient r^2=0.99.

As discussed earlier, (section 1.5.1) the degree of π-bonding, ie. the π bond order, can have a marked effect on the M-O bond length. Miller and Wentworth[93] investigated the relationship between the ^{17}O chemical shift and the M-O bond length for a series of oxomolybdenum complexes and a plot comparing these two parameters, as illustrated in figure 1.19 was found to be linear indicating that there is indeed a close inverse relationship between π bond order and M-O bond length.

Complex	$\upsilon_1(A_1)$	$\upsilon_2(F_2)$	$\upsilon_3(E)$	$\upsilon_4(F_2)$	K_{FC}
$[VO_4]^{3-}$	826	336 [b]	804	336 [b]	4.80
$[CrO_4]^{2-}$	846	349	890	378	5.65
$[MoO_4]^{2-}$	897	317 [b]	837	317 [b]	5.93
$[WO_4]^{2-}$	931	325 [b]	838	325 [b]	6.48
$[MnO_4]^{-}$	839	360	914	430	5.92
$[TcO_4]^{-}$	912	325	912	336	6.78
$[ReO_4]^{-}$	971	332 [b]	920	332 [b]	7.56
RuO_4	882	323	914	334	6.96
OsO_4	965	333	960	323	8.29

[b] The υ_2 and υ_4 bands cannot be resolved

Table 1.6

Complex	π-bond order	δ(M=Cr)	δ(M=Mo)
$[O_3MOMO_3]^{2-}$ (bridging)	0	345	248
$[MO_4]^{2-}$	0.75	835	532
$[O_3MOMO_3]^{2-}$ (terminal)	1.0	1129	715
MO_2X_2 [b]	1.5	1460	921

[a] ^{17}O chemical shift (versus $H_2{}^{17}O$) from refs.
[b] For Cr, X=Cl; for Mo, X=ethylcystienyl

Table 1.7

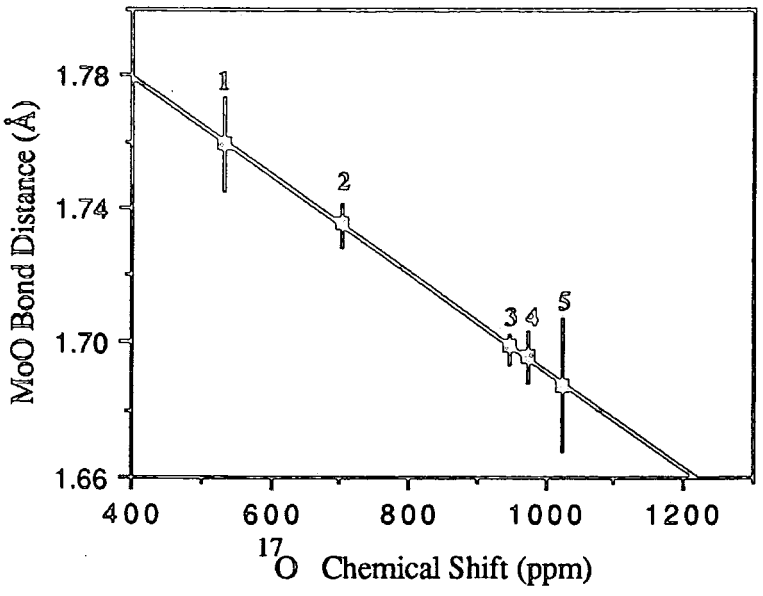

Figure 1.19, *Plot of ^{17}O chemical shift (ppm) versus M-O bond distance (Å).*

1.7 Uses.

1.7.1 Direct Oxidation by Oxometal (M=O) Reagents.

The stoichiometric oxidation of organic substrates by oxometal (M=O) reagents, such as permanganate[95], chromic acid and chromyl compounds[96], SeO_2[97-100], OsO_4[101], RuO_4[102,103], and MnO_2[104] are well known. These reagents have traditionally played an important role in organic synthesis owing to their capacity for selective oxygen transfer to a wide variety of substrates (Figure 1.20). Participation by one or more M=O groups is a key mechanistic feature common to virtually all of these reactions.

The simple tetraoxo species MnO_4^-, OsO_4 and RuO_4 all react with alkynes to give the α-diketone (Equation 1.2), whilst secondary alcohols react with a variety of d^0 oxometal reagents including RuO_4, MnO_4^- and oxochromium (VI) to afford the corresponding ketone (Equation 1.3).

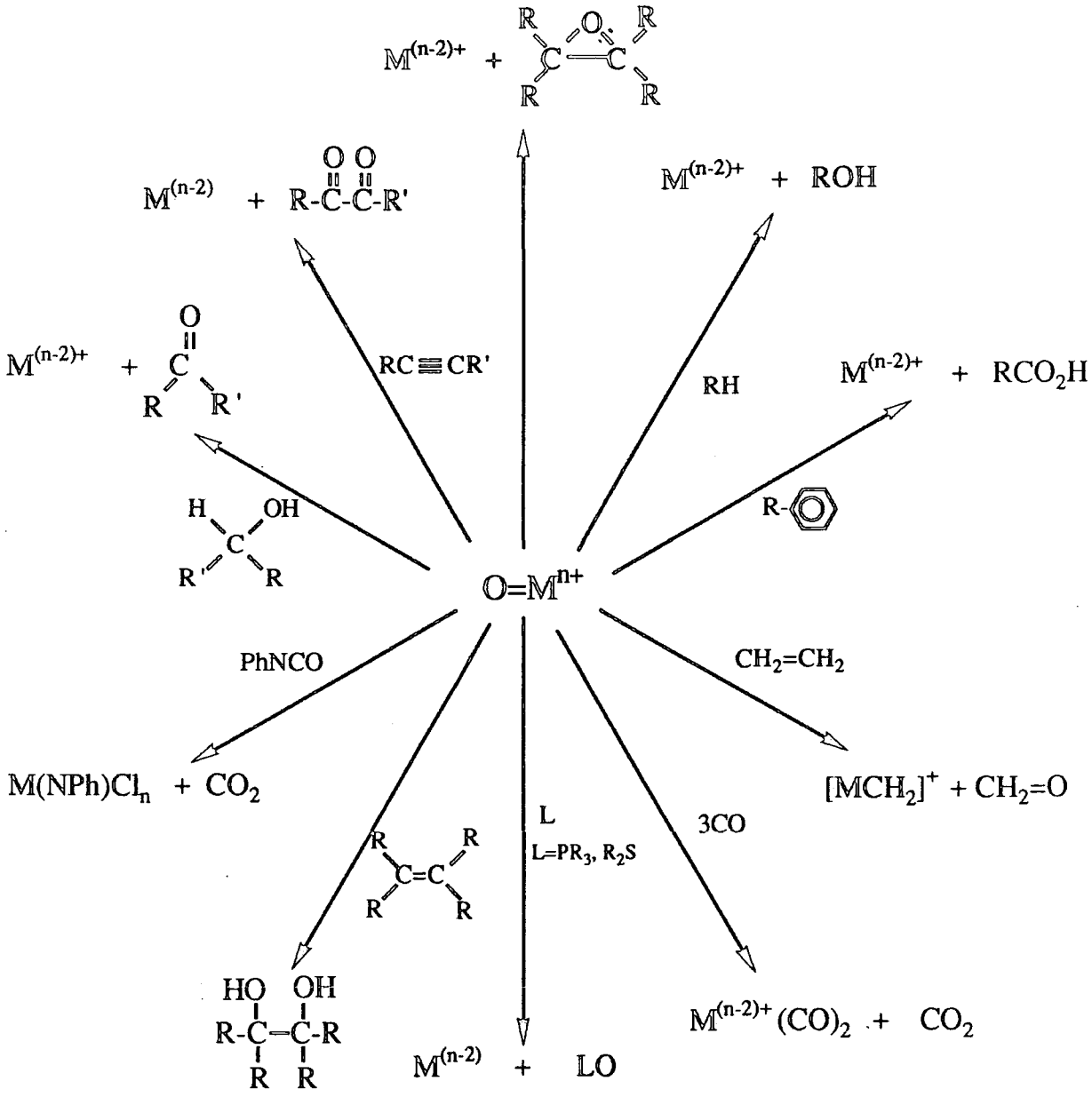

Figure 1.20, *Oxidative Transformations of M^{n+}=O.*

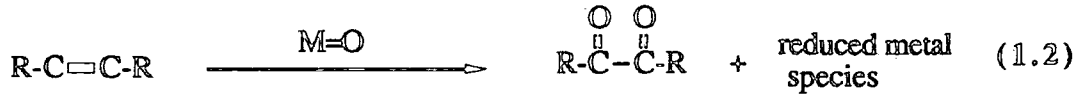

(1.2)

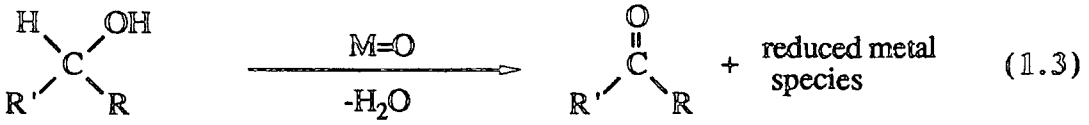

(1.3)

Selenium dioxide is one of the most commonly used oxometal reagents in direct oxidation reactions; in particular for the allylic oxidation of alkenes[97-100]. The mechanism for this reaction has been shown by Sharpless and co-workers[105-107] to involve an initial ene addition of an Se=O (Se^{+}-O^{-}) moiety to produce an organoselenium intermediate (ie. an allylselennic acid) first suggested by Stewart[96] (Equation 1.4).

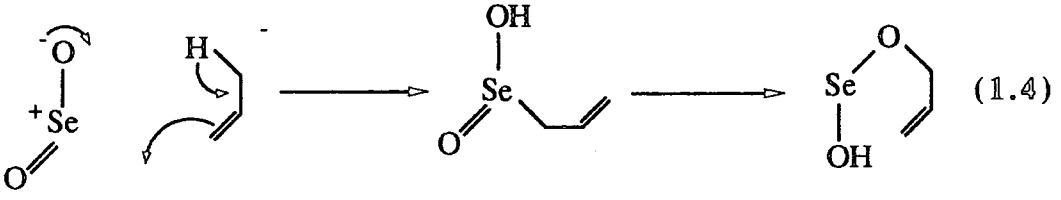

(1.4)

The insertion is followed by oxidative elimination to give the carbonyl compound (Equation 1.5), or hydrolysis to alcohols (Equation 1.6).

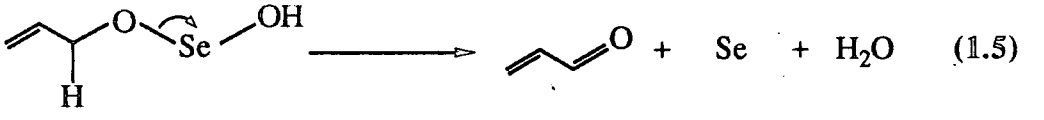

(1.5)

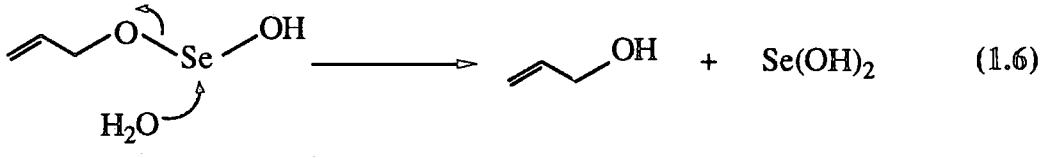

(1.6)

Oxometal reagents in addition to being useful allylic oxidants can also effect oxidative cleavage of double bonds. A characteristic feature of oxometal reagents that

effect the oxidative cleavage of double bonds is a cis- dioxometal functionality. Reaction with a double bond can produce cleavage via a [4+2]- or a [2+2]- cycloaddition. The reaction of OsO_4 with alkenes has long been considered to proceed via a thermally allowed [4+2]- cycloaddition involving attack on oxygen (Equation 1.7). Sharpless[66] has proposed an alternative [2+2]- cycloaddition to produce an organo-osmium (VIII) intermediate, followed by reductive insertion of the Os-C bond into an Os=O bond (Equation 1.8).

(1.7)

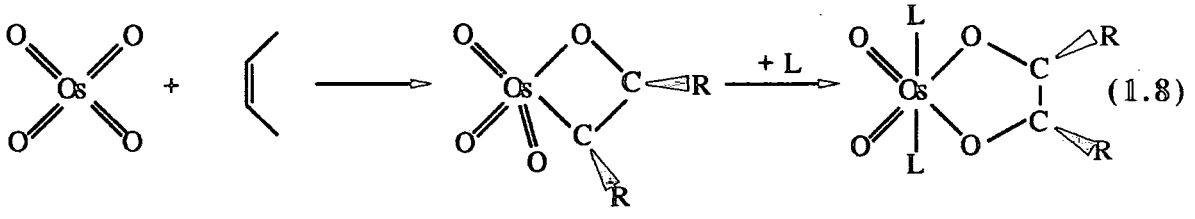

(1.8)

The latter is facilitated by the coordination of extra ligands (eg., L= pyridine with OsO_4). It has been suggested[109] that the mode of attack depends on (1) the degree of covalency or polarization of the M=O bond and (2) the presence of non-bonding electrons on the metal. High valent oxometal compounds having a polar M^+-O^- bond, and no non-bonding electrons generally effect [2+2]- cycloadditions.

A similar cis addition process for the epoxidation of alkenes by oxochromium (VI) reagents has been proposed[108,110] which involves attack of the substrate on the chromium centre to produce an organometallic intermediate (Equation 1.9), in contrast to the previous mechanisms that invariably invoked attack of the substrate on oxygen (Equation 1.10).

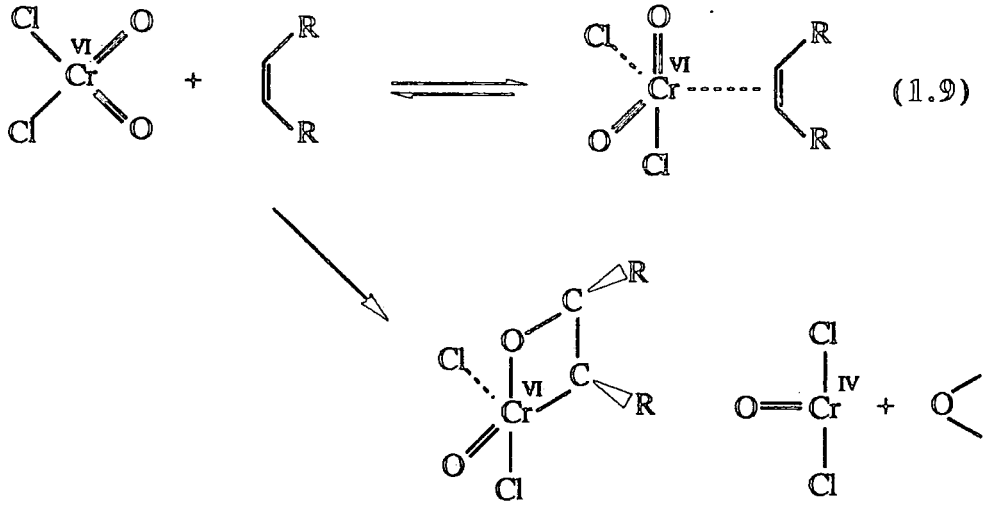

The latter constitutes a [2+2]- cycloaddition of an alkene to an oxometal function and has a precedent in the analogous stereospecific cycloaddition of sulphur trioxide to alkenes to afford cyclic sulfones[111].

1.7.2 Industrial Applications.

Eighty five per cent of industrial organic chemicals are currently produced by catalytic processes from petroleum and natural gas sources[112]. About one quarter are produced by the heterogeneous gas phase oxidation of hydrocarbons over metal oxide or mixed metal oxide catalysts[113]. These reactions are performed at elevated temperatures (300-600°C) and form the basis of a number of important petrochemical processes[114], namely allylic oxidation and ammoxidation, epoxidation, aromatic oxidation and oxidation of alkanes.

Perhaps the best known of these are the vapour phase oxidation and ammoxidation of propylene to acrolein and acrylonitrile respectively over bismuth molybdate catalysts[115] (Equation 1.11).

$$CH_3CH{=}CH_2 + O_2 \xrightarrow{[Bi_2Mo_2O_9]} CH_2{=}CHCHO + H_2O$$

$$CH_3CH{=}CH_2 + O_2/NH_3 \xrightarrow{[Bi_2Mo_2O_9]} CH_2{=}CHCN + 2H_2O \qquad (1.11)$$

The precise mechanism for acrolein formation is however unknown, although it is generally accepted that the initial step of the reaction involves formation of an allylic intermediate, by a rate limiting alpha-hydrogen abstraction. However, the nature of the allylic species together with oxygen insertion remain less well defined. Figure 1.21 shows the redox catalytic cycle which indicates that the catalyst should possess:-

a) an alpha-hydrogen abstracting site

b) an oxygen insertion site

c) a redox component

d) a solid matrix capable of rapid O^{2-} diffusion to reconstitute the catalytically active surface.

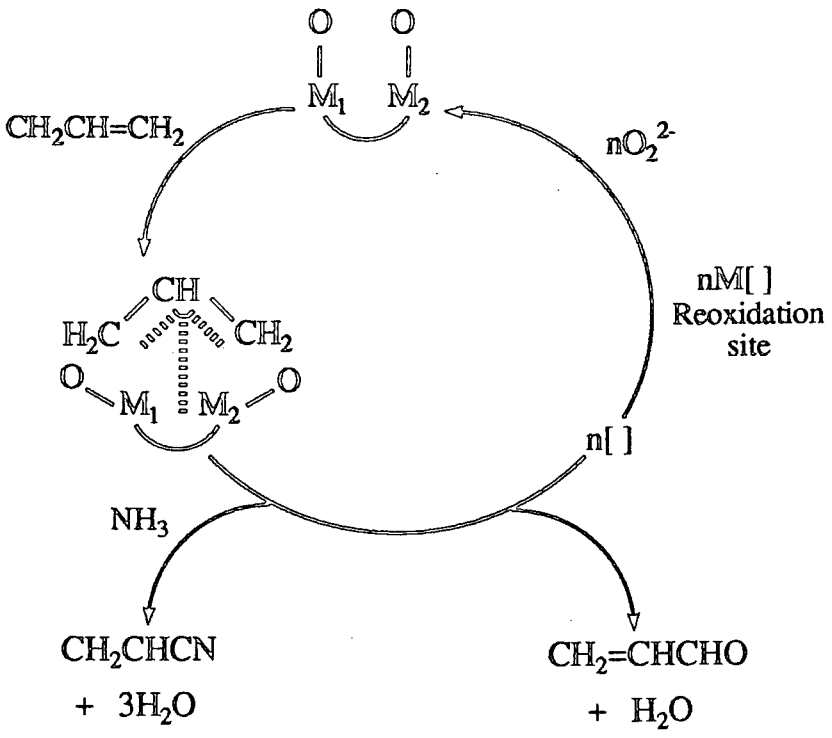

M_1 = α hydrogen abstraction element
M_2 = olefin chemisorption O & N insertion element
M = reoxidation element
[ ] = oxygen vacancy
O^{2-} = lattice oxygen

Figure 1.21, *Redox catalytic cycle for allyic oxidation mechanism.*

From the results of surface studies using probes, Grasselli[116] devised a more detailed general mechanism using Bi_2MoO_6 as his model. This mechanism involves propylene chemisorption on a coordinatedly saturated molybdenum di-oxo centre with a rate determining alpha-hydrogen abstraction by oxygen atoms associated with the bismuth. Raman studies carried out indicated that the lattice oxygens involved in the alpha-hydrogen abstraction and oxygen insertion steps are distinct. Further results indicated that Bi-O sites are associated with alpha-hydrogen abstraction, while Mo=O sites are associated with oxygen insertions. Hence the representation of the catalytically active site of Bi_2MoO_6 was postulated as shown (Figure 1.22).

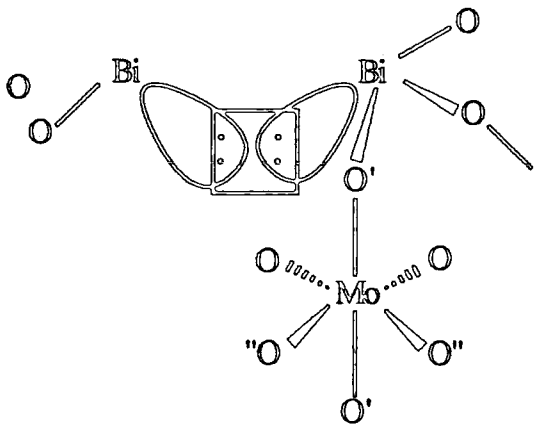

□ = Proposed centre for O_2 reduction and dissociative chemisorption
O' = Oxygen responsible for alpha-hydrogen abstraction
O" = Oxygen associated with molybdenum responsible for insertion into allyic intermediate

Figure 1.22, *Schematic representation of the proposed catalytically active site of* Bi_2MoO_6.

Calculations by Allison and Goddard[51] lend support to the above mechanism with the exception of the one centre beta-hydrogen elimination. Thermodynamic results calculated for the cis-di oxo moeity indicated that the process of trapping the allyl group with a dioxo molybdenum unit was more favourable than with a mono oxo unit. Hence, Goddard et al. put forward the idea that collections of adjacent dioxo groups are critical to the selective oxidation process together with the all important proposal that the rate determining beta-hydrogen abstraction is by an adjacent dioxo group with the hydrogen bonding to the 'spectator oxo group'[51] due to its increased electron density caused by the 'neighbouring oxo atom effect'.

Similarly, the MoO_3-SiO_2 system is of interest for catalysing oxidation or ammoxidation reactions. In the selective oxidation of ethanol to ethanal[117], Lavelley et al.have also shown that the active surface species contains a terminal cis-dioxo unit[118]. Structural information derived from the molybdenum oxo methoxide complex $[Mo_2O_5(OCH_3)_2]$[119] suggests that the chemisorption of methanol occurs at the surface oxygens at points of coordinative unsaturation, that is at oxygen atoms which possess a degree of multiple bond character.

1.7.3 Biochemical Oxidations.

A constant supply of dioxygen is essential for the existence of most living organisms. Oxidation reactions are involved in many fundamental biological processes, such as energy transformation and storage, as well as the biosynthesis of essential amino acids, vitamins, hormones etc. One of the most important biological processes is the enzymatic oxidation reaction. An enzyme is a protein having both catalytic activity and specificity for its substrates. Enzymes that play a vital role in oxidation reactions and produce similar catalytic activity to oxo metal catalysts are called oxygenases.

Interest in the study of chemical models that mimic oxygenases has developed for two reasons: first, to provide a basis for understanding enzymatic oxidations and second, to develop simple catalytic systems that, under mild conditions, exhibit the high selectivities characteristic of enzymatic oxidations. It is not surprising therefore, that most studies have concentrated on chemical models for the cytochrome P-450 monooxygenases, which mediate the selective hydroxylation of alkanes. These reactions bear a marked similarity to stoichiometric oxidations such as those effected by chromyl chloride.

Cytochrome P-450 is a protein containing ferriprotoporphyrin IX. It is a component of a significant group of enzymes that have been extensively studied. One such monooxygenase camphor 5 oxygenase is a multicomponent enzyme that contains in addition to cytochrome $P\text{-}450_{cam}$, a flavoprotein and an iron-sulphur protein. Cytochrome $P\text{-}450_{cam}$ has been isolated in crystalline form[120] and the mechanism of oxygen activation and transfer to substrate has been thoroughly studied[121]. The reaction sequence involves six well defined steps[121,122] (scheme 1.1).

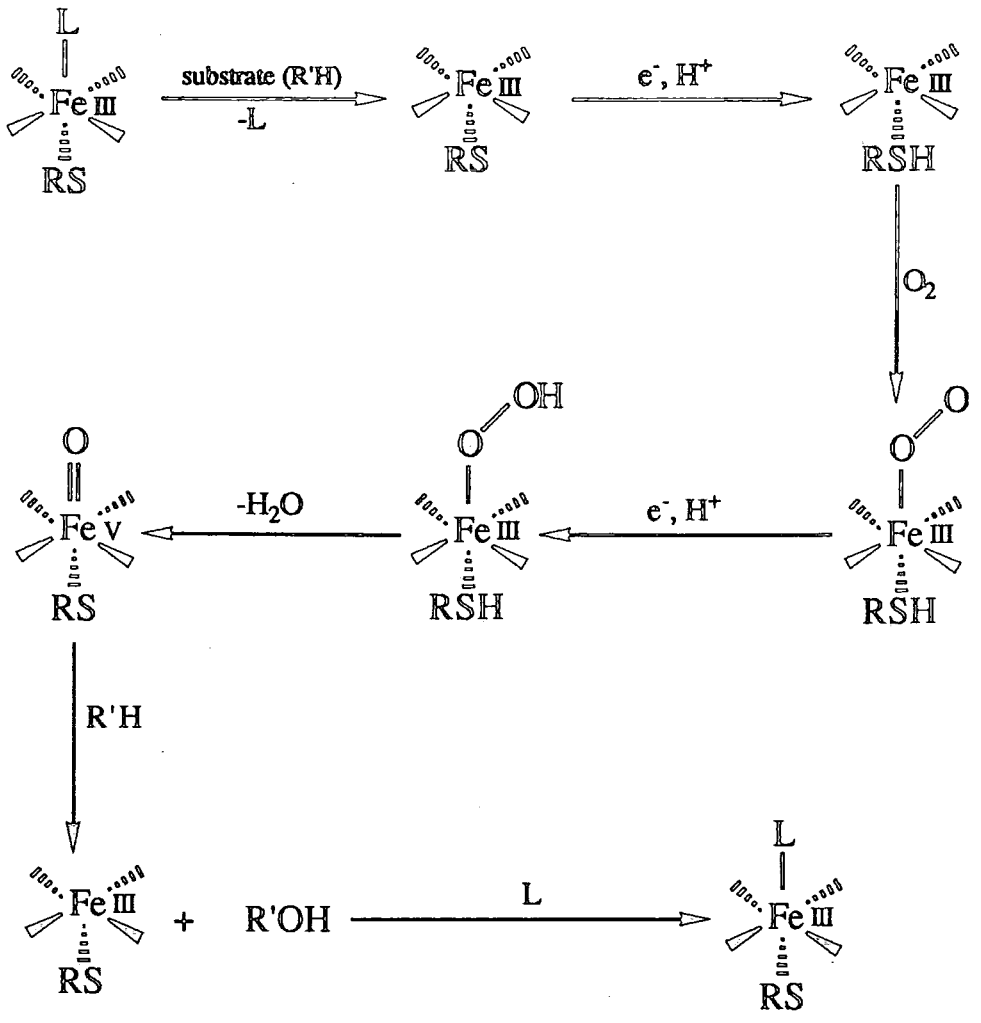

Scheme 1.1

The active intermediate is believed to be a perferryl cytochrome [O=Fe(V)]. Oxygen transfer then occurs from the perferrylcytochrome to either the C-H bond or the P stem of the substrate. The same active intermediate has been found in the structure of haemoglobin. The essential difference between the oxygen carrier (haemoglobin) and the oxygen activator (cytochrome P-450) being the presence in the latter of a second electron donor site, cysteinyl mercaptide (RS). The exact role of the mercaptide is not clearly defined although the facile one electron change ($RS^- \rightarrow RS\cdot + e$) is undoubtedly important in mediating electron transfer.

Before elaborating further as to the mechanism and possible reactions of the electrophilic [O=Fe(V)] intermediate, it is appropriate to consider the possible canonical

structures of this oxenoid species, since various structures can be written in which the odd electron and charges are delocalized onto the ligands (Equation 1.12).

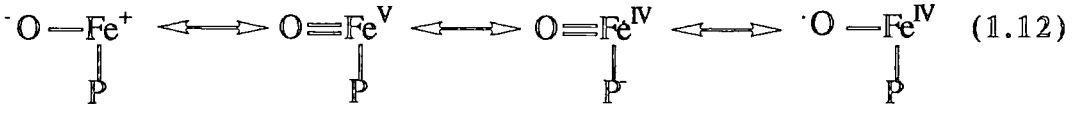

(1.12)

{P = porphyrin}

In addition to catalyzing the hydroxylation of aliphatic C-H bonds (see scheme 1.1). Cytochrome P-450 monooxygenases also mediate the epoxidation of alkenes. In light of the above canonical forms a [2+2]- cycloaddition can be envisaged for the stereospecific epoxidation of alkenes, analogous to that proposed by Sharpless for the epoxidation of alkenes by oxochromium (VI) reagents as discussed in section 1.7.1 (Equation 1.13).

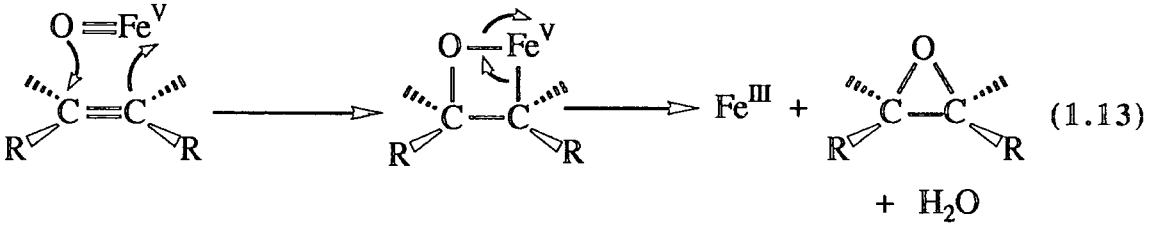

(1.13)

Another family of redox enzymes that promotesthe addition of an oxygen atom to, or it's removal from, a substrate are the molybdenum "oxo-transferase s". These include hydroxylases such as xanthine oxidase, aldehyde oxidase and sulphite oxidase. It is now generally believed that these enzymes function, at least in some cases, by direct transfer of the oxo ligand to the organic substrate. This model is supported by experiments involving the enzymatic oxidation of xanthine to uric acid with ^{18}O-labelled nicotinamide N-oxide as stoichiometric oxidant (Equation 1.14).

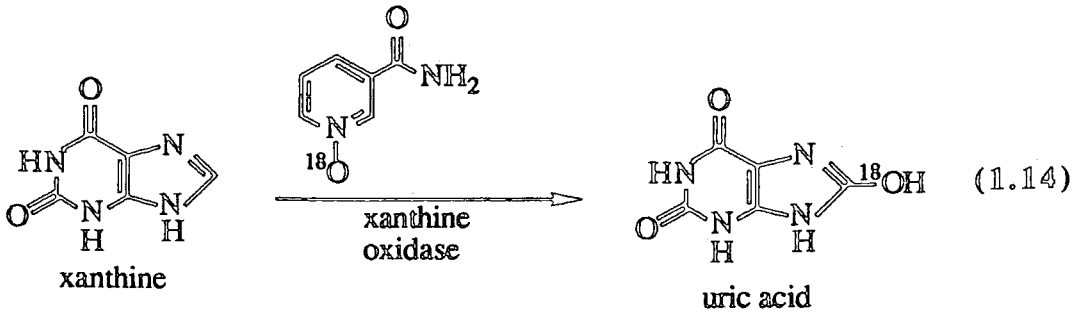

(1.14)

The amine oxide transfers its oxygen to molybdenum(IV) to give oxomolybdenum(VI); this in turn transfers the oxo moiety to the substrate. This and other model studies relevant to oxo transferase activity have been reviewed[123].

1.8 Summary.

This chapter has served to outline the many facets of transition metal oxo chemistry from their occurrence through to their properties and typical characterising data, and finally their applications in a number of important hydrocarbon oxidation reactions. The subsequent chapters in this thesis describe the synthesis and characterisation of a variety of new oxo and sulphido compounds of the early transition metals, and a study of their stability and reactivity.

1.9 References.

1. D.W. Phelps, *Inorg. Chem.*, 1975, 14, 2486.
2. P.T. Cheng and S.C. Nyburg, *Inorg. Chem.*, 1975, 14, 327.
3. R.A. Holwerda and J.S Petersen, *Inorg. Chem.*, 1980, 19, 1775.
4. K.F. Tebbe and H.G. von Schnering, *Z. Anorg. Allg. Chem.*, 1973, 396, 66.
5. D.A. Cartwright, W.P. Griffith, M. Schroder and A.C. Skapski, *J. Chem. Soc., Chem. Commun.*, 1978, 853.
6. S.C. Chang and G.A. Jeffrey, *Acta. Crystallogr. Sect. B*, 1970, 26, 673.
7. F.A. Cotton and W. Wang, *Inorg. Chem.*, 1982, 21, 2675.

8. A.R.E. Baike, M.B. Hursthouse, D.B. New and P. Thornton, *J. Chem. Soc. Chem. Commun.*, 1978, 62.

9. J.E. Baumann, S.T. Wilson, D.J. Salman, P.L. Hood and T.J. Meyer, *J. Am. Chem. Soc.*, 1979, 101, 2916.

10. K. Wieghardt, K. Pohl, I. Jibril ang G. Huttner, *Angew. Chem. Int. Ed. Engl.*, 1984, 23, 77.

11. G. Ciani, A. Sironi and V.G. Albano, *J. Chem. Soc. Dalton Trans.*, 1977, 1667.

12. A. Bino, F.A. Cotton and Z. Dori, *J. Am. Chem. Soc.*, 1981, 103, 243.

13. D. Bright, *J. Chem. Soc. Chem. Commun.*, 1970, 1169.

14. F. Bottomley, D.E. Paez and P.S. White, *J. Am. Chem. Soc.*, 1982, 104, 5651; F. Bottomley and F. Grein, *Inorg. Chem.*, 1982, 21, 4170.

15. M. Cousins and M.L.H. Green, *J. Chem. Soc. (A)*, 1969, 16.

16. W.H. Bragg, *Nature* (London), 1923, 111, 532.

17. J.A. Bertrand, *Inorg. Chem.*, 1967, 6, 495.

18. A. Olin and R. Soderguist, *Acta. Chem. Scand.*, 1972, 26, 3505.

19. T.P. Kee, Ph.D.Thesis, Durham University, 1989.

20. J. Catterick, P. Thornton and B.W. Fitzsimmons, *J. Chem. Soc. Dalton Trans.*, 1977, 1420.

21. K. Mertis and G. Wilkinson, *J. Chem. Soc. Dalton Trans.*, 1976, 1488.

22. A.B. Blake, F.A. Cotton and J.S. Wood, *J. Am. Chem. Soc.*, 1964, 86, 3024.

23. J.F. Rowbottom and G. Wilkinson, *J. Chem. Soc. Dalton Trans.*, 1972, 826.

24. I. Feinstein-Jaffe, D. Gibson, S.J. Lippard, R.R. Schrock and A. Spool, *J. Am. Chem. Soc.*, 1984, 106, 6305.

25. C. Couldwell and K. Prout, *Acta. Crystallogr. Sect. B*, 1978, B34, 933.

26. M. Herberhold, W. Kremnitz, A. Razairi, H. Schollhorn and U. Thewalt, *Angew. Chem.*, 1985, 97, 603.

27. J.D. Fellman, R.R. Schrock and D.D. Traficante, *Organometallics*, 1982, 1, 481.

28. E.A. Carter and W.A. Goddard III, *J. Am. Chem. Soc.*, 1986, 108, 2180.

29. T. Veki, A. Zalkin and D.H. Templeton, *Acta. Crystallogr.*, 1965, 19, 157.

30. K.V. Kotegov, O.N. Paulov and V.P. Shuedov, Advan. *Inorg. Chem. Radiochem.*, 1968, 2, 1.

31. K.W. Chiu, D. Lyons, G. Wilkinson, M. Thotnton-Pett and M.B. Hursthouse, *Polyhedron*, 1983, 2, 803.

32. B. Krebs and K.D. Hasse, *Acta. Cryst.*, 1976, B32, 1332.

33. K. Tijama and S. Shibata, *Chem. Lett.*, 1972, 1033.

34. F. Fairbrother, "The Chemistry of Niobium and Tantalum." Elsevier, Amsterdam, (1967) p. 148.

35. P.C.H. Mitchell, *Coord. Chem. Rev.*, 1966, 1, 315.

36. A.A. Woolf, *Quart. Rev.*, 1961, 15, 372.

37. R.V. Parish, *Advan. Inorg. Chem. Radiochem.*, 1966, 9, 315.

38. R. Colton, "Chemistry of Technetium and Rhenium." Interscience, London (1966) p 461.

39. W.P. Griffith, *Coord. Chem. Rev.*, 1970, 5, 459.

40. W. Hasse and H. Hoppe, *Acta. Cryst.*, 1968, B24, 282.

41. W. Hiller, J. Strahle, W. Kobel and M. Hanack, *Z. Kristallogr*, 1982, 159, 173.

42. P.N. Dwyer, L. Duppe, J.W. Buchler and W.R. Scheidt, *Inorg. Chem.*, 1975, 14, 1782.

43. E.M. Shustorovich, M.A. Porai-Koshits and A.Y. Buslaev, *Coord. Chem. Rev.*, 1975, 17, 1.

44. P. Stauropoulos, P.G. Edwards, T. Behling, G. Wilkinson, M. Motevalli and M.B. Hursthouse, *J. Chem. Soc. Dalton Trans.*, 1987, 169.

45. N.D. Silauwe, M.Y. Chiang and D.R. Tyler, *Inorg. Chem.*, 1985, 24, 4219.

46. J.M. Mayer, D.L. Thorn and T.H. Tulip, *J. Am. Chem. Soc.*, 1985, 107, 7454 and references therein.

47. D.C. Brower, J.L. Templeton and D.M.P. Mingos, *J. Am. Chem. Soc.*, 1987, 109, 5203.

48. K. Tatsumi and R. Hoffman, *Inorg. Chem.*, 1980, 19, 2656.

49. J.E. Huheey, "Inorganic Chemistry." 3rd ed., Harper and Row, New York (1983) pp. 71 ff, 256 ff.

50. D.M.P. Mingos, *J. Organomet. Chem.*, 1979, 179, C29.

51. J.N. Allison ands W.A. Goddard III, *Solid State Chemistry in Catalysis, A.C.S. Symposium Series*, 1985, no. 279, p 23.

52. F.A. Cotton and R.M. Wing, *Inorg. Chem.*, 1965, 4, 867.

53. B. Graham, C.D. Garner, L.H. Hill, F.E. Mabbs, K.D. Hargrave and A.T. McPhail, *J. Chem. Soc. Dalton Trans.*, 1977, 1726.

54. H. Ledon and B. Mentzen, *Inorg. Chim. Acta.*, 1978, 31, L393.

55. K. Iijima and S. Shibata, *Chem. Lett.*, 1972, 1033.

56. S. Jurisson, M. McPartlin and P.A. Tasker, *Inorg. Chem.*, 1986, 25, 3659.

57. K. Hagen, R.J. Hobson and D.A. Rice, *Inorg. Chem.*, 1986, 25, 3659.

58. K.J. Palmer, *J. Am. Chem. Soc.*, 1938, 60, 2360.

59. B. Kamenar and M. Penavic, *Acta. Cryst.*, 1976, B32, 1334.

60. M.G.B. Drew, G.W.A. Fowles, D.A. Rice and K.J. Stanton, *J. Chem. Soc. Chem. Commun.*, 1974, 614.

61. M.E. Kastner, M.J. Lindsay and M.J. Clarke, *Inorg. Chem.*, 1982, 21, 2037.

62. K.D. Hasse and B. Krebs, Acta. Cryst., 1976, B32, 1337.

63. J.A. McGinnety, *Acta. Cryst.*, 1972, B28, 2845.

64. G.J. Palenik, *Inorg. Chem.*, 1967, 6, 507.

65. R. Faggiani, C.J.L. Lock and J. Poce, *Acta. Cryst*, 1980, B36, 231.

66. L. Schafer and H.M. Seip, *Acta. Chem. Scand.*, 1967, 21, 737.

67. C.G. Barraclough, J. Lewis and R.S. Nyholm, *J. Chem. Soc.*, 1959, 3552.

68. M. Pasquali, F. Marchetti, C. Floriani and S. Merlino, *J. Chem. Soc. Dalton Trans.*, 1977, 139.

69. F.A. Miller and L.R. Cousins, *J. Chem. Phys.*, 1957, 26, 329.

70. E.G. Samsel and J.K. Kochi, *J. Am. Chem. Soc.*, 1985, 107, 7606.

71. P. Richard and R. Guilard, *Nouv. J. Chim.*, 1985, 9, 119.

72. J.F. Mitchell and P.T. Wolczanski, *J. Am. Chem. Soc.*, 1986, 108, 6382.

73. R.L. Deutscher ands D.L. Kepert, *Inorg. Chem. Acta.*, 1970, 4, 645.

74. E.G. Hope, P.G. Jones and J.W. Turff, *J.Chem. Soc. Dalton Trans.*, 1985, 529.

75. J.T. Groves, T. Takahashi and W.M. Butler, *Inorg. Chem.*, 1983, 22, 884.

76. J.R.M. Kress, M.J.M. Russell, M.G. Wesolek and J.A. Osborn, *J. Chem. Soc. Chem. Commun.*, 1980, 431.

77. W. Levason, J.S. Ogden, A.J. Rest and J.W. Turff, *J. Chem. Soc. Dalton Trans.*, 1981, 2501.

78. M. Herberhold, H. Kniesel and L. Haumaier, *J. Organomet. Chem.*, 1986, 107, 7454.

79. J.M. Mayer, D.L. Thorn and T.H. Tulip, *J. Am. Chem. Soc.*, 1985, 107, 7454.

80. C.L. Hill and F.J. Hollander, *J. Am. Chem. Soc.*, 1982, 104, 7318.

81. A. Davison, A.G. Jones and M.J. Abrams, *Inorg. Chem.*, 1981, 20, 4300.

82. F.A. Cotton, A. Davison, V.W. Day, L.D. Gage and H.S. Trop, *Inorg. Chem.*, 1979, 18, 3024.

83. T. Lis and B.J. Trzebiatowska, *Acta. Cryst.*, 1977, B33, 1248.

84. R.J. Collin, W.P. Griffith and D. Pawson, *J. Mol. Struct.*, 1973, 19, 531.

85. N. Bartlett and N.K. Jha, *J. Chem. Soc. A*, 1968, 536.

86. A.S. Alues, D.S. Moore and G. Wilkinson, *Polyhedron*, 1982, 1, 83.

87. M.L.H. Green, A.H.L. Lynch and M.G. Swanwick, *J. Chem. Soc. Dalton Trans.*, 1972, 1445.

88. N.D. Silauve, M.Y. Chiang and D.R. Tyler, *Inorg. Chem.*, 1985, 24, 4219.

89. Silverstein, Bassler and Morill, "Spectrometric Identification of Organic Compounds." 4th Ed., Wiley, New York (1981).

90. A. Muller and E.D. Iemann, "MTP International Review of Science, Inorganic Chemistry." Series 2, vol 5, D.W.A. Sharp ed., Butterworths, London (1974) pp. 71-110.

91. B.N. Figgis, R.G. Kidd and R.S. Nyholm, *Proc. Roy. Soc. Ser. A*, 1962, 269, 469.

92. N.F. Ramsey and E.M. Purcell, *Phys. Rev.*, 1952, 85, 143.

93. K.F. Miller and R.A.D. Wentworth, *Inorg. Chem.*, 1979, 18, 984.

94. R.G. Kidd, *Can. J. Chem.*, 1967, 45, 605.

95. R. Stewart, *in* "Oxidation in Organic Chemistry" (K.B. Wiberg ed), Part A, p. 2. Academic Press, New York (1965).

96. R. Stewart, *in* "Oxidation in Organic Chemistry" (K.B. Wiberg ed), Part A, p. 69. Academic Press, New York (1965).

97. H.J. Reich, *in* "Oxidation in Organic Chemistry" (W.S. Trahanovsky ed), Part C, p. 1. Academic Press, New York (1978).

98. E.N. Trachtenberg, *in* "Oxidation." (R.L. Augustine ed), Vol 1, Ch 3. Dekker, New York (1969).

99. N. Rabjohn, *Org. React.*, 1978, 24, 261.

100. R.A. Jerussi, *in* "Selective Organic Transformations" (B.S. Thyagarajan ed), p. 301. Wiley, New York (1970).

101. M. Schroeder, *Chem. Rev.*, 1980, 80, 187.

102. D.G. Lee, *in* "Oxidation in Organic Chemistry" (W.S. Trahanovsky ed). Academic Press, New York (1978).

103. M. Schroder and W.P. Griffith, *J. Chem. Soc. Chem. Commun.*, 1979, 58.

104. A.J. Fatiadi, *Synthesis*, 1976, 65

105.K.B. Sharpless, *J. Am. Chem. Soc.*, 1972, 94, 7154.

106. K.B. Sharpless and R.F. Laver, *J. Org. Chem*, 1975, 40, 264.

107. D. Arigoni, A. Vasella, K.B. Sharpless and H.P. Jensen, *J. Am. Chem. Soc.*, 1973, 95, 7917.

108. K.B. Sharpless, A.Y. Teranishi and J.E. Backvall, *J. Am. Chem. Soc.*, 1977, 99, 3120.

109. K.B. Sharpless, Pap., *Int. Symp. Oxygen. Activation Selective Oxidations Catalysed Transitiomn Met.*, 1979.

110. K.B. Sharpless and A.Y. Teranishi, *J. Org. Chem.*, 1973, 38, 185.

111. S. Noda and O. Okumursa, *J. Chem. Soc. Chem. Commun.*, 1973, 841.

112. R.K. Grasselli and J.D. Burrington, *J. Catal.*, 1984, 87, 363.

113. R.A. Sheldon and J.K. Kochi, "Metal-Catalysed Oxidations of Organic Compounds." Academic Press, New York (1981).

114. D.J. Hucknall, "Selective Oxidation of Hydrocarbons." Academic Press, New York (1974).

115. J.L. Callahan, R.K. Grasselli, E.C. Milberger and H.A. Strecker, *Ind. Eng. Chem. Prod. Rsch. Dev.*, 1970, 9, 134.

116. R.K. Grasselli, *J. Chem. Ed.*, 1986, 63, 3, 216.

117. Y. Iwasawa, Y. Nakano and S. Ogasawars, *J. Chem. Soc. Faraday Trans.*, 1978, 74, 2968.

118. M. Cornac, A. Janin and J.C. Lavalley, *Polyhedron*, 1986, 5, 183.

119. E.M. McCarron, H.H. Staley and H.W. Sleight, *Inorg. Chem.*, 1984, 23, 1043.

120. C.A. Yu and I.C. Gunsalus, *Biochem. Biophys. Res. Commun.*, 1970, 40, 1431.

121. I.C. Gunsalus, J.R. Meeks, j.D. Lipscomb, P. Debrunner and E. Munck, *in* "Molecular Mechanisms of Oxygen Activation", p. 561. Academic Press, New York (1974).

122. V. Ullrich, *J. Mol. Catal.*, 1980, 7, 159.

123. R.H. Holm and J.M. Berg, *Acc. Chem. Res.*, 1986, 19, 363.

Chapter Two

Synthesis of Oxo- and Sulphido-Halides of the Early Transition Metals.

2.1 Introduction.

2.1.1 General.

The previous chapter outlined the central role played by oxo complexes in a variety of laboratory, industrial and biological oxidation processess. Progress towards understanding the reactivity of the metal-oxo moiety in these systems is largely dependent upon the availability of convenient and generally applicable routes to complexes through which the properties of the oxo ligand can be addressed.

The oxohalides provide suitable starting materials for the preparation of molecular oxo complexes; likewise sulphidohalides for molecular sulphido complexes. However, a generally applicable, rapid, low temperature synthetic route has not hitherto been available and in many cases furnace procedures are necessary. Previously established routes to the oxohalides of metals under consideration in this chapter are collected in table 2.1 and those more commonly employed are indicated by an asterisk.

Transition metal sulphidohalides have proved more readily accessible by the treatment of transition metal halides with the sulphides of boron or antimony in CS_2 solvent over 1-3 days. Other routes usually require more forcing conditions (Table 2.2).

In this chapter, uses of the commercially available reagents Me_3SiYR (R = alkyl, $SiMe_3$; Y = O,S) for the convenient, high yield synthesis of oxohalide and sulphidohalide compounds of tungsten, molybdenum, niobium and tantalum are described. In addition, this methodology allows the preparation of mixed oxosulphidohalide materials and, in certain cases, intermediate alkoxo(siloxo) halide compounds have been isolated.

Species	Reagents	Conditions	Ref.
$WOCl_4$	WO_3 + CCl_4	Reflux, 36h	1
	WCl_6 + liq. SO_2	RT, 1week, 75%	2
	$2WCl_6$ + WO_3	Sealed tube, 100°C, 1day 150°C, 2h	3
	WCl_6 + Cl_3CNNO_2	70°C, 95%	4
	WO_3 + CCl_4	Sealed tube, 250-320°C	5
	W + SO_2Cl_2	Sealed tube,300°C	6
	WO_2Cl_2	Pyrolysis, 360°C	7
	WO_2 + CCl_2F_2	525°C, 2-5h	8
	*WO_3 + $SOCl_2$	200°C, 6-12h	9
	WO_3 + C_5Cl_8	Reflux, 285°C, 10min	10
	*$WO_3.xH_2O$ + $SOCl_2$	Reflux, 6h	11
	WO_3 + Cl_2/CCl_4	200°C, 3h	12
	WCl_6 + Me_3SiOMe	CH_2Cl_2, 25°C, 24h	13(a), 13(b)
WO_2Cl_2	$WOCl_4$ + Cl_3CNO_2	70°C	4
	*WCl_6 + $2WO_3$	Sealed tube, 100°C, 1day, 150°C, 2h	3
	WO_2 + O_2/CCl_4	370°c, 1h	14
	WO_2 + Cl_2/N_2	Furnace, 500-550°C	7
	WO_2 + CCl_4	Sealed tube, 250°C	5
	WO_2 + CCl_4	Sealed tube, 310-370°C	15
	WO_3/C + Cl_2	600°C	16
	WO_3 + HCl/CCl_4	600°C	17

Table 2.1, *Routes to the Oxohalides of the Early Transition Metals* .

Species	Reagents	Conditions	Ref.
MoO_2Cl_2	Mo + Cl_2/O_2	Flow system, 250-350°C	18
	$MoOCl_3$	> 215°C	19
	*MoO_2 + Cl_2	350-550°C	20, 21
	MoO_2 + O_2/CCl_4	360°C	14
	MoO_3 + NaCl	400-700°C	22
	$MoCl_5$ + MoO_3	120-130°C	23
	MoO_3 + Cl_2	Flow system, 600°C	18
	MoS_2 + O_2/Cl_2	650°C	24
$MoOCl_3$	*$MoCl_5$ liq. SO_2	Sealed tube, RT	25
	*$MoCl_5$ +Sb_2O_3	Vacuum, 80-150°C, 9h	26
	$MoCl_5$ + MoO_3		23
	$MoCl_5$ + MoO_2Cl_2		27
	$MoCl_5$ + $SOCl_2$	RT, 5-6 weeks	18
	$MoOCl_4$	< 200°C	18
	$MoOCl_4$ + C_6H_5Cl	Reflux	28
$NbOCl_3$	*$NbCl_5$ + Sb_2O_3 + Cl_2	Flow system,	29
	*$NbCl_5$ + O_2	150°C	30
	*$NbCl_5(OEt_2)$	Solid state pyolysis, 90°C	30
	Nb_2O_5 + $3CCl_4$	200°C	31
	Nb_2O_5 + $SOCl_2$	Reflux, 24h	9, 32
	$NbCl_5$ + Nb_2O_5	Melt, 250°C	33
$TaOCl_3$	*$TaCl_5$ + Sb_2O_3 + Cl_2	Flow system, 95°C	34
	*$TaCl_5(OEt_2)$	90°C, 17h	30
	$TaCl_5$ + OCl_2 + CCl_4	-30°C	35
	NO[$TaOCl_4$]	Vacuum, 97°C	4

Species	Reagents	Conditions	Ref.
$WSCl_4$	$W + S_2Cl_2 + S$	425°C, 2d	36
	$WCl_6 + S$	170°C, 8h	37
	*$WCl_6 + Sb_2S_3$	CS_2, 140°C, 3d	38, 39
	$WCl_6 + B_2S_3$	CS_2, 120°C, 1d	40
WS_2Cl_2	$WOCl_4 + H_2S$	C_6H_6 or CS_2	38, 41
	*$WSCl_4 + Sb_2S_3$	CS_2, RT, 1-3d	42
$MoSCl_3$	$MoCl_5 + Sb_2S_3$	140°C, 7d	38
	*$MoCl_5 + Sb_2S_3$	CS_2, RT, 2d	42
	$MoCl_5 + B_2S_3$	190°C, 1d	40
$NbSCl_3$	*$NbCl_5 + Sb_2S_3$	CS_2, RT, 1-3d	42
	$NbCl_5 + B_2S_3$	90°C, 1d	42
$TaSCl_3$	*$TaCl_5 + Sb_2S_3$	CS_2, RT, 1-3d	42
	$TaCl_5 + PhNCS$		43
	$TaCl_5 + B_2S_3$	80°C, 1d	40

Table 2.2, *Routes to the Sulphidohalides of the Early Transition Metals.*

2.1.2 Me_3SiYR Compounds as a Source of 'Y' and 'YR'.

Me_3SiOR (R=$SiMe_3$, Me, Et) reagents have received attention as sources of 'O' and 'OR' groups but mostly in main group systems. Reactions generally occur according to equations 2.1 and 2.2.

$$Me_3SiOR + [M]\text{-}Cl \rightleftharpoons Me_3SiCl + [M]\text{-}OR \quad (2.1)$$

$$(Me_3)_2SiO + [M]\text{-}Cl_2 \rightleftharpoons 2Me_3SiCl + [M]{=}O \quad (2.2)$$

For example, Emeléus has shown that $(R_3Si)_2O$ compounds react with BCl_3 to afford the corresponding trialkylsiloxyboron dichloride which subsequently decomposes at room temperature to afford B_2O_3 according to equation 2.3[44]

$$(Me_3Si)_2O + BCl_3 \xrightarrow{-78°C} [(Me_3Si)_2OBCl_3] \xrightarrow{-78°C} Me_3SiOBCl_2 + Me_3SiCl \quad (2.3)$$

For the transition metals, $W(O)F_4(CH_3CN)$[45] has been obtained by treatment of WF_6 with $(Me_3Si)_2O$ in acetonitrile (Equation 2.4), and following an initial observation by Handy.*et al*[13a], Schrock and co-workers have demonstrated that $W(O)Cl_4$ is accessible at room temperature through the reaction of WCl_6 with Me_3SiOMe[13b].

$$(Me_3Si)_2O + WF_6 \xrightarrow{MeCN} \text{O=W(F)(F)(F)(F)(NCMe)} + 2Me_3SiF \quad (2.4)$$

Alkylthioethers have been used by Boorman *et al*[46] to prepare a range of transition metal thiolates according to the general reaction shown in equation 2.5.

$$MCl_x + n(CH_3)_3SiSR \longrightarrow MCl_{x-n}(SR)_n + nMe_3SiCl \quad (2.5)$$

These workers have also found that the alkylthiolates decompose by two possible pathways (Equation 2.6), path (A) being analogous to the reaction in equation 2.1

(A) Elimination of RCl

$$MCl_x(SR) \longrightarrow MCl_{x-1}S + RCl$$

(B) Reductive elimination of R_2S_3

$$2MCl_x(SR)_y \longrightarrow M_2Cl_{2x}(SR)_{2y-2} + R_2S_3 \qquad (2.6)$$

Müller has extended this methodology to the group IV triad: titanium tetrachloride reacts with hexamethyldisilthiane to afford the titanium sulphidohalide, $Ti(S)Cl_2$ (Equation 2.7).[47]

$$TiCl_4 + (Me_3Si)_2S \longrightarrow Ti(S)Cl_2 + 2Me_3SiCl \qquad (2.7)$$

2.2 Synthesis and Characterisation of Oxo- and Sulphido-Halide Compounds of Molybdenum and Tungsten.

All the compounds (1-11) described in this section have been characterised by elemental analysis (M, X, S), infrared and mass spectroscopies and important characterising data are given in table 2.3. Full experimental details are described in chapter 7, section 7.2. Where more than one solvent has been investigated the procedure affording the higher yield and purity of product is reported.

2.2.1 Reaction of WCl_6 and $W(O)Cl_4$ with $(Me_3Si)_2O$:

Synthesis of $W(O)Cl_4$ (1), $W(O)_2Cl_2$ (2), $W(O)_2Cl_2(CH_3CN)_2$(3) and $W(O)_2Cl(OSiMe_3)$ (4).

Tungsten hexachloride reacts readily with equimolar amounts of $(Me_3Si)_2O$ in dichloromethane solvent at room temperature over a period of 1h, leading to deposition of $W(O)Cl_4$ in the form of red, moisture sensitive crystals (Equation 2.8)

$$WCl_6 + (Me_3Si)_2O \longrightarrow \underset{\textbf{(1), 99\%}}{W(O)Cl_4} + 2Me_3SiCl \qquad (2.8)$$

No.	Product	Colour	Analysis(%)												Yield %	Infra-red Spectra (cm^{-1})		
			Found						Calculated									
			M	Y	X	C	H	N	M	Y	X	C	H	N		M=Y	M-O-M	M-X
1.	$W(O)Cl_4$	Red	53.9		41.2				53.8		41.5				99		880-900 (s, br)	387(s, br), 368(m, sh), 334(s, sp), 320(m, sh), 308(w, sh)
2.	$W(O)_2Cl_2$	Yellow	63.7		24.4				64.1		24.7				95		800-830 (s, br)	415(s), 395(s, sh), 385(s, sh), 347(s), 300(m, sh), 290(m, sh), 279(s), 260(m, sh)
3.	$W(O)_2Cl_2(CH_3CN)_2$	White	50.1		19.3	13.0	1.7	7.6	49.8		19.2	13.0	1.6	7.6		980 (s, sp)		379(s, sp), 394(s, br), 380(m, sh)
4.	$W(O)_2Cl(OSiMe_3)$	Pale blue	55.9		10.1	10.2	2.5		56.7		10.9	11.1	2.8		70		700-900 (s, br)	280-360(s, br)
5.	$MoOCl_3$	Dark brown			48.7						48.7				98	1007 (s, sp)		398(s), 352(s), 309(m), 295(m, sh)
6.	$Mo(O)_2Cl_2$	Yellow			35.7						35.7				97		800-830 (s, br)	443(s, sp), 425(m, sh), 409(m, sh), 385(s, sp), 354(s, sp), 291(m, sp)
7.	$W(S)Cl_4$	Red	51.5	9.0	39.5				51.4	9.0	39.6				80	560 (s, sp)		392(m, sh), 355(s), 306(m, sh), 285(w)
8.	$W(S)_2Cl_2$	Black	57.6	20.0	21.7				57.7	20.0	20.0				81	538 (s, sp)		365(m, sh), 321(s, br), 287(m, sh)
9.	$Mo(S)Cl_3$	Olive green		14.4	45.3					13.7	45.4				87			398(s, br), 375(m, sh), 354(m), 346(w, sh), 290(m, br)
10.	$W(O)(S)Cl_2$	Light brown	60.1	9.8	22.8				60.7	10.6	23.4				82	540 (s,sp)	815 (s,br)	410(s), 372(m,br), 343(s, sp)
11.	$Mo(O)(S)Cl_2$	Light brown		15.1	32.8					14.9	33.0				86	982 (s, sp)		473(s, sp), 378(s), 369(m,sh), 325(s, sp), 298(s, sh), 255(m)

Table 2.3, *Characterising Data for Compounds (1-11).*

Previous syntheses of $W(O)Cl_4$ described in the introductory section invariably require further purification by sublimation[2,3]. The purity of the material obtained by the method described here does not necessitate a further purification step.

Attempts to prepare $W(O)_2Cl_2$ by addition of two molar equivalents of $(Me_3Si)_2O$ to WCl_6 in dichloromethane solvent at room temperature were unsuccessful. Instead, precipitation of a grey amorphous solid of indeterminate stoichiometry resulted. This solid is totally insoluble in common organic solvents and was found to be thermally stable up to 150°C (10^{-4} Torr). Its infrared spectrum revealed strong absorbtions at 1250 cm^{-1} and 1000 cm^{-1} assignable to a $\upsilon_s(CH_3)$ vibration and υ(Si-O-R) stretching vibration respectively[48], and a broad absorbtion at 800-850 cm^{-1} may be assigned to a υ(W-O-W) stretch[49] indicating that the compound is a heavily bridged oxo-siloxide.

$W(O)_2Cl_2$ can be prepared, however, by warming $W(O)Cl_4$ with an equimolar amount of $(Me_3Si)_2O$ in octane at 80°C for 4h. (Equation 2.9)

$$WOCl_4 + (Me_3Si)_2O \longrightarrow \underset{\text{(2), 95\%}}{W(O)_2Cl_2} + 2Me_3SiCl \qquad (2.9)$$

The product is deposited as a pale yellow amorphous powder. Prolonged exposure of this material to the reaction medium can result in a darkening of the product with evidence (infrared) for contamination by siloxide groups, presumably due to a back reaction with the Me_3SiCl formed. If isolated as soon as all the $W(O)Cl_4$ has been consumed (typically 4h as indicated by the absence of an orange colouration to the solution) the yellow powder is found to be analytically pure (Table 2.3)

If the reaction is carried out in a coordinating solvent such as acetonitrile, then the solvent adduct $W(O)_2Cl_2(CH_3CN)_2$ (3) may be obtained in 70% yield (Equation 2.10).

$$WOCl_4 + (Me_3Si)_2O \xrightarrow[RT/2h]{CH_3CN} \underset{\text{(3)}}{W(O)_2Cl_2(CH_3CN)_2} \qquad (2.10)$$

The $W(O)_2Cl_2(CH_3CN)_2$ may be selectively crystallized from the supernatant solution as colourless moisture sensitive needles, although care must be taken to avoid crystallization of the blue contaminant which is slightly more soluble. The synthesis described here offers a direct route to the acetonitrile complex (3) which has been previously prepared only by dissolution of $W(O)_2Cl_2$ in acetonitrile over 2 weeks at 90°C in a sealed tube[50].

Complete replacement of all the chloride groups of WCl_6 to give WO_3 is not possible using the $(Me_3Si)_2O$ reagent. When $W(O)Cl_4$ is reacted with 2 molar equivalents of $(Me_3Si)_2O$ in dichloromethane solvent at room temperature, dissolution of the starting oxohalide occurs with the formation of a pale blue solution. A light blue micro-crystalline moisture sensitive solid of formula $W(O)_2Cl(OSiMe_3)$ (4) may be isolated from this solution upon cooling (Equation 2.11).

$$WOCl_4 + 2(Me_3Si)_2O \longrightarrow \underset{(4),\ 70\%}{W(O)_2Cl(OSiMe_3)} + 3Me_3SiCl \quad (2.11)$$

Characterisation was provided by elemental analysis, infrared and ^1H NMR spectroscopies. In particular, strong absorptions at 1255 cm^{-1} and 1000 cm^{-1} may be assigned to the $\upsilon_s(CH_3)$ vibration and υ(Si-O-R) stretching vibration respectively of coordinated -$OSiMe_3$[48]. The broad absorbtion at 700-900 cm^{-1} is indicative of oxygen bridged metal atoms, in this case a υ(W-O-W) stretching vibration[49]. The 250 MHz ^1H NMR of (4) ($CDCl_3$) gives a singlet resonance at δ 0.42 attributable to the nine equivalent methyl hydrogens of a trimethylsiloxide ligand. Attempts to prepare WO_3 via elimination of Me_3SiCl from (4) were unsuccessful even after prolonged heating at 100°C.

2.2.2 Reactions of $MoCl_5$ and $Mo(O)Cl_4$ with $(Me_3Si)_2O$:

Synthesis of $Mo(O)Cl_3$ (5) and $Mo(O)_2Cl_2$ (6).

Molybdenum pentachloride reacts with equimolar amounts of $(Me_3Si)_2O$ in dichloromethane solvent at room temperature overnight to yield a dark brown amorphous solid and a colourless solution (Equation 2.12)

$$MoCl_5 + (Me_3Si)_2O \longrightarrow \underset{\text{(5), 98\%}}{Mo(O)Cl_3} + 2Me_3SiCl \qquad (2.12)$$

The solid was collected and subsequently characterised as $Mo(O)Cl_3$ (5) by elemental analysis; its infrared spectrum also shows the characteristic terminal oxo stretch at 1007 cm^{-1}.

$Mo(O)_2Cl_2$ (6) was isolated in high yield by allowing $Mo(O)Cl_4$ to react with an equimolar amount of $(Me_3Si)_2O$ in a similar manner (Equation 2.13).

$$Mo(O)Cl_4 + (Me_3Si)_2O \xrightarrow[RT/4h]{CH_2Cl_2} \underset{\text{(6), 97\%}}{Mo(O)_2Cl_2} + 2Me_3SiCl \qquad (2.13)$$

Compound (6) was deposited from solution as a yellow amorphous solid (6) and found to be very sensitive to moisture. Thus exposure to air for *ca.* 30 sec. resulted in complete decomposition with formation of hydroxide species ligands as shown by the presence of strong, absorbtions at 3300 cm^{-1} and 1650 cm^{-1} in the infrared spectrum.

2.2.3 Reactions of WCl_6, $W(S)Cl_4$ and $MoCl_5$ with $(Me_3Si)_2S$:

Synthesis of $W(S)Cl_4$ (7), $W(S)_2Cl_2$ (8) and $Mo(S)Cl_3$ (9).

In contrast to the analogous reaction with $(Me_3Si)_2O$, the reaction of tungsten-hexachloride with $(Me_3Si)_2S$ proceeds with such exothermicity that cooling is required. Thus dropwise addition of a chilled (*ca.*-30°C) dichloromethane solution of $(Me_3Si)_2S$ to a suspension of WCl_6 in dichloromethane at *ca.*-78°C, followed by warming of the

mixture to room temperature with stirring allowed the preparation of the known sulphidohalide compound $W(S)Cl_4$ (7) (Equation 2.14) in high yield. Compound (7) was isolated in 80% yield as red, moisture sensitive crystals.

$$WCl_6 + (Me_3Si)_2S \longrightarrow \underset{(7),\ 80\%}{W(S)Cl_4} + 2Me_3SiCl \qquad (2.14)$$

Treatment of $W(S)Cl_4$ with a further molar equivalent of $(Me_3Si)_2S$ in dichloromethane solvent at *ca.*-78°C affords $W(S)_2Cl_2$ (8) as an insoluble black amorphous solid in 81% yield (Equation 2.15)

$$W(S)Cl_4 + (Me_3Si)_2S \longrightarrow \underset{(8)}{W(S)_2Cl_2} + 2Me_3SiCl \qquad (2.15)$$

Full characterising data for (8) has not previously been available despite its reported preparation by Multani[41] and Fowles[42]. Infrared spectroscopy indicates the presence of a terminal (W=S) moiety with a strong sharp absorption band at 538 cm^{-1} and bands at 365 cm^{-1}, 321 cm^{-1} and 287 cm^{-1} are normal for W-Cl stretches. The mass spectrum gives an envelope at m/z 318 assignable to $[M]^+$ (^{32}S, ^{35}Cl, ^{184}W) with daughter fragments at m/z 286, 251 and 216 corresponding to $[M-S]^+$, $[M-S,Cl]^+$ and $[M-S_2,Cl]^+$ respectively.

$Mo(S)Cl_3$ is prepared by the reaction of molybdenum pentachloride with $(Me_3Si)_2S$ in dichloromethane solvent at *ca.*-78°C. Compound (9) was found to be similar in all respects to the previously reported $Mo(S)Cl_3$[42] (Table 2.1).

2.2.4 Reaction of $W(O)Cl_4$ and $Mo(O)Cl_4$ with $(Me_3Si)_2S$: *Synthesis of the Mixed Oxosulphidohalide Compounds $W(O)(S)Cl_2$ (10) and $Mo(O)(S)Cl_2$ (11).*

The successful application of $(Me_3Si)_2Y$ reagents to the synthesis of $W(O)Cl_4$ (1) and $W(S)Cl_4$ (7) under relatively mild conditions prompted us to investigate syntheses of the mixed oxosulphidohalide compounds $W(O)(S)Cl_2$ and $Mo(O)(S)Cl_2$

using a similar strategy. $W(O)(S)Cl_2$ has previously been reported[42,51] although no characterising data are available. $Mo(O)(S)Cl_2$ is hitherto unknown.

We envisaged that $W(O)(S)Cl_2$ would be most readily accessible by treatment of $W(S)Cl_4$ with $(Me_3Si)_2O$ (Equation 2.16) rather than $W(O)Cl_4$ with $(Me_3Si)_2S$ since hexamethyldisilthiane has been used on previous occasions to exchange oxo for sulphido ligands[52, 53]. In the event our concerns were unfounded as $W(O)(S)Cl_2$ may be prepared by either permutation, presumably due to the low temperature conditions employed (oxide for sulphide exchange invariably requires prolonged reaction at room temperature)[53].

$$W(S)Cl_4 + (Me_3Si)_2O \longrightarrow \underset{(10)}{W(O)(S)Cl_2} + 2Me_3SiCl \quad (2.16)$$

Thus chilled (*ca.*-78°C) solutions of either tungsten oxide tetrachloride or tungsten sulphide tetrachloride in dichloromethane solvent reacted readily with equimolar amounts of $(Me_3Si)_2S$ or $(Me_3Si)_2O$ respectively to yield colourless solutions and in both cases an identical pale brown solid. The solid was characterised as $W(O)(S)Cl_2$ (10) by elemental analysis, infrared and mass spectroscopies (Table 2.3). The infrared spectrum reveals a characteristic $\upsilon(W=S)$ stretching vibration at 540 cm^{-1} and the $\upsilon(W-Cl)$ vibrations are found between 420-340 cm^{-1}. Significantly, a strong broad absorption at 815 cm^{-1} may be assigned to the stretching vibrations of bridging oxo ligands. No bands in the region 850-1000 cm^{-1} attests to the absence of terminal oxo ligands. The formation of a W-O-W bridge rather than a W-S-W bridge between neighbouring units of $W(O)(S)Cl_2$ is directly comparable to the difference in structure between $W(O)Cl_4$ (oxygen bridged polymer)[54] and $W(S)Cl_4$ (weakly chlorine bridged dimer with terminal sulphur)[38]. Similar preferences are also seen in the molecular species $W(S)Cl_4 \cdot W(O)(S)Cl_2 \cdot [CH_3OCH_2]_2$ arising from the reaction of $W(S)Cl_4$ with $[CH_3OCH_2]_2$[51] (Figure 2.1). Mass spectroscopy (EI) reveals an envelope at m/z 304 corresponding to $[M]^+$ with daughter fragments at m/z 269, m/z 253, m/z 237, m/z 218 and m/z 198 corresponding to $[M-Cl]^+$, $[M-O,Cl]^+$,$[M-S,Cl]^+$,$[M-O,Cl_2]^+$and $[M-S,Cl_2]^+$ respectively (Figure 2.2).

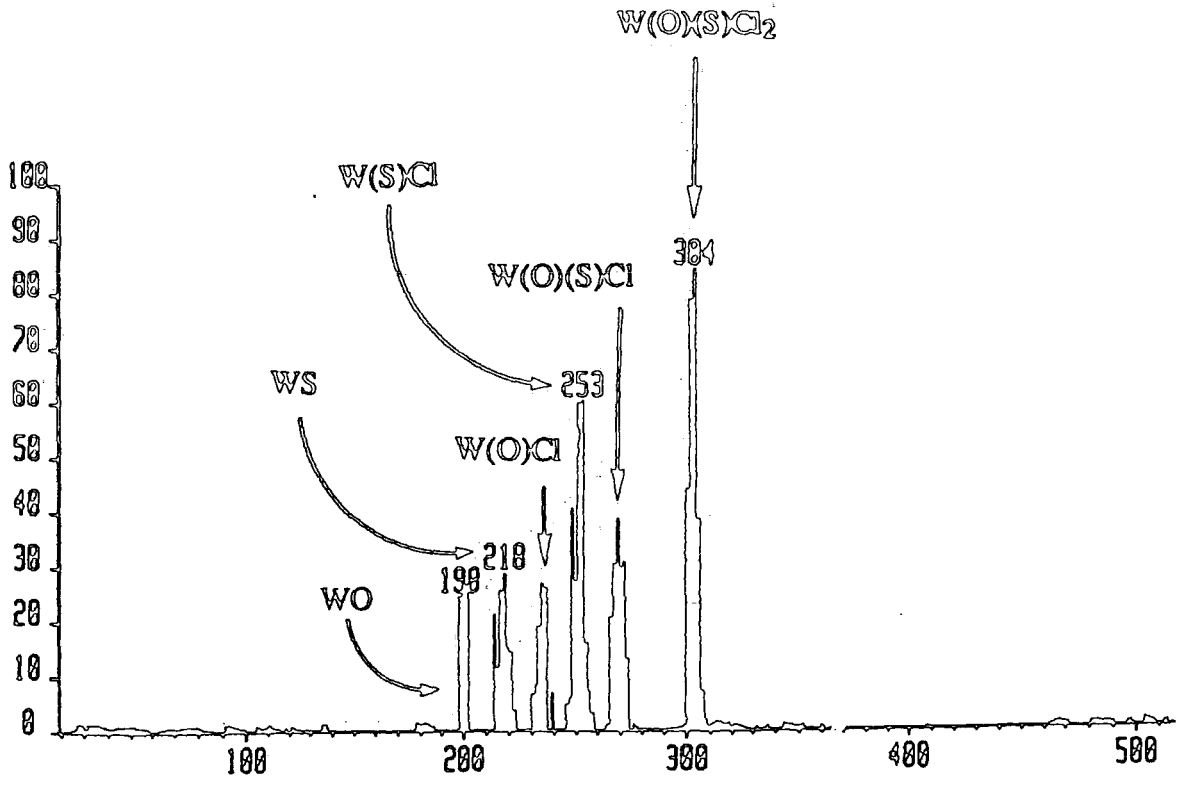

Figure 2.2, *Mass spectrum of W(O)(S)Cl$_2$ (10) (m/z, EI, 70eV, ^{184}W, ^{35}Cl, ^{32}S).*

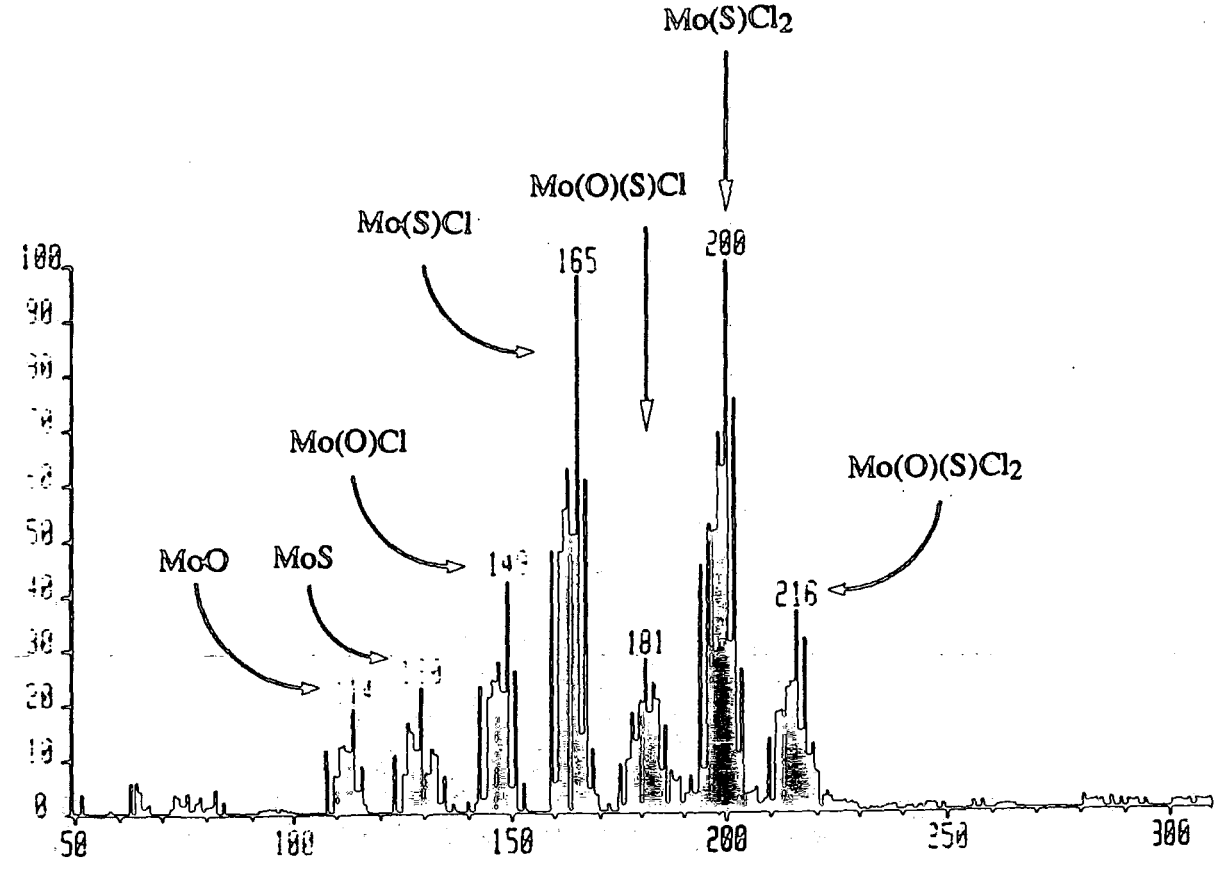

Figure 2.3, *Mass spectrum of Mo(O)(S)Cl$_2$ (11) (m/z, EI, 70eV, ^{96}Mo, ^{35}Cl, ^{32}S).*

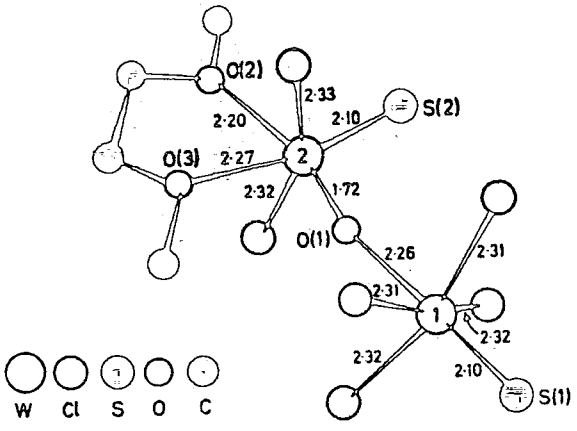

Figure 2.1, *Molecular structure of* $W(S)Cl_4 \cdot W(O)(S)Cl_2 \cdot [CH_3OCH_2]_2$.

The synthesis of $Mo(O)(S)Cl_2$ (11) was best carried out using carbon disulphide solvent. Thus, when a chilled (*ca.*-30°C) carbon disulphide solution of $(Me_3Si)_2S$ was added dropwise to a stirred solution of $Mo(O)Cl_4$ in CS_2, an immediate reaction ensued resulting in a colourless solution and precipitation of a light brown amorphous solid. The solid was subsequently characterised as the previously unreported compound $Mo(O)(S)Cl_2$ (11) by elemental analysis, infrared and mass spectroscopies. In particular, the stoichiometry of Cl_2OSMo was established by microanalysis.

(see Table 2.3). The infrared spectrum reveals a characteristic υ(Mo=O) stretching vibration at 982 cm^{-1} and the υ(Mo-Cl) vibrations are found between 480-250 cm^{-1}. No bands in the region 500-600 cm^{-1} attests to the absence of terminal sulphide ligands. It is reasonable therefore to assume that the structure of $Mo(O)(S)Cl_2$ (11) contrasts that found for $W(O)(S)Cl_2$ (10), that is the bridging/terminal bonding modes of the O and S groups are reversed. This is also consistent with the observed preference found in $Mo(O)Cl_3$[55,56] and $W(O)Cl_4$[54]. The former has a terminal oxo ligand whereas the latter does not. Mass spectroscopy (EI) reveals an envelope at m/z 214 corresponding to $[M]^+$ with daughter fragments at m/z 198, m/z 179, m/z 163, m/z 147, m/z 128 and m/z 112 corresponding to $[M\text{-}O]^+$, $[M\text{-}Cl]^+$,$[M\text{-}O,Cl]^+$,$[M\text{-}S,Cl]^+$,$[M\text{-}O_2,Cl_2]^+$ and $[M\text{-}S_2,Cl]^+$ respectively (Figure 2.3).

2.2 Synthesis and Characterisation of Oxo- and Sulphido-Halide Compounds of Niobium and Tantalum.

Compounds (12-24) have been characterised by elemental analysis, infrared and mass spectroscopies. Some of this data is summarised in table 2.4. Mass spectra for $Nb(S)Cl_3$ (20) and $Ta(S)Cl_3$ (27) are shown in figures 2.4 and 2.5.

2.3.1 Reaction of $NbCl_5$ and $NbBr_5$ with $(Me_3Si)_2O$:

Synthesis of $Nb(O)Cl_3$ (12), $Nb(O)Cl_3(CH_3CN)_2$ (13 $Nb(O)Cl_3(THF)_2$ (14), $Nb(O)Br_3$ (15), $Nb(O)Br_3(CH_3CN)_2$ (16) and $Nb(O)Br_3(THF)_2$ (17).

$Nb(O)Cl_3$ (12) may be synthesised directly in high yield (*ca.*75%) by the treatment of niobium pentachloride with equimolar amounts of $(Me_3Si)_2O$ in 1,2-dichloroethane solvent at 80°C for 4.5h. according to equation 2.17. The product is deposited as a white amorphous powder. Prolonged exposure to the reaction medium, can result in a darkening of the product with evidence of siloxide species in the infrared spectrum.

$$NbCl_5 + (Me_3Si)_2O \xrightarrow[CH_2Cl_2]{80°C} \underset{(12)}{Nb(O)Cl_3} + 2Me_3SiCl \qquad (2.17)$$

By analogy, treatment of niobium pentabromide with $(Me_3Si)_2O$ in 1,2 dichloroethane solvent gives yellow $Nb(O)Br_3$ (15) in 92% yield.

If these reactions are carried out in acetonitrile solvent at room temperature, colourless crystals of $Nb(O)Cl_3(CH_3CN)_2$ (13) and yellow crystals of $Nb(O)Br_3(CH_3CN)_2$ (16) may be isolated in 95% and 63% yields respectively. Compounds (13) and (16) both exhibit strong absorbtions in the infrared spectrum at 960 cm^{-1} (13) and 953 cm^{-1} (16) which may be assigned to the υ(Nb=O) stretching

No.	Product	Colour	Analysis(%)												Yield %	Infra-red Spectra (cm^{-1})		
			Found						Calculated									
			M	Y	X	C	H	N	M	Y	X	C	H	N		M=Y	M-O-M	M-X
12.	$Nb(O)Cl_3$	White	43.3		49.6				43.2		49.4				75		780(s, br)	414(s, br), 295(s)
13.	$Nb(O)Cl_3(CH_3CN)_2$	Colourless				15.9	2.1	9.4				16.2	2.0	9.4	95	960 (s, br)		370(s, br), 333(s), 250(m)
14.	$Nb(O)Cl_3(THF)_2$	White	22.8		26.3	26.1	4.4		22.8		26.1	26.7	4.5		90	960 (s, sp)		365(s, br), 327(s), 250(m)
15.	$Nb(O)Br_3$	Yellow	26.6		69.2				26.7		68.8				92		750(s,br)	341(m), 309(m, br), 294(s), 269(m)
16.	$Nb(O)Br_3(CH_3CN)_2$	Yellow				11.2	1.4	6.5				11.2	1.4	6.5	63	953 (s, sp)		311(s, sh), 295(s, sh), 275(s, br), 269(m)
17.	$Nb(O)Cl_3(THF)_2$	Yellow	18.9		46.6	20.2	3.3		18.9		48.6	19.5	3.3		56	960 (s)		270(s, br)
18.	$Nb(S)Cl_3$	Grey	39.6	14.1	44.0				40.2	13.9	46.0				87	550 (s, sp)		414(s, sh), 401(s, sh), 394(s, br), 355(m), 292(m)
19.	$Nb_2Cl_8S(CH_2Cl_2)$	Grey	31.9	5.4	61.1	2.0	0.3		31.7	5.5	60.5	2.1	0.3		11			410(m, sh), 390(s, sp), 380(m, sh), 365(w, sh)
20.	$Nb_3S_3Br_8$	lilac	27.3	10.1	62.8				27.5	9.5	63.0				90			310(m, sh), 298(m, sh), 280(s, br), 258(m, sh), 255(m, sh)
21.	$Nb(S)Cl_3(CH_3CN)_2$	Yellow	29.9	10.1	32.9	15.1	2.0	8.1	29.7	10.2	33.9	15.3	1.9	8.9	65	523 (s, sp)		379(m, sh), 370(m, sh), 354(s, sp), 334(s), 316(s, sp), 280(m)
22.	$Nb(S)Br_3(CH_3CN)_2$	Yellow	20.8	7.6	54.2	10.7	1.4	6.4	20.2	7.2	53.7	10.8	1.4	6.3	93	527 (s,sp)		351(m), 326(m), 260(s, br)
23.	$Nb(S)Cl_3(THF)_2$	Yellow	25.0	8.5	28.4	25.5	4.3		24.7	8.5	28.3	25.6	4.3		50	529 (s, sp)		352(s, br), 319(s, sh)
24.	$Ta(S)Cl_3$	Orange	56.7	11.3	31.1				56.7	10.0	32.9				82	460 (s, sp)		413(m, sh), 380(s, sh), 330(m, sh), 319(m), 279(m)

Table 2.4, *Characterising Data for Compounds (12-24).*

vibration of a terminal oxo ligand bound to niobium[41]. These contrast with the bridging oxo ligands in polymeric $Nb(O)Cl_3$[57] which give an absorbtion at 780 cm^{-1}. Compounds (13) and (16) are very sensitive to moisture. Thus exposure to air for *ca.* 30 sec. resulted in complete decomposition and the formation of an oxo-bridged species as evidenced by the presence of strong, broad absorbtions between 600-900 cm^{-1} in the infrared spectrum. $Nb(O)Cl_3(CH_3CN)_2$ has previously been prepared by dissolving $Nb(O)Cl_3$ in acetonitrile[58]. The molecular structure of (13) showed it to be monomeric with a cis-meridional arrangement of acetonitrile and chloro ligands (Figure 2.6) . It is reasonable to assume, based on the available data that (16) will be isostructural.

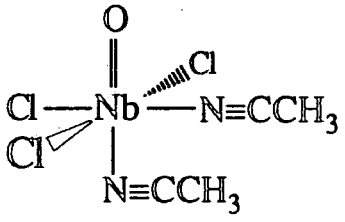

Figure 2.6, *Molecular structure of* $Nb(O)Cl_3(CH_3CN)_2$ *(13).*

Attempts to prepare the THF adduct of $Nb(O)Cl_3$ and $Nb(O)Br_3$ by analogous treatment of $NbCl_5$ and $NbBr_5$ with $(Me_3Si)_2O$ in THF solvent did not afford $Nb(O)Cl_3(THF)_2$ (14) and $Nb(O)Br_3(THF)_2$ (17) cleanly. Instead (14) and (17) were obtained in 90% and 56% yields respectively by the dissolution of (13) and (16) in THF. $Nb(O)Cl_3(THF)_2$ may be obtained as colourless crystals upon addition of cold petroleum ether to the oily residue formed upon removal of solvent. Similar treatment produced $Nb(O)Br_3(THF)_2$ as yellow crystals. Infrared spectroscopy revealed, for both compounds, a strong absorbtion at 960 cm^{-1} which is consistent with a terminal (Nb=O) moiety[57], and the similarity of the niobium-chlorine stretching frequencies below 400 cm^{-1} suggests that (13), (14), (16) and (17) are likely to be isostructural. Complexes (14), (16) and (17) have not been reported previously although the existence of $Nb(O)Cl_3(OEt_2)_2$ in solution was proposed on the basis of solution

infrared measurements [965 cm^{-1}, υ(Nb=O)][59]. The preparations of (13), (14), (16) and (17) are summarised in scheme 2.1.

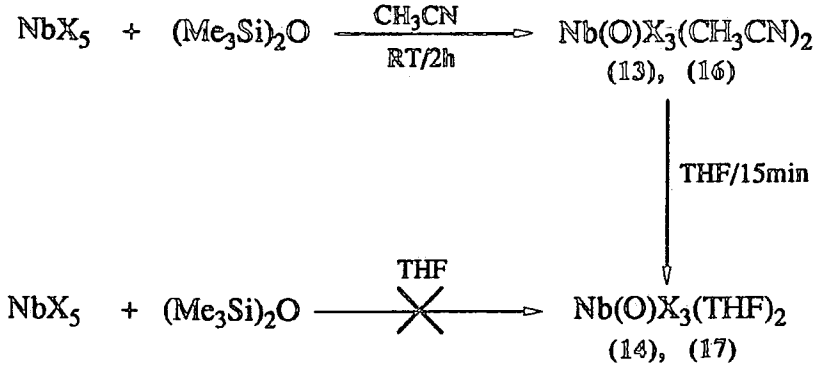

Scheme 2.1, *Synthesis of (13), (14), (16) and (17).*

2.3.2 Reaction of $NbCl_5$, $NbBr_5$ and $TaCl_5$ with $(Me_3Si)_2S$:

Synthesis of $Nb(S)Cl_3$ (18), $Nb_2(S)Cl_8(CH_2Cl_2)$ (19), $Nb(S)Cl_3(CH_3CN)_2$ (21), $Nb(S)Cl_3(THF)_2$ (23), $Nb_3S_3Br_8$ (20), $Nb(S)Br_3(CH_3CN)_2$ (22) and $Ta(S)Cl_3$ (24).

Niobium pentachloride reacts readily with equimolar amounts of $(Me_3Si)_2S$ in dichloromethane solvent at *ca.*-78°C over a period of 30min. leading to deposition of $Nb(S)Cl_3$ (18) in the form of a grey, moisture sensitive amorphous solid in 87% yield. Filtration of the supernatant solution followed by concentration and cooling to *ca.*-78°C also afforded a second grey, moisture and thermally sensitive crystalline compound, $Nb_2(S)Cl_8(CH_2Cl_2)$ (19) in 11% yield. Compound (18) is spectroscopically identical to previously reported $Nb(S)Cl_3$[41] which in pure form is yellow. The $Nb(S)Cl_3$ prepared in this reaction is slightly impure, although the small amount of grey contaminant, possibly arising from the decomposition of (19) (*vide infra*), does not adversely affect subsequent derivatisation of (18). If the synthesis of $Nb(S)Cl_3$ (18) is performed in CS_2 solvent the product is found to be lighter in colour and of a higher purity as shown by elemental analysis. This is the experimental procedure reported in section 7.2. Compound (19) was hitherto unknown and has been characterised by

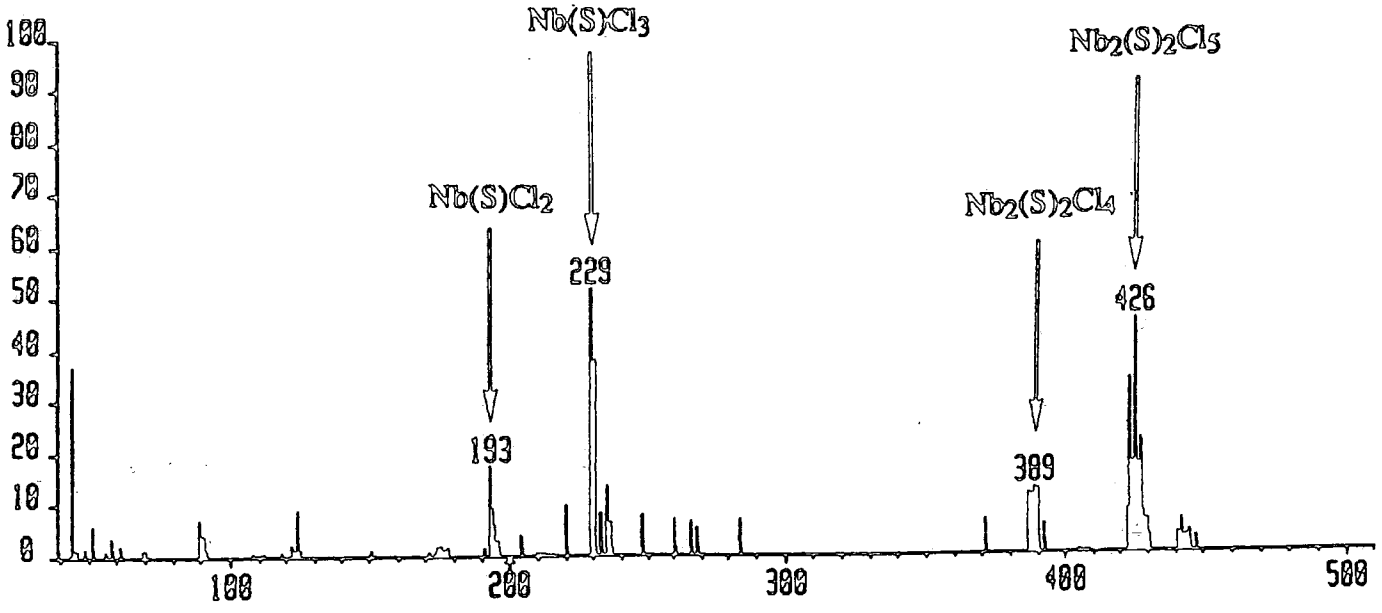

Figure 2.4, *Mass spectrum of Nb(S)Cl3 (18) (m/z, EI, 70eV, ^{93}Nb, ^{35}Cl, ^{32}S).*

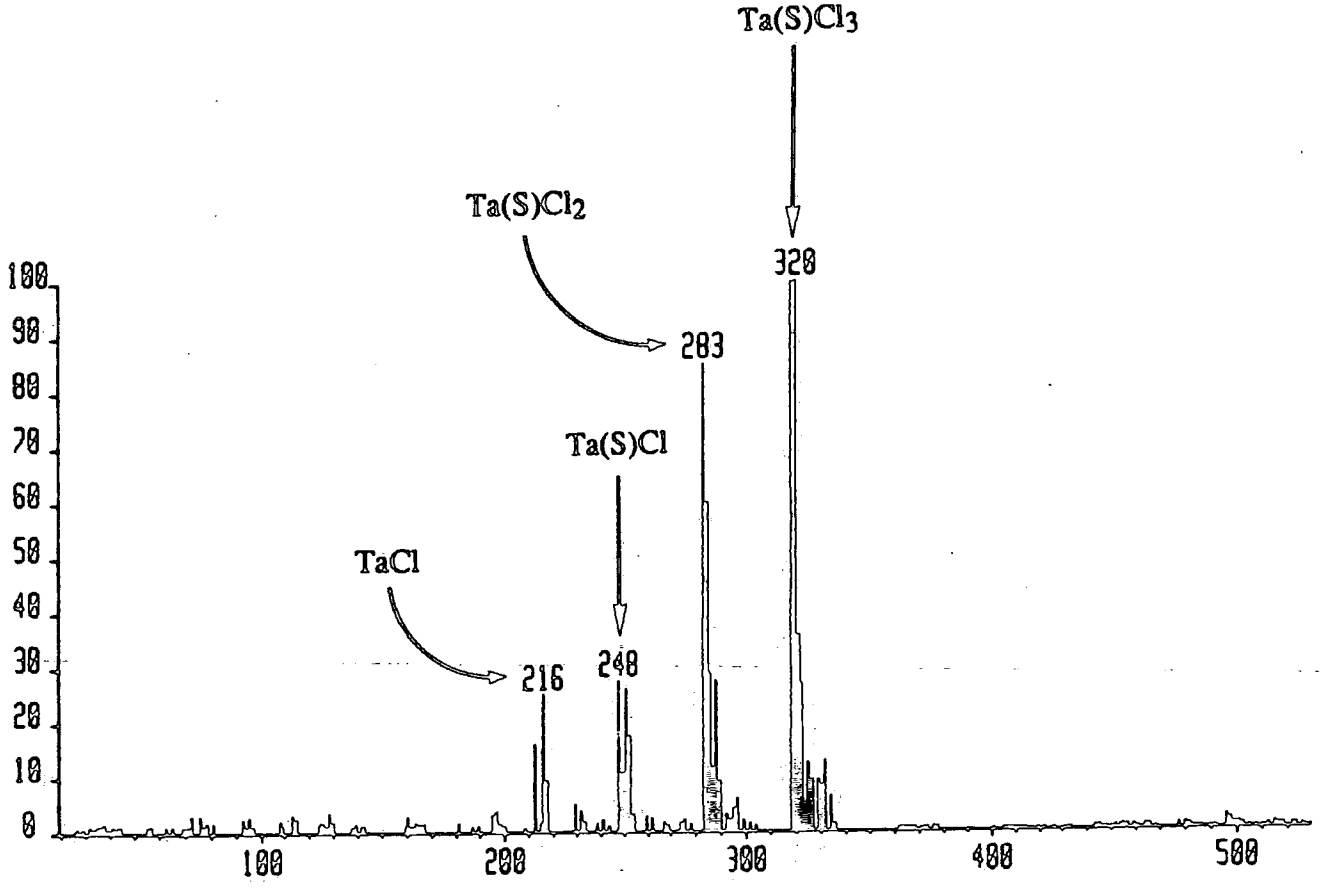

Figure 2.5, *Mass spectrum of Ta(S)Cl3 (24) (m/z, EI, 70eV, ^{181}Ta, ^{35}Cl, ^{32}S).*

elemental analysis, infrared and ^1H NMR spectroscopy (Table 2.4). In particular, the stoichiometry of $CH_2Cl_{10}SNb_2$ was established by microanalysis:

Found (Required): %Nb, 31.9 (31.7); %S, 5.4 (5.5); %Cl, 61.1 (60.5)
%C, 2.0 (2.1); %H, 0.3 (0.3)

(19) is presumed to be unstable in solution since a 250 MHz ^1H NMR spectrum (d^6-benzene) gives a singlet resonance at δ 5.28 attributable to the 2 methylene hydrogens of free dichloromethane and a grey amorphous precipitate is in evidence. The infrared spectrum of (19) reveals characteristic υ(Nb-Cl) vibrations between 410-360 cm^{-1} but no bands between 500-600 cm^{-1}, the region typical for terminal Nb=S linkages. Since the stoichiometry indicates a S : Nb ratio of 1: 2 it is reasonable to propose a Nb-S-Nb linkage. Unfortunately (19) was not sufficiently stable in hydrocarbon solvents for molecular weight measurements but on the basis of the established stoichiometry and its apparent solubility in dichloromethane, a binuclear structure for (19) containing one bridging sulphur ligand is favoured as shown in figure 2.7.

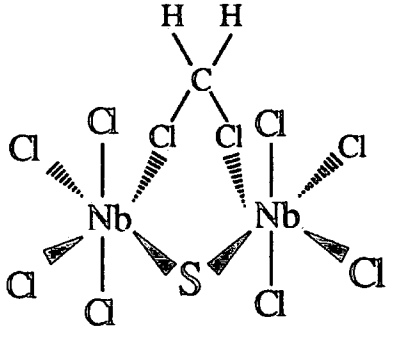

Figure 2.7, *Proposed structure of* $Nb_2(S)Cl_8(CH_2Cl_2)$ *(19).*

Attempts to prepare $Nb(S)Br_3$ by analogous treatment of $NbBr_5$ with $(Me_3Si)_2S$ in dichloromethane solvent were unsuccessful. Instead treatment of niobium pentabromide with $(Me_3Si)_2S$ in CH_2Cl_2 at *ca* .-78°C, afforded a clear purple solution from which lilac crystals of $Nb_3S_3Br_8$ (20) were isolated in 90% yield. Compound (20) is formulated as a cluster compound (Figure 2.8) by analogy to the

(20) is formulated as a cluster compound (Figure 2.8) by analogy to the reported red-brown $Nb_3S_3Cl_8$[60].

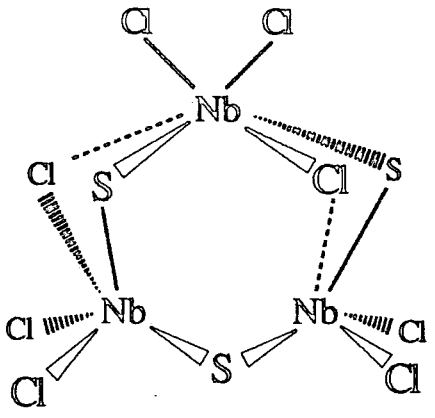

Figure 2.8, *Proposed structure of $Nb_3S_3Cl_8$ (20).*

Mass spectrometry provides some support for a cluster formulation with decomposition fragmentation ions at m/z 682, m/z 650, m/z 365, and m/z 317 corresponding to $[Nb_2S_3Br_5]^+$, $[Nb_2S_2Br_5]^+$, $[NbSBr_3]^+$ and $[NbS_2Br_2]^+$ respectively. $Nb_3S_3Br_8$ and $Nb_3S_3Cl_8$ appear to originate from the disproportionation of the metal sulphidohalide although the greater propensity for the bromide to decompose completely to the cluster in favour of the tribromide sulphide is unclear.

Treatment of niobium pentachloride or niobium pentabromide with $(Me_3Si)_2S$ in acetonitrile solvent at room temperature, afforded yellow crystals of $Nb(S)Cl_3(CH_3CN)_2$ (21) and $Nb(S)Br_3(CH_3CN)_2$ (22) which were isolated in 65% and 93% yields respectively. Compounds (21) and (22) give strong absorptions in the infrared spectrum at 523 cm^{-1} and 527 cm^{-1} respectively which may be assigned to the υ(Nb=S) stretching vibration. These species are likely to be monomeric, octahedral compounds by analogy with $Nb(O)Cl_3(CH_3CN)_2$ (13) and $Nb(O)Br_3(CH_3CN)_2$ (16) which have been proposed to possess a cis-meridional arrangement of acetonitrile and chloro ligands (Figure 2.6).

Dissolution of $Nb(S)Cl_3(CH_3CN)_2$ in tetrahydrofuran afforded a yellow solution, which after filtration, concentration and addition of cold petroleum ether (*ca.*-30°C) yielded yellow crystals of $Nb(S)Cl_3(THF)_2$ (23). A strong absorption in the infrared spectrum at 529 cm^{-1} is characteristic of a terminal sulphide ligand and the similarity between the υ(Nb-Cl) stretching vibrations for (23) and $Nb(O)Cl_3(THF)_2$ (14) suggest that they are isostructural.

Tantalum pentachloride reacts readily with equimolar amounts of $(Me_3Si)_2S$ in either dichloromethane or carbon disulphide solvent at *ca.*-78°C over a period of 30 min. leading to dissolution of the $TaCl_5$ to afford a clear yellow solution. Warming to room temperature and stirring overnight gave a colourless solution and an orange amorphous solid whose spectroscopic data agree in all respects to the previously reported $Ta(S)Cl_3$ (24) (Table 2.4). The $Ta(S)Cl_3$ produced when dichloromethane is employed as the reaction medium is frequently contaminated with a minor product which discolours the $Ta(S)Cl_3$ but does not significantly affect its purity or prove troublesome in subsequent transformations.

2.4 Reaction of Metal Halides with Me_3SiYR (R = Me, Et, $SiMe_3$) Mechanistic Considerations.

2.4.1 General Aspects.

The reaction of a metal halide with Me_3SiYR (R = Me, Et, $SiMe_3$) reagents is presumed to proceed according to scheme 2.2 in which an initial ether or sulphidoether) adduct eliminates RCl to give an intermediate alkoxide (or thiolate) which undergoes a further elimination to the oxo or sulphidohalide product.

$$MCl_n + Me_3SiYR \longrightarrow [Cl_nMYR(SiMe_3)]$$

$$[Cl_nMYR(SiMe_3)] \longrightarrow MCl_{n-1}YR + Me_3SiCl$$

$$MCl_{n-1}YR \longrightarrow M(Y)Cl_{n-2} + RCl$$

Scheme 2.2, *Reaction of metal halides with silylethers and thioethers.*

We have attempted to verify this reaction pathway by isolating some of the key intermediates. Cowley and Fairbrother have described the diethylether adducts $MCl_5{\cdot}OEt_2$ (M = Nb, Ta) and demonstrated that they decompose to the oxotrichlorides with condensation of EtCl (Equation 2.18). The alkoxide intermediate, however is not observed in this reaction.

$$MCl_5.OEt_2 \xrightarrow[\text{Reduced pressure}]{\Delta} M(O)Cl_3 + 2EtCl \qquad (2.18)$$

M=Nb; 90°C; 3.5h
M=Ta; 65°C; 17h

The diethyl ether adducts are likely to be analogous to the initial interaction of $(Me_3Si)_2O$ with MCl_5, although in the latter case these adducts are not sufficiently stable for isolation.

Nevertheless, it has proved possible to obtain a single crystal of $NbCl_5(OEt_2)$ and confirm it's structure by X-ray crystallography. The crystal was grown by T.P. Kee in this laboratory and the crystal data analysis confirms the octahedral geometry and interaction of Et_2O with the niobium centre (Figure 2.9). The full crystallographic data is given in appendix 1A and selected bond distances and angles are given in table 2.6.

The compound has the stoichiometry $NbCl_5(OEt_2)$ and is monomeric, the niobium atom occupying the centre of the octahedron. The diethyl etherate ligand lies trans to a slightly elongated Nb–Cl bond and at a distance of 2.194(7) Å from the niobium atom. The (Nb–O) bond length is typical of niobium-oxygen dative covalent

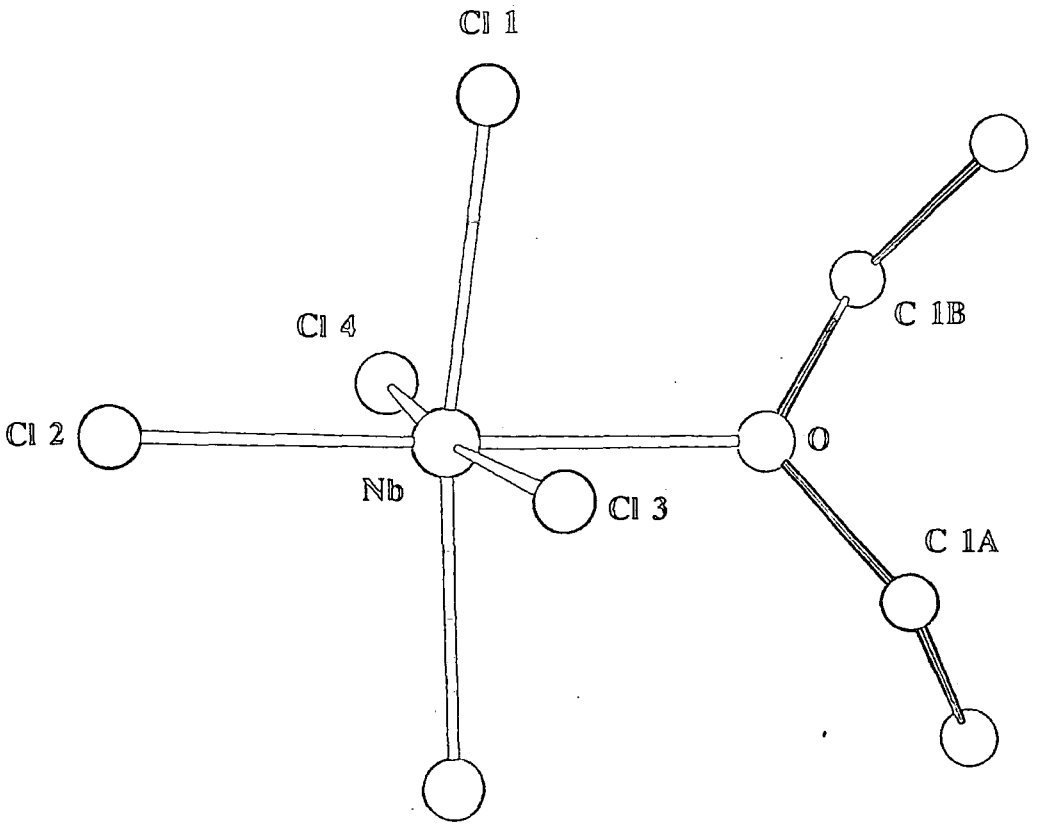

Figure 2.9, *Molecular structure of $NbCl_5(OEt_2)$.*

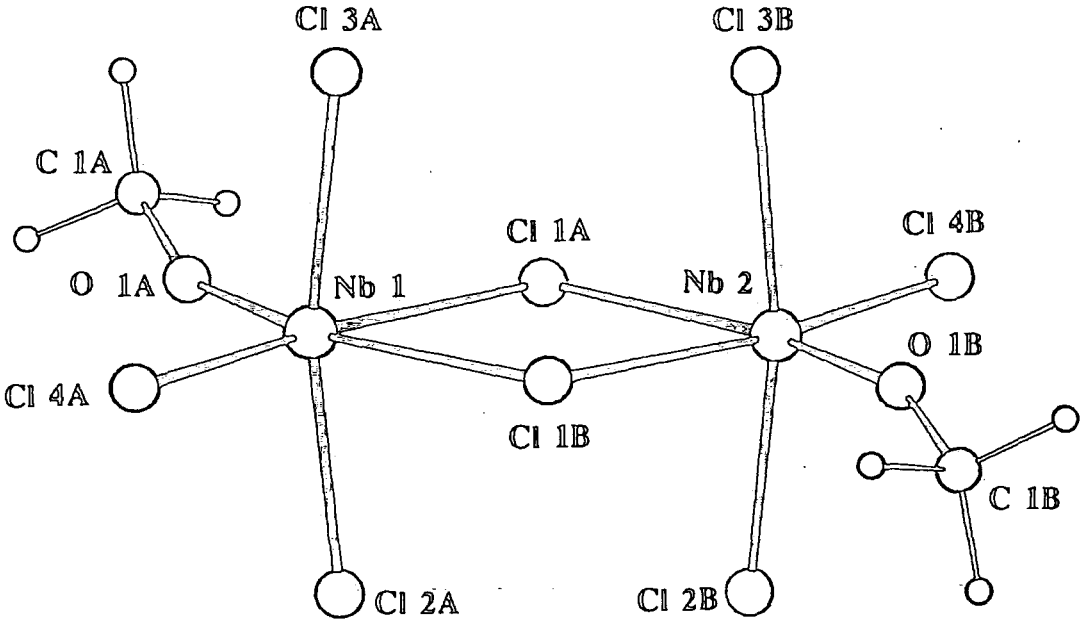

Figure 2.10, *Molecular structure of $[NbCl_4(OMe)]_2$.*

Nb - Cl (1) 2.312 (2)
Nb - Cl (2) 2.267 (4)
Nb - Cl (3) 2.325 (3)
Nb - Cl (4) 2.315 (4)

Nb - O 2.194 (7)

Cl (1) - Nb - Cl (3) 89.2 (1)
Cl (1) - Nb - Cl (4) 90.1 (1)
Cl (2) - Nb - Cl (3) 95.9 (1)
Cl (2) - Nb - Cl (4) 94.4 (1)
Cl (3) - Nb - Cl (2) 93.9 (1)
Cl (3) - Nb - Cl (4) 169.7 (1)

O - Nb - Cl (1) 86.1 (1)
O - Nb - Cl (2) 179.6 (1)
O - Nb - Cl (3) 84.5 (2)
O - Nb - Cl (4) 85.2 (2)

Nb - O - C (1A) 123.8 (6)
Nb - O - C (1B) 122.6 (7)

C (1A) - O - C (1B) 113.6 (10)

C (2) - C (1A) - O 112.5 (10)
C (2) - C (1B) - O 111.6 (10)

Table 2.5, *Selected bond distances (Å) and angles (°) for* $NbCl_5(OEt_2)$.

Nb (1) - Nb (2) 3.970(1)

Nb (1) - Cl (1a) 2.552(2)
Nb (1) - Cl (1b) 2.585(2)
Nb (1) - Cl (2a) 2.332(3)
Nb (1) - Cl (3a) 2.317(3)
Nb (1) - Cl (4a) 2.296(3)

Nb (1) - O (1a) 1.785(6)

Nb (2) - Cl (1a) 2.578(2)
Nb (2) - Cl (1b) 2.541(2)
Nb (2) - Cl (2b) 2.313(3)
Nb (2) - Cl (3b) 2.328(3)
Nb (2) - Cl (4b) 2.303(3)

Nb (2) - O (1b) 1.781(6)

Nb (1) - Cl (1a) -Nb(2) 101.4 (1)
Nb (1) - Cl (1b) -Nb(2) 101.5 (1)
Cl (2a) - Nb (1) -Cl(1a) 87.3 (1)
Cl (3a) - Nb (1) -Cl(1a) 86.7 (1)
Cl (3a) - Nb (1) -Cl(2a) 168.3 (1)
Cl (4a) - Nb (1) -Cl(1a) 169.8 (1)
Cl (4a) - Nb (1) -Cl(2a) 92.4 (1)
Cl (4a) - Nb (1) -Cl(3a) 91.8 (1)
Cl (1b) - Nb (1) -Cl(1a) 78.3 (1)
Cl (1b) - Nb (1) -Cl(2a) 84.3 (1)
Cl (1b) - Nb (1) -Cl(3a) 84.5 (1)
Cl (1b) - Nb (1) -Cl(4a) 91.4 (1)

O (1a) - Nb (1) -Cl(1a) 86.5 (2)
O (1a) - Nb (1) -Cl(2a) 92.4 (2)
O (1a) - Nb (1) -Cl(3a) 97.3 (2)
O (1a) - Nb (1) -Cl(4a) 103.7 (2)
O (1a) - Nb (1) -Cl(1b) 164.7 (2)

Cl (1b) - Nb (2) -Cl(1a) 78.7 (1)
Cl (2b) - Nb (2) -Cl(1a) 85.1 (1)
Cl (2b) - Nb (2) -Cl(1b) 87.5 (1)
Cl (3b) - Nb (2) -Cl(1a) 85.3 (1)
Cl (3b) - Nb (2) -Cl(1b) 86.4 (1)
Cl (3b) - Nb (2) -Cl(2b) 169.4 (1)
Cl (4b) - Nb (2) -Cl(1a) 90.8 (1)
Cl (4b) - Nb (2) -Cl(1b) 169.4 (1)
Cl (4b) - Nb (2) -Cl(2b) 93.2 (1)
Cl (4b) - Nb (2) -Cl(3b) 91.1 (1)

O (1b) - Nb (1) -Cl(1a) 165.8 (2)
O (1b) - Nb (2) -Cl(1b) 87.2 (2)
O (1b) - Nb (2) -Cl(2b) 92.4 (2)
O (1b) - Nb (2) -Cl(3b) 95.9 (2)
O (1b) - Nb (2) -Cl(4b) 103.3 (2)

C(1a) - O(1a) - Nb(1) 157.1 (7)
C(1b) - O(1b) - Nb(2) 159.1 (7)

Table 2.6, *Selected bond distances (Å) and angles (°) for* $[NbCl_4(OMe)]_2$.

bonds as, for example, in $[Cp'NbCl_3(H_2O)]_2(\mu\text{-}O)$ where $[Nb\text{-}O(H_2O)]$ is 2.19 Å [Cp' = C_5H_4Me].

Although $NbCl_5(OEt_2)$ converts to $Nb(O)Cl_3$ upon warming in the solid state at 90°C, the intermediate ethoxide cannot be observed unambiguously. T.P.Kee[61] studied the decomposition of $TaCl_5 \cdot OEt_2$ and found that it decomposes in d-chloroform at 60°C to give EtCl and broad, poorly resolved ^1H NMR signals at δ 5.56 and δ 5.43 which are assignable to the methylene hydrogens of tantalum ethoxide species. The anticipated $[TaCl_4(OEt)]_n$ intermediate could not be identified unambiguously. However, it has proved possible to isolate intermediates of this kind by treatment of $NbCl_5$ with Me_3SiOR (R = Me, Et) at room temperature. The methoxide product $NbCl_4(OMe)$ was initially formulated as a dimeric species on the basis of infrared and mass spectrometry[62]. The infrared spectrum gives bands at 600 cm^{-1} and 595 cm^{-1} indicative of terminal methoxide ligands in contrast to the structure proposed for $[NbCl_4(OPh)]_2$[63] in which phenoxide bridges prevail. The preference for terminally coordinated MeO may be attributed to its enhanced π donating ability over OPh. Strong π donating ligands have also been shown to prefer terminal coordination in other bio-octahedral complexes; $[W(O)(OMe)_4]_2$[64] is such an example.

The molecular structure of $[NbCl_4(OMe)]_2$ has been determined by Dr. M. McPartlin and coworkers at the Polytechnic of North London (Appendix 1B) and the results are discussed below. The molecular structure is illustratred in figure 2.10 and selected bond distances and angles are given in table 2.6.

The compound is dimeric, with an edge shared biooctahedral geometry. The niobium atoms, occupying the centres of the octahedra, are joined by two chloride bridges and possess a terminal methoxide ligand on each niobium atom. Each metal atom is pentavalent and consequently direct metal-metal bonds are not required to interpret the structure. Consistently, the metal-metal distance of 3.970(1) Å [Nb(1) - Nb(2)] is significantly longer than those normally found in (Nb-Nb) bonded systems (typically *ca.* 2.7 - 3.0 Å)[64]. A consideration of the two bridging Cl ligands [Cl(1a) and Cl(1b)] shows them to bridge in an angular manner with Nb(1)-Cl(1a)-Nb(2) and

Nb(1)-Cl(1b)-Nb(2) angles of 101.4(1)° and 101.5(1)° respectively. Each bridge is asymmetrical with Nb(1)-Cl(1a) =2.552(3)Å and Nb(2)-Cl(1a) = 2.578(2) due to the strongly π-donating OMe group. These values maybe compared with the average (Nb-μ_2-Cl) distances of 2.555(2)Å in Nb_2Cl_{10}[65]. The Nb(1)-Cl(1a)-Nb(2) angle of 101.4(1)° is also comparable to the Nb(1)-Cl(1a)-Nb(2) angle of 101.3(1)° in Nb_2Cl_{10}. Also, the terminal Nb-Cl bonds trans to the shortened Nb-Cl bridge bonds are, on average, 0.023(3)Å longer than the terminal Nb-Cl bond cis to the bridge.

The terminal methoxide ligands lie trans to the lengthened Nb-Cl bridge bond. The large C(1a)-O(1a)-Nb(1) and C(1b)-O(1b)-Nb(2)O-Nb-C bond angles of 157.1(7)° and 159.1(7)° respectively coupled with the extremely short terminal niobium-oxygen bonds (av. 1.783(6)Å) provides further evidence for a significant π contribution to the bonding. Indeed, these niobium-oxygen distances are closer to the range anticipated for double bonds (typically 1.63-1.75Å eg.$Nb(O)Cp_2[C_7H_5(CF_3)_2]$[66] and $[Nb(O)F_5]^{2-}$ $[N_2H_6]^{2+}$ [67]) than those for Nb-OR groups which fall in the range 1.87-1.91Å eg. $Nb_2(OMe)_{10}$[68] and $Nb(O)Cl_2(OEt)bipy$[69].

On heating to 80°C in dichloromethane, $[NbCl_4(OMe)]_2$ undergoes elimination of RCl to give white $Nb(O)Cl_3$. The ethoxide derivative $[NbCl_4(OEt)]_2$, which would be the anticipated intermediate in the formation of $Nb(O)Cl_3$ from $NbCl_5(OEt_2)$, undergoes a similar decomposition reaction. Elimination of EtCl from this species occurs at 70°C over 6h., conditions less forcing than for formation of $Nb(O)Cl_3$ directly from $NbCl_5(OEt_2)$. This suggests that the elimination of the 2nd equivalent of EtCl occurs at a lower temperature than for the first and therefore may explain why the intermediate ethoxide cannot be observed during the conversion of $NbCl_5$ to $Nb(O)Cl_3$.

A schematic illustration of the reaction between $NbCl_5$ and Me_3SiOMe is shown in scheme 2.3. In CH_2Cl_2 solution, bioctahedral Nb_2Cl_{10} exists in equilibrium with monomeric $NbCl_5$ which binds Me_3SiOMe to give the ether adduct. Either an inter-or intramolecular elimination of Me_3SiCl will afford $NbCl_4OMe$ which, in solution, most probably exists in a monomer-dimer equilibrium *c.f.* $NbCl_5$. Either the monomer or dimer may eliminate RCl in an intra or intermolecular fashion to give the oxohalide

product. Which path is followed will have an influence on the nature of the growing oxohalide lattice. The observation of residual Me_3SiO groups, especially in the pyrolosis of $TaCl_5/(Me_3Si)_2O$ is consistent with a stepwise condensation process.

The thioether adducts and thiolate intermediates eliminate Me_3SiCl more readily than their oxide counterparts for thermodynamic reasons (*vide infra*) and this may lead to alternative reaction pathways e.g. in the reaction of $NbCl_5$ with $(Me_3Si)_2S$, the intermediate $NbCl_4(SSiMe_3)$ appears also to react with the starting halide to afford $Nb_2Cl_9(SSiMe_3)$ rather than solely self condensation to give $Nb(S)Cl_3$. (Scheme 2.4).

2.4.2 Thermodynamic Considerations.

The thermodynamics of metal chalcogenide formation is dependent upon the energies of the various constituent bonds in the system. While the strengths of Si-X and Si-Y bonds are well known (Table 2.7) those of M-X and M-Y are not.

Bond	D_o	
	KJ mol^{-1}	Kcal mol^{-1}
Si-Cl	381	91
Si-Br	310	74
Si-O	452	108
Si-S	293	70

Table 2.7, *Bond dissociation energies for Si-X and Si-Y X=Cl, Br; Y=O, S.*

For the system shown in equation 2.19, the forward reaction i.e. cleavage of two Si-O bonds and formation of 2Si-Cl bonds is endothermic by 34 Kcal mol^{-1}.

$$MCl_n + (Me_3Si)_2O \underset{}{\overset{\Delta +ve\ 34\ Kcal}{\rightleftharpoons}} M(O)Cl_{n-2} + 2Me_3SiCl \qquad (2.19)$$

The driving force for the formation of $M(O)Cl_{n-2}$ is likely to be not only strongly influenced by the strength of the M-O interaction but also dependent upon the nature of the lattice and whether terminal or bridging oxo ligands predominate. In addition, 2 equivalents of highly volatile Me_3SiCl may result in a favourable entropy factor to drive the reaction to completion. This has considerable support from the observation that, whilst at room temperature the reaction of $W(O)Cl_4$ and $(Me_3Si)_2O$ in CH_2Cl_2 produces an intermediate siloxide species, the same reaction performed at elevated temperature *ca.* 80°C in octane produces analytically pure $W(O)_2Cl_2$ with no evidence of organic contamination. The strength of the M-O interaction and possibly the influence of an inert oxide lattice is highlighted from the observation that WO_3 will not react, even under rigorous heating, with Me_3SiCl to generate $W(O)_2Cl(OSiMe_3)$ (4) or $W(O)_2Cl_2$ (2).

For the system shown in equation 2.20 , the cleavage of two Si-S bonds and formation of 2Si-Cl bonds is exothermic by 42 Kcal mol^{-1}. This is supported by the observation that reactions of $(Me_3Si)_2S$ with metal halides are noticeably exothermic and proceed rapidly under ambient conditions, thus cooling is required to administer control over the reaction.

$$MCl_n + (Me_3Si)_2S \xrightleftharpoons{\Delta\text{ -ve 42 Kcal}} M(S)Cl_{n-2} + 2Me_3SiCl \qquad (2.20)$$

2.5 Summary.

Treatment of the halides (or oxohalides) of the group 5 and 6 metals with commercially available hexamethyldisiloxane and hexamethyldisilthiane facilitates the introduction of oxygen and sulphur atoms into the metal coordination sphere in a controlled, mild fashion, with minimal risk of product contamination as the sole by-product, Me_3SiCl is volatile and hence readily removed. The pertinent features of this transformation are shown in equation 2.21

$$[M]X_2 + (Me_3Si)_2Y \longrightarrow [M]{=}Y + Me_3SiX \qquad (2.21)$$

X=Cl, Br; Y=O, S; M=Mo, W, Nb, Ta

Both base-free and solvent adducts are accessible using this methodology and the treatment of $NbCl_5$ with silylalkyl ethers has allowed the isolation of key mono-alkoxide niobium intermediates. Thus, the preparations described in this chapter offer ready accessibility to a range of metal oxo- and sulphido-halide materials by rapid solution syntheses and represent a welcome alternative to the well-established hot-tube/furnace procedures.

2.6 References.

1. J.E. Drake and G.W.A. Fowles, *J. Less-Common Metals*, 1960, 2, 401.
2. G.W.A. Fowles and J.L. Frost, *J. Chem. Soc.* (A), 1967, 671.
3. P.C. Crouch, G.W.A. Fowles and R.A. Walton, *J. Inorg. Nucl. Chem.*, 1970, 32, 329.
4. H. Prinz, K. Dehnicke and U. Müller, *Z. Anorg. Allg. Chem.*, 1982, 488, 49.
5. E.R. Epperson and H. Frye, *Inorg. Nucl. Chem. Letts.*, 1966, 2, 223.
6. D.A. Edwards and A.A. Woolf, *J. Chem. Soc.* (A), 1966, 91.
7. A.V. Komandin and D.N. Tarasenkov, *J. Gen. Chem. USSR*, 1940, 10, 1333.
8. A.D. Webb and H.A. Young, *J. Am. Chem. Soc.*, 1950, 72, 3356.
9. H. Hecht, G. Jander and H. Schlapmann, *Z. Anorg. Allg. Chem.*, 1947, 254, 261.
10. S.E. Feil, S.Y. Tyree, F.N. Collier, R.E. McCarley and P.B. Fleming, *Inorg. Synth.*, 1967, 9, 123.
11. a. R. Colton, I.B. Tomkins and P.W. Wilson, *Aust. J. Chem.*, 1964, 17, 496.
    b. R.H. Crabtree and G.G. Hlatky, *Polyhedron*, 1985, 4, 521.
12. A. Michael and A. Murphy, *Am. Chem. J.*, 1910, 44, 382.
13. (a) S.F. Pedersen and R.R. Schrock, *J. Am. Chem. Soc.*, 1982, 104, 7483.
    (b) L.B. Handy, K.G. Sharp and F.E. Brinkman, *Inorg. Chem.*, 1972, 11, 523.
14. F. Zado, *J. Inorg. Nucl. Chem.*, 1963, 25, 1115.
15. S.A. Schhukarev, G.I. Novikov, A.V. Suvorov and A.K. Baev, *Zh. Neorg. Khim.*, 1958, 3, 2630.

16. K. Funaki and K. Uchimura, *Denki Kagaku*, 1962, 30, 35.

17. F. Schroeder, *Naturwissenschaften*, 1965, 52, 389.

18. R. Colton and I.B. Tomkins, *Aust. J. Chem.*, 1965, 18, 447.

19. I.A. Glukhov and S.S. Eliseev, *Russ. J. Inorg. Chem.*, 1963, 8, 50.

20. R.L. Graham and L.G. Helper, *J. Phys. Chem.*, 1959, 63, 723.

21. H.M. Neumann and N.C. Cook, *J. Am. Chem. Soc.*, 1957, 79, 3026.

22. A.N. Zelikman and N.N. Gorovits, *Zh. Obshsh. Khim.*, 1954, 24, 1916.

23. I.A. Glukhov and S.S. Eliseev, *Russ. J. Inorg. Chem.*, 1962, 7, 40.

24. I.A. Glukhov and G.A. Bekhtle, *Trudy. Akad. Nauk. Tadzh. SSR.*, 1958, 35, 84.

25. D.A. Edwards, J. *Inorg. Nucl. Chem.*, 1970, 32, 329.

26. P.C. Crouch, G.W.A. Fowles, I.B. Tomkins and R.A. Walton, *J. Chem. Soc.* (A), 1969, 2412.

27. I.A. Glukhov and S.S. Eliseev, *Izv. Akad. Nauk. Tadzh. SSr.*, 1959, 79.

28. M.L. Larson and F.W. Moore, *Inorg. Chem.*, 1966, 5, 801.

29. C. Djordilevic and V. Katovic, *J. Inorg. Nucl. Chem.*, 1963, 25, 1099.

30. A.H. Cowley, F. Fairbrother and N. Scott, *J. Less-Common Metals*, 1959, 1, 206.

31. D.E. Sands, A. Zalkin and R.F. Elson, *Acta. Crystallogr.*, 1959, 12, 21.

32. H. Hecht, G. Jander and H. Schlapmann, *Z. Anorg. Allg. Chem.*, 1952, 267, 213.

33. H. Schafer and F. Kahlenberg, *Z. Anorg. Allg. Chem.*, 1960, 305, 327.

34. I.S. Morozov and A.I. Morozov, *Russ. J. Inorg. Chem.*, 1966, 11, 182.

35. K. Dehnicke, *Angew. Chem. Int. Ed. Engl.*, 1961, 73, 535.

36. F.A. Cotton, P.A. Kibala and R.B.W. Sandor, *Inorg. Chem.*, 1989, 28, 2485.

37. N.S. Fortunatov and N.I. Timoschenko, *Ukrain. Khim. Khur.*, 1969, 35, 1207.

38. D.A. Britnell, G.W.A. Fowles and D.A. Rice, *J. Chem. Soc. Dalton Trans.*, 1974, 2191.

39. M.G.B. Drew and R. Mandyczewsky, *J. Chem. Soc.* (A), 1970, 2815.

40. A.O. Baghlef and A. Thompson, *J. Less-Common Metals*, 1977, 53, 291.

41. K.M. Sharma, S.K. Anand, R.K. Multani and B.D. Jain, *Chem. and Ind.*, 1969, 1556.

42. G.W.A. Fowles, R.J. Hobson, D.A. Rice and K.J. Shanton, *J. Chem. Soc. Chem. Commun.*, 1976, 552.

43. H. Bohland and F.M. Schneider, *Z. Chem.*, 1972, 12, 28.

44. H.J. Emeléus, W. Gerrard and J.A. Strickson, J. Chem. Soc., 1960, 4701.

45. O.R. Chambers, M.E. Harman, D.S. Rycroft, D.W.A. Sharp and J.M. Winfield, *J. Chem. Res.*, 1977, 1849.

46. P.M. Boorman, T. Chivers, K.N. Mahadev and B.D. O'Dell, *Inorg. Chim. Acta.*, 1976, 19, L35.

47. U. Müller and V. Krug, *Angew. Chem. Int. Ed. Engl.*, 1988, 27, 293.

48. R.M. Silverstein, G.C. Bassler and T.C. Morill, 'Spectrometric Identification of Organic Compounds', *Butterworth Scientific Publications* (1960).

49. C. Eaborn, 'Organosilicon Compounds',*Butterworth Scientific Publications* (1960).

50. B.J. Brisdon, *Inorg. Chem.*, 1967, 6, 1791.

51. D. Britnell, M.G.B. Drew, G.W.A. Fowles and D.A. Rice, *J. Chem. Soc. Chem. Commun.*, 1972, 462.

52. Y. Sola, D. Youngkyu, J.M. Berg and R.H. Holm, *Inorg. Chem.*, 1985, 24, 1706.

53. Y. Do, ED. Simhon and R.H. Holm, *Inorg. Chem.*, 1983, 22, 3809.

54. H. Hess and H. Hartung, *Z. Anorg. Allg. Chem.*, 1966, 157, 344.

55. M.G.B. Drew and I.B. Tomkins, *Acta. Crystallogr. Sect. B*, 1970, 26, 1161.

56. D.E. Sands, A. Zalkin and R.E. Elson, *Acta. Crystallogr. Sect. B*, 1959, 12, 21.

57. V. Katovic and C. Djordjevic, *Inorg. Chem.*, 1970, 9, 1729.

58. C. Chavant, J.C. Duran, Y. Jeaanin, G. Constant and R. Morancho, *Acta. Cryst.*, 1975, B31, 1828.

59. C. Santini-Scampucci and J.G. Riess, *J. Chem. Soc. Dalton Trans.*, 1974, 1433.

60. D.A. Rice, *Coord-Chem. Rev.*, 1978, 25, 199.

61. T.P. Kee, Ph.D.Thesis, Durham University, 1989.

62. M. Schoenherr and L.Kolditz, *Z. Chem.*, 1970, 10, 72.

63. K.C. Malhotra, U.K. Banerjee and S.C. Chaudhry, J. Ind. Chem. Soc., 1980, 57, 868.

64. J.R Errington, Personnel Communication.

65. A. Zalkin and D.E. Sands, *Acta. Cryst.*, 1958, 11, 615.

66. R, Mercier, J. Douglade, J. Amaudrat, J. Sala-Pala and J.E. Guerchais, *J. Organomet. Chem.*, 1983, 244, 145.

67. Yu. Gorbunov, V.I. Pakhomov and E.S. Kovaleva, *Zh. Strukh. Khim.*, 1972, 13, 165.

68. A.A. Pinkerton, D. Schwarzenbach, L.G. Huert-Pfalzgraf and J.G. Riess, *Inorg. Chem.*, 1976, 15, 1196.

69. B. Kamenar and C.K. Prout, *J. Chem. Soc.* (A), 1970, 2379.

Chapter Three

Synthesis and Reactivity Studies on Molecular Oxo Complexes of Molybdenum and Tungsten.

3.1 Introduction.

Interest in molecules which contain both organic and oxo groups attached to a metal atom derives from the expectation that their chemistry will provide some insight into how metal oxides homogeneously or heterogeneously catalyse various organic transformations[1]. Of particular importance are industrial oxidation processes based on molybdenum oxide catalysts. Here, the active sites for many of the processes are thought to involve terminal oxo groups, either singly (I) or as a cis-dioxo unit (II) (Figure 3.1).

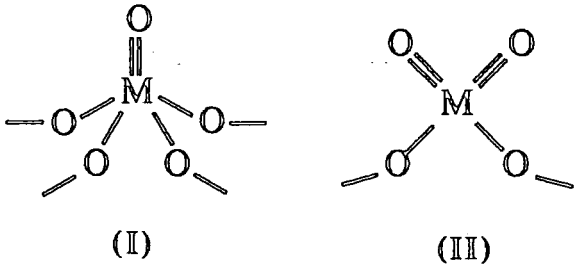

(I) (II)

Figure 3.1

Both of these sites have been observed on the surface of active catalysts, for example by Trifiro and co-workers, using reflectance UV. and IR. spectroscopy[2], and by Lavelley et al by FTIR spectroscopy[3].

In this chapter, studies are described towards the preparation of molybdenum and tungsten oxo complexes which mimic the surface catalyst sites (I) and (II) with ancillary alkoxide or aryloxide ligands to model the lattice oxygens. The molybdenum and tungsten oxohalides described in the previous chapter provide the starting materials for these investigations. For simplicity, mononuclear species were sought which necessitated the use of sterically demanding OR groups. Ancillary aryloxide ligands were chosen for the following reasons:

1) A wide variety of phenols are readily available.

2) They are readily introduced into a metal coordination sphere, either by

metathesis using LiOAr reagents or by phenol exchange.

3) 2,6- disubstituted phenols provide suitably hindered aryloxides to facilitate the stabilisation of mononuclear complexes.

4) Electron withdrawing or releasing substituents may be incorporated to influence the electronic environment of the attendant oxo ligands and thereby influence the relative contributions to the metal oxo canonical forms.

5) Functionalised substituents e.g. those containing alkene groups may also be employed to test reactivity of the oxo ligand towards unsturated organic substrates.

Although compounds of the type $M(O)(OAr)_4$ and $M(O)_2(OAr)_2$ (M = Mo, W) are unknown apart from $W(O)(OPh)_4$[8,9], simple alkoxide complexes of this type are known with a variety of ligands as shown in tables 3.1 and 3.2 respectively. X-ray diffraction studies on the base stabilised mono oxo complex $W(O)(O\text{-}t\text{-}Bu)_4(THF)$[7] and the di-oxo complex $Mo(O)_2(O\text{-}i\text{-}Pr)_2(bpy)$[4] have shown them to be monomeric with 5 coordinate distorted octahedral structures. However, the base free compounds are most likely to be dimeric in the solid state with weak association through RO bridge formation leading to the more favourable octahedral coordination for Mo and W (Figure 3.2).

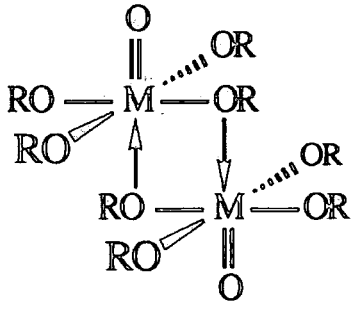

Figure 3.2

Indeed, $W(O)(OMe)_4$ has been shown by X-ray diffraction to be dimeric with bridging alkoxides[10] (Figure 3.3).

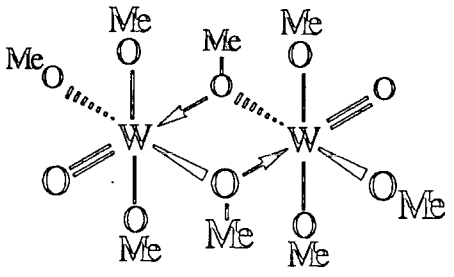

Figure 3.3, *Molecular structure of* $[W(O)(OMe)_4]_2$.

Since, metal alkoxides and aryloxides have not been discussed explicitly in the introductory chapter, a brief discussion is included here.

3.2 Alkoxides and Aryloxides.

3.2.1 Definition and Nomenclature.

Metal alkoxides and aryloxides can be considered to be derivatives of alcohols (ROH) and phenols (ArOH) in which the hydroxylic hydrogen has been replaced by a metal (M).

A characteristic feature of an alkoxy ligand is its ability to readily form bridges between two (μ_2) or even three (μ_3) metal atoms. Such oligomerisation proceeds in order to satisfy the metal atoms desire to attain a preferred coordination geometry and increase its electron count. Oligomerisation may be suppressed by the use of sterically demanding aryloxide ligands and, in this way unusual coordination numbers and geometries may be imposed. For example, Nb^V and Ta^V alkoxides exist as dimers when the alkoxy group is not too sterically demanding eg. MeO, EtO (Figure 3.4)[11], but as 5 coordinate monomers with bulky aryloxides such as $(O\text{-}2,6\text{-}Me_2C_6H_3)$[12].

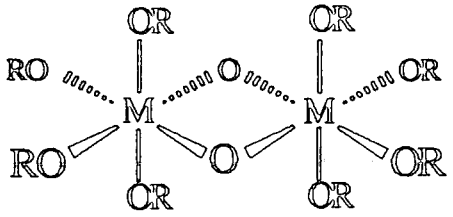

M=Nb, Ta

Figure 3.4

The ethoxides and methoxides of titanium (IV) adopt a tetrameric structure in the solid state (Figure 3.5)[13] whereby each metal atom achieves an octahedral coordination geometry. In benzene solution the titanium ethoxide dissociates into a trimer while for the bulky DIPP ligand, a monomeric, 4 coordinate $Ti(DIPP)_4$[14] is found.

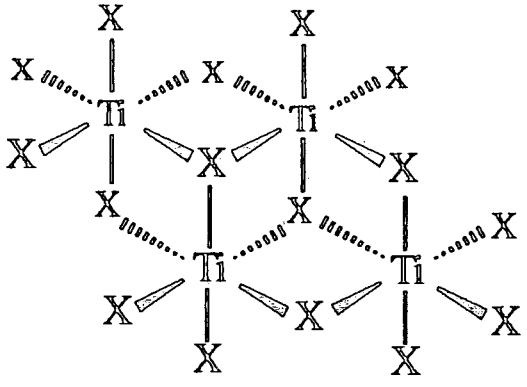

Figure 3.5, *Molecular structure of $Ti(X)_4$ (X=MeO, EtO).*

The use of sterically demanding aryloxide ligands has recently received increasing attention and several reports have described complexes of a number of metals[15-17]. Another novel example is the use of the tritox ligand in Figure 3.6[18].

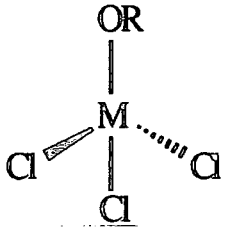

M=Ti
R= $C(C(CH_3)_3)_3$

Figure 3.6

Models indicate that in the example shown (Figure 3.6) the methyl hydrogens overhang the oxygen in a manner sufficient to prevent the formation of alkoxide bridges that are prevalent for small RO ligands (R = Me, Et, Pr^i).

It should also be emphasised that alkoxide ligands may act as π-donor ligands RO→M effectively contributing 3 electrons to the metal count. Within the same molecule M-O distances can differ by up to 0.4 Å following the order M-OR (μ_3) > (μ_2) > terminal. Shorter terminal M-O distances are also characteristically associated with larger M-O-C angles which may be close to 180°. This is rationalised as being due to partial rehybridisation at the oxygen to promote the non bonding lone pairs into π orbitals of correct symmetry for overlap with metal d orbitals. In the exteme case, a linear M-O-C unit containing sp-hybridised oxygen would in theory allow the π donation of four electrons to the metal. However such a situation is rare as suitable orbitals at the metal are normally lacking. Conversely, relatively long terminal M-OR distances are associated with small M-O-C angles, typically in the range 120-130°. The strength of early transition metal-alkoxide bonds can be attributed to this phenomenon, as can the fact that as one decreases the electron deficiency of the metal (ie. moves to the right across the period) then the number and stability of metal alkoxides decrease.

3.2.2 Preparation.

The method chosen for the synthesis of an alkoxide is generally determined by the electropositive character of the metal concerned. Highly electropositive elements such as the alkali metals and alkaline earth metals react directly with alcohols and phenols with the liberation of hydrogen and formation of metal alkoxides[20,21] according to equation 3.1.

$$2M + 2ROH \longrightarrow 2MOR + H_2 \qquad (3.1)$$

Lithium alkoxides are best prepared by the addition of n-butyllithium to a cooled hexane solution of the alcohol or phenol[18].

In the case of less electropositive metals, the alkoxides are generally synthesised by the reactions of their chlorides with alcohols either alone or in the presence of a base acting as a hydrogen chloride acceptor. In this manner $W(O)(OR)_4$ (R=Me, Et, Pr^n, Pr^i, Bu^n or benzyl) compounds were first prepared over 25 years ago[22] (Equation 3.2). Although useful for the synthesis of simple alkoxides and aryloxides of Si, Ge, Ti, Zr, Hf, V, Nb, Ta and Fe, as well as a number of lanthanides[23-26], the method fails to produce pure t-butoxides of a number of metals[27].

$$W(O)Cl_4 + 4ROH \xrightarrow[C_6H_6]{4Et_3N} W(O)(OR)_4 + 4Et_3N^+HCl^- \qquad (3.2)$$

Metal alkoxides and aryloxides can also be prepared by reaction of the metal halide with alkali metal alkoxides and aryloxides. The metathetical exchange of alkoxide or aryloxide for halide is possible using either lithium or sodium salts. For instance, thorium tetraalkoxides[28] are best obtained from the reaction shown in equation 3.3.

$$ThCl_4 + 4NaOR \longrightarrow Th(OR)_4 + 4NaCl \qquad (3.3)$$

The use of sodium salts has been successful in the synthesis of a large number of metal alkoxides including nearly all of the lanthanides[29-31]. However, one problem sometimes encountered in this method is the formation of double alkoxides with alkali metals. In particular, zirconium forms complexes of the type $M_2Zr(OR)_6$ from which removal of the parent alkoxide is difficult[31]. The use of sterically demanding alkoxides and aryloxides of the alkali metals can sometimes lead to only partial substitution. Hence, although lithium 2,6-dimethylphenoxide will totally substitute $TaCl_5$ to give the mononuclear pentaaryloxide the much more sterically demanding 2,6-di-t-butylphenoxide (OAr') will only substitute twice to yield $Ta(OAr')_2Cl_3$[12].

The use of alcohols to synthesise new alkoxides by the process of alcohol interchange has been widely applied for a large number of elements (Equation 3.4)

$$M(OR)_n + nR'OH \longrightarrow M(OR')_n + nROH \quad (3.4)$$

In general, the facility of interchange of alkoxy and aryloxy groups by alcoholysis follows the order aryl > phenyl > tertiary alkyl > secondary alkyl > primary alkyl[32]. (aryl denotes a substituted phenol). Hence the t-butoxides of titanium and zirconium will undergo rapid exchange with methanol or ethanol[33]. An extra driving force here is the larger degree of oligomerisation of methoxides or ethoxides in general over t-butoxides[33]. Similarly it follows that a less substituted aryl group will substitute a more sterically hindered phenol.

Alcoholysis reactions of the type shown in equation 3.5 have also been employed in the synthesis of metal alkoxides when other procedures are inapplicable, for example, in the synthesis of $W(OPh)_6$[6], $V(OR)_4$[34] and $M(OR)_3$ (where M=Mo[35,36] and W[37,36]).

$$M(NMe_2)_n + nROH \longrightarrow M(OR)_n + nHNMe_2 \quad (3.5)$$

3.3 Synthesis and Characterisation of Mononuclear Mono-oxo Complexes of Molybdenum and Tungsten.

3.3.1 Reaction of $W(O)Cl_4$ with LiO-2,6-$Pr^iC_6H_3$ (1), LiO-2,4,6-MeC_6H_2 (2), LiO-2,6-MeC_6H_3 (3):

Preparation of $W(O)(OAr)_4$ (1-3).

$W(O)Cl_4$ reacts readily with four equivalents of LiOAr in toluene solvent at room temperature leading to dissolution of the starting oxo halide and the formation of intense

red solutions. Red, crystalline moisture sensitive solids of general formula $W(O)(OAr)_4$ (1-3) were isolated from these solutions in high yields (Equation 3.6).

$$W(O)Cl_4 + 4LiOAr \xrightarrow[RT,\ 12h.]{tol.} W(O)(OAr)_4 + 4LiCl \quad (3.6)$$

OAr = O-2,6-$Pr^i_2C_6H_3$(DIPP) (1) 79%
O-2,4,6-$Me_3C_6H_2$(TMP) (2) 75%
O-2,6-$Me_2C_6H_3$(DMP) (3) 77%

These compounds may also be prepared by addition of excess Et_3N to a room temperature 1:4 mixture of $W(O)Cl_4$ and the phenol in toluene (Equation 3.7). The mixture is stirred for 2h. at room temperature followed by removal of the solvent under reduced pressure. The resulting residue is then washed with cold petroleum ether (b.p. 40-60°C) to remove unreacted Et_3N and phenol and the products extracted with petroleum ether. Crystallisation from pentane at -30°C affords large red prisms.

$$W(O)Cl_4 + 4ArOH + 4Et_3N \longrightarrow W(O)(OAr)_4 + 4Et_3N^+HCl^- \quad (3.7)$$

Compounds (1-3) are soluble in aromatic hydrocarbon solvents; (1) and (2) possess appreciable solubility in petroleum ether. Elemental analysis (Chapter 7, section 7.3) confirmed the stoichiometry of (1-3). 250 MHz ^1H NMR spectra (C_6D_6) of (1-3) indicate the presence of coordinated aryloxide ligands which occupy equivalent solution environments at room temperature. A doublet resonance at δ1.22 is observed for the isopropyl methyl groups of $W(O)(DIPP)_4$ (1) and a septet at δ3.72 is attributable to the isopropyl methine hydrogen. Similarly, sharp singlets are observed at δ2.40 and δ2.03 (ratio 2:1) in the ^1H NMR spectrum of $W(O)(TMP)_4$ (2) due to the ortho and para methyl substituents respectively of the TMP ligand, whilst $W(O)(DMP)_4$ (3) gives a sharp singlet at δ2.34 due to equivalent methyl groups of the O-2,6-$Me_2C_6H_3$ ligand. The ^1H NMR spectrum (C_7D_8) of (1) at -83°C revealed considerable broadening of all resonances associated with the phenoxide ligand

reflecting restricted rotation of the bulky groups on the NMR time scale at low temperature.

Infrared spectra of (1-3) reveal strong bands characteristic of oxo and phenoxide ligands. In particular, strong bands in the range 960-970 cm^{-1} (which are not present in the parent phenol) may be attributed to $\upsilon(W=O)$ while absorptions in the region 1190-1220 cm^{-1} and 870-905 cm^{-1} may be tentatively assigned to $\upsilon(C-O)$ and $\upsilon(O-W)$ respectively although coupling of these stretching modes often complicates a precise assignment[38].

A single crystal, X-ray structural determination on (1) confirms that the complex is a 5 coordinate monomer in which the coordination geometry may be best described as that of a square-based pyramid with the oxide ligand occupying the apical site and the four aryloxide oxygens forming the basal plane. A full description of the structure is presented in section 3.3.1.1 Compounds (2) and (3) are presumed to be isostructural with (1). . . .

3.3.1.1 Molecular Structure of $W(O)(O\text{-}2,6\text{-}Pr^{i}_{2}C_{6}H_{3})_{4}$ (1).

A petroleum ether solution of (1) cooled at -20°C afforded red prismatic crystals. A suitable crystal of dimensions was selected for an X-ray study and mounted in a Lindeman capillary tube under an inert atmosphere. The structural parameters are collected in appendix 1C. The molecular structure is illustrated in figures 3.7 and 3.8 and selected bond angles and distances are collected in table 3.3.

The coordination geometry is square pyramidal with the oxo group occupying the apical position. The tungsten atom is displaced above the plane defined by the four basal oxygens O(1) - O(4) and at a distance of 1.72 Å from the terminal oxygen atom. This value lies in the range expected for a terminal oxo ligand bound to tungsten VI[39]. The O(5) - W - O angles between the terminal oxo group and the phenoxide oxygens (102 - 105°) are consistent with values typically observed in square pyramidal complexes of this type[40-42]. The angles O(1) - W - O (3) and O(2) - W - O (4), at

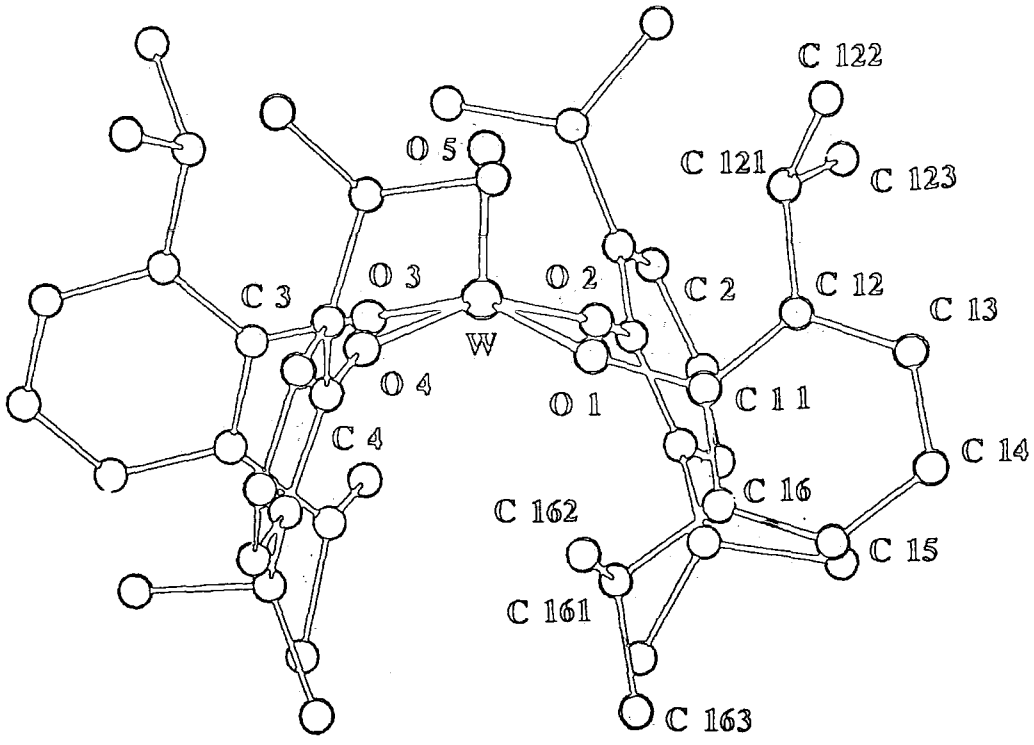

Figure 3.7, *Molecular structure of W(O)(O-2,6-Pr$^i_2$C$_6$H$_3$)$_4$.*

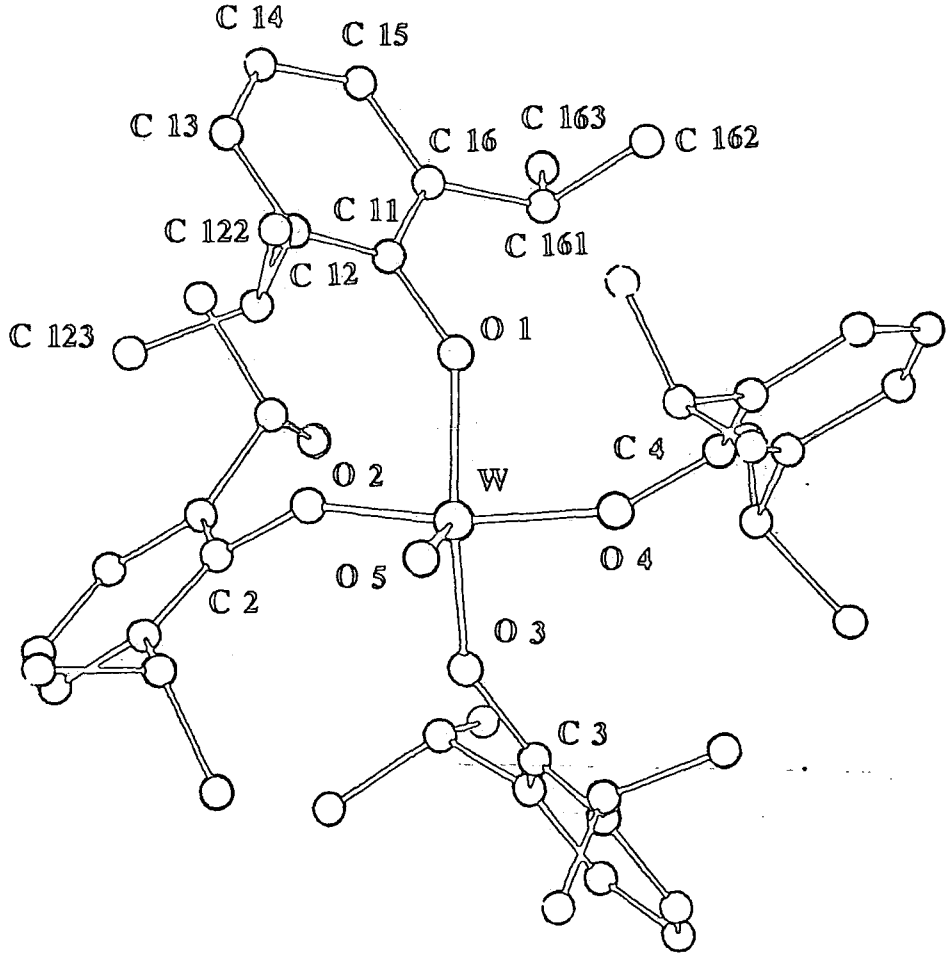

Figure 3.8 ,*View down the oxygen-tungsten vector of W(O)(O-2,6-Pr$^i_2$C$_6$H$_3$)$_4$ (1).*

W - O(1) 1.863(7)
W - O(2) 1.903(7)
W - O(3) 1.859(7)
W - O(4) 1.897(7)

W - O(5) 1.719(9)

O(1) - C(11) 1.365(12)
O(2) - C(21) 1.375(13)
O(3) - C(31) 1.397(13)
O(4) - C(41) 1.371(14)

C(12) - C(121) 1.515(23)
C(16) - C(161) 1.527(25)
C(22) - C(221) 1.525(18)
C(26) - C(261) 1.518(19)
C(32) - C(321) 1.503(20)
C(36) - C(361) 1.520(15)
C(42) - C(421) 1.517(22)
C(46) - C(461) 1.498(18)

C(121) - C(122) 1.560(25)
C(121) - C(123) 1.560(22)
C(161) - C(162) 1.590(3)
C(161) - C(163) 1.550(3)
C(221) - C(222) 1.552(17)
C(221) - C(223) 1.594(24)
C(261) - C(262) 1.565(20)
C(261) - C(263) 1.543(23)
C(321) - C(322) 1.540(18)
C(321) - C(323) 1.566(19)
C(361) - C(362) 1.575(20)
C(361) - C(363) 1.570(3)
C(421) - C(422) 1.548(19)
C(421) - C(423) 1.555(19)
C(461) - C(462) 1.548(19)
C(461) - C(463) 1.510(3)

O(2) - W - O(1) 86.4(3)
O(3) - W - O(1) 153.6(4)
O(3) - W - O(2) 85.1(3)
O(4) - W - O(1) 88.4(3)
O(4) - W - O(2) 153.1(4)
O(4) - W - O(3) 88.0(3)
O(5) - W - O(1) 103.0(4)
O(5) - W - O(2) 104.4(4)
O(5) - W - O(3) 103.4(4)
O(5) - W - O(4) 102.4(3)

C(11) - O(1) -W 153.5(7)
C(21) - O(2) -W 143.8(6)
C(31) - O(3) -W 149.7(7)
C(41) - O(4) -W 148.4(6)

C(12) - C(11) -O(1) 119(1)
C(16) - C(11) -O(1) 118(1)
C(16) - C(11) -C(12) 123(1)
C(13) - C(12) -C(11) 119(1)

C(121) - C(12) -C(11) 123(1)
C(121) - C(12) -C(13) 119(1)
C(14) - C(13) -C(12) 118(2)
C(15) - C(14) -C(13) 124(1)
C(16) - C(15) -C(14) 118(2)
C(15) - C(16) -C(11) 117(1)
C(161) - C(16) -C(11) 123(1)
C(161) - C(16) -C(15) 120(1)

C(22) - C(21) -O(2) 121(1)
C(26) - C(21) -O(2) 115(1)
C(221) - C(22) -C(21) 123(1)
C(221) - C(22) -C(23) 119(1)
C(261) - C(26) -C(21) 122(1)
C(261) - C(26) -C(25) 122(1)

C(32) - C(31) -O(3) 119(1)
C(36) - C(31) -O(3) 117.2(9)
C(321) - C(32) -C(31) 123(1)
C(321) - C(32) -C(33) 119(1)
C(361) - C(36) -C(31) 123(1)
C(361) - C(36) -C(35) 121(1)

C(42) - C(41) -O(4) 121(1)
C(46) - C(41) -O(4) 116(1)
C(421) - C(42) -C(41) 125(1)
C(421) - C(42) -C(43) 117(1)
C(461) - C(46) -C(41) 122(1)
C(461) - C(46) -C(45) 120(1)

C(122) - C(121) -C(12) 112(1)
C(123) - C(121) -C(12) 110(1)
C(123) - C(121) -C(122) 111(1)
C(162) - C(161) -C(16) 111(2)
C(163) - C(161) -C(16) 110(1)
C(163) - C(161) -C(162) 110(2)
C(222) - C(221) -C(22) 114(1)
C(223) - C(221) -C(22) 108(1)
C(223) - C(221) -C(222) 111(1)
C(262) - C(261) -C(26) 111(1)
C(263) - C(261) -C(26) 114(1)
C(263) - C(261) -C(262) 109(1)
C(322) - C(321) -C(32) 112(1)
C(323) - C(321) -C(32) 111(1)
C(323) - C(321) -C(322) 110(1)
C(362) - C(361) -C(36) 111(1)
C(363) - C(361) -C(36) 113(1)
C(363) - C(361) -C(362) 109(1)
C(422) - C(421) -C(42) 111(1)
C(423) - C(421) -C(42) 112(1)
C(423) - C(421) -C(422) 113(1)
C(462) - C(461) -C(46) 110(1)
C(463) - C(461) -C(46) 113(1)
C(463) - C(461) -C(462) 119(1)

Table 3.3, *Selected bond distances (Å) and angles (°) for W(O)(O-2,6-$Pr^i_2C_6H_3$)$_4$ (1).*

153.6(4)° and 153.1(4)° respectively are also in the range expected for square pyramidal geometries, and are considerably less than those found in the molecular structure of $W(O\text{-}2,6\text{-}Pr^i_2C_6H_3)_4$[43] (168°) which has an approximate square planar geometry. They are also free of the distortion observed in the structure of $W(O)(NMe_2)_4$[44]. The W - O bond lengths of the phenoxide ligands lie in the range 1.86 - 1.90 Å, which on average are slightly longer than the values found in $W(DIPP)_4$ (1.85 - 1.87 Å)[43]. This is consistent with decreased π-donation from the phenoxide ligands of (𝟙), which are in competition with the strongly π-donating oxo ligand. Accordingly, the W - O - C angles in (𝟙) (145 - 154°) are less obtuse than those observed in $W(DIPP)_4$ (154 - 159°), although this effect may also be partially influenced by non bonding interactions within the highly crowded coordination sphere of (𝟙). The cis- O -W - O angles in (𝟙) (85 - 89°) are only slightly reduced relative to $W(DIPP)_4$ and $W(DMP)_4$ while O - C distances are identical within the error of the structural determinations.

. The six-membered rings of the phenoxide ligands are orientated in a propeller fashion which is evident in Figure 3.8. The 'tilt' of each phenoxide C_6 ring, determined by the angle between its normal and the normal of the WO_4 basal plane, lies in the range 61 - 75° cf. a 60° 'tilt' for square planar $W(DMP)_4$[43]. This parameter is likely to be strongly influenced by the non bonding interactions which are particularly pronounced for (𝟙). The congestion is quite apparent from the space-filled view shown in figure 3.12 , and is particularly severe in the vicinity of the oxo ligand where the four van der Waals spheres of the iso-propyl methine hydrogens are seen to be in contact with the central oxygen atom. The corresponding intramolecular O·····H contact distances lie in the range 2.38 - 2.50 Å (Table 3.3). This congestion is further manifested in reduced thermal parameters for the iso-propyl methyl groups adjacent to the oxo ligand consistent with restricted rotation. No such effect is observed for the isopropyl substituents projecting to the less hindered side of the WO_4 plane suggesting that these are rotate without inhibition.

3.3.2 Reactivity Studies on $W(O)(OAr)_4$ (1-3).

3.3.2.1 Exchange Reactions Involving Alcohols and Phenols: *Preparation of $W(O)(OPh)_4$ (4).*

$W(O)(DIPP)_4$ (1) reacts instantly with four equivalents of HO-2,6-$Me_2C_6H_3$, HO-2,4,6-$Me_3C_6H_2$, HO-C_6H_5 or $HOBu^t$ to give the corresponding tetraaryloxide or tetra-t-butoxide complexes according to equation 3.8 These reactions are quantitative by ^1H NMR and take advantage of the ready displacement of the bulky DIPP ligand by a less hindered aryloxide or alkoxide[32]. Consistently a mixture of $W(O)(DIPP)_4$ (1) and four equivalents of HO-2,6-$Bu^t{}_2C_6H_3$ remained unchanged after prolonged treatment at 100°C.

$$W(O)(DIPP)_4 + 4ROH \rightleftharpoons W(O)(OR)_4 + 4HO\text{-}2,6\text{-}Pr^i \quad (3.8)$$

OR = O-2,6-$Me_2C_6H_3$
O-2,4,6-$Me_3C_6H_2$
OBu^t
OC_6H_5

Although this method has been exploited to prepare metal alkoxide derivatives which have not proved accessible by alternative routes[45], difficulties associated with removal of excess substituted phenol from the hydrocarbon soluble $W(O)(OAr)_4$ and $W(O)(OBu^t)_4$ products makes a direct synthesis (eg. those shown in Equations 3.6 and 3.7) more advantageous.

However, this is not the case for the parent aryloxide $W(O)(OPh)_4$ (4) which is precipitated as an amorphous orange solid upon addition of 4 equivalents of HO-C_6H_5 to a solution of $W(O)(DIPP)_4$ in toluene. The solid is isolated by filtration and any excess phenol or substituted phenol is easily removed by washing with light petroleum ether. The solid is dried *in vacuo* and collected in 87% yield. Compound

(4), which is insoluble in all common solvents has been reported previously and is believed to be polymeric[8,9].

3.3.2.2 Mass Spectral Studies on $W(O)(OAr)_4$ Complexes: *Evidence for Alkylation of the Terminal Oxo Group of $W(O)(O\text{-}2,6\text{-}Me_2C_6H_3)_4$ (3)* .

Positive chemical ionization mass spectra were recorded for (1-3). The principle tertiary ions observed using isobutane carrier gas are collected in table 3.4 .

Compound	Fragment Ions (m/e)	% relative abundance
$W(O)(DMP)_4$	742 $[W(O^tBu)(DMP)_4]$ 700 $[W(OMe)(DMP)_4]$ 609 $[W(OMe)_2(DMP)_3]$ 563 $[W(O)(DMP)_3]$	12.2 41.7 10.1 100.0
$W(O)(TMP)_4$	755 $[W(OMe)(TMP)_4]$ 651 $[W(OMe)_2(TMP)_3]$ 605 $[W(O)(TMP)_3]$	30.7 3.9 100.0
$W(O)(DIPP)_4$	732 $[W(O)(DIPP)_3]$	100.0

Table 3.4, *Principle Fragment Ions arising in the Positive Chemical Ionisation Mass Spectra of (1-3) (isobutane, carrier gas, % relative abundance).*

For $W(O)(DIPP)_4$ (1), the highest mass fragment occurs at m/z 732 (^{184}W) and is attributable to $[W(O)(DIPP)_3]^+$ arising by loss of an aryloxide group. For $W(O)(DMP)_4$ (3), however, additional to a fragment ion at m/z 563 due to $[W(O)(DMP)_3]^+$, envelopes at m/z 742 (12.2%) and 700 (41.7%) are assignable to $[W(OBu^t)(DMP)_4]^+$ and $[W(OMe)(DMP)_4]^+$ respectively. Similar behaviour is observed for $W(O)(TMP)_4$ (2) which affords the methylated ion $[W(OMe)(TMP)_4]^+$ at m/z 755.

The formation of these higher mass species may be rationalised by attack of the secondary ions (^{t}butyl and methyl) generated from the iso-butane carrier gas, on the neutral $W(O)(OAr)_4$ molecules (Equation 3.9).

$$W(O)(OAr)_4 + R^+ \longrightarrow [W(OR)(OAr)_4]^+ \qquad (3.9)$$

$$R = Me, Bu^t$$

Consistently, mass spectra recorded using argon carrier gas revealed no fragments to a mass higher than $[M\text{-}OAr]^+$ confirming that the source of alkyl cations is the iso-butane carrier gas rather than the substituents of the aryloxide ligands. Furthermore, time resolved, selected ion monitoring of $[W(OMe)(DMP)_4]^+$ and $[W(O)(DMP)_3]^+$ suggests that the methylation of the parent ion occurs before fragmentation to give $[W(O)(DMP)_3]^+$.

In order to confirm that the noticeable difference in behaviour between $W(O)(DIPP)_4$ and $W(O)(OAr)_4$ (OAr = DMP, TMP) was not attributable to the conditions present in each of the individual experiments, a mass spectrum was recorded on a 50:50 mixture of $W(O)(DMP)_4$ and $W(O)(DIPP)_4$. The resultant spectrum showed molecular ions corresponding to $[W(OMe)(DMP)_4]^+$, $[W(O)(DIPP)(DMP)_3]^+$, $[W(OMe)(DMP)_3]^+$ and $[W(O)(DIPP)_3]^+$. Significantly no alkylation of a W species containing DIPP as a ligand could be detected. This apparent alkylation of the terminal oxo ligands of (2-3) by gas phase cations is worthy of consideration since, to date, there has been only one report of alkylation of an oxo ligand in a molecular complex. In that case the bridging oxo ligands of $Mo_{12}PO_{40}^{3-}$ and $W_{12}PO_{40}^{3-}$ were methylated using $[Me_3O]^+ [BF_4]^-$ [46].

An explanation for the failure to alkylate the oxo ligand in (1) as opposed to compounds (2-3) which alkylate readily under similar conditions may be provided by considering the environment around the oxo group in these compounds. Figure 3.9 shows a space-filled diagram of $W(O)(DIPP)_4$ (1) viewed side-on to the W=O unit. The oxo ligand is largely obscured by the isopropyl substituents of the phenoxide

ligands and consequently is not sufficiently exposed to attack by electrophiles. On the other hand a similar space-filled view of $W(O)(DMP)_4$ (3), modelled using the coordinates for (1) (Figure 3.10) shows that the oxo ligand protrudes beyond the organic periphery and is far more accessible to attacking electrophiles. A similar picture will prevail for $W(O)(TMP)_4$ (2) where the para methyl groups do not affect the congestion in the vicinity of the oxo ligand.

These observations are consistent with the findings of Schrock and co-workers[43], who have studied four coordinate $W(OAr)_4$ complexes. They have found that whereas $W(DMP)_4$ is capable of deoxygenating a variety of reagents to give $W(O)(DMP)_4$ (3), $W(DIPP)_4$ is unreactive, even towards molecular oxygen due to the steric inhibition afforded to the metal centre by the bulky isopropyl groups of the DIPP ligands.

The mass spectral evidence for alkylation of the terminal oxo ligand by gas-phase cations led us to attempt to reproduce this reactivity on a laboratory scale. Reactions of $W(O)(DMP)_4$ with $[Me_3O]^+ [BF_4]^-$ or CF_3SO_3Me in a variety of chlorocarbon, ether and aromatic solvents over the temperature range -30 - +50°C, however did not afford tractable products.

The failure to alkylate the terminal oxo ligand in compound (3) prompted us to prepare the mono-oxo complex $W(O)(O\text{-}t\text{-}Bu)_4$ (5) described previously by Chisholm et al[6]. (5) is assumed to be monomeric by analogy with the thio derivative $W(S)(OBu^t)_4$[47] (Figure 3.11) and molybdenum analogue $Mo(O)(OBu^t)_4$.

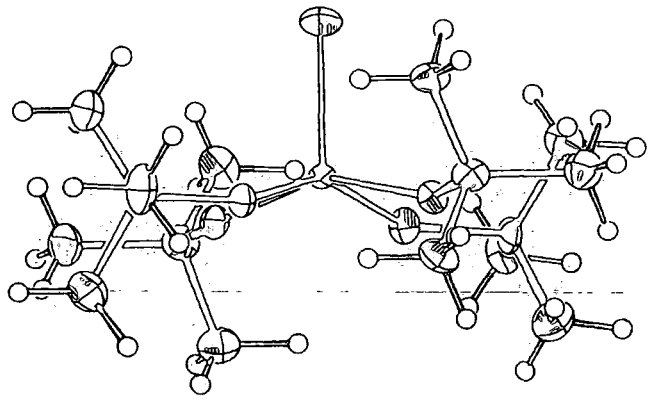

Figure 3.11, *Molecular structure of $W(S)(OBu^t)_4$.*

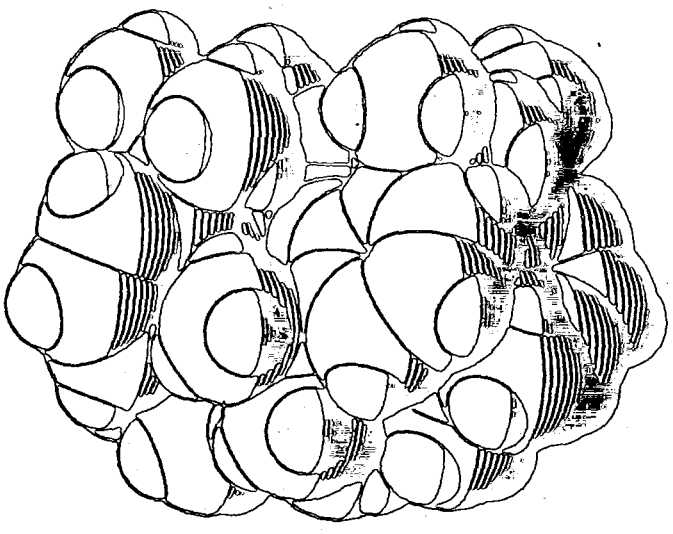

Figure 3.9 , *Side on space filled view of W(O)(DIPP)$_4$ (1).*

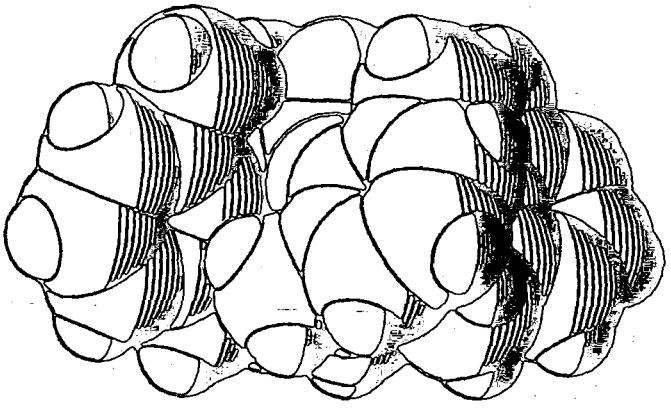

Figure 3.10, *Computer simulated side on space filled view of W(O)(DMP)$_4$ (3).*

It was envisaged that the increased electron donating ability of the tertiary butoxide ligands over the aryloxide ligands in (3) should lead to an increase in electron density on the oxo ligand and a corresponding lengthening of the W=O bond. This appears to be confirmed by a lowering of the υ(W=O) stretching frequency from 961 cm^{-1} for (3) to 940 cm^{-1} for $W(O)(O\text{-}t\text{-}Bu)_4$. The positive chemical ionization spectrum of (5) however, gave a principle tertiary ion at m/z 549 due to the alkylated species $[W(OBu^t)_5]^+$. Once again mass spectra recorded using argon carrier gas revealed no fragments to a mass higher than $[M\text{-}OR]^+$. Unfortunately, reactions of $W(O)(OBu^t)_4$ (5) with a range of alkylating agents on a laboratory scale were again unsuccessful.

3.3.2.3 Other Reactions of $W(O)(OAr)_4$ (1-3).

Several other reactions were carried out on compounds (1-3) and monitored by ^1H NMR spectroscopy. These results are described briefly below.

Rothwell et al have reported[48] the metalation behaviour of the compound $Ta(O\text{-}2,6\text{-}Bu^t_2C_6H_3)_2(Me)_3$ in which thermolysis at 120°C leads to loss of 2 equivalents of methane and cyclometalation of a tertiary butyl substituent. This is in contrast to the stability of $Ta(O\text{-}2,6\text{-}Me_2C_6H_3)_2Me_3$ which does not generate methane even when heated to 120°C for 7 days. This is a clear indication that the hydrogen abstraction observed is sterically induced as proposed by Schrock[49]. It was of interest to establish whether similar reactivity could be observed for (1-3) and to establish if the terminal oxo ligand may influence intramolecular cyclometallation reactions. However, heating solutions of (1-3) in C_6D_6 through the temperature range RT $\rightarrow$ 150°C, whilst monitoring by ^1H NMR, gave no evidence for a reaction; the starting materials remaining unchanged after heating for several days.

Despite the vacant coordination site lying trans to the oxo ligands of (1-3), there was no evidence for coordination of PMe_3 or other bases (CH_3CN, THF) after

mixing for one week at either ambient or higher temperatures. This may possibly reflect, the strong trans influence of the multiply bonded oxo group or more likely, the steric constraints in the metal coordination sphere.

Similarly there was no evidence for reaction between (1-3) and unsaturated organic substrates such as ethylene, butadiene and phenyl acetylene even upon prolonged heating at elevated temperature.

3.3.3 Reaction of $Mo(O)Cl_4$ with $LiO\text{-}2,6\text{-}Me_2C_6H_3$:

Preparation of $Mo(O)(O\text{-}2,6\text{-}Me_2C_6H_3)_4$ (6).

$Mo(O)Cl_4$ reacted readily with four equivalents of LiOAr in diethyl ether solvent at -78°C leading to dissolution of the starting oxohalide and the formation of an intense blue solution. Dark blue, moisture sensitive crystals of (6) were isolated from solution in 71% yield (Equation 3.10).

$$Mo(O)Cl_4 + 4LiOAr \xrightarrow[-78°C,\ 12h.]{Et_2O} Mo(O)(OAr)_4 \qquad (3.10)$$

$OAr = 2,6\text{-}Me_2C_6H_3$ (DMP)

(6)

Compound (6) is soluble in aromatic hydrocarbon solvents and possesses partial solubility in petroleum ether.

The infrared spectrum of (6) reveals bands characteristic of terminal oxo and alkoxide ligands. In particular a strong band at 982 cm^{-1} may be attributed to $\upsilon(Mo{=}O)$ while absorbtions in the region 1150 - 1265 cm^{-1} and 820 - 950 cm^{-1} may be tentatively assigned to $\upsilon(C\text{-}O)$ and $\upsilon(O\text{-}Mo)$ respectively. The 250 MHz ^1H NMR spectrum (C_6D_6) indicates the presence of coordinated aryloxide ligands which occupy equivalent solution enviroments at room temperature. A singlet resonance at δ 2.35 ppm is served for the ortho methyl substituents of the DMP ligand, whilst a triplet and a doublet at δ 6.55 ppm and δ 6.69 ppm are consistent with the resonance pattern expected for the aromatic hydrogens. In the mass spectrum (CI), as for the tungsten analogue, the ion

of highest mass corresponds to $Mo(OMe)(DMP)_4^+$. Consistently, mass spectra recorded using argon carrier gas revealed no fragments to a mass higher than [M-OAR]$^+$.

A single crystal, X-ray structural determination on (6) confirms that the complex is a 5 coordinate monomer with a square based pyramidal geometry similar to (1). A full description of the structure is presented in the following section.

3.3.3.1 Molecular Structure of $Mo(O)(O\text{-}2,6\text{-}Me_2C_6H_3)_4$ (6).

A petroleum ether solution of (6) cooled at -20°C afforded purple prismatic crystals. A suitable crystal was selected for an X-ray study and mounted in a Lindeman capillary tube under an inert atmosphere. The structural parameters are collected in appendix 1D. The molecular structure is illustrated in figures 3.12 and 3.13 and selected bond angles and distances are collected in table 3.5.

The overall coordination geometry is essentially identical to (1) consisting of a square based pyramid with the oxo ligand occupying the apical site and the four aryloxide oxygen atoms lying in the basal sites. The most marked difference between (1) and (6) is a slight distortion in (1) such that the four *trans* O–W–O angles are inequivalent giving the molecule a one fold symmetry axis, whereas the analogous angles in (6) are equivalent giving the molecule a four fold axis of symmetry. The molybdenum atom is 1.719 Å from the terminal oxygen atom with all the other Mo–O distances being equal [1.878(6) Å] as required by the crystallographic symmetry. The Mo=O bond distance lies at the far end of the range expected for a terminal oxo ligand bound to molybdenum[39] (typically 1.65 - 1.70 Å). Comparative values of selected parameters for (1) and (6) are displayed in table 3.6. It can be seen that the (M=O), (M-O) and (O-C) distances are identical within the error of the structure determinations.

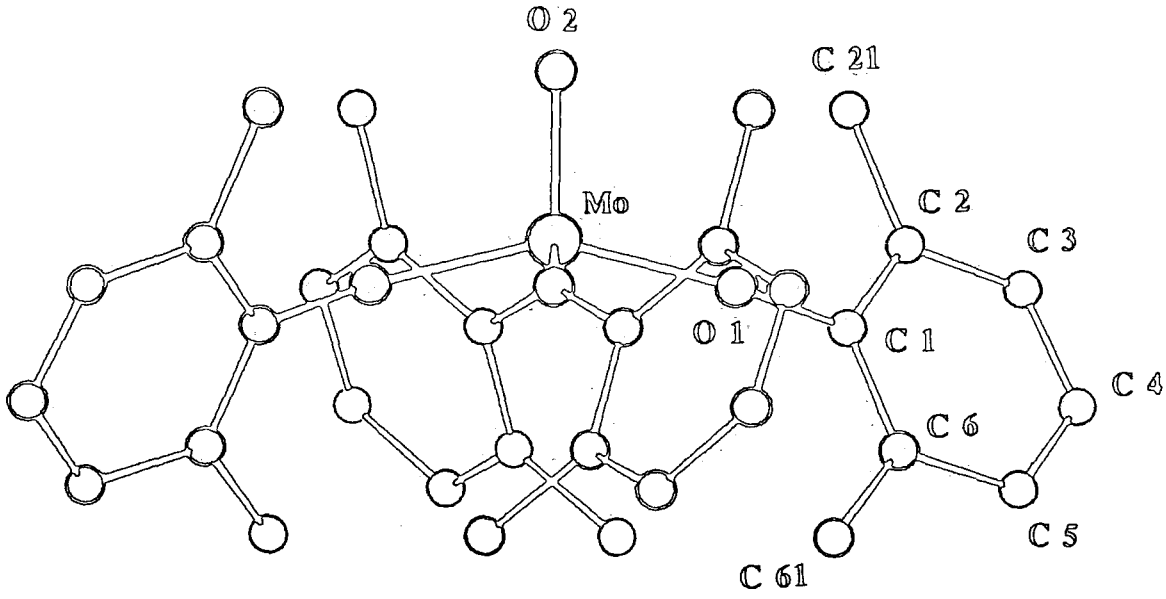

Figure 3.12, *Molecular structure of Mo(O)(O-2,6-$Me_2C_6H_3$)$_4$.*

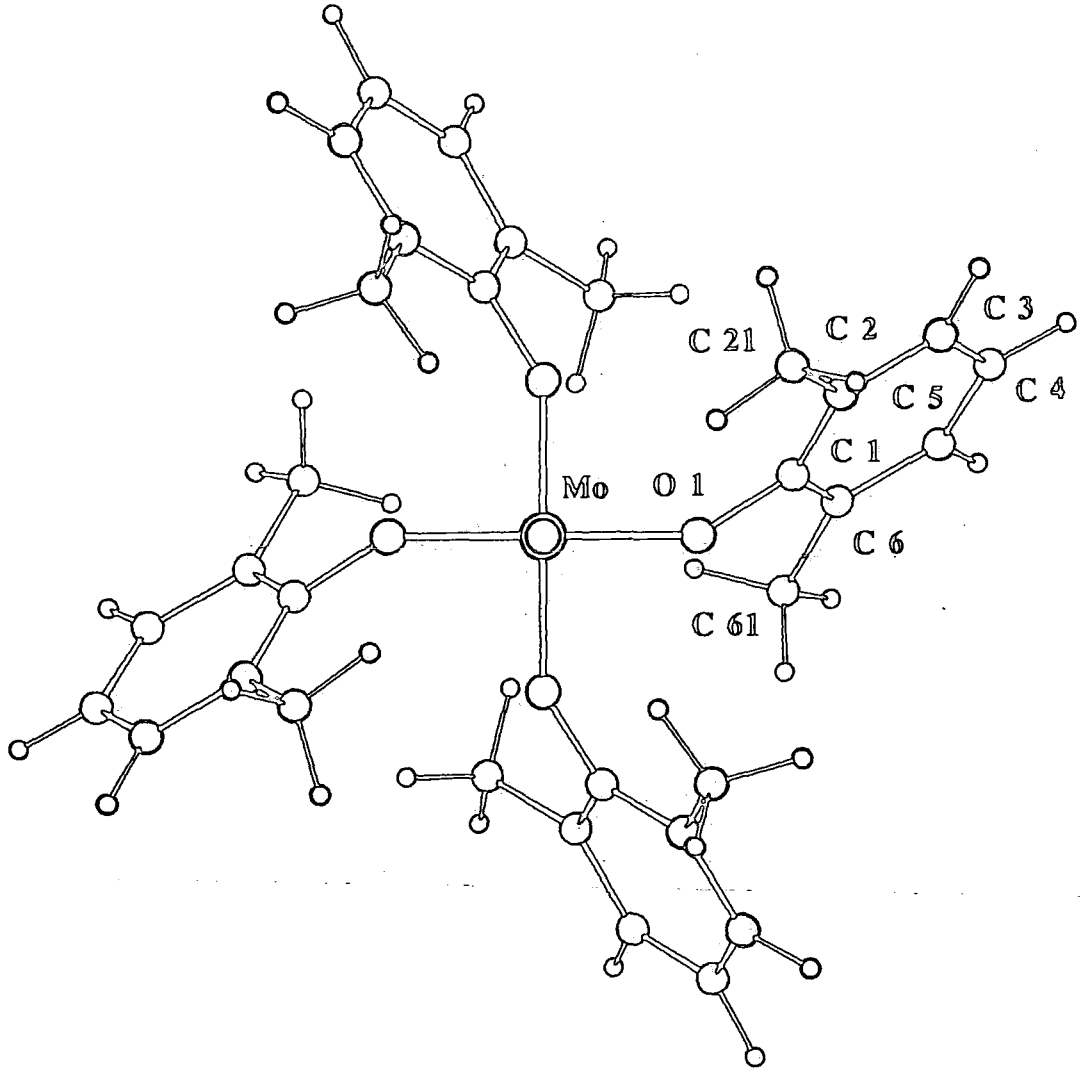

Figure 3.13 *View down the oxygen-molybdenum vector of Mo(O)(O-2,6-$Me_2C_6H_3$)$_4$ (6).*

Mo - O(1) 1.878(6)

Mo - O(2) 1.719(14)

O(1) - C(1) 1.359(10)

C(1) - C(2) 1.372(13)
C(1) - C(6) 1.388(12)
C(2) - C(3) 1.399(15)
C(2) - C(21) 1.517(17)
C(3) - C(4) 1.342(15)
C(4) - C(5) 1.379(15)
C(5) - C(6) 1.395(13)
C(6) - C(61) 1.498(13)

O(1) - Mo - O(1) 86.5(1)
O(1) - Mo - O(2) 104.3(2)

C(1) - O(1) -Mo 148.6(6)

C(2) - C(1) -O(1) 119.3(9)
C(6) - C(1) -O(1) 117.6(9)
C(6) - C(1) -C(2) 123(1)
C(3) - C(2) -C(1) 118(1)
C(21) - C(2) -C(1) 123.1(9)
C(21) - C(2) -C(3) 122(1)
C(4) - C(3) -C(2) 120(1)
C(5) - C(4) -C(3) 122(1)
C(6) - C(5) -C(4) 120(1)
C(5) - C(6) -C(1) 117(1)
C(61) - C(6) -C(1) 121.6(9)
C(61) - C(6) -C(5) 121(1)

Table 3.5, *Selected bond distances (Å) and angles (°) for Mo(O)(O-2,6-$Me_2C_6H_3$)$_4$ (6).*

	(1)	(6)
M=O	1.719(9)	1.719(14)
M-O	1.881(7)	1.878(6)
O-C	1.377(13)	1.359(10)
O-M-O	103.3(4)	104.3(2)
O-M-O_{cis}	87.0(4)	86.5(1)
O-M-O_{trans}	153.4(4)	104.3(2)
M-O-C	148.9(6)	148.6(6)

Table 3.6, *Selected bond distances (Å) and angles (°) for (1) and (6) (Averaged where appropriate)*

3.3.4 Mono-oxo Tungsten Derivatives Containing Both Chloride and Aryloxide Ligands.

It was envisaged that oxo-aryloxide compounds containing ancillary chloride ligands would facilitate the introduction of other ligands such as an alkyl group relevant to hydrocarbon oxidation reactions. In particular, there is considerable interest in the migratory aptitude of alkyl groups to oxo ligands.

Basset[50] has found that the number of chloride ligands that may be substituted for phenoxide groups in WCl_6 is strongly dependent upon the nature, the number and the position of the substituents on the aromatic phenol ring, allowing three series of chloro-aryloxides $W(OAr)_4Cl_2$, $W(OAr')_3Cl_3$ and $W(OAr'')_2Cl_4$ (OAr = DMP, OAr' = DIPP, OAr'' = DPP) to be synthesised. Related results have been observed by Rothwell et al[12] with chloro aryloxides of tantalum and Johnson et al[51] have reported that the solution exchange of $Mo(O)Cl_4$ in dichloromethane with solid perfluoro-t-butoxide sodium gave fully and partially substituted compounds, depending on the stoichiometry of the reactants (Equation 3.11).

$$Mo(O)Cl_4 + n(NaOC_4F_9) \longrightarrow Mo(O)Cl_{4-n}(OC_4F_9)_n \; nNaCl \quad (3.11)$$

3.3.4.1 Reaction of $W(O)Cl_4$ with $LiO\text{-}2,6\text{-}Me_2C_6H_3$:

Preparation of $W(O)Cl(OAr)_3$ [Ar = 2,6-$Me_2C_6H_3$ (7)].

In an attempt to prepare a series of $W(O)Cl_x(OAr)_{4-x}$ (x = 1-3), $W(O)Cl_4$ was reacted with 1-3 equivalents of Li-O-2,6-$Me_2C_6H_3$ according to equation 3.12.

$$W(O)Cl_4 + nLiOAr \longrightarrow W(O)Cl_{4-n}(OAr)_n + nLiCl \quad (3.12)$$
$$n = 1\text{-}3$$

Of the three possible products for x = 1-3 only one could be isolated cleanly, namely $W(O)Cl(OAr)_3$ (7) in 49% yield from the reaction of $W(O)Cl_4$ with 2 equivalents of LiDMP. The dark, moisture sensitive red crystals of (7) are soluble in aromatic hydrocarbon solvents and partially soluble in petroleum ether.

Characterisation of (7) is provided by elemental analysis, infrared, NMR and mass spectroscopies(Chapter 7, section 7.3). In particular, the stoichiometry of $C_{24}H_{27}ClOW$ has been established by microanalysis.

Found (Required): %C, 48.14 (48.13); %H, 4.54 (4.48);
%Cl, 5.92 (5.89); %W, 29.66 (30.70).

The 250 MHz ^1H NMR spectrum (C_6D_6) indicates the presence of coordinated aryloxide ligands which occupy inequivalent solution environments at room temperature. Two singlet resonances are observable due to the methyl groups of the O-2,6-$Me_2C_6H_3$ ligand at δ 2.43 and δ 2.51 respectively in the ratio 2:1. The $^{13}C\{^1H\}$ NMR data in the aromatic region consistent with this, although the observation of only one singlet resonance at δ 16.77 is presumably due to coincidental overlap of the methyl carbon resonances. Infrared spectra of (7) reveal strong bands at 1200 and 1186 cm^{-1}, characteristic of 2 phenoxide ligands in different chemical environments. Strong bands in the range 990 - 980 cm^{-1} may be attributed to υ(W=O)

while absorptions in the region 885 - 905 cm^{-1} and at 400 cm^{-1} may be tentatively assigned to υ(O-W) and υ(W-Cl) respectively[38]. Mass spectrometry $(CI)^+$ reveals envelopes for $W(O)Cl(OAr)_3$, $W(O)(OAr)_3$ and $W(O)Cl_2(OAr)_2$ at m/z 598, m/z 563 and m/z 477 respectively, the latter is presumed to arise by OAr/Cl exchange.

In the absence of a structure determination the precise geometry of (7) remains unknown. However an attractive formulation is a mononuclear square based pyramid by analogy with crystallographically characterised (1) (Figure 3.14 (I)).

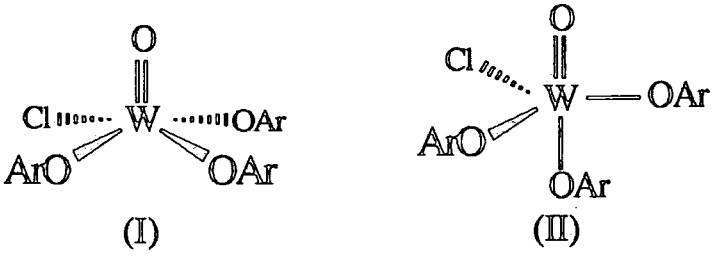

Figure 3.14, *Possible structures for (7).*

A dimeric structure is unlikely in the presence of 3 sterically demanding aryloxides, although the trigonal bypyramidal geometry (Figure 3.17 (II)) is not ruled out by the spectroscopic data.

Attempts to isolate compounds of the type $W(O)Cl_2(OAr)_2$ by treatment of $W(O)Cl_4$ with more sterically demanding aryloxides (OAr = 2,6-$Bu^t_2C_6H_3$) were unsuccessful. The only tractable products here were the parent phenol and the para-para coupled biphenol. Also, solution equilibration of an equimolar mixture of $W(O)Cl_4$ and $W(O)(OAr)_4$ afforded a range of mixed chloro aryloxide species. Schrock et al[52] have reported the exchange of t-butoxide groups of $W(NAr)(OBu^t)_2(CH_2\,Bu^t)_2$ for chloride groups using PCl_5. However, an attempt to prepare $W(O)Cl_2(DIPP)_2$ by reacting $W(O)(DIPP)_4$ with PCl_5 was also unsuccessful.

3.3.5 Summary.

A series of monomeric tungsten (VI) oxo-aryloxide compounds of the type $W(O)(OAr)_4$ (OAr = O-2,6-$Pr^i_2C_6H_3$ (DIPP), O-2,4,6-$Me_3C_6H_2$ (TMP), O-2,6-$Me_2C_6H_3$ (DMP) and the Mo derivative $Mo(O)(DMP)_4$ have been prepared by treatment of $W(O)Cl_4$ or $Mo(O)Cl_4$ with four equivalents of LiOAr in toluene, or the reaction of $W(O)Cl_4$ with ArOH in the presence of excess Et_3N. The X-ray structures of $W(O)(DIPP)_4$ (1) and $Mo(O)(OAr)_4$ (6) have been determined. The terminal oxo ligands in these environments have been found to be unreactive to all but the most potent electrophiles

*e.g.*gas-phase cationic alkyls generated during mass spectrochemical studies. Further, attempts to obtain a convenient entry into mixed chloro aryloxide derivatives appear complicated by facile aryloxide for chloride exchange processess leading to a mixture of products. Therefore, it was decided at this stage to focus attention on dioxo derivatives where it was believed that the neighbouring oxo atom effect may lead to enhanced oxo atom reactivity.

3.4 Attempted Synthesis of Mononuclear Di-Oxo Complexes of Molybdenum and Tungsten.

3.4.1 Reaction of $M(O)_2Cl_2$ with LiO-2,6-$Me_2C_6H_3$: *Preparation of $Mo_2(O)_3(O\text{-}2,6\text{-}Me_2C_6H_3)_6$ (8).*

Using the readily available $M(O)_2Cl_2$ reagents (M = Mo, W) described in chapter 2, we envisaged that reactions between $M(O)_2Cl_2$ and 2 equivalents of LiOAr may provide a convenient route to $M(O)_2(OAr)_2$ complexes according to equation 3.13

$$M(O)_2Cl_2 + 2LiOAr \longrightarrow M(O)_2(OAr)_2 + 2LiCl \quad (3.13)$$

Indeed, $Mo(O)_2Cl_2$ reacted instantly with two equivalents of LiOAr in toluene solvent at room temperature leading to dissolution of the starting oxohalide and the formation of an intense blue solution. Purple, moisture sensitive crystals were isolated from toluene in low yield. However, contrary to the anticipated $Mo(O)_2(OAr)_2$, the spectroscopic and analytical data are consistent with a binuclear oxide of formula $Mo_2(O)_3(OAr)_6$ (8) in which each molybdenum centre consumes three equivalents of LiOAr (Equation 3.14). Consistently, the yield of (8) may be improved substantially upon treatment of $Mo(O)_2Cl_2$ with three equivalents of LiOAr.

$$2MoO_2Cl_2 + 6LiOAr \xrightarrow[RT,\ 18h]{tol.} \underset{(8)}{Mo_2O_3(OAr)_6} + 4LiCl + Li_2O \quad (3.14)$$

$OAr = O\text{-}2,6\text{-}Me_2C_6H_3$ (DMP)

The mass spectrum $(CI)^+$ is consistent with a binuclear formulation giving envelopes for $[Mo_2O_3(OAr)_5]^+$, $[Mo_2O_2(OAr)_4]^+$ and $[Mo(O)(OAr)_3]^+$ at m/z 846, m/z 709 and m/z 475 respectively, while the 250 MHz ^1H NMR spectrum (C_6D_6) gives a singlet resonance at δ 2.35 due to equivalent aryloxide methyl groups. In the infrared spectrum, a band at 970 cm^{-1} can be assigned to a υ(Mo=O) stretch. Bands at 1207 cm^{-1} and 890 cm^{-1} are consistent with those expected for υ(C-O) and υ(Mo-O) stretches of the aryloxide ligands respectively. A strong absorbtion at 730 cm^{-1} is consistent with an asymmetric $Mo_2(\mu\text{-oxo})$ stretch of a system containing the O=Mo-O-Mo=O unit[53]. Thus, the coordination geometry of each metal is likely to be trigonal bypyramidal by comparison with the structurally characterised tungsten complex $W_2(O)_3(Np)_6$[54] (Figure 3.15).

In contrast the reaction of $W(O)_2Cl_2$ with two equivalents of LiOAr proceeds quite differently. Room temperature treatment of a finely divided toluene suspension of $W(O)_2Cl_2$ with powdered LiOAr under dry argon rapidly affords a dark moisture sensitive crystalline solid and a red-green dichroic supernatant solution according to Equation 3.15.

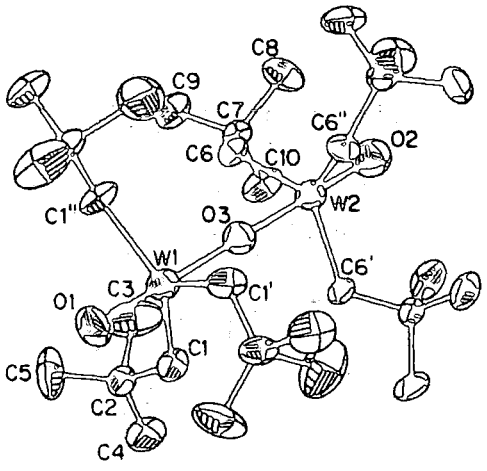

Figure 3.15, *Molecular structure of* $W_2(O)_3(Np)_6$.

$$W(O)_2Cl_2 + xLi(O\text{-}2,6\text{-}Bu^t{}_2C_6H_3) \longrightarrow W(O)_2Cl_2.Li_x + \text{'Organics'} \quad (3.15)$$

Analysis of the solid shows that the chlorides are not exchanged for aryloxide groups. Rather Li is incorporated into the $W(O)_2Cl_2$ lattice. This unexpected observation forms the basis of chapter 6.

3.4.2 Reaction of $W(O)_2Cl_2(CH_3CN)_2$ with Li-O-2,6-$Me_2C_6H_3$: *Preparation of* $W_2(O)_3(O\text{-}2,6\text{-}Me_2C_6H_3)_6$ *(9).*

The apparent inability of LiOAr to break up the $W(O)_2Cl_2$ lattice stimulated us to repeat the reaction, starting with the base stabilised monomer $W(O)_2Cl_2(CH_3CN)_2$.

$W(O)_2Cl_2(CH_3CN)_2$ reacted readily with two equivalents of LiOAr in toluene solvent at room temperature to give an intense red solution over a period of 18h. Red moisture sensitive crystals of compound (9), containing three aryloxides per tungsten could be isolated in low yield. When three equivalents of aryloxide reagent were used the yield was increased to 85%. Thus, a similar reaction to that observed between $Mo(O)_2Cl_2$ and LiOAr would appear to occur (Equation 3.16).

$$2W(O)_2Cl_2(CH_3CN)_2 + 6LiOAr \xrightarrow[RT,\ 18h.]{tol.} W_2O_3(OAr)_6 + 6LiCl \quad (3.16)$$

$OAr = O\text{-}2,6\text{-}Me_2C_6H_3$(DMP)

(9)

Compound (9) is soluble in aromatic hydrocarbon solvents and possesses partial solubility in petroleum ether. Characterisation is provided by elemental analysis, infrared, NMR and mass spectroscopies (Chapter 7, section 7.3).

Mass spectrometry $(CI)^+$ reveals envelopes for $W_2(O)_3(OAr)_5$ and $W_2O_3(OAr)_3$ at m/z 1022 and m/z 779 respectively which are analogous to the fragments observed for $Mo_2(O)_3(OAr)_6$. The 250 MHz, ^1H NMR spectrum (C_6D_6) of (9) indicates the presence of coordinated aryloxide ligands which occupy equivalent solution enviroments at room temperature. A singlet resonance is obtained for the methyl substituents at δ 2.30 ppm whilst a triplet and a doublet at δ 6.70 ppm and δ 6.91 ppm are consistent with the resonance pattern expected for the aromatic hydrogens. The $^{13}C\{^1H\}$ NMR data is consistent with the above. In the absence of crystallographic and molecular weight studies, the infrared spectra of (9) is quite informative. A strong, sharp absorption at 969 cm^{-1} may be assigned to a terminal υ(W=O) vibration, while strong broad absorbtions at 1208 and 900 cm^{-1} may be tentatively assigned to υ(C-O) and υ(O-W) respectively. The strong absorbtion at 730 cm^{-1} may be assigned to the asymmetric O=W-O-W=O stretch by comparison with other systems[54,53].

Therefore (9) most likely consists of two $W(O)(OAr)_3$ units joined by an oxo bridge analogous to the Mo compound described in section 3.4.1.

3.4.3 Other Attempts to Prepare $M(O)_2(OAr)_2$ Compounds.

The preparation of $Cr(O)_2(OBu^t)_2$ by room temperature treatment of chromium trioxide with tertiary butanol has recently been reported[55] (Equation 3.17).

$$CrO_3 + Bu^tOH \xrightarrow{CCl_4} Cr(O)_2(OBu^t)_2 + H_2O \quad (3.17)$$

It was envisaged that the reaction obetween WO_3 and either a phenol or the alkali metal phenoxide might provide a route to $W(O)_2(OAr)_2$ compounds according to equation 3.18.

$$\begin{matrix} WO_3 \\ " \end{matrix} + \begin{matrix} 2LiOAr \\ 2HOAr \end{matrix} \longrightarrow \begin{matrix} W(O)_2(OAr)_2 \\ " \end{matrix} + \begin{matrix} Li_2O \\ H_2O \end{matrix} \quad (3.18)$$

Toluene suspensions of WO_3 and either LiOAr or ArOH were refluxed for periods in excess of 48h., however on completion the starting reagents were found to be unreacted. Similar treatment of MoO_3 with LiOAr or ArOH also afforded starting materials only.

In chapter 2, $W(O)_2Cl(OSiMe_3)$ was prepared by the reaction of $W(O)Cl_4$ with 2 molar equivalents of $(Me_3Si)_2O$ in dichloromethane. It was envisaged that treatment of $W(O)_2Cl_2$ with Me_3SiOAr would yield $W(O)_2(OAr)_2$ by a similar metathetical exchange of chlorine for oxygen.

However, no reaction was observed between $W(O)_2Cl_2$ and Me_3SiOAr after 1 week at room temperature in CH_2Cl_2 or at higher temperatures in toluene solvent. The introduction of oxo ligands into a metal aryloxide coordination sphere by treatment with hexamethyldisiloxane according to equation 3.19 was also attempted.

$$WCl_4(OAr)_2 + 2(Me_3Si)_2O \longrightarrow W(O)_2(OAr)_2 + 4Me_3SiCl \quad (3.19)$$

$WCl_4(O\text{-}2,6\text{-}Ph_2C_6H_3)_2$ was prepared by the literature procedure[50] and then treated with one and subsequently two molar equivalents of $(Me_3Si)_2O$. Neither reaction proved conclusive, the only tractable products being the starting aryloxide.

3.4.4 Reaction of $Mo(O)_2Cl_2(CH_3CN)_2$ with Li-O-2,6-$Me_2C_6H_3$:

Preparation of $Mo(O)(O\text{-}2,6\text{-}Me_2C_6H_3)_4$ (6).

It has already been established that base free $Mo(O)_2Cl_2$ does not react with LiOAr to form $Mo(O)_2(OAr)_2$. Instead partial oxygen abstraction occurs with formation of $Mo_2(O)_2(\mu\text{-}O)(OAr)_6$ (9) and Li_2O. Hoffman[56] has shown that the solvent stabilised monomer $Mo(O)_2Cl_2(THF)_2$ reacts with 2 equivalents of the Grignard reagent mesitylMgBr to produce $Mo(O)_2(Mes)_2$. It was envisaged that the analogous bis(acetonitrile) complex $Mo(O)_2Cl_2(CH_3CN)_2$ might react similarly with aryloxide reagents to give $Mo(O)_2(OAr)_2$.

$Mo(O)_2Cl_2(CH_3CN)_2$ reacts with LiOAr in toluene over 18h. to produce a dark blue solution from which purple crystals can be isolated. The compound was subsequently characterised and found to be the previously prepared (Section 3.3.4) $Mo(O)(DMP)_4$ (6) (Equation 3.20) suggesting that the oxo group in $Mo(O)_2Cl_2$ is susceptible to metathetical exchange.

$$Mo(O)_2Cl_2(CH_3CN)_2 + 4LiDMP \xrightarrow[RT,\ 18h]{tol.} \underset{(6)}{Mo(O)(DMP)_4} + Li_2O + 2LiCl \quad (3.20)$$

3.4.5 Reaction of $Mo(O)_2Cl_2$ with Me_3SiO-2,6-$Me_2C_6H_3$:

Preparation of $Mo(O)Cl_2(O\text{-}2,6\text{-}Me_2C_6H_3)_2$ (10).

The apparent reactivity of the oxo groups of Mo(O)2Cl2 towards LiOAr reagents suggested that the milder reagent Me_3SiOAr may lead to selective metathesis of the chloride ligands according to equation 3.21.

$$MoO_2Cl_2 + 2Me_3SiOAr \longrightarrow Mo(O)_2(OAr)_2 + 2Me_3SiCl \quad (3.21)$$

$Mo(O)_2Cl_2$ did react at room temperature with 2 equivalents of Me_3SiOAr leading to formation of an intense blue solution over 2h. Purple, moisture sensitive crystals were isolated from the solution in 72% yield, and were found on analysis to be the previously unreported complex $Mo(O)Cl_2(O\text{-}2,6\text{-}Me_2C_6H_3)_2$ (10) in which an oxo group has been exchanged in preference to the chloro substituents.

The stoichiometry of $C_{16}H_{18}Cl_2O_3Mo$ was confirmed by elemental analysis.

Found (Required): %Mo, 22.56 (22.57), %C, 44.68 (45.20),
%H, 4.27 (4.27), %Cl, 16.82 (16.68).

The infrared spectrum of (10) revealed bands at 980 cm^{-1}, 905 cm^{-1} and 405-330 cm^{-1}, which can be assigned to υ(Mo=O), υ(Mo-O) and υ(Mo-Cl) stretches respectively. A band at 1200 cm^{-1} is consistent with the υ(C-O) stretching frequency encountered in coordinated aryloxides. The 250 MHz ^1H NMR spectrum (C_6D_6) shows only one type of environment for the coordinated aryloxide methyl groups. Mass spectrometry $(EI)^+$, reveals ions at m/z 510 and 475 corresponding to $[Mo(O)Cl(OAr)_3]^+$ and $[Mo(O)(OAr)_3]^+$ respectively. The other molybdenum containing ions in the spectrum are $[Mo(O)Cl_2(OAr)_2]^+$, $[Mo(O)Cl(OAr)_2]^+$, $[MoCl(OAr)_2]^+$, $[Mo(O)Cl_2(OAr)]^+$, $[MoCl_2(OAr)]^+$ and $[Mo(O)Cl(OAr)]^+$ at m/z 424, m/z 389, m/z 373, m/z 303, m/z 287 and m/z 268 respectively.

A cryoscopic molecular weight determination in dichloromethane on (10) showed that it is predominantly monomeric in solution with observed (calculated) molecular weights of 485 ± 50 (423). Since the observed molecular weight is slightly higher than that of the monomer, it is possible that there is a monomer- dimer equilibrium in solution with the position of the equilibrium favouring the monomer. Any dimeric form is likely to be associated through weak chloride bridges leading to octahedral coordination for molybdenum as shown in figure 3.16.

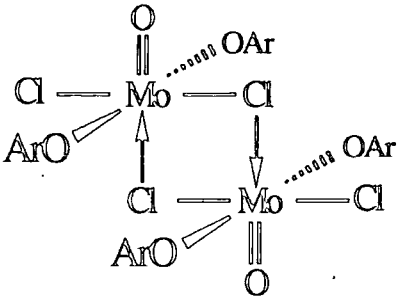

Figure 3.16, *Possible dimeric formulation for (10).*

3.4.7 Summary.

Although $W(O)Cl_4$ and $Mo(O)Cl_4$ react with lithium aryloxide reagents in a straight forward manner to give mononuclear $M(O)(OAr)_4$ (M = Mo, W) compounds, the preparation of di-oxo species of the type $M(O)_2(OAr)_2$ has proved somewhat problemmatical. A summary of the chemistry developed during attempts to prepare $Mo(O)_2(OAr)_2$ is shown in scheme 3.1.

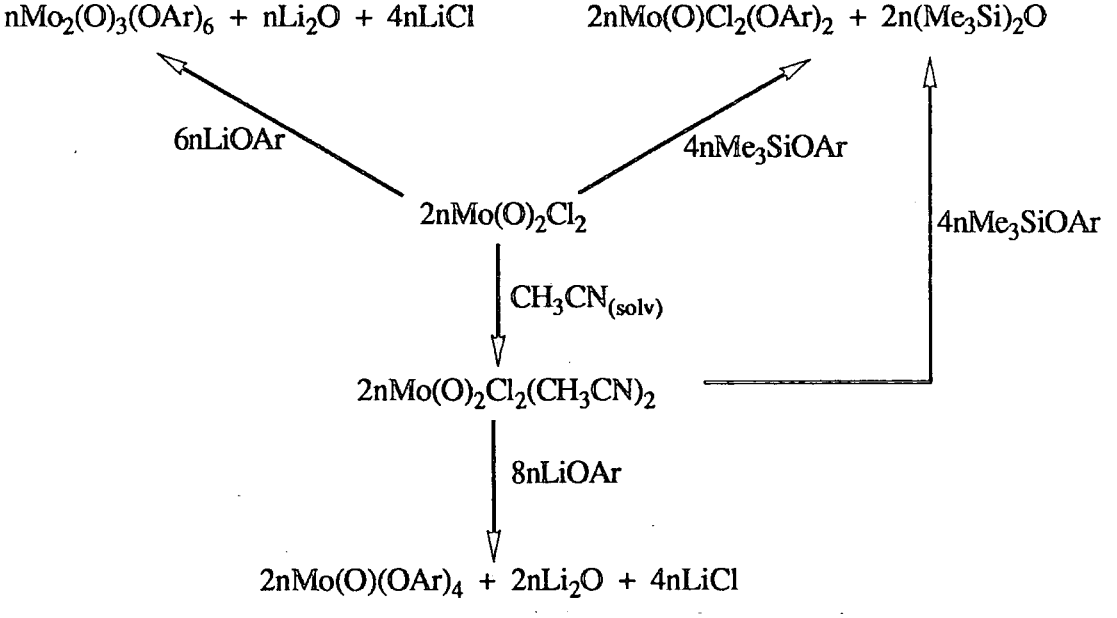

Scheme 3.1, *Reactions of $Mo(O)_2Cl_2$.*

The formation of $Mo(O)(OAr)_4$ (6) from the reaction of $Mo(O)_2Cl_2(CH_3CN)_2$ with LiOAr reflects the relative ease of substitution of one of the oxo atoms in the cis di-oxo moeity. This is further demonstrated in the reaction between $Mo(O)_2Cl_2$ and Me_3SiOAr. The formation of $Mo(O)Cl_2(OAr)_2$ (10) as opposed to $Mo(O)_2(OAr)_2$ is a clear indication of the preference for oxo abstraction over metathetical exchange of chloride groups. This apparent increase in reactivity of the molybdenum di-oxo unit over related mono-oxo species is not unexpected since molecular orbital calculations by Allison and Goddard have anticipated such a 'neighbouring oxo atom effect' and this may explain the difficulties encountered in isolate a four coordinate bis(aryloxide) cis di-oxo species.

3.5 References.

1. (a) R.A. Sheldon and J.K. Kochi, "Metal-Catalysed Oxidations of Organic Compounds", Academic Press, New York (1981). (b) R.K. Grasselli, *J. Chem. Educ.*, 1986, 63, 216. (c) W.A. Nugent and J.M. Mayer, "Metal-Ligand Multiple Bonds", John Wiley, New York (1988).
2. P.C.H. Mitchell and F. Trifiro, *J. Chem. Soc. A.*, 1970, 3183.
3. M. Cornac, A. Janin and J.C. Lavalley, *Polyhedron*, 1986, 5, 183.
4. M.H. Chisholm, K. Folting, J.C. Huffman and C.C. Kirkpatrick, *Inorg. Chem.*, 1988, 27, 264.
5. D.A. Johnson, J.C. Taylor and A.B. Waugh, *J. Inorg. Nucl. Chem.*, 1980, 42, 1271.
6. D.C. Bradley, M.H. Chisholm, M.W. Extine and M.E. Stager, *Inorg. Chem.*, 1977, 16, 1794.
7. F.A. Cotton, W. Schwotzer and E.S. Shamshoum, *J. Organomet. Chem.*, 1985, 296, 55.
8. H. Funk and G. Mohaupt, *Z. Anorg. Chem.*, 1962, 315, 204.
9. P.I. Mortimer and M. I. Strong, *Aust. J. Chem.*, 1965, 18, 1579.
10. R.J. Errington, Personnel Communication.
11. D.C. Bradley, Adv. *Inorg. Chem. Radiochem.*, 1972, 15, 259.
12. L.R. Chamberlain, I.P. Rothwell and J.C. Huffman, *Inorg. Chem.*, 1984, 23, 2575.
13. D.A. Wright and D.A. Williams, *Acta. Crystallogr.*, Sect. B., 1968, 24, 1107.

14. L.D. Durfee, S.I. Latesky, I.P. Rothwell, J.C. Huffman and K. Folting, *Inorg. Chem.*, 1985, 24, 4569.

15. L. Chamberlain, J.C. Huffman and I.P. Rothwell, *J. Am. Chem. Soc.*, 1982, 104, 7338.

16. L. Chamberlain, J. Keddington, J. C. Huffman and I.P. Rothwell, *Organometallics*, 1982, 1, 1538.

17. R.A. Jones, J.G. Hefner and T.C. Wright, *Polyhedron*, 1984, 3, 1121.

18. T.L. Lubben, P.T. Wolczanski and G.D.V. Duyne, *Organometallics*, 1984, 3, 977.

19. T.G. Appleton, H.C. Clark and L.E. Manzer, *Coord. Chem. Rev.*, 1972, 10, 335.

20. Ethyl. Corp., *Br. Pat.* 727923, 1955; *Chem. Abstr.*, 1956, 50, 5018.

21. L. Lochmann, D. Lim and J. Coupek, *Ger. Pat.* 2035260, 1971; *Chem. Abstr.*, 1971, 74, 87355.

22. H. Funk, M. Weiss and G. Mohaupt, *Z. Anorg. Allg. Chem.*, 1960, 304, 128.

23. R.C. Mehrotra and B.C. Pant, *J. Indian, Chem. Soc.*, 1962, 39, 65.

24. D.C. Bradley, R.C. Mehrotra and W. Wardlaw, *J. Chem. Soc.*, 1951, 280.

25. D.C. Bradley, F.M.A. Halim, E.a. Sadek and W. Wardlaw, *J. Chem. Soc.*, 1952, 2032.

26. D.C. Bradley, R.C. Mehrotra and W. Wardlaw, *J. Chem. Soc.*, 1953, 1634.

27. N.M. Cullinane and S.J. Chard, *Nature* (London), 1949, 164, 710.

28. D.C. Bradley, M.A. Saed and W. Wardlaw, *J. Chem. Soc.*, 1954, 1091.

29. A.J. Bloodworth and A.G. Davies, "Organotin Compounds", A.K. Sawyer Dekker, New York (1971).

30. W.J. Reagen and C.H. Brubaker, Jr., *Inorg. Chem.*, 1970, 9, 827.

31. D.C. Bradley and K.J. Fischer, MTP International Review of Science, 5, p. 6, H.J Emeleus and D.A. Sharp, Butterworth, London (1972).

32. I.D. Verma and R.C. Mehrotra, *J. Chem. Soc.*, 1960, 2966.

33. R.C. Mehrotra, *J. Ind. Chem. Soc.*, 1954, 31, 904.

34. I.M. Thomas, *Can. J. Chem.*, 1961, 39, 1386.

36. M.H. Chisholm, M.W. Extine and W.W. Reichert, *Adv. Chem. Ser.*, No. 150,273, 1976.

36. M.H. Chisholm and W.W. Reichert, *J. Am. Chem. Soc.*, 1974, 96, 1249.

37. M.H. Chisholm M.W. Extine, *J. Am. Chem. Soc.*, 1975, 97, 5625.

38. D.M. Adams, "Metal-ligand and Related Vibrations", Arnold, London (1967).

39. W.A. Nugent and J.M. Mayer, "Metal-ligand Multiple Bonds", John Wiley, New York (1988).

40. V.H. Hess and H.Z. Hartung, *Anorg. Allg. Chem.*, 1966, 334, 157.

41. J. Strahle, B. Knopp and K.P. Lorcher, *Z. Naturforsch.*, B, 1976, 1465.

42. J. Strahle, B. Knopp and K.P. Lorcher, *Anorg. Chem. Org. Chem.*, 1977, 32B, 1361.

43. M.L. Listermann, R.R. Schrock, J.C. Dewan and R.M. Kolodziej, *Inorg. Chem.*, 1988, 27, 264.

44. D.M. Berg and P.R. Sharp, *Inorg. Chem.*, 1987, 26, 2959.

45. D.C. Bradley, R.C. Mehrotra and D.P. Gour, "Metal Alkoxides", Academic Press: London, New York, San Francisco (1978).

46. W.H. Knoth and R.L. Harlow, *J. Am. Chem. Soc.*, 1981, 103, 4265.

47. M.H. Chisholm, J.C. Huffman and J.W. Pasterczyk, *Polyhedron*, 1987, 6, 1551.

48. L. Chamberlain, A.P. Rothwell and I.P. Rothwell, *J. Am. Chem. Soc.*, 1984, 106, 1847.

49. R.R. Schrock and J.D. Fellmann, *J. Am. Chem. Soc.*, 1978, 100, 3359.

50. F. Quignard, M. Leconte, J.M. Basset, Ly. Hsu, J.J. Alexander and S.G. Shore, *Inorg. Chem.*, 1987, 26, 4272.

51. D.A. Johnson, J.C. Taylor and A.B. Waugh, Inorg. *Nucl. Chem. Lett.*, 1979, 15, 205.

52. R.R. Schrock, S.A. Krouse, K. Knoll, J. Feldman, J.S. Murdzek and D.C. Yang, *J. Mol. Cat.*, 1988, 46, 243.

53. J.W. Buchler and K. Rohbock, *Inorg. Nucl. Chem. Lett.*, 1972, 8, 1073.

54. I.F. Jaffe, D. Gibson, S.J. Lippard, R.R. Schrock and A. Spool, *J. Am. Chem. Soc.*, 1984, 106, 6305.

55. T.G. Appleton, H.C. Clark and L.E. Manzer, *Synth. Comm.*, 1980, 10, 905.

56. B. Heyn and R. Hoffman, *Z. Chem.*, 1976, 16, 195.

57. C.G. Barraclough and J. Stals, *Aus. J. Chem.*, 1966, 19, 741.

Chapter Four

Bond Stretch Isomerism in Seven Coordinate Oxo- and Sulphido-Halides of Niobium and Tantalum.

4.1 Introduction.

Molecules in both the solid and solution states, which interconvert with varying degrees of ease, and whose only structural difference is a relatively small increment in the length of one or several bonds have been termed bond-stretch isomers[1] or distortional isomers[2].

The term "distortional isomerism" was first proposed by Chatt to account for blue and green forms of $Mo(O)Cl_2L_3$[4] which appeared to differ significantly only in the length of the Mo=O bond. An X-ray structure determination on the blue isomer, for L = PMe_2Ph, revealed a meridional-cis configuration (Figure 4.1). Therefore, a meridional-trans structure was assigned to the green form. However, the structure of a closely related green complex, with L=PEt_2Ph, also showed a meridional-cis structure[5] but with significantly different Mo-O and Mo-Cl (trans) bond lengths. More recently the structure of the green isomer of the original complex has been described, although not fully refined, and it too shows a similar cis-meridional geometry.[6].

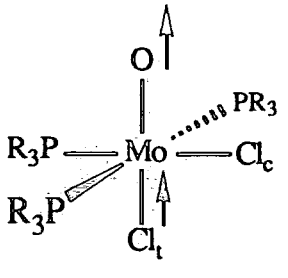

	(a), L=PMe_2Ph	(b), L=PEt_2Ph
Mo–O	1.676(7)	1.803(11)
Mo–Cl_t	2.551(3)	2.426(6)

Figure 4.1, *Molecular structures of $Mo(O)Cl_2L_3$ compounds.*

For the blue form with L = PMe_2Ph, the Mo-O bond distance is short and Mo-Cl_t long, while the reverse is true for the green form with L = PEt_2Ph (Figure 4.1).

Complex	Form	M-L (Å)	Ref.
$Mo(O)Cl_2(PEt_2Ph)_3$	Green	1.801(9)	5
$Mo(O)Cl_2(PMe_2Ph)_3$	Green	1.80(2)	4
$Mo(O)Cl_2(PMe_2Ph)_3$	Blue	1.676(7)	6
$Re(N)Cl_2(PEt_2Ph)_3$	Yellow	1.788(11)	8
$Re(N)Cl_2(PEt_2Ph)_3$	Yellow	1.660(8)	9
$[Mo(O)(CN)_4(H_2O)](PPh_4)_2$	Green	1.72(2)	10
$Mo(O)(CN)_4(H_2O)](AsPh_4)_2$	Blue	1.60(2)	10
$[Mo(O)Cl(HBpz_3)]_2(\mu\text{-}O)$	C_i form	1.779(6)	11
$[Mo(O)Cl(HBpz_3)]_2(\mu\text{-}O)$	C_2 form	1.671(4)	11
$[Mo(O)(OH)(dppe)_2]BF_4$		1.883(5)	12
$[Mo(O)Cl(dppe)_2]^+$		1.708(12)	13
$[Mo(O)Br_4]PPh_4$		1.726(14)	14
$[Mo(O)Cl_4]AsPh_4$		1.610(10)	15
$Mo(O)_2(ONCH_2CH_2CH_2CH_2CH_2)_2$		1.879(5), 1.701(5)	16
$Mo(O)_2(ONEt_2)_2$		1.714(2), 1.713(2)	17
$[W(O)Cl_2[C\text{-}(NMeCH_2CH_2)_3]PF_6$	Blue	1.719(18)	7
$W(O)Cl_2(C\text{-}(NMeCH_2CH_2)_3]PF_6$	Green	1.893(20)	7
$[Ru(O)Cl\text{-}C\text{-}(NMe)_4C_{10}H_{20}]ClO_4$		1.765(7)	18
$[Ru(O)Cl(Py)_4]ClO_4$		1.862(*)	19
$[Nb(O)Cl_5](AsPh_4)_2$		1.976(6)	20
$[Nb(O)F_5]^{2-}$		1.75(2)	21
$[Nb(O)Cl_3(PMe_3)_3]$	Green	2.087(5)	22
$[Nb(O)Cl_3(PMe_3)_3]$	Yellow	1.781(6)	22
$Nb(S)(S_2CNEt_2)_3$	Yellow	2.164	23
$Nb(S)(S_2CNEt_2)_3$	Yellow	2.112	23

Table 4.1, ***Bond stretch isomers and related species.***

Since Chatts proposals there have been a number of other structures reported with metal-ligand multiple bond distances more than 0.1Å longer than isomeric or very similar species (Table 4.1). In one case[7], Wieghardt and co-workers have shown that for $(LWOCl_2)^+$ complexes (L=N,N',N" trimethyl-1,4,7-triazacyclononane), the two isomers are stable in solution. This example indicates that distortional isomerism is not solely a solid state phenomenon arising due to crystal packing forces or disorder.

In the absence of more well characterised bond stretch isomer pairs, it is difficult to generalise as to the origin of the phenomenon. There are however some common characteristics in the compounds listed in table 4.1. First, there is always a large change in the metal-oxygen bond length between isomers (0.05 - 0.31Å) accompanied by more or less apparent variations of the other metal-ligand bond lengths. Secondly, colour differences, presumably due to L→ M charge transfer[7], often accompany the marked difference in metal-oxygen distance and lastly all the complexes are relatively high oxidation states of Mo, W or Nb and therefore electron deficient. Hoffmann, Burdett and co-workers have forwarded explanations of bond-stretch isomerism in terms of a frontier orbital crossing of (M-L) and (M-O) antibonding molecular orbitals or a second order Jahn-Teller effect (SOJT). The former rationale appears to be valid only for d^n systems where n>0 and is therefore not so generally applicable. The SOJT effect outlined by Hoffman predicts two energy minima as the (M-O) bond is lengthened and the equatorial bonds shortened. The effect has been shown to be sensitive to the π bonding capabilities of the ancillary ligands. In particular, π donor ligands trans to the oxygen atom favour a double minimum and hence bond-stretch isomerism. Undoubtedly, a better comprehension of this phenomenon may hold the key to an understanding of the bonding and reactivity of multiply-bonded main group atoms in the coordination sphere of transition metals and may also have important implications for bonding in general. But, as Hoffmann points out in his theoretical treatment, many more examples will be required before the phenomenon is well understood.

4.2 Bond Stretch Isomers of $Nb(O)Cl_3(PMe_3)_3$.

In 1988, the first tertiary phosphine adduct of $Nb(O)Cl_3$, *viz.* $Nb(O)Cl_3(PMe_3)_3$, was prepared by Dr. R.M. Sorrell in this laboratory and characterised by X-ray crystallography[24]. The molecular structure is illustrated in figures 4.2 and 4.3. Subsequent investigations by T.P. Kee revealed that an isomeric form could be isolated upon recrystallisation, and an X-ray structure determination on this compound revealed an exceptionally elongated Nb=O bond (2.09 Å), all other parameters within the molecule remaining essentially unchanged. For discussion purposes, the isomer with the shorter Nb=O distance is referred to as α-$Nb(O)Cl_3(PMe_3)_3$ while the isomer with the elongated Nb=O bond is refered to as β-$Nb(O)Cl_3(PMe_3)_3$.

In view of the importance of this phenomenon in assessing the bonding of main group atoms such as oxygen or sulphur to transition metals and the ready accessibility of niobium and tantalum oxo- and sulphido-halide starting materials from the studies described in chapter 2, we decided to prepare a series of complexes of the type $M(Y)X_3(P)_3$ where M = Nb, Ta; Y = O, S; X = Cl, Br and P = PR_3 to establish whether or not bond-stretch isomerism is a general phenomenon accompanying these seven coordinate complexes. Interestingly, although T.P. Kee was able to prepare the dimethyl phenyl phosphine analogue, $Nb(O)Cl_3(PMe_2Ph)_3$, this showed no evidence for bond-stretch isomerism. Therefore, our studies commenced with an investigation of compounds of the type $Nb(O)X_3(PMe_3)_3$ (X = Cl, Br).

4.3 Bond Stretch Isomers of $Nb(O)X_3(PMe_3)_3$ (X=Cl, Br).

4.3.1 Further Analysis of α- and β-$Nb(O)Cl_3(PMe_3)_3$ (1).

Although displaying behaviour typical of bond stretch isomers, the magnitude of the effect shown by $Nb(O)Cl_3(PMe_3)_3$ [Δ (Nb=O) ca. 0.3 Å] is considerably larger than that shown in both d^2 and d^1 systems (see Table 4.1). Crystal packing forces are

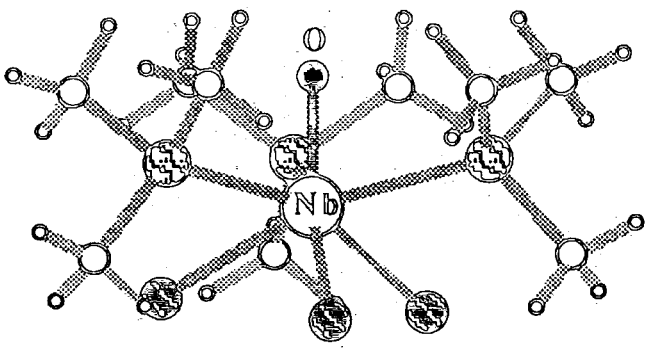

Nb=O 1.78 Å (2.09 Å)

Figure 4.2, *Molecular structure of* $Nb(O)Cl_3(PMe_3)_3$.

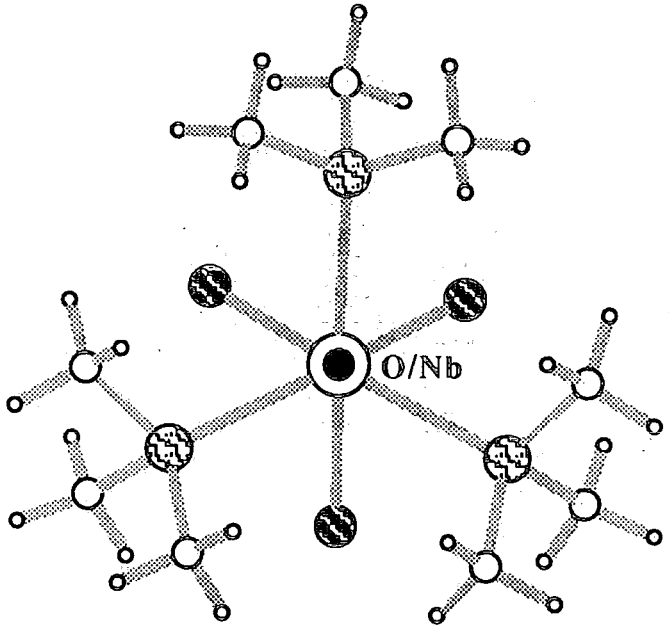

Figure 4.3, *View down the oxygen-niobium vector of* $Nb(O)Cl_3(PMe_3)_3$

unlikely to result in bond length changes > 0.1 Å[2], and since both (1)-α and (1)-β are isomorphous with similar intramolecular ligand conformations the (Nb-O) bond difference undoubtedly results from factors other than packing or conformational differences. In (1)-β, the (Nb=O) bond length of 2.087(5) Å, is comparable to the sum of the covalent radii of niobium and oxygen (2.1 Å)[25] suggesting that the bond order is close to unity. The possibility of the bond lengthened form being a hydroxide species was entertained since the hydroxide complex $H_2[Nb^{(v)}O(OH)(C_2O_4)_2.H_2O].4H_2O$ has a (Nb-OH) bond length 2.100(3) Å. The hydroxyl proton would not be evident in the X-ray structural analysis and the broadening of the ^1H NMR resonance could be the result of the transition from diamagnetic $Nb^{(V)}(O)Cl_3(PMe_3)_3$ to paramagnetic $Nb^{(IV)}(OH)Cl_3(PMe_3)_3$. The possibility that (1)-β contains a niobium hydroxide moiety as opposed to an oxo group is not supported however by infrared spectroscopy, which provides no evidence for a υ(OH) stretching vibration >3000 cm^{-1} and the υ(Nb=O) vibration at 871 cm^{-1} is comparable in both shape and intensity to that in (1)-α and is 300 cm^{-1} higher than is normally observed for metal hydroxide (M-O) vibrations[26].

In order to rule out unequivocally the possibility of a paramagnetic Nb(IV) hydroxide, a 250 mg sample was weighed into a glass ampoule, sealed and subjected to Vibrating Sample Magnetometry. A plot of magnetism (J/T/Kg) against field strength showed the sample to be fundamentally diamagnetic with only the slightest amount of paramagnetism possibly due to a Nb(IV) impurity arising by decomposition. Thus, all the evidence suggests that (1)-α and β are *bona fide* bond stretch isomers.

4.3.2 Reaction of $Nb(O)Br_3$ and $Nb(O)Br_3(CH_3CN)_2$ with PMe_3: *Preparation of α- and β-$Nb(O)Br_3(PMe_3)_3$ (2).*

The preparation of α-$Nb(O)Cl_3(PMe_3)_3$ from the reaction of $Nb(O)Cl_3$ with PMe_3 has been described previously. When the reaction is carried out using $Nb(O)Br_3$, prepared by the procedure outlined in chapter 2, a trimethylphosphine

complex of stoichiometry, $Nb(O)Br_3(PMe_3)_3$ is isolated in 67% yield. This orange, crystalline solid is moderately soluble in aromatic and chlorinated hydrocarbons and is moisture sensitive. Infrared spectroscopy revealed that this compound was essentially a mixture of two oxo complexes in the ratio 40:60 assuming the Nb-O bonds possess similar absorption coefficients. The Nb=O bands for these species occur at 882 and 871 cm^{-1} respectively with the lower wavenumber species being predominent. Remarkably, these stretching frequencies are identical to those observed for α- and β-$Nb(O)Cl_3(PMe_3)_3$ suggesting that replacement of the chloride ligands for bromide has little effect on υ(Nb=O). Dissolution of the mixture in toluene and cooling at -35°C for 2 weeks resulted in the selective crystallisation of the predominant complex (the β-isomer) as red cubes. This is in contrast to the crystallisation of a mixture of α- and β-$Nb(O)Cl_3(PMe_3)_3$ which under the same conditions affords the α-isomer.

Elemental analysis confirmed the stoichiometry as $Nb(O)Br_3(PMe_3)_3$. The infrared spectrum displays absorptions typical of coordinated PMe_3 at 1279 cm^{-1} [$\sigma(CH_3)$], 953 cm^{-1} [$\rho(CH_3)$] and 740 cm^{-1} [$\upsilon_{as}(PC_3)$][27] respectively. The strong absorption at 871 cm^{-1} is consistent with the presence of a terminal oxo ligand[28] and bands between ca. 250 - 350 cm^{-1} are assignable to (Nb-Br) stretching vibrations[26]. The 250 MHz ^1H NMR spectrum (C_6D_6) consists of a single broad resonance at δ 1.13 ($\Delta_{1/2}$ ca. 18 Hz). However, a signal could not be observed in the $^{31}P\{^1H\}$ spectrum at room temperature possibly due to the very weak sample or broadening due to the presence of small amounts of a paramagnetic impurity (solutions of (1) and (2), upon standing, release $O{=}PMe_3$ and deposit a paramagnetic solid.

The reaction between $Nb(O)Br_3(CH_3CN)_2$ and PMe_3 in dichloromethane has been used to selectively produce β-$Nb(O)Cl_3(PMe_3)_3$ since this is formed in the higher proportion by this route. However, the reaction of $Nb(O)Br_3(CH_3CN)_2$ and PMe_3 in CH_2Cl_2 affords a similar α:β ratio (45:55), and attempts to isolate the α-isomer by selective crystallisation from this mixture were unsuccessful. However, in light of the similarity between the infrared spectra for $Nb(O)Br_3(PMe_3)_3$ and $Nb(O)Cl_3(PMe_3)_3$ and in particular the identical υ(Nb=O) vibrational frequency of (1)-α (882 cm^{-1}) and

Figure 4.4, *Infrared spectra of α-, and β-Nb(O)Br3(PMe3)3 (2)*

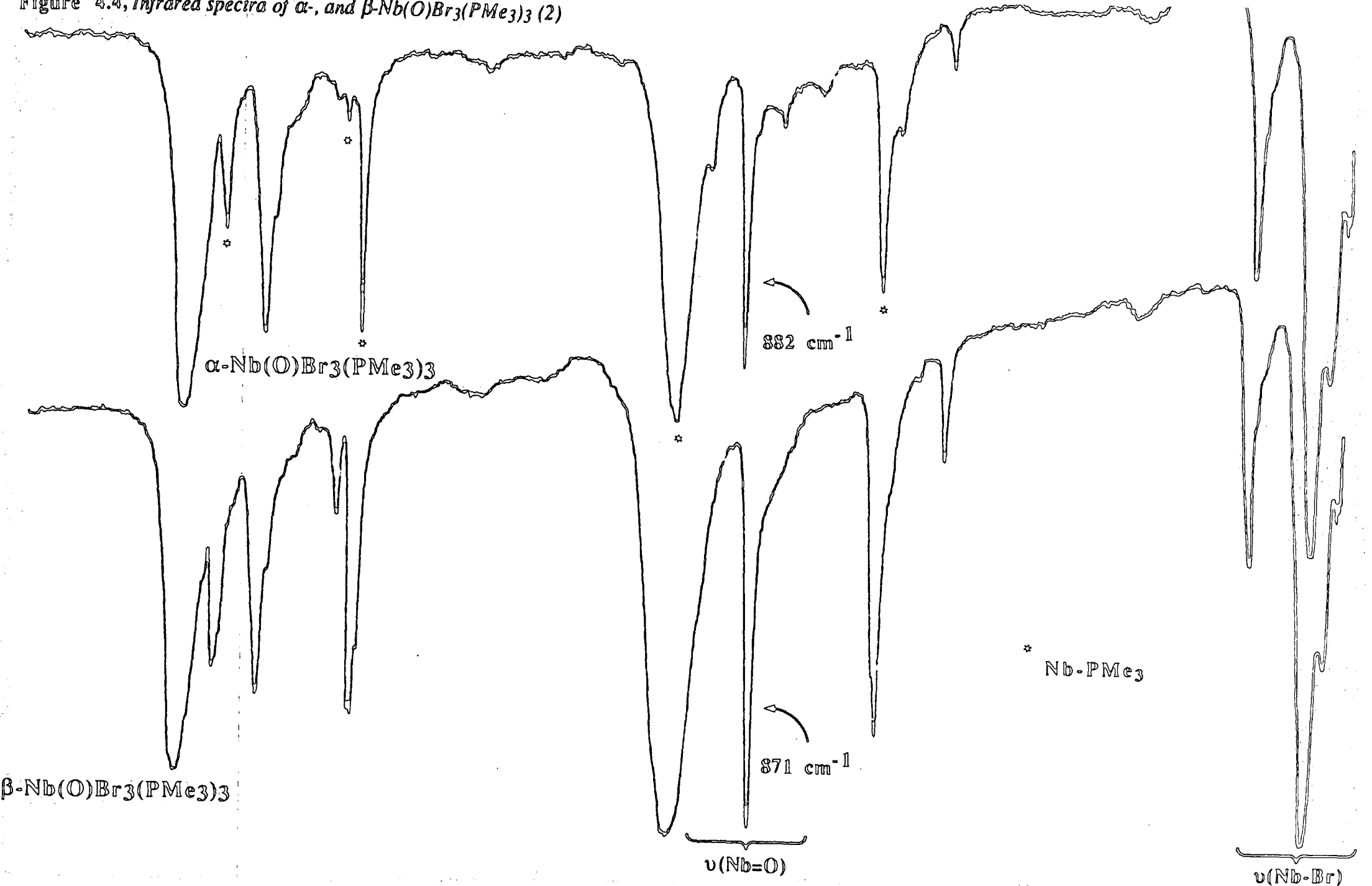

the second oxo species in the above mixture (882 cm^{-1}) (Figure 4.4), it is not unreasonable to assume that the non-isolated species is in fact the α- form of $Nb(O)Br_3(PMe_3)_3$ (2).

4.4 Bond Stretch Isomers of $Nb(S)X_3(PMe_3)_3$ (X=Cl, Br).

4.4.1 Reaction of $Nb(S)Cl_3$ and $Nb(S)Cl_3\cdot(L)_2$ (L = CH_3CN, THF) with PMe_3:

Preparation of α- and β-$Nb(S)Cl_3(PMe_3)_3$ (3).

The occurrence of bond-stretch isomers for the oxo-halides of niobium led us to investigate the analogous sulphide compounds. When $Nb(S)Cl_3$ is treated with PMe_3 in CH_2Cl_2, a complex of stoichiometry, $Nb(S)Cl_3(PMe_3)_3$ maybe isolated in 56% yield. This yellow, crystalline solid is moderately soluble in aromatic and chlorinated hydrocarbons and is moisture sensitive. Infrared spectroscopy revealed that this compound was essentially a mixture of two sulphido complexes in the ratio 20:80, the compound with the higher υ(Nb=S) being the predominent species. Dissolution of the mixture in toluene and cooling at -35°C for 2 weeks resulted in the selective crystallisation of this species as green cubes.

Elemental analysis confirmed the stoichiometry as $Nb(S)Cl_3(PMe_3)_3$. The infrared spectrum was recorded over the range 4000 - 250 cm^{-1}. Apart from absorptions due to trimethylphosphine ligands the spectrum showed bands assignable to metal-sulphur and metal-chlorine stretching modes. A most significant feature of the spectrum is the low value (489 cm^{-1}) observed for υ(Nb=S) vibration. With few exceptions, previously characterised compounds containing terminal niobium sulphur ligands usually give absorptions > ca. 500 cm^{-1} (Table 4.2). The low value for (3) presumably reflects the high coordination number and the presence of three highly basic PMe_3 ligands. The 250 MHz ^1H NMR spectrum (C_6D_6) of (3) consists of a single broad resonance at δ 1.33 ($\Delta_{1/2}$ ca. 13 Hz) while the $^{31}P\{^1H\}$ spectrum did not reveal

No.	Complex	de⁻	CN	Nb=S (Å)	υ (cm⁻¹)	Ref.
1.	$Nb(S)(SPh_4)^-$	0	5	2.171(2)	525	29
2.	$Nb(S)Cl_4^-$	0	5	2.085(5)	552	30
3.	$Nb(S)Cl_3(SPPh_3)$	0	5	2.114(4)	536	32
4.	$[Nb(S)Cl_3(SPPh_3)]_2$	0	6	2.129	537	22
5.	$Nb(S)Br_3(THT)_2$	0	6	2.09(8)		33
6.	$Nb_6S_{17}^{4-}$	0	6	2.196(4)	483	34
7.	$Nb(S)(S_2CNEt_2)_3$	0	7	2.122(1)	493	35
8.	$Nb(S)(S_2CNEt_2)_3$	0	7	2.168(1)	500	35
9.	$Nb(S)(S_2CNEt_2)_3$	0	7	2.112(3)	500	23
10.	$Nb(S)(S_2CNEt_2)_3$	0	7	2.164(3)	500	23
11.	α-$Nb(S)Cl_3(PMe_3)_3$	0	7	2.194(2)	455	This work
12.	β-$Nb(S)Cl_3(PMe_3)_3$	0	7	2.296(1)	489	This work
13.	$Nb(S)Cl_3$	0	6		542	36
14.	$Nb(S)Br_3$	0	6		552	37
15.	$Nb(S)Cl_3(MeCN)_2$	0	6		524	This work
16.	$Nb(S)Cl_3(MeCN)_2$	0	6		528	This work
17.	$Nb(S)Cl_3(THF)_2$	0	6		529	This work

Table 4.2

any signal at room temperature again possibly due to its low solubility or the presence of paramagnetic impurities arising by partial decomposition.

The reaction between $Nb(S)Cl_3(CH_3CN)_2$ and PMe_3 in dichloromethane proceeded in a similar manner to above although the product mixture contained the two sulphido complexes in different proportions 45:55 the compound with the higher υ(Nb=S) still being the predominant species. Dissolution of the mixture in toluene and cooling at -35°C for 4 weeks resulted in the selective crystallization of the other species as orange cubes.

Elemental analysis confirmed the stoichiometry as $Nb(S)Cl_3(PMe_3)_3$ implicating an isomer of (3). Infrared spectroscopy revealed that this compound was essentially analogous to (3) apart from a shift in the υ(Nb=S) stretching frequency of 34 Hz to lower wavenumber (Figure 4.5). The 250 MHz ^1H NMR spectrum (C_6D_6) locates the PMe_3 hydrogens as a slightly broadened doublet resonance at δ 1.41 [$^2J(PH)$ = 8.9 Hz] suggesting equivalent solution enviroments for the phosphine ligands. A signal could not be observed in the $^{31}P\{^1H\}$ spectrum at room temperature.

Single crystal, X-ray diffraction studies on both the green and orange forms confirmed that they are isomorphous with a significant difference only in the metal sulphur bond parameter (Section 4.4.2). For discussion purposes, the orange isomer will be referred to as (3)-α (the shorter Nb-S bond) and the green isomer as (3)-β (the longer Nb-S bond).

Curiously, the Nb-S stretching frequency does not appear to correlate with Nb-S bond distance for these isomers, which is somewhat surprising since reasonable correlation is usually found for niobium sulphides (a selection taken from Table 4.2 are represented graphically in Figure 4.6). (3)-β, instead of having a lower frequency υ(Nb=S) stretch is shifted 34 Hz to higher wavenumber than (3)-α. A possible explanation for this anomaly is discussed in section 4.5.

Figure 4.5, *Infrared spectra of α-, and β-Nb(S)Cl3(PMe3)3 (3).*

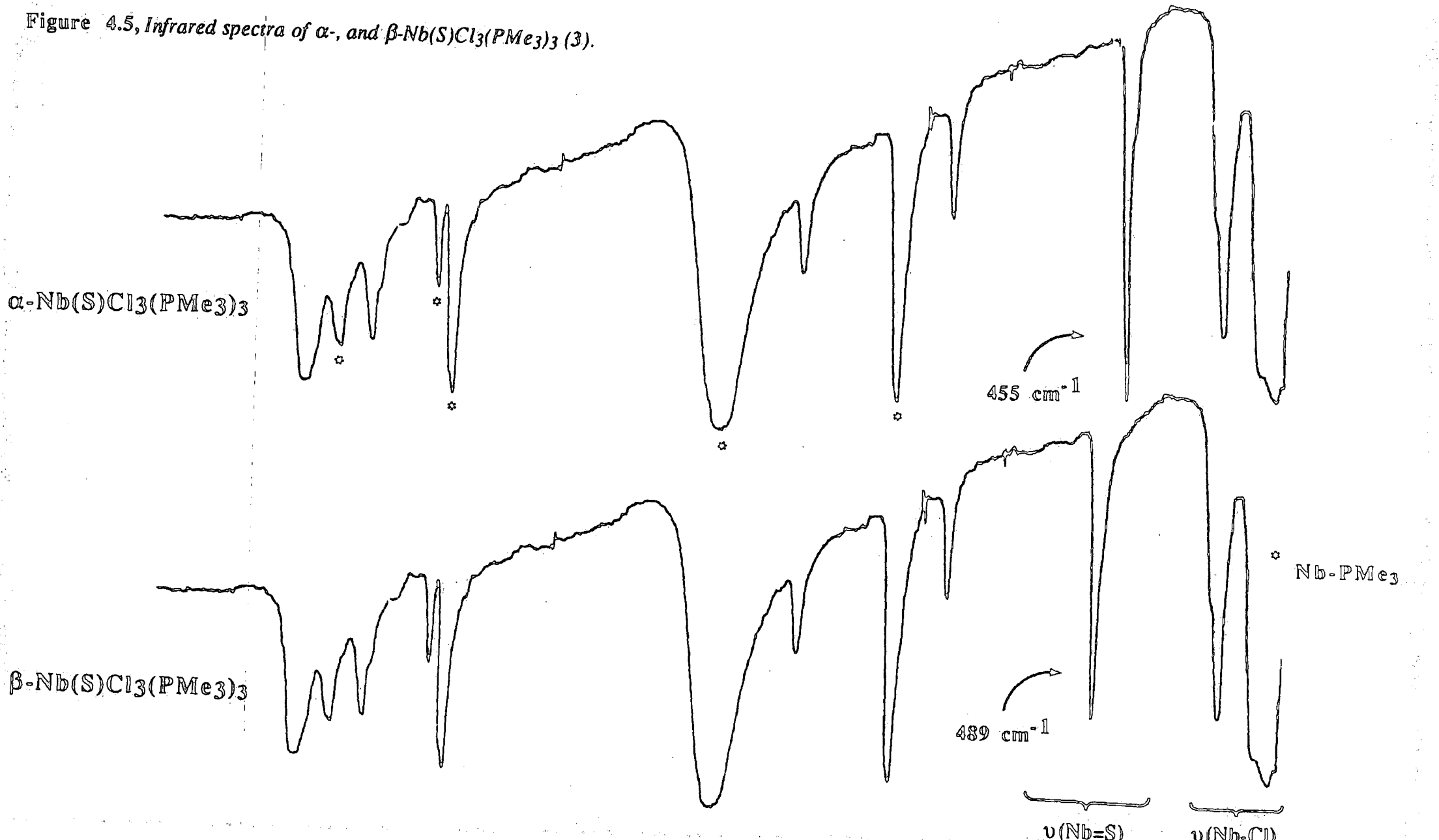

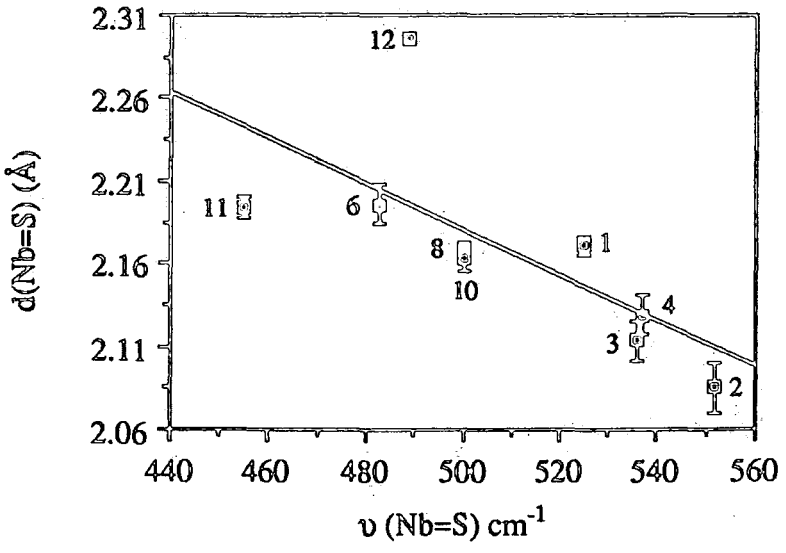

Figure 4.6, *Plot of d(Nb=S) (Å) versus υ(Nb=S) cm^{-1}.*

4.4.2 The Molecular Structures of α- and β-$Nb(S)Cl_3(PMe_3)_3$.

The isolation of two isomeric compounds with the formula $Nb(S)Cl_3(PMe_3)_3$ was described in section 4.4.1. Both forms, orange (3)-α and green (3)-β have been subjected to X-ray diffraction analysis by Dr. M. McPartlin and coworkers at the Polytechnic of North London and the results of these studies are described below.

The Orange Isomer, (3)-α.

The crystal data are collected in appendix 1E and the molecular structure is illustrated in figures 4.7 and 4.8. Selected bond angles and distances are given in table 4.3.

The complex is monomeric for which the coordination geometry is best described as distorted, monocapped octahedral (Figure 4.7) with facial arrangements of chloro and trimethylphosphine ligands giving the molecule virtual C_{3v} symmetry (Figure 4.8). The sulphido group is in a site capping the face defined by the phosphine ligands and lies above the P(1), P(2), P(3) plane, with the niobium atoms below this plane. This coordination is similar to that observed in $NbCl_4(PMe_3)_3$[38], yet very

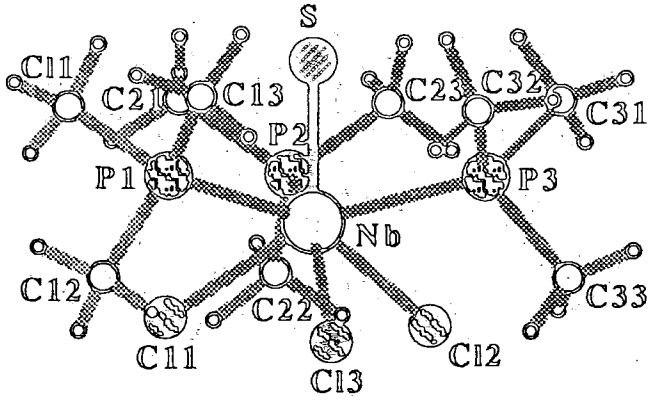

Figure 4.7, *Molecular structure of α-Nb(S)Cl$_3$(PMe$_3$)$_3$.*

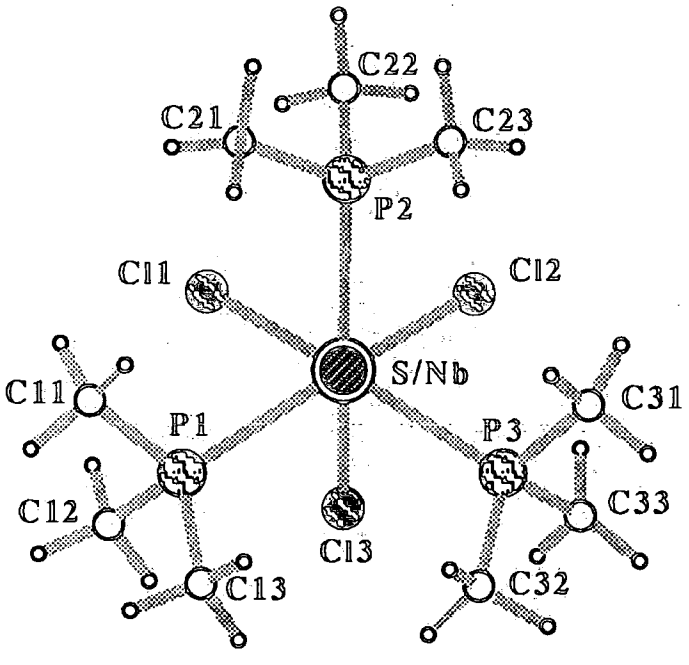

Figure 4.8, *View down the sulphur-niobium vector of α-Nb(S)Cl$_3$(PMe$_3$)$_3$*

Nb - Cl(1) 2.490(2)
Nb - Cl(2) 2.516(2)
Nb - Cl(3) 2.491(2)

Nb - P(1) 2.640(2)
Nb - P(2) 2.640(2)
Nb - P(3) 2.636(2)

Nb - S 2.194(2)

P(1) - C(11) 1.816(10)
P(1) - C(12) 1.827(11)
P(1) - C(13) 1.807(11)
P(2) - C(21) 1.824(11)
P(2) - C(22) 1.835(10)
P(2) - C(23) 1.824(10)
P(3) - C(31) 1.821(10)
P(3) - C(32) 1.808(9)
P(3) - C(33) 1.812(10)

Cl(2) - Nb - Cl(1) 88.8(1)
Cl(3) - Nb - Cl(1) 87.2(1)
Cl(3) - Nb - Cl(2) 91.2(1)

P(1) - Nb - Cl(1) 74.8(1)
P(1) - Nb - Cl(2) 158.9(1)
P(1) - Nb - Cl(3) 75.2(1)
P(2) - Nb - Cl(1) 75.3(1)
P(2) - Nb - Cl(2) 73.7(1)
P(2) - Nb - Cl(3) 156.8(1)
P(3) - Nb - Cl(1) 153.7(1)
P(3) - Nb - Cl(2) 73.7(1)
P(3) - Nb - Cl(3) 74.0(1)

P(2) - Nb - P(1) 113.5(1)
P(3) - Nb - P(1) 116.4(1)
P(3) - Nb - P(2) 116.5(1)

S - Nb - Cl(1) 128.8(1)
S - Nb - Cl(2) 123.4(1
S - Nb - Cl(3) 125.7(1)

S - Nb - P(1) 77.7(1)
S - Nb - P(2) 77.5(1)
S - Nb - P(3) 77.5(1)

C(11) - P(1) - Nb 113.1(3)
C(12) - P(1) - Nb 119.2(4)
C(13) - P(1) - Nb 114.1(6)
C(21) - P(2) - Nb 114.4(4)
C(22) - P(2) - Nb 117.2(4)
C(23) - P(2) - Nb 113.3(4)
C(31) - P(3) - Nb 113.6(4)
C(32) - P(3) - Nb 113.5(4)
C(33) - P(3) - Nb 119.3(4)

C(12) - P(1) - C(11) 101.5(6)
C(13) - P(1) - C(11) 104.3(6)
C(13) - P(1) - C(12) 102.8(6)
C(22) - P(2) - C(21) 103.2(5)
C(23) - P(2) - C(21) 102.3(5)
C(23) - P(2) - C(22) 104.8(5)
C(32) - P(3) - C(31) 103.5(6)
C(33) - P(3) - C(31) 103.1(5)
C(33) - P(3) - C(32) 102.0(5)

Table 4.3, *Selected bond distances (Å) and angles (°) for α-Nb(S)Cl$_3$(PMe$_3$)$_3$ (3).*

different to the seven coordinate complex $Nb(S)(S_2CNEt_2)_3$[23], in which the niobium atom is at the centre of a distorted pentagonal bypyramid.

The (Nb=S) bond length of 2.194(1) Å is at the far end of the range of distances usually observed in four to seven coordinate sulphido-niobium complexes (2.085(5) - 2.196(4) Å) (Table 4.2). This presumably arises due to the presence of three, highly electron releasing PMe_3 ligands within the crowded coordination sphere of (3)-α.

The compounds (3)-α and $NbCl_4(PMe_3)_3$[38] are isomorphous (space group $P2_{1/c}$). The average (Nb-Cl) distances in (3)-α [2.499(2) Å] are slightly longer than the average facial (Nb-Cl) distances in $NbCl_4(PMe_3)_3$ [2.453(13) Å] the opposite of the trend predicted on the basis of oxidation state. Since both compounds possess average $P\text{-}Nb\text{-}Cl_{trans}$ angles of ca. 157°, a similar average trans influence is anticipated due to the sulphido ligand. Therefore, the average lengthening observed in (3)-α may be attributed to the presence of the sulphido ligand.

Interestingly, the Nb-Cl (2) bond is the longest [2.501(1) Å] whilst also having the most acute S-Nb-Cl angle of 121.8°, an observation at variance with a sulphido ligand trans influence. However, since the trans P-Nb-Cl angle for Cl(2) is the largest (158.9°), this atom may experience a slightly larger PMe_3 trans influence.

The (Nb-P) bonds have an average length of 2.639(1) Å in (3)-α and 2.651(6) Å in $NbCl_4(PMe_3)_3$, the former having the slightly shorter distances as expected for niobium (V) over niobium (IV).

The acute S-Nb-P angles [average 77.6(1)°] lead to a staggered arrangement of PMe_3 substituents with respect to the capping sulphur atom (as viewed along the P-Nb vector) in order to minimise interligand repulsions. A similar arrangement is found in $NbCl_4(PMe_3)_3$. Consequently, close S....H contacts result, in the range 2.83 - 3.03 Å. Indeed these distances are comparable to the sum of the Van der Waals radii of niobium and sulphur (3.0 Å)[25]. Figure 4.9 (a) represents a space filling diagram of

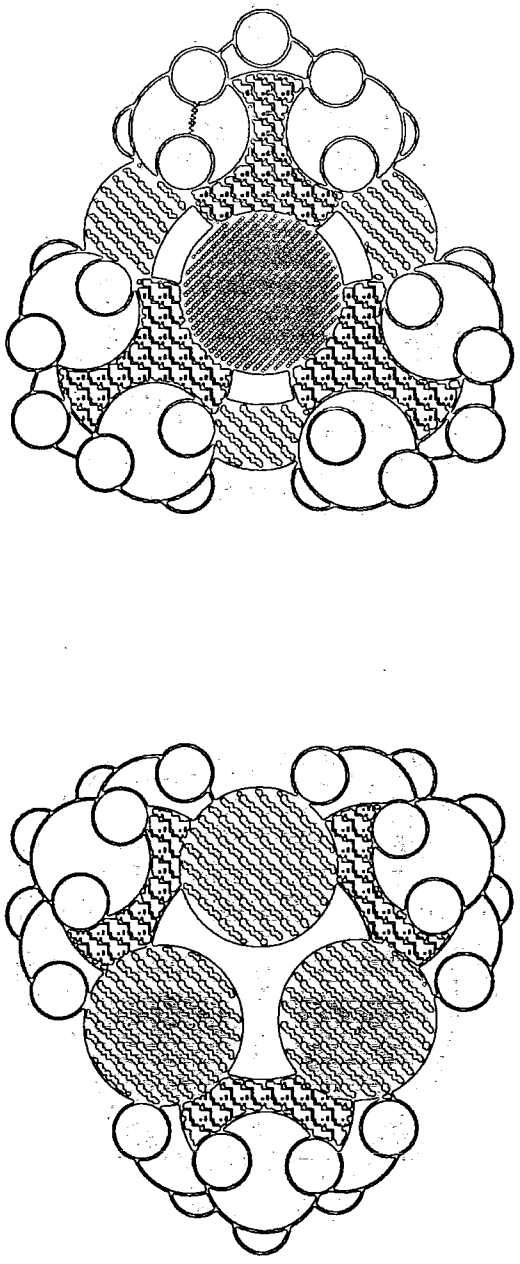

Figure 4.9, *Space filling diagrams of α-Nb(S)Cl_3(PMe_3)$_3$;*
(a) View down the sulphur-niobium vector;
(b) View down the chloro face.

(3)-α viewed down the (S=Nb) vector illustrating the extremely close contacts between the sulphur atom and six phosphine-methyl hydrogens (H-H). Figure 4.9 (b) is a similar diagram viewed through the facial chlorine plane.

The Green Isomer, (3)-β.

The crystal data are collected in appendix 1F and the molecular structure is illustrated in figures 4.10 and 4.11. Selected bond angles and distances are given in table 4.4 and comparative values of selected parameters for (3)-α, (3)-β and for a tantalum analogue (5-β) described later are displayed in table 4.5.

Parameter	(3)-α	(3)-β	(5)-β
(M=S)	2.194(2)	2.296(1)	2.219(2)
$(M\text{-}Cl)_{av}$	2.499(2)	2.486(1)	2.486(2)
$(M\text{-}P)_{av}$	2.639(2)	2.649(1)	2.635(2)
$S\text{-}M\text{-}Cl_{av}$	126.0(1)	125.8(1)	126.4(1)
$S\text{-}M\text{-}P_{av}$	77.6(1)	76.3(1)	77.5(1)
$P\text{-}M\text{-}P_{av}$	115.5(1)	114.6(1)	115.4(1)
$Cl\text{-}M\text{-}Cl_{av}$	89.1(1)	89.3(1)	88.3(1)
$P\text{-}M\text{-}Cl_{trans,\ av}$	156.5(1)	157.7(1)	156.1(1)

Table 4.5, *Comparitive values of some parameters for (3)-α, (3)-β α and (5)-β.*

The green compound (3)-β is isomorphous to (3)-α (space group $P2_{1/c}$, appendix 1F) and the average interatomic distances and angles are essentially identical, although the β-isomer shows larger individual deviations.

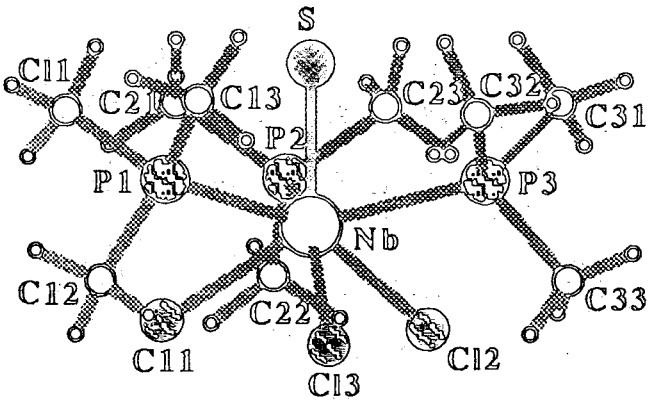

Figure 4.10, *Molecular structure of β-Nb(S)Cl$_3$(PMe$_3$)$_3$.*

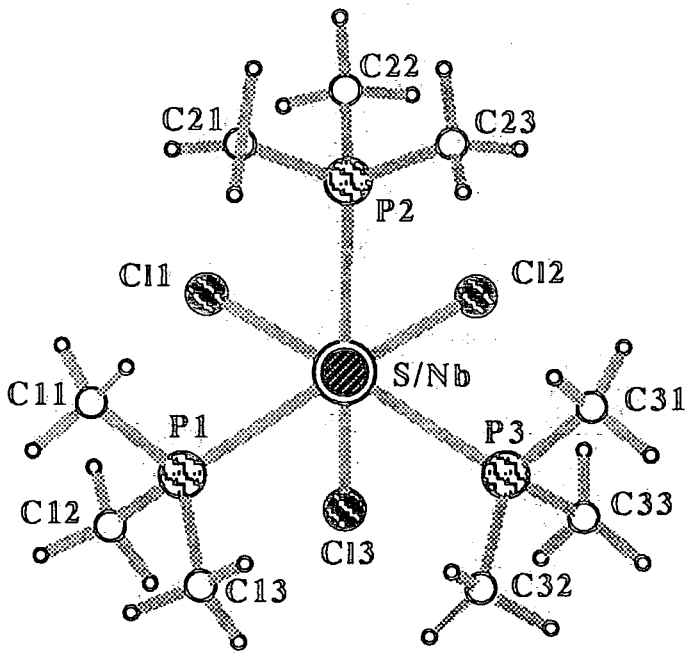

Figure 4.11, *View down the sulphur-niobium vector of β-Nb(S)Cl$_3$(PMe$_3$)$_3$*

Nb - Cl(1) 2.475(1)
Nb - Cl(2) 2.501(1)
Nb - Cl(3) 2.482(1)

Nb - P(1) 2.647(1)
Nb - P(2) 2.654(1)
Nb - P(3) 2.647(1)

Nb - S 2.296(1)

P(1) - C(11) 1.813(6)
P(1) - C(12) 1.817(6)
P(1) - C(13) 1.811(6)
P(2) - C(21) 1.826(6)
P(2) - C(22) 1.812(6)
P(2) - C(23) 1.828(6)
P(3) - C(31) 1.826(5)
P(3) - C(32) 1.802(5)
P(3) - C(33) 1.819(5)

Cl(2) - Nb - Cl(1) 88.2(1)
Cl(3) - Nb - Cl(1) 86.6(1)
Cl(3) - Nb - Cl(2) 93.1(1)

P(1) - Nb - Cl(1) 76.0(1)
P(1) - Nb - Cl(2) 161.2(1)
P(1) - Nb - Cl(3) 76.1(1)
P(2) - Nb - Cl(1) 76.2(1)
P(2) - Nb - Cl(2) 74.8(1)
P(2) - Nb - Cl(3) 159.0(1)
P(3) - Nb - Cl(1) 153.0(1)
P(3) - Nb - Cl(2) 74.4(1)
P(3) - Nb - Cl(3) 74.2(1)

P(2) - Nb - P(1) 110.4(1)
P(3) - Nb - P(1) 116.1(1)
P(3) - Nb - P(2) 117.3(1)

S - Nb - Cl(1) 131.2(1)
S - Nb - Cl(2) 121.8(1)
S - Nb - Cl(3) 124.4(1)
S - Nb - P(1) 76.8(1)
S - Nb - P(2) 76.4(1)
S - Nb - P(3) 75.8(1)

C(11) - P(1) - Nb 114.4(2)
C(12) - P(1) - Nb 117.8(2)
C(13) - P(1) - Nb 113.5(2)
C(21) - P(2) - Nb 116.2(2)
C(22) - P(2) - Nb 117.0(2)
C(23) - P(2) - Nb 112.7(2)
C(31) - P(3) - Nb 113.2(2)
C(32) - P(3) - Nb 114.2(2)
C(33) - P(3) - Nb 117.9(2)

C(12) - P(1) - C(11) 103.1(3)
C(13) - P(1) - C(11) 103.8(2)
C(13) - P(1) - C(12) 102.6(3)
C(22) - P(2) - C(21) 102.9(3)
C(23) - P(2) - C(21) 103.0(3)
C(23) - P(2) - C(22) 103.2(3)
C(32) - P(3) - C(31) 104.4(2)
C(33) - P(3) - C(31) 102.7(2)
C(33) - P(3) - C(32) 103.0(2)

Table 4.4, *Selected bond distances (Å) and angles (°) for β-Nb(S)Cl$_3$(PMe$_3$)$_3$ (3).*

The (Nb-Cl) distances are slightly shorter and the (Nb-P) distances marginally longer for the β-isomer.

Without doubt, the most marked difference between the isomers is the length of the niobium-sulphur bond. In (3)-β this bond has been lengthened by ca. 0.10 Å over that in (3)-α and is ca. 0.15 Å longer than is usually found in niobium sulphido compounds. Indeed this distance is approaching the sum of the covalent radii of niobium and sulphur (2.39 Å)[25] and therefore must be regarded as a bond order considerably less than 2.

4.4.3 Reaction of $Nb_3S_3Br_8$ and $Nb(S)Br_3(CH_3CN)_2$ with PMe_3 Preparation of α- and β-$Nb(S)Br_3(PMe_3)_3$ (4)

The reaction between $Nb_3S_3Br_8$ and PMe_3 in dichloromethane afforded a pale yellow precipitate and a clear red solution. Filtration of the solution followed by concentration and cooling gave red, moisture sensitive crystals in 54% yield. Elemental analysis (Chapter 7, section 7.4.3) confirmed the stoichiometry as $Nb(S)Br_3(PMe_3)_3$ (4) and infrared spectroscopy indicated the presence of a terminal Nb=S ligand with $\upsilon(Nb{=}S)$ = 489 cm^{-1}. The 250 MHz ^1H NMR spectrum (C_6D_6) revealed a single resonance at δ 1.42 ($\Delta_{1/2}$ ca. 18 Hz) while the $^{31}P\{^1H\}$ spectrum did not reveal any signal at room temperature.

Due to the similarity of the infrared spectra of β-$Nb(S)Cl_3(PMe_3)_3$ and (4), and the similarly broad resonances found in the ^1H NMR spectra, it is presumed that (4) is the β (bond lengthened) form of $Nb(S)Br_3(PMe_3)_3$ and can therefore be expected to possess a similar coordination geometry, i.e. a facial arrangement of chloro and trimethylphosphine ligands with the sulpur atom capping the P_3 face.

The reaction between $Nb(S)Cl_3(CH_3CN)_2$ and PMe_3 in dichloromethane proceeded in a similar manner to above although the product mixture contained three sulphido complexes in the proportions 35:30:35, the component constituting 30% of the mixture may be assigned to β-$Nb(S)Br_3(PMe_3)_3$ (4) whilst the other two

components exhibit υ(Nb=S) stretches at 505 cm^{-1} and 455 cm^{-1} respectively. It was previously found that exchange of chloride for bromide ligands in the oxides $Nb(O)X_3(PMe_3)_3$ had no effect upon the Nb-O stretching frequency. Therefore, given the similarity of υ(Nb=S) for (3)-β and (4)-β, it is not unreasonable to assign the absorbtion at 455 cm^{-1} to the υ(Nb=S) stretching frequency of α–$Nb(S)Br_3(PMe_3)_3$. Attempts to isolate this isomer by selective crystallization of a saturated toluene solution of the mixture were, however, unsuccessful. The identity of the third species remains unknown.

4.5 Bond Stretch Isomers of $Ta(S)Cl_3(PMe_3)_3$.

4.5.1 Reaction of $Ta(S)Cl_3$ with PMe_3:

Preparation of α- and β-$Ta(S)Cl_3(PMe_3)_3$ (5).

The reaction of $Ta(S)Cl_3$ with PMe_3 in dichloromethane gives a yellow solid which is found to be a mixture of two tantalum-sulphido compounds. The infrared spectrum gives absorptions at 430 and 470 cm^{-1} in the ratio 90:10 due to Ta-S stretching vibrations. Elemental analysis also confirms a stoichiometry of $Ta(S)Cl_3(PMe_3)_3$ (Chapter 7, section 7.4.4).

This yellow crystalline compound is moderately soluble in aromatic and chlorinated hydrocarbons and is less moisture sensitive than either (1) or (3). The infrared spectrum of (5) also displays absorptions typical of coordinated PMe_3 at 1301 cm^{-1} [$\sigma(CH_3)$], 950 cm^{-1} [$\rho(CH_3)$] and 733 cm^{-1} [$\upsilon_{as}(PC_3)$] respectively[27], and metal halide stretching vibrations are found in the region 285 - 350 cm^{-1}.

The most significant feature of the spectrum is the extremely low value (430 cm^{-1}) observed for the υ(Ta=S) vibration of the 90% abundant species. Previously characterised molecular compounds containing terminal tantalum sulphur ligands invariably give absorbtions > 460 cm^{-1} (Table 4.6). The low value for (5) probably reflects the high coordination number, as in $Ta(S)(S_2CNEt_2)_3$[39], and the

presence of three, sterically demanding, strongly basic PMe_3 ligands as in $Nb(S)Cl_3(PMe_3)_3$. The 250 MHz ^1H NMR spectrum (C_6D_6) locates the PMe_3 hydrogens as a slightly broadened doublet resonance at δ 1.41 [$^2J(PH)$ = 8.9 Hz] suggesting equivalent solution environments for the phosphine ligands. The $^{31}P\{^1H\}$ spectrum did not give a signal at room temperature. Dissolution of the compound in toluene and cooling at -35°C for 2 days did not give crystals of the 90% abundant species but rather large orange prisms of the minor component. Clearly conversion had taken place in solution to account for the now large quantity of orange product.

Complex	de⁻	CN	Ta=S (Å)	ν (cm⁻¹)	Ref.
$Ta(S)(S_2CNEt_2)_3$	0	7	2.181(1)	479	39
$Ta(S)Cl_3(bpte)$	0	6	2.204(5)	516	40
α-$Ta(S)Cl_3(PMe_3)_3$	0	7		430	This work
β-$Ta(S)Cl_3(PMe_3)_3$	0	7	2.219(2)	470	This work
$Ta(S)Br_3$	0	6		448	41
$Ta(S)Cl_3$	0	6		460	This work
$Ta(S)Cl_3(MeCN)_2$	0	6		510	40
$Ta(S)Br_3(MeCN)_2$	0	6		508	40
$Ta(S)Cl_3(tht)_2$	0	6		505	40
$Ta(S)Br_3(tht)_2$	0	6		504	40
$Ta(S)Cl_3(dms)_2$	0	6		510	40
$Ta(S)Br_3(dms)_2$	0	6		506	40
$Ta(S)Br_3(bpte)_2$	0	6		512	40

Table 4.6.

Figure 4.12, *Infrared spectra of α-, and β-Ta(S)Cl$_3$(PMe$_3$)$_3$ (5).*

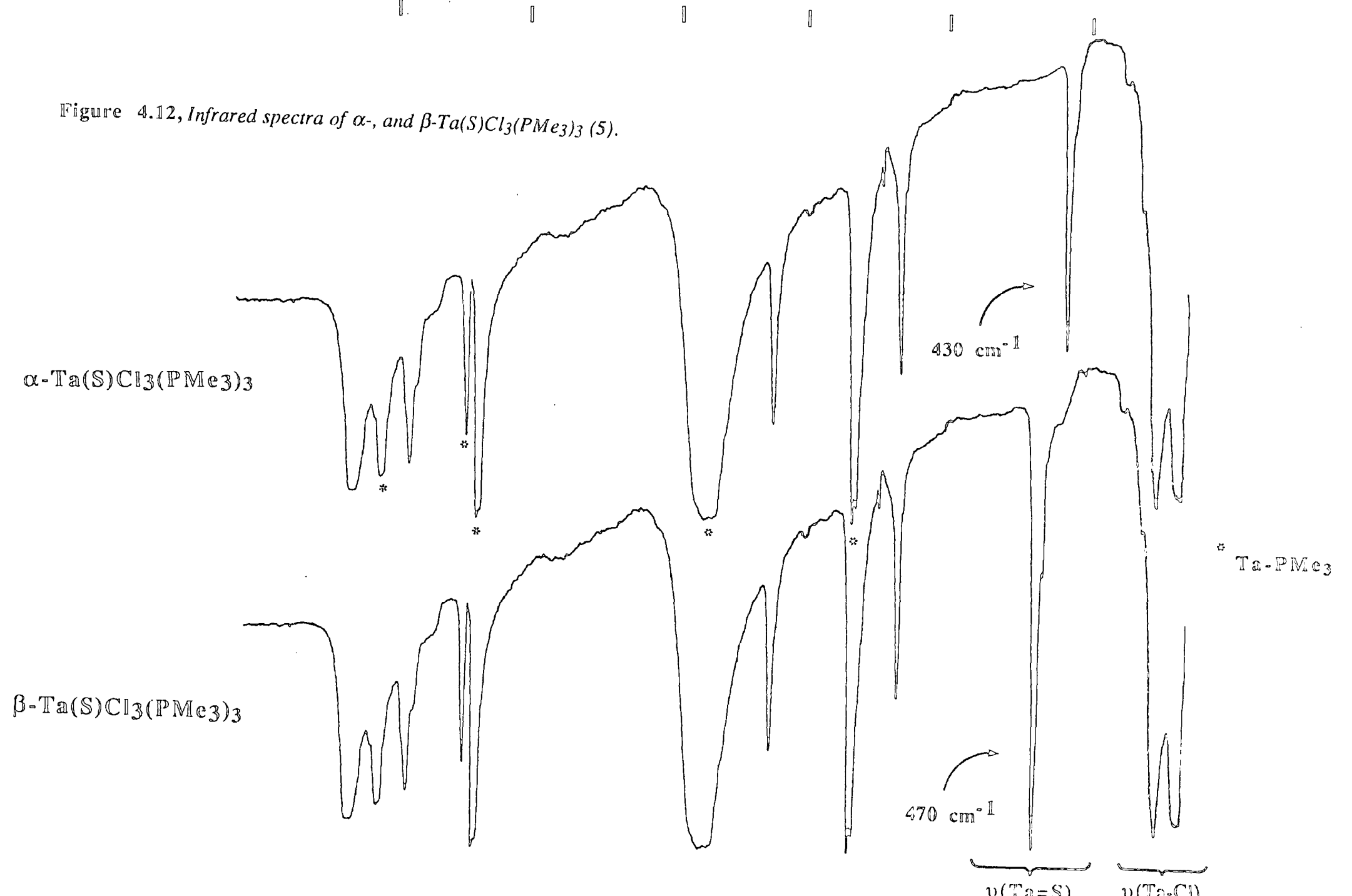

Elemental analysis on the orange compound also confirmed a stoichiometry of $Ta(S)Cl_3(PMe_3)_3$ and its infrared spectrum showed the higher frequency Ta-S stretch at 470 cm^{-1}. The 250 MHz ^1H NMR spectrum (C_6D_6) consists of a broad singlet resonance at δ 1.40 ($\Delta_{1/2}$ ca. 18 Hz) while the $^{31}P\{^1H\}$ spectrum did not give a signal at room temperature. The mass spectrum (CI^+, ^{181}Ta, ^{35}Cl, ^{32}S) displays an envelope at m/z 546 attributable to the parent ion and daughter fragments at m/z 470, m/z 435 and m/z 400 attributable to $[M\text{-}PMe_3]^+$, $[M\text{-}PMe_3,Cl]^+$ and $[M\text{-}PMe_3,2Cl]^+$ respectively.

An X-ray structural determination of the orange compound confirms that the complex is a seven coordinate monomer and is isomorphous to β-$Nb(S)Cl_3(PMe_3)_3$ (3). A description of the structure is presented in the following section.

In the case of α- and β-$Nb(S)Cl_3(PMe_3)_3$, an X-ray structural determination on both crystal forms allowed an unequivocal assignment of the α- and β-isomers. In the above, the X-ray determination shows that the orange form possess a (Ta=S) bond length of 2.219(2) Å, a length in between the α- and β-forms of $Nb(S)Cl_3(PMe_3)_3$. Given the apparent anomoly in the infrared data, this can no longer be used for an unambiguous assignment of α- and β-forms. However, if the same anomoly operates for the Ta compounds, then the structurally characterised derivative would be the β-form. This would also be consistent with the observation that the thermodynamic product is usually the bond lengthened (i.e. β) isomer. Thus, the orange compound is tentatively formulated as β-$Ta(S)Cl_3(PMe_3)_3$ and the yellow complex as α-$Ta(S)Cl_3(PMe_3)_3$.

4.5.2 Molecular Structure of β-$Ta(S)Cl_3(PMe_3)_3$ (5).

Orange (5)-β has been subjected to X-ray diffraction analysis by Dr. M. McPartlin and coworkers at the Polytechnic of North London. The crystal data are collected in

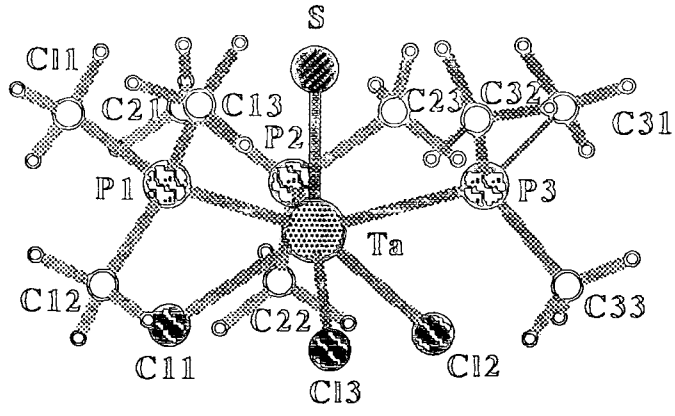

Figure 4.13, *Molecular structure of β-Ta(S)$Cl_3(PMe_3)_3$.*

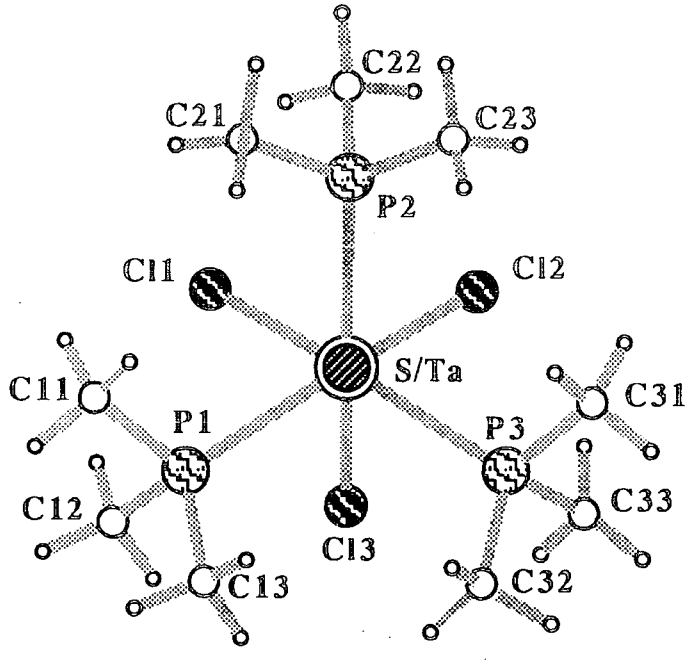

Figure 4.14, *View down the sulphur-tantalum vector of β-Ta(S)$Cl_3(PMe_3)_3$*

Ta - Cl(1) 2.479(2)
Ta - Cl(2) 2.501(2)
Ta - Cl(3) 2.479(2)

Ta - P(1) 2.631(2)
Ta - P(2) 2.639(2)
Ta - P(3) 2.636(2)

Ta - S 2.219(2)

P(1) - C(11) 1.822(9)
P(1) - C(12) 1.819(8)
P(1) - C(13) 1.821(9)
P(2) - C(21) 1.829(9)
P(2) - C(22) 1.827(9)
P(2) - C(23) 1.816(8)
P(3) - C(31) 1.822(8)
P(3) - C(32) 1.808(8)
P(3) - C(33) 1.811(8)

Cl(2) - Ta - Cl(1) 88.0(1)
Cl(3) - Ta - Cl(1) 86.3(1)
Cl(3) - Ta - Cl(2) 90.7(1)

P(1) - Ta - Cl(1) 75.2(1)
P(1) - Ta - Cl(2) 158.8(1)
P(1) - Ta - Cl(3) 75.5(1)
P(2) - Ta - Cl(1) 75.4(1)
P(2) - Ta - Cl(2) 74.1(1)
P(2) - Ta - Cl(3) 156.4(1)
P(3) - Ta - Cl(1) 153.0(1)
P(3) - Ta - Cl(2) 74.0(1)
P(3) - Ta - Cl(3) 74.2(1)

P(2) - Ta - P(1) 113.0(1)
P(3) - Ta - P(1) 116.3(1)
P(3) - Ta - P(2) 117.0(1)

S - Ta - Cl(1) 129.7(1)
S - Ta - Cl(2) 123.4(1)
S - Ta - Cl(3) 126.2(1)
S - Ta - P(1) 77.8(1)
S - Ta - P(2) 77.3(1)
S - Ta - P(3) 77.3(1)

C(11) - P(1) - Ta 113.0(3)
C(12) - P(1) - Ta 119.0(3)
C(13) - P(1) - Ta 113.3(3)
C(21) - P(2) - Ta 114.4(3)
C(22) - P(2) - Ta 117.7(3)
C(23) - P(2) - Ta 112.3(3)
C(31) - P(3) - Ta 113.6(3)
C(32) - P(3) - Ta 113.5(3)
C(33) - P(3) - Ta 118.4(3)

C(12) - P(1) - C(11) 103.1(5)
C(13) - P(1) - C(11) 104.5(5)
C(13) - P(1) - C(12) 102.3(4)
C(22) - P(2) - C(21) 102.7(4)
C(23) - P(2) - C(21) 103.6(5)
C(23) - P(2) - C(22) 104.5(4)
C(32) - P(3) - C(31) 103.1(4)
C(33) - P(3) - C(31) 103.1(4)
C(33) - P(3) - C(32) 103.3(4)

Table 4.7, *Selected bond distances (Å) and angles (°) for β-Ta(S)Cl$_3$(PMe$_3$)$_3$ (5).*

appendix 1H and the molecular structure is illustrated in figures 4.13 and 4.14. Selected bond angles and distances are given in table 4.7.

The compound is isomorphous to (3)-α and (3)-β (space group $P_{21/c}$, appendices 1F and 1G). Values of selected parameters for (5)-β are displayed along side (3)-α and (3)-β in table 4.5 and essentially, the average bond lengths and angles are identical.

The most significant feature is the length of the tantalum-sulphur bond. In (5)-β this is 0.015 Å longer than the longest (Ta=S) bond previously reported for six coordinate $Ta(S)Cl_3(bpte)$[40] and 0.038 Å longer than the seven coordinate complex $Ta(S)Cl_3(S_2CNEt_2)_3$[39].

4.6 Infrared Spectroscopy of Bond Stretch Isomers.

The very small difference in the υ(Nb=O) stretching frequencies (11 cm^{-1}) for α-and β-$Nb(O)X_3(PMe_3)_3$ (X = Cl, Br) and the reversal of the anticipated υ(M=S) vibrations for α-and β-$Nb(S)Cl_3(PMe_3)_3$ and α-and β-$Ta(S)Cl_3(PMe_3)_3$ are not readily explained. For a full understanding of the origin of these bands, mixing of all the vibrations (i.e. the normal coordinates) of the molecule may have to be considered. However, comparison of α-and β-$Nb(O)Cl_3(PMe_3)_3$ with α-and β-$Nb(O)Br_3(PMe_3)_3$, which possess identical υ(Nb=O) stretching frequencies, suggests that the Nb–O stretch is not significantly perturbed by changes in the ancillary halide ligand set. Moreover, since the M–P and M–Cl distances and inter-ligand angles for *all* of the isomers are almost the same within the bounds of the structure determinations (Table 4.5), the ancillary ligand bond lengths and geometries do not appear to have an important influence on the M-Y stretching frequencies. We have entertained the possibility that one of the isomers may possess a subtle but significant interaction with the closeby PMe_3 groups. However, in this case changes in the bands due to M–PMe_3 (asterisked in Figures 4.4, 4.5 and 4.12) would be anticipated: no such changes are observed. A more probable explanation for these unusual effects may lie in an

enhanced ionic contribution to the elongated Nb–Y bond resulting in a form reminiscent of Me_3N^+–O^- or the canonical form (III) shown below in figure 4.15.

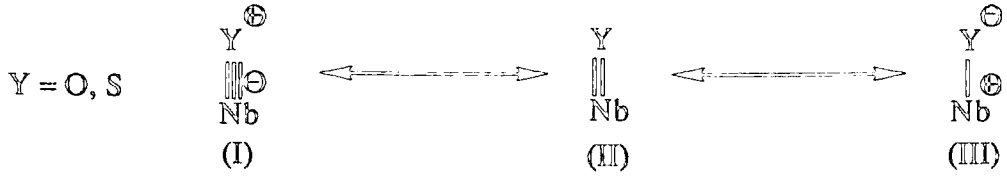

Figure 4.15

This would adequately account for why the M–Y stretching frequency does not correlate with covalent bond order and also the reversal of the M=S stretching frequencies should the ionic contribution increase in dominance. It would also be consistent with the shorter Ta-S distance in β-$Ta(S)Cl_3(PMe_3)_3$ compared with β-$Nb(S)Cl_3(PMe_3)_3$ since the Ta-S bond is expected to be more highly polarised due to the greater electropositivity of tantalum (all other factors e.g. ionic radii being equal).

More studies involving correlation of infrared and possibly Raman spectroscopies with the results of M.O. calculations will undoubtedly be required before a full explanation of this remarkable phenomenom is forthcoming. These studies are in progress.

4.7 Reactivity Studies.

The factors which govern the stability and interconversion of the isomers are of central importance to an understanding of the phenomenon of bond stretch isomerism. The observations in the preceding sections clearly show that conversion between isomers does occur in solution. This invariably involves a transformation of the α-form into the apparently thermodynamically preferred β-form. This section is concerned with a further investigation of the solution and solid state stability of the bond-stretch isomer pairs.

T.P.Kee observed[24] (^{1}H NMR) that α- and β-$Nb(O)Cl_3(PMe_3)_3$ decompose readily in solution within 24 h., to give a paramagnetic species and $O{=}PMe_3$. $Nb(O)Br_3(PMe_3)_3$ decomposes similarly. The niobium sulphides $Nb(S)X_3(PMe_3)_3$ (X=Cl, Br), however, are markedly more stable in solution although eventually their decomposition follows a similar pattern affording $SPMe_3$ and a paramagnetic species. By far the most stable are the isomers of $Ta(S)Cl_3(PMe_3)_3$ which degrade only after prolonged standing in solution at room temperature (typically 2 weeks). Therefore, these were chosen for more detailed examination.

A sample of $Ta(S)Cl_3(PMe_3)_3$ (§) (90%α, 10%β) stored under argon at room temperature for one week in a sealed glass tube, showed by infrared analysis a mixture of (§)-β (56%) and a significant reduction in intensity of the signal due to (§)-α (44%) suggesting that a solid state conversion of (§)-α to (§)-β is occuring. When the experiment was repeated on a fresh sample under similar conditions but in the absence of light, the infrared revealed a 49:51 mixture of (§)-α to (§)-β indicating that the process proceeds thermally. However, a sample sealed in a glass tube and exposed to ultraviolet radiation, gave a mixture of (§)-α (51%) and (§)-β (49%) after only 2h, suggesting that the conversion, although thermally induced, is also enhanced photochemically. Interestingly, a sample of pure (§)-β remains unchanged when exposed to both uv or heat suggesting that the conversion of α→β is irreversible. A more detailed kinetic analysis of this solid state transformation is currently in progress.

In solution, the conversion is assumed to be rapid since signals are observed (^{1}H NMR (C_6D_6)) for both α and β isomers immediately upon mixing. Significant features of the ^{1}H NMR spectrum are a virtually coupled triplet resonance at δ 1.72 and a doublet resonance at δ 1.03 [^2J (PH) = 14.7 Hz] which continue to grow over a period of several days at room temperature. The signal at δ 1.03 is consistent with the shift reported for $SPMe_3$ (Chapter 7, section 7.1). Indeed, when $SPMe_3$ is added to the solution this signal is enhanced confirming that $SPMe_3$ is generated by the solution decomposition of $Ta(S)Cl_3(PMe_3)_3$ (§). The origin of the virtually coupled triplet is as

yet unknown although the pattern could indicate the presence of trans phosphines[43]. Since $SPMe_3$ is generated it is highly likely that $Ta(S)Cl_3(PMe_3)_3$ (5) decomposes (*via* loss of $SPMe_3$) to give $TaCl_3(PMe_3)_2$ which is known to dimerise to the binuclear tantalum species shown in equation 4.1.

$$2Ta(S)Cl_3(PMe_3)_3 \longrightarrow Ta_2Cl_6(PMe_3)_4 + 2SPMe_3 \quad (4.1)$$

The rate of decomposition of (5) is unaffected by ultraviolet light. However, upon heating a solution of (5) in C_6D_6 at 70°C, the generation of $SPMe_3$ and the consequent decomposition of $Ta(S)Cl_3(PMe_3)_3$ is accelerated.

Attempts to prepare bond-stretch isomers with other tertiary phosphines have thus far not been successful. However, the room temperature treatment of β-$Ta(S)Cl_3(PMe_3)_3$ with 2 equivalents of PMe_2Ph in C_6D_6 resulted (by ^1H NMR) in partial phosphine exchange suggesting that mixed phosphine derivatives of (5) could be accessible.

4.8 Summary.

A series of monomeric, seven coordinate niobium and tantalum trimethyl phosphine complexes of the general type $M(Y)X_3(PMe_3)_3$ (M=Nb; Y=O, S; X=Cl, Br and M=Ta; Y=S; X=Cl) have been prepared that exhibit the phenomenom of bond-stretch isomerism.

The X-ray structures of α-$Nb(S)Cl_3(PMe_3)_3$, β-$Nb(S)Cl_3(PMe_3)_3$ and β-$Ta(S)Cl_3(PMe_3)_3$ have been determined. For each pair there is a significant difference in the length of the metal-oxygen and metal-sulphur bond with little or no change in the other structural parameters.

Preliminary investigations into the stability of the isomers have revealed that decomposition occurs *via* loss of $Y=PMe_3$ (Y=O, S) and that the α-isomers invariably convert to the β-form. Remarkably, this transformation takes place in the solid state for

$Ta(S)Cl_3(PMe_3)_3$. Clearly, much more work will be required before this phenomenon is fully understood. However, the X-ray determinations described in this chapter offer a firm base for future theoretical analyses.

4.9 References.

1. (a) Y. Lean, A. Lledos, J.K. Burdett and R. Hoffmann, *J. Chem. Soc. Chem. Commun.*, 1988, 140.
   (b) Y. Lean, A. Lledos, J.K. Burdett and R. Hoffmann, *J. Am. Chem. Soc.*, 1988, 110, 4506.
2. J. Chatt, L. Manojlovic-Muir and W.K. Muir, *J. Chem. Soc. Chem. Commun.*, 1971, 655.
3. F.A. Cotton, M.P. Diebold and W.J. Roth, *Inorg. Chem.*, 1987, 26, 2848.
4. A.V. Butcher and J. Chatt, *J. Chem. Soc. A*, 1970, 2652.
5. L. Manojlovic-Muir and K.W. Muir, *J. Chem. Soc. Dalton Trans.*, 1972, 686.
6. B.L. Haymore, W.A. Goddard and J.N. Allison, *Proc. Int. Conf. Coord. Chem. 23rd.*, 1984, 535.
7. K. Wieghardt, G. Backes-Dahmann, B. Nuker and J. Weiss, *Angew. Chem. Int. Ed. Engl.*, 1985, 24, 777.
8. P.W.R. Corfield, R.J. Doedens and J.A. Ibers, *Inorg. Chem.*, 1967, 6, 197.
9. E. Forsellini, U. Casellato, R. Graziani and L. Magon, *Acta. Cryst.*, 1982, B38, 3081.
10. K. Wieghardt, G. Backes-Dahmann and G. Holzbach, *Z. Anorg. Allg. Chem.*, 1983, 499, 44.
11. S.Lincoln and S.A. Koch, *Inorg. Chem.*, 1986, 25, 1594.
12. M.R. Churchill and F.J. Rotella, *Inorg. Chem.*, 1978, 17, 668.
13. M.W. Bishop, J. Chatt and J.R. Dilworth, *J. Chem. Soc. Dalton Trans.*, 1979, 1603.
14. F. Weller and K. Dehnicke, *Z. Anorg. Allg. Chem.*, 1982, 495, 135.
15. C.D. Garner, L.H. Hill, F.E. Mabbs and D.L. McFadden, *J. Chem. Soc. Dalton Trans.*, 1977, 853.
16. K. Wieghardt, B. Nuber and J. Weiss, *Angew. Chem. Int. Ed. Engl.*, 1985, 24, 790.
17. L. Saussine, H. Mimoun, A. Mitschler and J. Fischer, *Nouv. J. Chim.*, 1980, 4, 235.

18. C.M. Che, Y.K. Wang and T.C.W. Mak, *J. Chem. Soc. Chem. Commun.*, 1985, 988.

19. K. Aoyagi, Y. Yukawa, K. Shimuzu and M. Mukaida, *Bull. Chem. Soc. Jpn.*, 1986, 59, 1493

20. U. Mullerr and I. Lorenz, *Z. Anorg. Allg. Chem*, 1980, 463, 110.

21. Y. Gorbunov, V.I. Pakhomov and E.S. Kovaleva, *Zh. Strukh. Khim.*, 1972, 13, 165.

22. K. Gebreyes, J. Zubieta, T.A. George and L.M. Koczon, *Inorg. Chem.*, 1986, 25, 405.

23. M.G.B. Drew, D.A. Rice and D.M. Williams, *J. Chem. Soc. Dalton Trans.*, 1985, 1821.

24. (a) V.C. Gibson, T.P. Kee, R.M. Sorrell, A.P. Bashall and M. McPartlin, *Polyhedron*, 1988, 7, 2221.
(b) T.P. Kee, Ph.D.Thesis, Durham University, 1989.

25. W.W. Porterfield, "Inorganic Chemistry-A Unified Approach", Addison-Wesley, New York (1984).

26. D.M. Adams, "Metal-Ligand and Related Vibrations", Edward Arnold, London (1967).

27. J. Nieman, J.H. Teuben, J.C. Huffman and K.G. Caulton, *J. Organometallic Chem.*, 1983, 255, 193.

28. V. Katovic and C. Djordjevic, *Inorg. Chem.*, 1970, 9, 1729.

29. G. Christou, J.C. Huffman and J.L. Seela, *Polyhedron*, 1989, 8, 1797.

30. P. Klingelhofer and U. Muller, *Z. Anorg. Allg. Chem.*, 1984, 510, 109.

31. M.G.B. Drew, R.J. Hobson, G.W.A. Fowles and D.A. Rice, *Inorg. Chim. Acta..*, 1976, L35, 20.

32. M.G.B. Drew and R.J. Hobson, *Inorg. Chim. Acta.*, 1983, 72, 233.

33. M.G.B. Drew, D.A. Rice and D.M. Williams, *J. Chem. Soc. Dalton Trans.*, 1983, 2251.

34. J.M. Berg and R.H. Holm, *Inorg. Chem.*, 1985, 24, 1706.

35. Y. Do and R.H. Holm, *Inorg. Chim. Acta.*, 1985, 104, 33.

36. M.G.B. Drew and I.B. Tomkins, *J. Chem. Soc. A*, 1970, 22.

37. G. Ferguson, M. Mercer and D.W.A. Sharp, *J. Chem. Soc. A*, 1969, 2415

38. F.A. Cotton, M.P. Diebold and W.J. Roth, *Polyhedron*, 1985, 4, 1103.

39. T.M. Brown, R.B. von Dreele and E.J. Peterson, *Inorg. Chem.*, 1978, 14, 1410.

40. M.G.B. Drew, D.A. Rice and D.M. Williams, *J. Chem. Soc. Dalton Trans.*, 1984, 845.

41. M.G.B. Drew and I.B. Tomkins, *Acta. Crystallogr.Sect. B*, 1970, 26, 1161.

42. S.M. Rocklage, H.W. Turner, J.D. Fellman and R.R. Schrock, *Organometallics*, 1982, 1, 703

43. A.P. Sattelberger, R.B. Wilson and J.C. Huffman, *J. Am. Chem. Soc.*, 1980, 102, 7111; *Inorg. Chem.*, 1982, 21, 2392.

Chapter Five

Synthesis and Reactivity Studies on Half-Sandwich Oxo Complexes of Niobium and Tantalum.

5.1 Introduction.

The (η^5-C_5R_5) ligand (R=H, alkyl) has proved particularly suitable for the solubilisation and stabilisation of high oxidation state metal complexes containing hard ligands such as oxygen. The first half-sandwich organometal oxide to be described, was $CpV(O)Cl_2$ (Cp=η^5-C_5H_5), reported by Fischer[1] as long ago as 1958. Other organometallic oxides exhibiting terminal oxo functionalities have since been made (Table 5.1) and include a number of early molybdenum derivatives described by Cousins and Green[2]. The structure of one, cis-$[CpMo(O)]_2(\mu\text{-}O)_2$, was later proved by X-ray diffraction[3] and the analogous chromium complex, trans-$[Cp^*Cr(O)]_2(\mu\text{-}O)_2$ (Cp^*=η^5-C_5Me_5) has been characterised recently[4]. The rhenium system Cp^*ReO_3 has also been the subject of extensive investigations[5]. However, despite considerable progress in the synthesis of other Group 6 organometal oxides[6], half-sandwich oxo complexes of the heavier group 5 metals have proved particularly elusive.

Compound	Author	Ref.
$CpV(O)X_2$ (X=Cl, Br)	Fischer (1958)	1
CpNb(O)Cl	Triechel (1968)	7
$[Cp_2Nb(O)(C_7H_5(CF_3)_2]$	Amaudrut (1983)	8
$Cp^*V(O)Cl_2$	Bottomley (1986)	9
$[Cp^*V(O)(\mu\text{-}O)]_3$	Bottomley (1987)	10
$Cp^*V(O)(S_5)$	Herberhold (1988)	11
$Cp^*V(O)Cl_2$	Herrmann (1989)	12

Table 5.1a, *Group V.*

Compound	Author	Ref.
$CpMo(O)_2$ $CpMo(O)_2Cl$ $[CpMo(O)]_2[\mu\text{-}O]_2$ (cis) $[CpMo(O)_2]_2[\mu\text{-}O]$	Green (1964)	13
$Cp_2W(O)$	Green (1972)	14
$(\eta^5\text{-}C_5Et_5)W(O)_2(O^tBu)$	Schrock (1984)	15
$[Cp^*Cr(O)]_2[\mu\text{-}O]_2$	Herberhold (1985)	16
$[Cp^*_2Mo(O)]_2[\mu\text{-}O]_2$ (cis)	Herrmann (1985) Arzoumanian (1985)	17
$CpW(O)_2CH_2SiMe_3$	Legzdins (1985)	18
$[Cp^*Mo(O)]_2[\mu\text{-}O]$ (cis)	Herberhold (1985)	6
$[Cp^*W(O)]_2[\mu\text{-}O]_2$	Herrmann (1985)	5
$(\eta^5\text{-}C_5H_4Me)_2Mo(O)$	Tyler (1985)	19
$CpW(O)(\pi\text{-}C_2H_2)Me$	Alt (1985)	20
$[(\eta^5\text{-}CH_2C_5Et_4)W(O)_2(O\text{-}C_4H_9)]_2$ $[(\eta^5CH_2C_5Et_4)W(O)Cl_3]_2$	Schrock (1985)	21
$CpW(O)_2Fc$	Herberhold (1986)	22
$Cp^*(CO)_3W\text{-}W(O)_2Cp^*$	Alt (1987)	23
$[Cp^*M(O)_2]_2[\mu\text{-}O]$ $Cp^*M(O)_2Cl$	Faller (1988)	24
$Cp^*Cr(O)Br_2$	Rauchfuss (1989)	25
$Cp^*_2W(O)$ $Cp^*W(O)_2(OC_5Me_5)$	Bercaw (1989)	26
$Cp^*M(O)(\mu\text{-}O_2)Cl$ $Cp^*M(O)Cl_3$	Faller (1989)	27

Table 5.1b, *Group VI.*

Compound	Author	Ref.
$Cp^*Re(O)_3$	Herrmann (1984)	28
$Cp^*Re(O)(O_2C{=}CPh_2)$	Herrmann (1984)	29
$Cp^*Re(O)(\mu\text{-}O)_2Re(OReO_3)_2Cp^*$	Herrmann (1984)	29
$Cp^*Re(O)[(CMeCMe)_2]$	De Boer (1986)	30
$Cp^*Re(O)Cl_2$	Herrmann (1987)	31
$Cp^*Re(O)(\mu\text{-}O)_2Re(Cl)_2Cp^*$	Herrmann (1987)	31
$Cp^*Re(O)(Me)_2$	Herrmann (1987)	31
$Cp^*Re(O)(CH_2Ph)_2$	Herrmann (1987)	31
$Cp^*Re(O)(OCH_2CH_2O)$	Herrmann (1987)	32

Table 5.1c, *Group VII.*

In chapter 2 we described the convenient high yield preparations of a range of transition metal oxohalides by exploiting the reaction between transition metal halides and hexamethyldisiloxane according to the general equation 5.1.

$$MCl_x + (Me_3Si)_2O \longrightarrow M(O)Cl_{x-2} + 2Me_3SiCl \quad (5.1)$$

It was envisaged that the readily available half-sandwich metal halides, $CpMCl_4$[33] (M=Nb,Ta) and Cp^*TaCl_4[34] would provide a convenient entry into the half-sandwich oxo chemistry of niobium and tantalum and in particular, the elusive $CpM(O)Cl_2$ (M=Nb,Ta) systems. (Equations 5.2 and 5.3).

$$CpMCl_4 + (Me_3Si)_2O \xrightarrow[\{M=Nb,\ Ta\}]{} CpM(O)Cl_2 + 2Me_3SiCl \quad (5.2)$$

$$Cp^*TaCl_4 + (Me_3Si)_2O \longrightarrow Cp^*Ta(O)Cl_2 + 2Me_3SiCl \quad (5.3)$$

In this chapter, a number of new half-sandwich oxo compounds of niobium and tantalum are described and an investigation into the reactivity of $Cp^*Ta(O)Cl_2$[35], the first heavy metal analogue of Fischer's complex is presented.

5.2 Reaction of $CpNbCl_4$ with $(Me_3Si)_2O$:

Preparation of $[CpNbCl_3]_2[O]$ (1).

The reaction of $CpNbCl_4$ with one equivalent of $(Me_3Si)_2O$ in dichloromethane at room temperature proceeded smoothly to afford $[CpNbCl_3]_2[O]$ as an insoluble orange powder. Yield, 0.52g (64%). Characterisation was provided by elemental analysis, infrared and mass spectroscopies (Chapter 7, section 7.5.1). In particular, elemental analysis was consistent with the stoichiometry $C_{10}H_{10}Cl_6Nb_2O$.

Found (Required): %C, 22.07 (22.05), %H, 1.73 (1.85),
%Cl, 39.08 (39.05), %Nb, 34.15 (34.11).

Compound (1) is moisture sensitive and is insoluble in aromatic and chlorocarbon solvents. Its poor solubility has prevented a solution molecular weight determination. However, a low resolution mass spectrum gives an envelope at m/z 526 (^{35}Cl) consistent with a dimeric formulation (no higher mass fragments are observed) and the infrared spectrum shows strong bands at 660 cm^{-1} and in the range 400-280 cm^{-1} indicating the presence of υ(Nb-O-Nb) and υ(Nb-Cl) stretches respectively[36]. A structure determination[37] on a closely related derivative $[\{Nb(\eta^5\text{-}C_5H_4SiMe_3)Cl_3\}_2][O]$ has recently been reported by Oro and co-workers. These studies revealed a dimeric structure with two bridging chloride ligands and a single oxygen bridge as shown in figure 5.1.

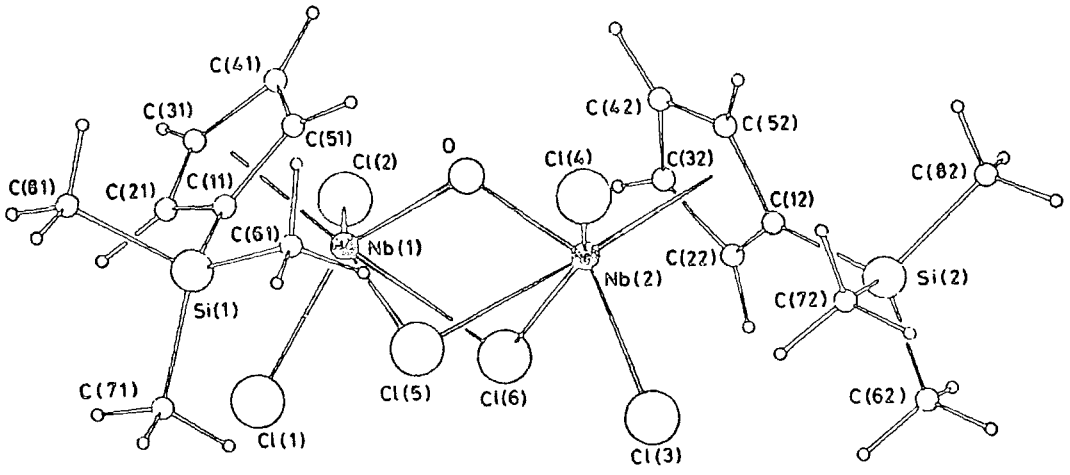

Figure 5.1, *Molecular structure of [{Nb(η5-C5H4SiMe3)Cl3}2] [O].*

(1) is thus formulated as an analogue such that a more accurate representation is [CpNbCl2]2[μ2-Cl]2[μ2-O] (Figure 5.2).

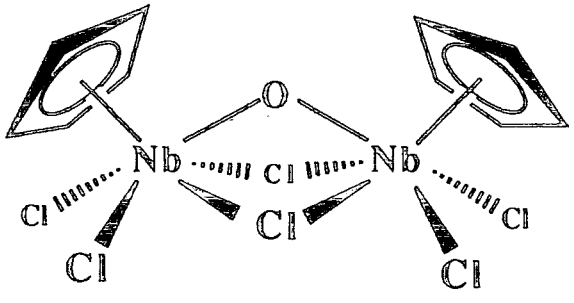

Figure 5.2

Therefore, (1) may be envisaged to form according to equation 5.4.

$$2CpNbCl_4 + (Me_3Si)_2O \xrightarrow[RT]{CH_2Cl_2} \underset{(1)}{[CpNbCl_3]_2[O]} + 2Me_3SiCl \quad (5.4)$$

The formation of a mono-bridged oxide in preference to the desired $CpNb(O)Cl_2$ might suggest an enhanced propensity for inter-molecular elimination of the second Me3SiCl or alternatively may be favoured by binuclear siloxide intermediates.

5.3 Reaction of $CpTaCl_4$ with $(Me_3Si)_2O$:

Preparation of $[CpTaCl_3]_2[O]$ (2).

In an analogous experiment to that described in 5.2, $CpTaCl_4$ was reacted with $(Me_3Si)_2O$ to give a yellow amorphous solid (87% yield) whose infrared spectrum is closely related to that described for (1). In particular, strong bands at 695 cm^{-1} and 335-285 cm^{-1} are attributable to υ(Ta-O-Ta) and υ(Ta-Cl) stretching vibrations respectively[12].

$$2CpTaCl_4 + (Me_3Si)_2O \xrightarrow[RT]{CH_2Cl_2} \underset{(2)}{[CpTaCl_3]_2[O]} + 2Me_3SiCl \quad (5.5)$$

Also, a stoichiometry consistent with $[CpTaCl_3]_2[O]$ was readily established by microanalysis. As for (1) compound (2) is moisture sensitive and is insoluble in aromatic and chlorocarbon solvents. However, their close similarity in the M-Cl stretching region suggests related structures with bridging chloro and oxo ligands .i.e.$[CpTaCl_2]_2[\mu_2\text{-}Cl]_2[\mu_2\text{-}O]$ (Figure 5.3).

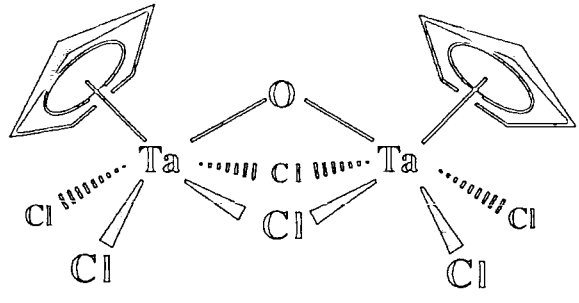

Figure 5.3

The factors governing the formation of (2) are presumed to be similar to those described for (1).

5.4 Reaction of Cp^*TaCl_4 with $(Me_3Si)_2O$:

Preparation of $[Cp^*TaCl_3]_2[O]$ (3).

The reaction between Cp^*TaCl_4 and $(Me_3Si)_2O$ (one equivalent) was performed in methylene chloride at room temperature. The product precipitated from the solution in the form of yellow crystals in 53% yield and was subsequently characterised as $[Cp^*TaCl_3]_2$ [O] (3), the pentamethylcyclopentadienyl analogue of (2) recently reported by Geoffroy and co-workers upon hydrolysis of Cp^*TaCl_4[38].

A stoichiometry of $C_{20}H_{30}Cl_6Ta_2O$ was established by microanalysis:

Found (Required): %C, 27.58 (27.89); %H, 3.69(3.52);
%Cl, 24.65 (24.70); %Ta, 42.01 (42.03).

(3) is partially soluble in aromatic and chlorocarbon solvents. Its 250 MHz ^1H NMR spectrum (d^6-benzene) gives a singlet resonance at δ 2.07 attributable to the equivalent Cp^* methyl hydrogens. The infrared spectrum of (3) gives a strong broad band centred at 690 cm^{-1} attributable to a υ(Ta-O-Ta) stretching vibration with bands in the region 430-275 cm^{-1} consistent with υ(Ta-Cl) vibrations. The mass spectrum reveals peaks at m/z 402 and m/z 420 assignable to $[Cp^*Ta(O)Cl_2]^+$ and $[Cp^*TaCl_3\text{-}H]^+$ respectively.

Geoffroy, converted (3) into the hexamethyl derivative $[Cp^*TaMe_3]_2[\mu\text{-}O]$, which has been studied by X-ray diffraction. The structure reveals a single bridging oxo group with terminal methyls[38] (an ORTEP drawing of $[Cp^*TaMe_3]_2[O]$ is shown in Figure 5.4). However, this structure is likely to have little relevance to (3) since its spectroscopic data are more closely related to (1) and (2). Thus, the $[Cp^*TaCl_2]_2[\mu\text{-}Cl]_2[\mu\text{-}O]$ structure shown in figure 5.5 is believed to be a more accurate representation. It is worth mentioning that the method described here allows the isolation of pure (3) in ca. 53% yield which is a considerable improvement on the 8% yield reported by the hydrolytic procedure.[38]

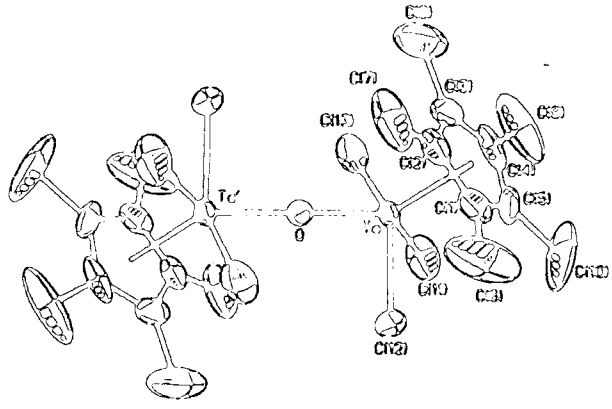

Figure 5.4, *Molecular structure of [Cp*TaMe3]2[O].*

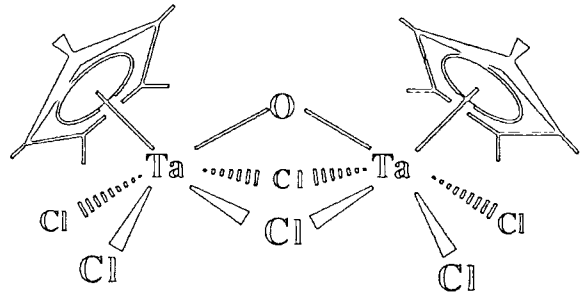

Figure 5.5

Compound (3) can also be prepared, albeit more slowly, when the reaction between Cp^*TaCl_4 and $(Me_3Si)_2O$ is conducted at room temperature in a hydrocarbon solvent such as toluene. Also, if a co-ordinating solvent such as acetonitrile is used, (3) may be isolated in 38% yield after stirring for 18h. at room temperature. There was no evidence for the formation of an acetonitrile adduct, commonly observed for simple oxohalide materials using this methodology.

5.4.1 Mechanism of Formation of $[Cp^*TaCl_3]_2[O]$:

Isolation of Intermediate $Cp^*TaCl_3(OSiMe_3)$ (4) and $[Cp^*TaCl_4 \cdot Cp^*TaCl_3(OSiMe_3)]$ (5).

Geoffroy et al have proposed[38] that the formation of $[Cp^*TaCl_3]_2[O]$ (3), upon hydrolysis of Cp^*TaCl_4, proceeds according to scheme 5.1.

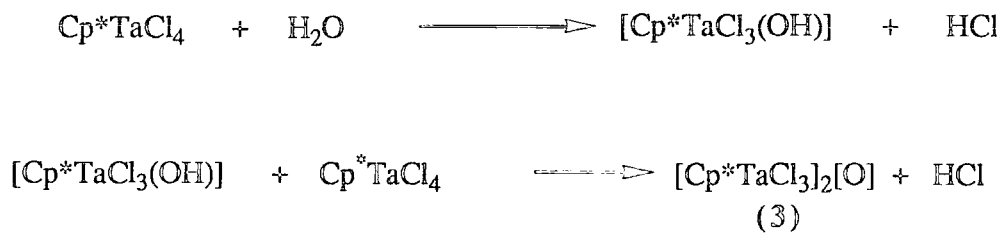

Scheme 5.1, *Proposed pathway for the formation of (3) from Cp^*TaCl_4 and H_2O.*

$(Me_3Si)_2O$ may be considered as a 'protected' water molecule and so an analogous reaction sequence may be considered for the reaction of Cp^*TaCl_4 with $(Me_3Si)_2O$. Reactions of Cp^*TaCl_4 with $(Me_3Si)_2O$ in CH_2Cl_2 and toluene were examined in close detail with a view to identifying intermediates. The results of these studies are summarised.

In either solvent the reaction is presumed to proceed via initial co-ordination of $(Me_3Si)_2O$ to the tantalum complex forming a 1:1 adduct, a situation analogous to that described for the formation of $Nb(O)Cl_3$ in chapter 2. Consistently, a sample of $Cp^*TaCl_4(PMe_3)$, prepared by the literature method, does not react with $(Me_3Si)_2O$ (1 equiv.) in CH_2Cl_2 over a period of 48h. at 60°C suggesting that co-ordination of $(Me_3Si)_2O$ is required prior to elimination of Me_3SiCl.

Rapid condensation of Me_3SiCl will then afford the mono-siloxide $[Cp^*TaCl_3(OSiMe_3)]$ (4), a species analogous to $Cp^*TaCl_3(OH)$ postulated by Geoffroy.

Compound (4) was isolated as a yellow crystalline compound in 10% yield and ca. 90% purity from the 2nd. of four crystallised fractions arising from the supernatant solution of the reaction performed between Cp^*TaCl_4 and $(Me_3Si)_2O$ in CH_2Cl_2. A number of other unidentified siloxide species comprised the 3rd. and 4th. fractions, unreacted Cp^*TaCl_4 being the only compound present in the 1st. Microanalysis on impure (4) is given below which shows it to be most consistent with a stoichiometry of $C_{13}H_{24}Cl_3SiOTa$.

Found (Required): %C, 28.46 (30.51); %H, 4.13 (4.73);

%Cl, 19.23 (20.78); %Ta,Si 41.45 (40.85)

The 250 MHz ^{1}H NMR spectrum in (d^6-benzene) is also consistent with a mono-siloxide formulation showing a singlet resonance at δ 2.09 attributable to the 15 equivalent Cp^* hydrogens and a singlet resonance at δ 0.22 attributable to the $SiMe_3$ hydrogens. The infrared spectrum reveals a characteristic Cp^* ring breathing vibration at 1025 cm^{-1},[40] $\upsilon_{as}(CH_3)$ and $\upsilon_s(CH_3)$ vibrations of the $OSiMe_3$ ligand at 1425 and 1252 cm^{-1} [15] respectively, a υ(Si-R) stretching vibration at 920 cm^{-1},[41,42] and bands at 700 cm^{-1} and 390-270 cm^{-1}[15] due to υ(Ta-O-Si) and υ(Ta-Cl) respectivly.

In contrast, when the reaction is carried out in toluene, the supernatant solution affords an intermediate whose elemental analysis is consistent with the formulation $[Cp^*TaCl_4 \cdot Cp^*TaCl_3(OSiMe_3)]$ (5):

Found (Required): %C, 27.87 (28.49); %H, 4.01 (4.05);

%Cl, 25.48 (25.59), %Ta,Si 40.69 (40.22).

This compound may be regarded as a simple adduct of $Cp^*TaCl_3(OSiMe_3)$ (4) and Cp^*TaCl_4 and displays bands in the infrared due to υ(Si-R)(1090 cm^{-1}) and υ(Ta-O-Si)(800 cm^{-1}). Also, it must be at least binuclear; a feasible structure is shown in scheme 5.2. It is possible that (5) has an opportunity to form due to the reduced solubility of Cp^*TaCl_4 in toluene which leads to its slower consumption in the presence of $(Me_3Si)_2O$. It has not proved possible to obtain satisfactory NMR data on this compound, partially due to its low solubility and also the close similarity of the Cp^* ^{1}H NMR shifts to other Cp^* containing species in this mixture. However a singlet resonance attributable to the methyls of a siloxide ligand is observable at δ 0.29.

The formation of (3) is then believed to arise by condensation of Me_3SiCl from the intermediate $[Cp^*TaCl_4 \cdot Cp^*TaCl_3(OSiMe_3)]$ (5).

The isolation of intermediates in this system is undoubtedly complicated by their reactivity towards Me_3SiCl, which is an ever present component of the reaction mixture. Independent experiments carried out on these compounds with excess Me_3SiCl has shown that $[Cp^*TaCl_3(OSiMe_3)]$ reacts principally to give Cp^*TaCl_4 and $(Me_3Si)_2O$. $[Cp^*TaCl_3]_2[O]$ is also formed presumably via reaction of $Cp^*TaCl_3(OSiMe_3)$ with Cp^*TaCl_4, whilst a suspension of $[Cp^*TaCl_3]_2[O]$ in C_6D_6, treated with Me_3SiCl generates $Cp^*TaCl_3(OSiMe_3)$ and Cp^*TaCl_4 in addition to $(Me_3Si)_2O$. These observations suggest that an equilibrium mixture of the oxide, siloxides and chlorides prevail in the presence of Me_3SiCl. This is not surprising since similar reactivity of metal oxides towards Me_3SiCl has been seen in other systems e.g. equation 5.6[26].

$$Cp^*_2W{=}O \;+\; 2Me_3SiCl \longrightarrow Cp^*_2WCl_2 \;+\; (Me_3Si)_2O \qquad (5.6$$

Failure to isolate $Cp^*Ta(O)Cl_2$ from the treatment of Cp^*TaCl_4 with $(Me_3Si)_2O$ under the range of conditions described and the predominence of $[Cp^*TaCl_3]_2[O]$ as the reaction product suggests that the reaction proceeds via intermolecular elimination of Me_3SiCl from a monosiloxide rather than the desired intramolecular pathway outlined in scheme 5.2.

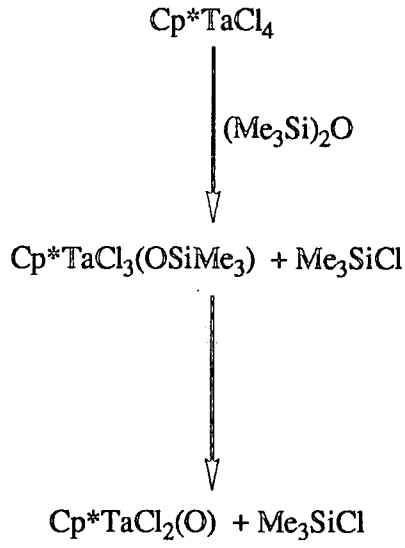

Scheme 5.2

No evidence for the formation of $Cp^*Ta(O)Cl_2$ was obtained upon heating $Cp^*TaCl_3(OSiMe_3)$ for 18h. at 60°C in toluene in the absence of excess Me_3SiCl and $[Cp^*TaCl_3]_2[O]$ and Me_3SiCl are formed when $Cp^*TaCl_3(OSiMe_3)$ is treated with Cp^*TaCl_4 in C_6D_6 at room temperature.

Only trace amounts of intermediate siloxides may be isolated during the formation of (1) and (2) which prevented a detailed investigation of the reaction pathway followed for these species. However, given the similarity of the starting materials, reaction conditions and isolated products, it is not unreasonable to propose a reaction pathway closely related to that shown in scheme 5.2. The higher yields of (1) and (2) may be influenced by their reduced solubility in the reaction media which may shift the equilibria in favour of the less soluble oxide products. Likewise the differing solubilities of Cp^*TaCl_4 and the siloxide intermediates (4) and (5) may account for the differing observations in CH_2Cl_2 and toluene respectively.

5.5 Reactivity of $[Cp^*TaCl_2]_2[O]_2$ (6).

Despite the failure of the reaction of Cp^*TaCl_4 with $(Me_3Si)_2O$ to give $Cp^*Ta(O)Cl_2$ (6) the latter may be prepared in 40% yield from the reaction of $Cp^*TaCl_2(PMe_3)_2$ with carbon dioxide according to equation 5.7.[43]

$$2Cp^*TaCl_2(PMe_3)_2 \xrightarrow[\text{tol. 12h.}]{CO_2} \underset{\substack{40\% \\ (6)}}{Cp^*Ta(O)Cl_2} + \underset{ca.\ 20\%}{Cp^*TaCl_2(CO)_2(PMe_3)} \quad (5.7)$$

Given the observations in the previous sections, it was of considerable interest to establish whether or not (6) is stable to the reaction conditions employed in its attempted preparation and, if not, whether some unusual reactivity of the oxygen atoms in these enviroments might account for the instability of this type of molecule.

5.5.1 Reaction of $[Cp^*TaCl_2]_2[O]_2$ (6) with Me_3SiCl.

$[Cp^*TaCl_2]_2[O]_2$ does indeed react with Me_3SiCl (2 equivalents) in (d^6-benzene) at 70°C to afford a major insoluble component, identified as $[Cp^*TaCl_3]_2[O]$ (3) by comparison of its spectroscopic data with those of an authentic sample. Also, a soluble siloxide species is formed which may be identified as $Cp^*TaCl_3(OSiMe_3)$ (4) by ^1H NMR spectroscopy; $(Me_3Si)_2O$ and Cp^*TaCl_4 are also observable. The formation of these species may be rationalised according to scheme 5.3. These observations confirm that (6) is unstable under the reaction conditions employed in its attempted preparation using $(Me_3Si)_2O$.

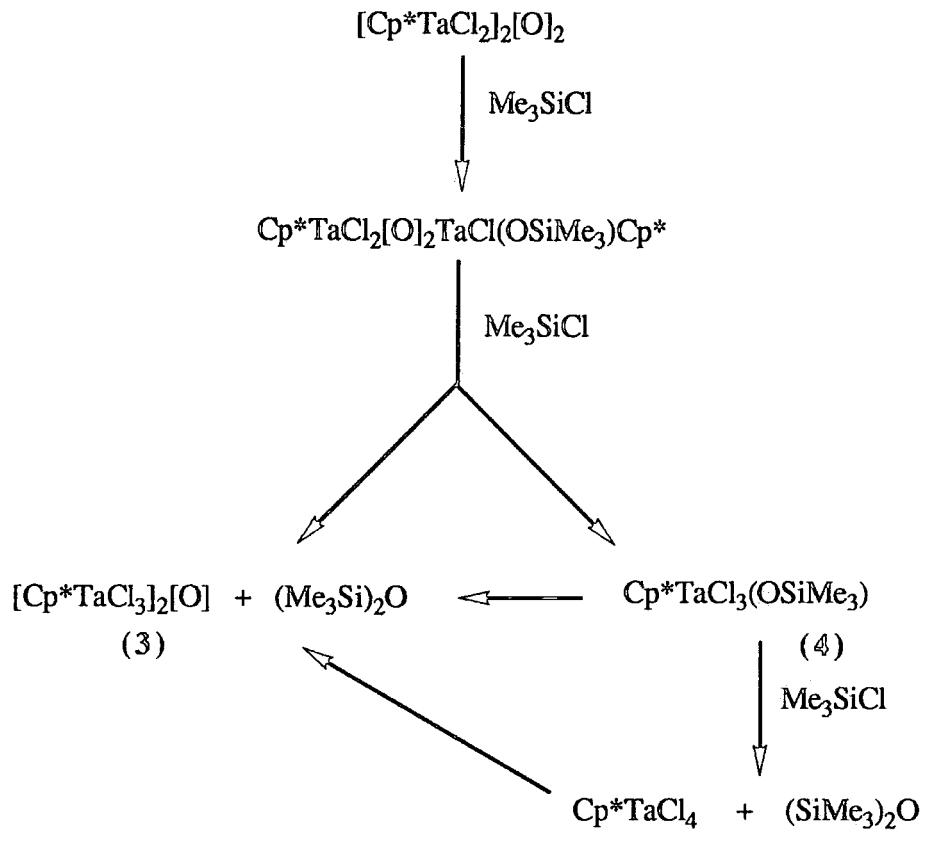

Scheme 5.3, *Possible mechanism for the formation of the observed products in the reaction of [Cp*TaCl$_2$]$_2$[O]$_2$ (6) with Me$_3$SiCl.*

5.5.2 Decomposition of [Cp*TaCl2]2[O]2 (6) in Chloroform.

Rather more surprising is the instability of (6) in the absence of Me3SiCl; chloroform solutions of [Cp*TaCl2]2[O]2 are found to be unstable even at room temperature. After several days at 25°C, (6) is converted cleanly to a mixture of [Cp*TaCl3]2[O] (3) (^{1}H NMR) and a species which gives singlets in the ^{1}H NMR spectrum at δ 2.21 and δ 2.19 . The latter may be identified as the trinuclear cluster (Cp*3Ta3O4Cl4) (7) reported by Geoffroy and coworkers.[36] The formation of (7) from (6) lends support to Geoffroy's postulation that (6) is involved in the conversion of [Cp*Ta(OH)Cl2]2[O] to Cp*3Ta3O4Cl4 the latter being conceptually assembled from the fragments Cp*Ta(O)Cl2 and Cp*(O)ClTa-O-TaCl(O)Cp* and that complex (3) may be formed from the fragments Cp*Ta(O)Cl2 and Cp*TaCl4. Further support for the involvement

of $Cp^*Ta(O)Cl_2$ in the formation of the trinuclear cluster may be derived from monitoring (^1H NMR) the reaction of a $CDCl_3$ solution of $[Cp^*TaCl_2]_2[O]_2$ with a limited amount of H_2O in a sealed NMR tube.[35] A complex equilibrium is formed between the mononuclear hydroxo complex $Cp^*TaCl_3(OH)$ [δ 2.52 (s)], $[Cp^*TaCl_2]_2[O]_2$ [δ 2.45 (s)], $[Cp^*TaCl_3]_2[O]$ [δ 2.39 (s)], $[Cp^*Ta(OH)Cl_2]_2[O]$ [δ 2.29 (s)] and the trinuclear cluster $Cp^*_3Ta_3O_4Cl_4$ [δ 2.21 (s) and δ 2.19 (s)]. Cp^*TaCl_4 is not observed since its hydrolysis is rapid in solution and it is reasonable to assume that it will hydrolyse more rapidly than $[Cp^*Ta(O)Cl_2]_2[O]$. Nevertheless, the observation of $Cp^*TaCl_3(OH)$ alongside $[Cp^*Ta(OH)Cl_2]_2[O]$ may indicate that the initial decomposition products arising from $[Cp^*TaCl_2]_2[O]_2$ in $CDCl_3$ are indeed Cp^*TaCl_4 and $[Cp^*Ta(O)Cl_2]_2[O]$ since they would be the initial hydrolysis products arising from these species. The following mechanism, shown in scheme 5. , would be consistent with these observations.

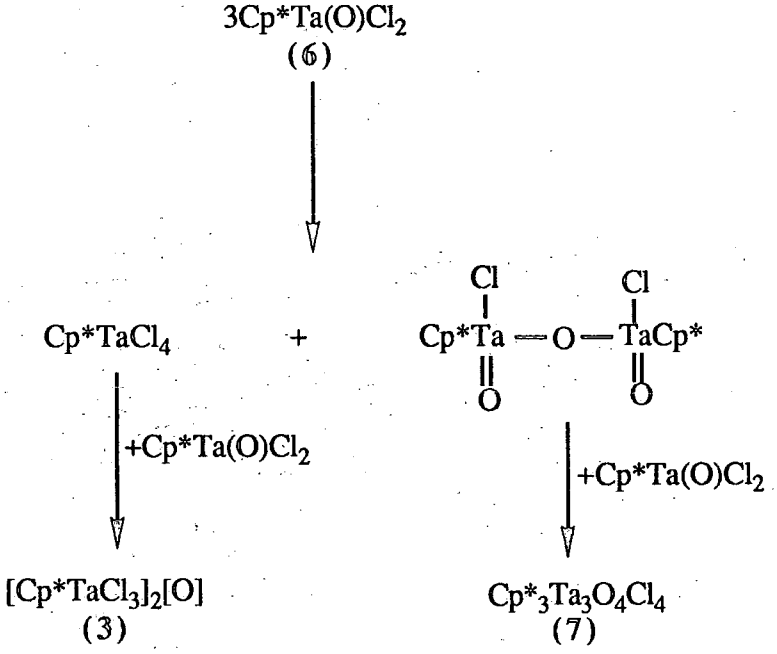

Scheme 5.4, *Proposed decomposition pathway of $[Cp^*TaCl_2]_2[O]_2$ in chloroform.*

5.5.3 Thermolysis of $[Cp^*TaCl_2]_2[O]_2$ (6) in Toluene: *Isolation and Characterisation of $Cp^*_3Ta_3O_4Cl_4$ (7).*

Solutions of (6) in toluene or benzene are stable indefinitely at room temperature. However, upon warming a C_6D_6 solution of (6) at 90°C over several days, a slow conversion ($t_{0.5}$=15h.) to $[Cp^*TaCl_3]_2[O]$ (3) and a toluene soluble species giving a single Cp^* proton resonance at δ 2.15 (C_6D_6) was observed. After one week at 90°C no $[Cp^*TaCl_2]_2[O]_2$ remains.

Pale yellow crystals of the δ 2.15 species grow readily from toluene solution and an X-ray structure analysis (see following section) has revealed a toluene solvate of the recently identified trinuclear cluster, $Cp^*_3Ta_3O_4Cl_4$ (7) obtained by Geoffroy and coworkers by the quantitative transformation of $[Cp^*Ta(OH)Cl_2]_2[O]$ in air (6h, 185°C)[12]. Crystals of (7) grown by these workers from Et_2O afforded a partial (disordered) structure determination. The single δ 2.15 ^1H NMR resonance for (7) in C_6D_6 arises due to coincidental overlap of the Cp^* methyl resonances. It is worth pointing out that the above reaction products are identical to those formed when $[Cp^*TaCl_2]_2[O]_2$ is treated with chloroform and it seems probable that the decomposition mechanism in both cases is the same. Therefore, there is no reason to propose an exchange of chloride ligands with the chloro groups of chloroform. The propensity for $[Cp^*TaCl_2]_2[O]_2$ to decompose at 25°C in $CDCl_3$ as opposed to 90°C in toluene may be associated with the higher polarity of the chlorocarbon which may serve to disrupt the oxide bridges.

5.5.4 The Molecular Structure of $Cp^*_3Ta_3O_4Cl_4$ (7).

A crystal of (7) of dimensions 0.72 x 0.10 x 0.18 mm was sealed under argon in a pyrex capillary and the crystal structure determination was performed by Dr.W.Clegg at the University of Newcastle-upon-Tyne. The structural parameters are

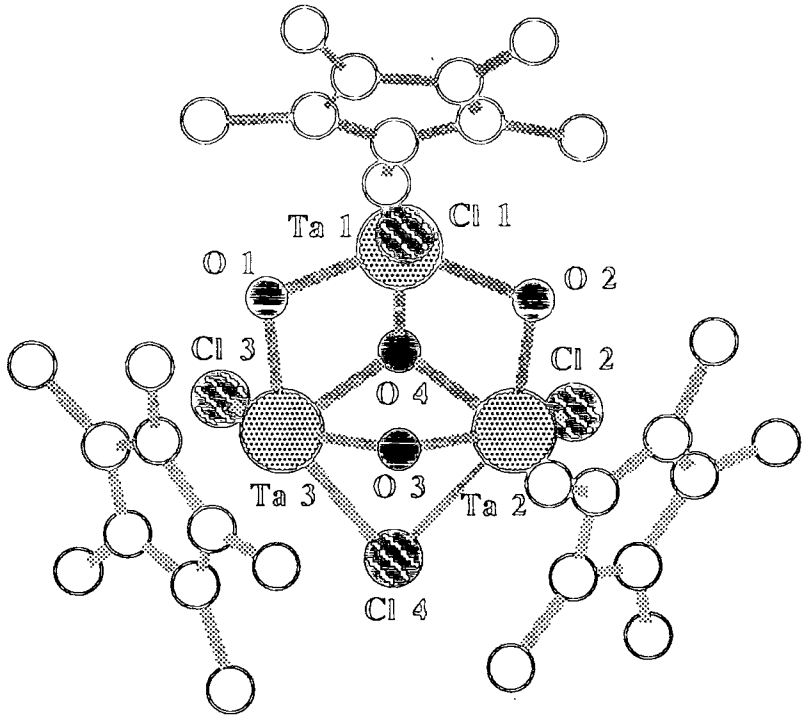

Figure 5.6, *Molecular structure of* $Cp^*_3Ta_3O_4Cl_4$.

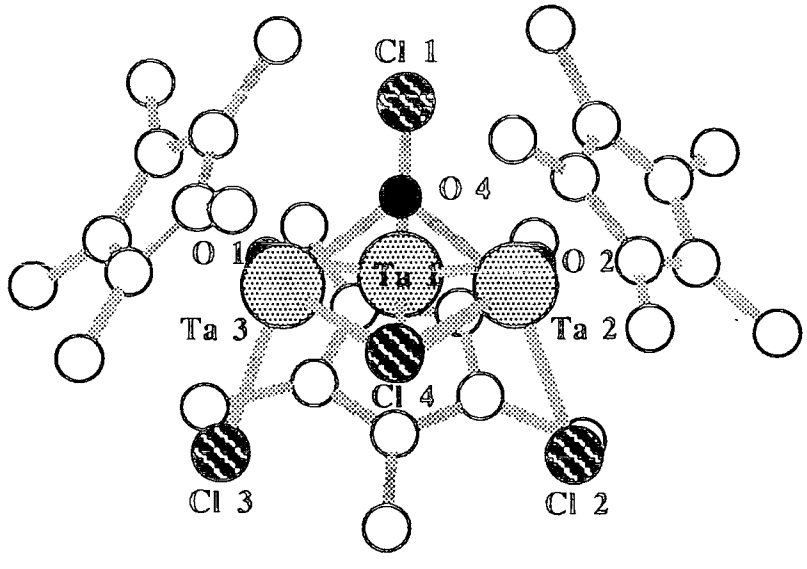

Figure 5.7, *Molecular structure of* $Cp^*_3Ta_3O_4Cl_4$ *viewed in* Ta_3 *plane.*

Ta (1)-Ta(2)	3.015(1)
Ta(1)-Ta(3)	3.029(1)
Ta(2)-Ta(3)	3.155(1)
Ta(1)-O(1)	1.943(8)
Ta(1)-O(2)	1.947(10)
Ta(1)-O(4)	2.011(8)
Ta(2)-O(2)	1.911(8)
Ta(2)-O(3)	1.969(10)
Ta(2)-O(4)	2.075(9)
Ta(3)-O(1)	1.953(9)
Ta(3)-O(3)	1.976(9)
Ta(3)-O(4)	2.102(8)
Ta(1)-Cl(1)	2.386(4)
Ta(2)-Cl(2)	2.411(4)
Ta(2)-Cl(4)	2.690(4)
Ta(3)-Cl(3)	2.405(4)
Ta(3)-Cl(4)	2.630(4)

Ta(1)-Ta(2)-Ta(3)	58.8(1)
Ta(1)-Ta(3)-Ta(2)	58.3(1)
Ta(2)-Ta(1)-Ta(3)	62.9(1)
Ta(1)-Ta(3)-O(1)	38.9(3)
Ta(2)-Ta(1)-O(4)	43.3(2)
Ta(3)-Ta(1)-O(1)	39.1(3)
Ta(3)-Ta(1)-O(2)	100.7(2)
Ta(3)-Ta(1)-O(4)	43.8(2)
Ta(3)-Ta(2)-O(2)	97.4(3)
Ta(3)-Ta(2)-O(3)	37.0(3)
Ta(1)-Ta(3)-O(3)	64.3(3)
Ta(2)-Ta(3)-O(4)	40.6(2)
Ta(2)-Ta(1)-O(2)	38.2(2)
Ta(3)-Ta(2)-O(4)	41.3(2)
Ta(1)-Ta(2)-O(3)	64.7(3)
Ta(1)-Ta(2)-O(2)	39.0(3)
Ta(1)-Ta(3)-O(4)	41.4(2)
Ta(2)-Ta(3)-O(3)	36.8(3)
Ta(2)-Ta(3)-O(1)	96.4(3)
Ta(1)-Ta(2)-O(4)	41.7(2)
Ta(2)-Ta(1)-O(1)	101.2(3)
Ta(1)- O(1)-Ta(3)	102.0(5)
Ta(1)- O(2)-Ta(2)	102.8(4)
Ta(1)- O(4)-Ta(2)	95.1(3)
Ta(1)- O(4)-Ta(3)	94.8(4)
Ta(2)- O(3)-Ta(3)	106.2(4)
Ta(2)- O(4)-Ta(3)	98.1(3)
O(1)- Ta(1)- O(2)	137.1(4)
O(1)- Ta(1)- O(4)	77.8(4)
O(1)- Ta(3)- O(3)	89.6(4)
O(1)- Ta(3)- O(4)	75.4(4)
O(2)- Ta(1)- O(4)	75.4(3)
O(2)- Ta(2)- O(3)	91.7(4)
O(2)- Ta(2)- O(4)	74.6(4)
O(3)- Ta(2)- O(4)	72.5(4)
O(3)- Ta(3)- O(4)	71.8(3)

Table 5.2, *Selected distances (Å) and angles (°) for $Cp^*_3Ta_3O_4Cl_4$ (7).*

collected in appendix 1H. The molecular structure is illustrated in figures 5.6 and 5.7 and selected bond angles and distances are collected in table 5.2.

The structure consists of a triangle of Cp^*Ta units, each edge being bridged by an oxide ligand and the triangular face capped by a single μ_3- oxide ligand. Each Ta possesses a terminal chloride with two of the Ta atoms being bridged by a fourth chloride. The metal atoms are pentavalent and consequently direct metal-metal bonds are not required to interpret the structure. Consistently, the metal-metal distances of 3.015 (1) Å [Ta(1)-Ta(2)], and 3.029 (1) Å [Ta(1)-Ta(3)] are significantly longer than those normally found in (Ta-Ta) bonded systems (typically ca. 2.6-2.8 Å)[44]. A Ta-Ta distance of 2.835 Å in the diamagnetic $(C_5Me_4Et)_2Ta_2Cl_3Me(\mu\text{-}H)_2$ has been assigned as a Ta(IV)-Ta(IV) single bond[45].

Analysis of the three μ_2-O ligands [O(1), O(2) and O(3)] shows them to bridge in an unsymmetrical manner with ∠ Ta(1)-O(1)-Ta(3) = 102.0 (5), ∠Ta(1)-O(2)-Ta(2) = 102.8 (4) and ∠Ta(2)-O(3)-Ta(3) = 106.2 (4). Each bridge itself is slightly asymmetrical with Ta(1)-O(2) = 1.947 (10) Å, Ta(2)-O(2) = 1.911 (8) Å, Ta(1)-O(1) = 1.943 (8) Å, Ta(3)-O(1) = 1.953 Å, Ta(2)-O(3) = 1.969 (10) Å, Ta(3)-O(3) = 1.976 (9) Å. These values are comparable to the average (Ta-μ_2O) distances of 1.95 Å in the recently reported compounds $(Cp^*Ta)_4(\mu_2\text{-}O)_4(\mu_3\text{-}O)_2(\mu_4\text{-}O)(OH)_2$[46] and $[Cp^*_3Ta_3O_5Cl(H_2O)_2]^+Cl^-$[38]. However the bonds are longer than those found in linear (Ta-μ_2-O) systems such as $[(Ta_2Cl_{10})(\mu\text{-}O)]^{2-}$; 1.880 (1) Å[23] and $(Cp^*TaMe_3)_2(\mu\text{-}O)$; 1.909 (7) Å[38] presumably due to more effective pπ -dπ interactions in the latter compounds[47].

The μ_3- oxo ligand [O(4)] caps the triangular face defined by Ta(1), Ta(2) and Ta(3) in an asymmetrical manner, with an average (Ta–μ_3-O) distance and Ta-(μ_3-O)-Ta angle of 2.06 (1) Å and 96.0° respectively. This compares favourably with the distance of 2.10 (1) Å and Ta-(μ_3-O)-Ta angle of 101.3(2)° found in $(Cp^*Ta)_4(\mu_2\text{-}O)_4(\mu_3\text{-}O)_2(\mu_4\text{-}O)(OH)_2$. These parameters for the (M-μ_3-O) moeity are also comparable to the corresponding average parameters for the half-sandwich cluster compounds of other transition metals shown in table 5.3.

Compound	Average d(M-O)/Å	Average ∠MOM(°)	Average d(M-M)/Å	Ref.
$Cp^*Ta_3O_4Cl_4$	2.06(1)	96.0	3.07	#
$Cp^*_4TaO_7(OH)_2$	2.10(1)	92.7	3.04	46
$[Cp^*_3Ta_3O_5Cl(H_2O)_2]Cl$	2.13	92.7	----	38
$Cp_6Ti_6O_8$	1.97	94.2	2.89	48
$Cp_5V_5O_6$	1.86 a 2.00 e	91.1 86.9	2.75	49
$Cp_4Cr_4O_4$	1.94	92.8	2.81	49

Table 5.3, *Average d(M-μ_3-O) and ∠M-(μ_3-O)-M parameters for some [Cp'nMnOx] compounds. {# This work; a=Axial; e=Equatorial}.*

5.5.5 Reaction of $[Cp^*TaCl_2]_2[O]_2$ (6) with LiO-2,6-$Me_2C_6H_3$: *Preparation of $Cp^*Ta(O)(O\text{-}2,6\text{-}Me_2C_6H_3)_2$ (8).*

$[Cp^*TaCl_2]_2[O]_2$ reacted smoothly within minutes at room temperature with LiO-2,6-$Me_2C_6H_3$ (2 equivalents) to afford a single product by ^1H NMR spectroscopy. The equivalent Cp^* methyl hydrogens resonate at δ 1.89 whilst the presence of two equivalent -O-2,6-$Me_2C_6H_3$ ligands is indicated by a singlet resonance at δ 2.34. (Me) and an AX_2 pattern at δ 6.93 (d) and δ 6.77 (t) (^3J (HH) = 7.3 Hz) assignable to the aryl hydrogens . Attempts to isolate (8) were, however, unsuccessful since the product could be obtained only as an oil containing small amounts of the uncomplexed phenol (^1H NMR spectroscopy). In addition to the NMR data the infrared spectrum of (8) is quite informative. A strong, broad absorption at 919 cm^{-1} (that is not present in the parent phenol) may be assigned to a terminal υ(Ta=O) vibration[50,51]. Furthermore, the presence of bands in the region 1150-1300 cm^{-1} and 770-920 cm^{-1} may be tentatively assigned to υ(C-O) and υ(O-Ta) respectively. The bands at 575 cm^{-1} and 535 cm^{-1} (again absent in the parent phenol)

are indicative of terminal aryloxide ligands[52] (bridging phenoxide ligands invariably give bands to lower frequencies). Therefore, (8) may be reasonably formulated as $Cp^*Ta(O)(O\text{-}2,6\text{-}Me_2C_6H_3)_2$ according to equation 5.8 and is anticipated to possess a monomeric 3-legged piano stool geometry related to the trigonal pyramidal structure of recently reported $Ta(O)[N(CHMe_2)_2]_3$[29].

$$\underset{(6)}{Cp^*Ta(O)Cl_2} + 2LiOAr \xrightarrow{\{Ar=2,6\text{-}Me_2C_6H_3\}} \underset{(8)}{Cp^*Ta(O)(OAr)_2} + 2LiCl \qquad (5.8)$$

5.5.6 Other Reactions of $[Cp^*TaCl_2]_2[O]_2$ (6).

Several further reactions were performed with $[Cp^*TaCl_2]_2[O]_2$ and monitored by ^1H NMR spectroscopy, the results of which are described (briefly) below.

Reaction with methyl chloride

Compound (6) showed no indication of reaction with MeCl (3 equivalents) after 1 week at room temperature in C_6D_6. Warming at 70°C led to the decomposition outlined in scheme 6.6 with the MeCl taking no apparent part in the transformation.

Reaction with ethene.

No reaction was observed between (6) and ethene (2 equivalents) after 2 weeks in C_6D_6 at room temperature. Higher temperatures resulted in decomposition to (7) as outlined in scheme 6.6.

Reaction with trimethylphosphine

No reaction was observed between (6) and PMe_3 (2 equivalents) after 1 week at room temperature or at higher temperatures. Again, only decomposition to (7) is observed.

Reaction with substituted alkynes, PhC≡CR (R=Ph,H)

No reaction was observed between (6) and either PhC≡CPh or PhC≡CH after 1 week at room temperature or at higher temperatures. Decomposition to (7) only is observed.

5.6 Summary.

Half-sandwich oxo compounds of the type $[Cp'MCl_3]_2(O)$ have proved readily accessible by the reaction of $Cp'MCl_4$ compounds with $(Me_3Si)_2O$. $Cp'M(O)Cl_2$ derivatives are not accessible via this route or by analogous hydrolytic procedures. It has been demonstrated that $Cp^*Ta(O)Cl_2$ is highly reactive towards Me_3SiCl and hence presumably also HCl, the product of any hydrolysis reaction with Cp^*TaCl_4. This may account for why the heavier metal analogues of $CpV(O)Cl_2$ have proved elusive for such a considerable period of time. However, the results presented in this chapter also show that the oxygen atoms in these enviroments are inherently unstable. Further studies are required to allow further understanding of this instability. However, the low valent synthesis discovered for $[Cp^*TaCl_2]_2[\mu\text{-}O]_2$ (6) offers potential for preparing analogous $Cp'M(O)Cl_2$ compounds and thus facilitating a detailed investigation of these phenomena.

5.7 References.

1. E.O. Fischer and S. Vigoureux, *Chem. Ber.*,1958, 91, 1342.
2. M. Cousins and M.L.H. Green, *J. Chem. Soc.*,1964, 1567.
3. C. Couldwell and K. Prout, *Acta Crystallogr., Sect. B: Struct. Crystallogr., Cryst. Chem.*, 1978, 33, 1334.
4. M. Herberhold, W. Kremnitz, A. Razain, H. Schollhorn and U. Thewalt, *Angew. Chem.*, 1985, 97, 603.
5. W.A. Herrmann, E. Herdtweck, M. Floel, J. Kulpe, U. Kusthardt and J. Okuda, *Polyhedron*, 1987, 6, 1165, and references therein; E.J.M. deBoer, J. de With and A.G. Orpen, *J. Am. Chem. Soc.*, 1986, 108, 8271.
6. See for example, J.W. Faller and Y. Ma, *J. Organomet. Chem.*, 1988, 340, 56; M. Herberhold, W. Kremnitz, A. Razavi, H. Schollhorn and H. Thewalt, *Angew. Chem., Int. Ed. Engl.*, 1985 24, 601; H. Arzoumanian, A. Baldy, M. Pierrot and J-F. Petrignani, *J. Organomet. Chem.*, 1985, 294, 327; K. Wieghardt, M. Hahn, W. Swindoff and J. Weiss, *Angew. Chem., Int. Ed. Engl.*, 1983, 22, 491.

7. P.M. Treichel and G.P. Werber. *J. Am. Chem. Soc.*, 1968, 90, 1753.

8. R. Mercier, J. Douglade and J. Amaudrut, *J. Organometallic Chem.*, 1983, 244, 145

9. F. Bottomley, J. Darkwa, L. Sutin and P.S. White, *Organometallics*, 1986, 6, 11.

10. F. Bottomley and L. Sutin, *J. Chem. Soc. Chem. Commun.*, 1987, 1112.

11. M. Herberhold, M. Kuhnlein, B. Nuber and M.L. Ziegler, *J. Organometallic Chem.*, 1988, 349, 131.

12. W.A. Herrmann, E. Herdtweck and G. Weichselbaumer, *J. Organometallic Chem.*, 1989, 362, 321.

13. M. Cousins and M.L.H. Green, *J. Chem. Soc.*, 1964, 1567.

14. M.L.H. Green, A.H.L. Lynch, and M.G. Swanwick, *J. Chem. Soc. Dalton Trans.*, 1972, 1445.

15. R.R. Schrock, S.F. Pederson, M.R. Churchill and J.W. Ziller, *Organometallics*, 1984, 3, 1574.

16. M. Herberhold, W. Kremnitz, A. Razain, H. Schollhorn and U. Thewalt, *Angew. Chem.*, 1985, 97, 603.

17. H. Arzoumanian, A. Baldy, M. Pierrot and J.F. Petrignani, *J. Organometallic Chem..*, 1985, 294, 327.

18. P. Legzdins, S.J. Rettig and L. Sanchez, *Organometallics*, 1985, 4, 1470.

19. N.D. Silauwe, M.Y. Chiang and D.R. Tyler, *Inorg. Chem.*, 1985, 24, 4219.

20. H.G. Alt and H.I. Hayen. *Angew. Chem. Int. Ed. Engl.*, 1985, 24, 497.

21. J.H. Wengrovious, J. Sancho and R.R. Schrock, *J. Am. Chem. Soc.*, 1981, 103, 3932.

22. M. Herberhold, H. Kniesel, L. Haumaier, A. Gieren and C. Ruiz-Perez, *Z. Naturforsch, B*, 1986, 41, 1431.

23. H.G. Halt, H.I. Hayen and R.D. Rogers, *J.Chem. Soc. Chem. Commun.*, 1987, 1795.

24. J.W. Faller and Y. Ma, *J. Organometallic Chem..*, 1988, 340, 59.

25. D.B. Morse, T.B. Rauchfuss and S.R. Wilson, *J. Am. Chem. Soc.*, 1988, 110, 8234.

26. G. Parkin and J.E. Bercaw, *J. Am. Chem. Soc.*, 1989, 111, 391.

27. J.W. Faller and Y. Ma, *J. Organometallic Chem..*, 1989, 368, 45.

28. W.A. Herrmann, R. Serrano and H. Bock, *Angew. Chem.*, 1984, 96, 364.

29. W.A. Herrmann, r. Serrano, U. Kusthardt, M.L. Ziegler, E. Guggotz and

T. Zahn, *Angew. Chem., Int. Ed. Engl.*, 1984, 23, 515.

30. E.J.M. DeBoer, J. Dewith and A.G. Orpen, *J. Am. Chem. Soc.*, 1986, 108, 8271.

31. W.A. Herrmann, E. Herdtweck, M. Floel, J. Kulpe, U. Kusthardt and J. Okuda, *Polyhedron*, 1987, 6, 1165.

32. W.A. Herrmann, D. Marz, E. Herdtweck, A. Schafer, W. Wagner and H-J. Kneuper, *Angew. Chem., Int. Ed. Engl.*, 1987, 26, 462.

33. M.J. Bunker, A. De Cain, M.L.H. Green, J.J.E. Moreau and N. Siganporia, *J. Chem. Soc.Dalton Trans.*, 1980, 2155.

34. V.C. Gibson, J.E. Bercaw, W.J. Bruton Jr. and R.D. Sanner, *Organometallics*, 1986, 5, 976.

35. V.C. Gibson and T.P. Kee, Unpublished results.

36. V. Katovic and C. Djordjevic, *Inorg. Chem.*, 1970, 9, 1729.

37. A. Andreu, F.A. Jalon, A. Oro and P. Royo. *J. Chem. Soc. Dalton. Trans.*, 1987, 953.

38. P. Jernakoff, C. De Meric De Bellefen, G.L. Geoffroy, A.L. Rheingold and S.J. Geib, *Organometallics*, 1987, 6, 1362.

39. (a) F.A. Cotton and R.C. Najjor, *Inorg. Chem.*, 1981, 20, 1866.
(b) M.H. Chisholm, J.C. Huffman and L-S. Tan, *Inorg. Chem.*, 1981, 20, 1859.

40. R.M. Silverstein, G.C. Bassler and T.C. Morill, "Spectrometric Identification of Organic Compounds", 4th Ed., J. Wiley, New York (1981).

41. A.G Davies, P.G. Harrison and T.A.G. Silk, *Chem. and Ind.*, 1968, 949.

42. C. Eaborn, "Organosilicon Compounds", Butterworth Scientific Publications (1960)

43. V.C. Gibson and T.P. Kee, *J. Chem. Soc. Chem. Commun.*, 1989, 656.

44. C.E. Holloway and M. Melnik, *Rev. Inorg. Chem.*, 1985, 7, 1.

45. P.A. Belmonte, R.R. Schrock and C.S. Day, *J. Am. Chem. Soc.*, 1982, 104, 3082.

46. V.C. Gibson and T.P. Kee, Unpublished results.

47. F.A. Cotton and R.C. Najjar, *Inorg. Chem.*, 1981, 20, 1866.

48. J.C. Huffman, J.G. Stone, W.C. Krusell and K.G. Caulton, *J. Am. Chem. Soc.*, 1977, 99, 5829.

49. G.Stucky and R.E. Rundle, *J. Am. Chem. Soc.*, 1964, 86, 4821.

50. R.E. LaPointe, P.J. Wolczanski and J.F. Mitchell, *J. Am. Chem. Soc.*, 1986, 108, 6382.

51. R.L. Deutscher and D.L. Kepert, *Inorg. Chim. Acta.*, 1970, 4, 645.

52. K.C. Malhotra, U.K. Banerjee and S.C. Chaudhry, *J. Ind. Chem. Soc.*, 1980, 57, 868.

Chapter Six

Synthesis and Properties of Some Tungsten Halide Bronzes.

6.1 Introduction.

In chapter 3, reactions of molybdenum and tungsten oxohalides with lithium aryloxides were described and a number of molecular complexes were isolated and characterised. However, $W(O)_2Cl_2$ displayed exceptional behaviour in these reactions affording, instead of molecular oxo-aryloxide complexes, insoluble crystalline compounds with a metallic lustre. The colour of the solids ranged from blue to purple to black depending on the amount of lithium reagent employed and their overall characteristics appeared typical of tungsten bronze materials. These observations form the background to this chapter which includes an investigation into the mechanism of intercalation by alkali metal aryloxide reagents, X-ray characterisation of the materials formed and a preliminary assessment of some of their properties.

6.1.1 Background.

Intercalation compounds may be defined as solid hosts into which guest atoms or molecules may be inserted or removed. The tungsten bronzes, first discovered by Wohler[1] in 1823, represent one of the most extensively studied classes of intercalation compound combining novel electrical, optical and magnetic properties with remarkable chemical inertia[2].

Intercalation compounds may be divided into three groups, 1-D, 2-D and 3-D, depending on whether the guest species migrate along tunnels, within layers or in a three dimensional network. 3-D intercalation compounds are characterised by rigid structures with channels, the dimensions of which are generally matched to a particular guest e.g. alkali metal cations. Typical examples of such compounds are the spinels Mn_3O_4, $LiMn_2O_4$ and Fe_3O_4[3-6]. Tungsten bronzes arise by intercalation of alkali metals into the three dimensional oxygen-bridged lattice of WO_3[7].

The two dimensional, or layered, intercalation compounds offer the advantage of high structural stability in two of the dimensions coupled with a very flexible third dimension due to weak van der Waals bonding between the layers. This permits the insertion of a wide variety of both charged and neutral guest species that span a range of atomic and molecular dimensions. Three groups of 2-D intercalates have received significant attention to date.

1. The layered sulphides, e.g. TiS_2. This compound is built from hexagonal close packed S^{2-} ions. Li^+ ions may be readily and reversibly intercalated between the pairs of van der Waals bonded sulphur layers[8].

2. The layered oxides e.g. $LiCoO_2$. These solids are similar to the sulphides but with a different orientation of the anions. The cations are arranged in alternate Li^+ and Co^{3+} layers and a significant proportion of the lithium ions may be removed[9].

3. The layered halides e.g. α-$RuCl_3$. The anion arrangement again consists of close packed layers. A number of cationic species have been intercalated into this structure.

Layered oxides are attractive intercalation hosts particularly for use as cathodes in lithium batteries because the transition metal ions may be maintained in high oxidation states thus offering high battery voltages and the Li^+ ions are highly mobile between the layers. However, van der Waals bonding between oxide layers is frequently too weak to stabilise the structure. Layered intercalation compounds with mixed anions offer some distinct advantages here since, if one of the anions is an oxide, high oxidation states can still be maintained while, if the second anion is, for example a halide, the layers may be effectively bonded together by the van der Waals forces between the X^- ions. Therefore, the most desirable features of each anion may be incorporated into one compound.

In general, intercalation compounds with mixed anions have received relatively little attention. For the bronzes, work has been limited to a handful of fluoride derivatives of the type $WO_{3-x}F_x$ obtained by high temperature and pressure treatment of WO_3 with metallic tungsten in HF[10]. However, these were found to behave essentially as the pure oxides. Studies on mixed anion hosts of the type MOCl where M = Fe, V, Cr[8] etc. have proved much more promising.

In chapter 2, a convenient low temperature synthesis of $W(O)_2Cl_2$ was described. In light of its unexpected behaviour towards LiOAr reagents, it came as some surprise that this class of high valent tungsten mixed anion compound had not been investigated previously as an intercalation host. This, may possibly be attributed to its relative inaccessibility by a convenient synthetic procedure.

Some interesting comparisons can be made between $W(O)_2X_2$ and its oxide counterpart, WO_3. Tungsten trioxide is not stable in a layered structure and crystallises as a 3-D framework compound. However it is of interest as a material for electrochromic display devices because of the colour change from white to blue upon intercalation of Li^+ ions which is associated with the reduction of W^{VI} to W^V. Unfortunately, Li^+ ion diffusion is relatively slow in WO_3 thus limiting the write/erase times; it may be anticipated that lithium ion diffusion will be significantly faster between the van der Waals bonded X layers in $W(O)_2X_2$, this type of compound may therefore offer some advantages over WO_3 in electrochromic applications. Of the series of tungsten oxohalides $W(O)_2Cl_2$, $W(O)_2Br_2$ and $W(O)_2I_2$, only the structure of $W(O)_2Cl_2$ has been fully determined[11] (Figure 6.1). The idealised structure consists of layers containing both W and O atoms in which the tungsten atoms are coordinated by a square planar arrangement of oxygens. The W-O layers are sandwiched between two layers of Cl atoms such that each W in the central layer is coordinated by one Cl from the layer above and one from the layer below, thus providing octahedral coordination around each tungsten atom. Each one of the layer units is stacked upon another, the layer units being held by weak van der Waals bonds. As is evident in figure 6.1, each one of the layer units is laterally displaced from those adjacent to it. Examination of the

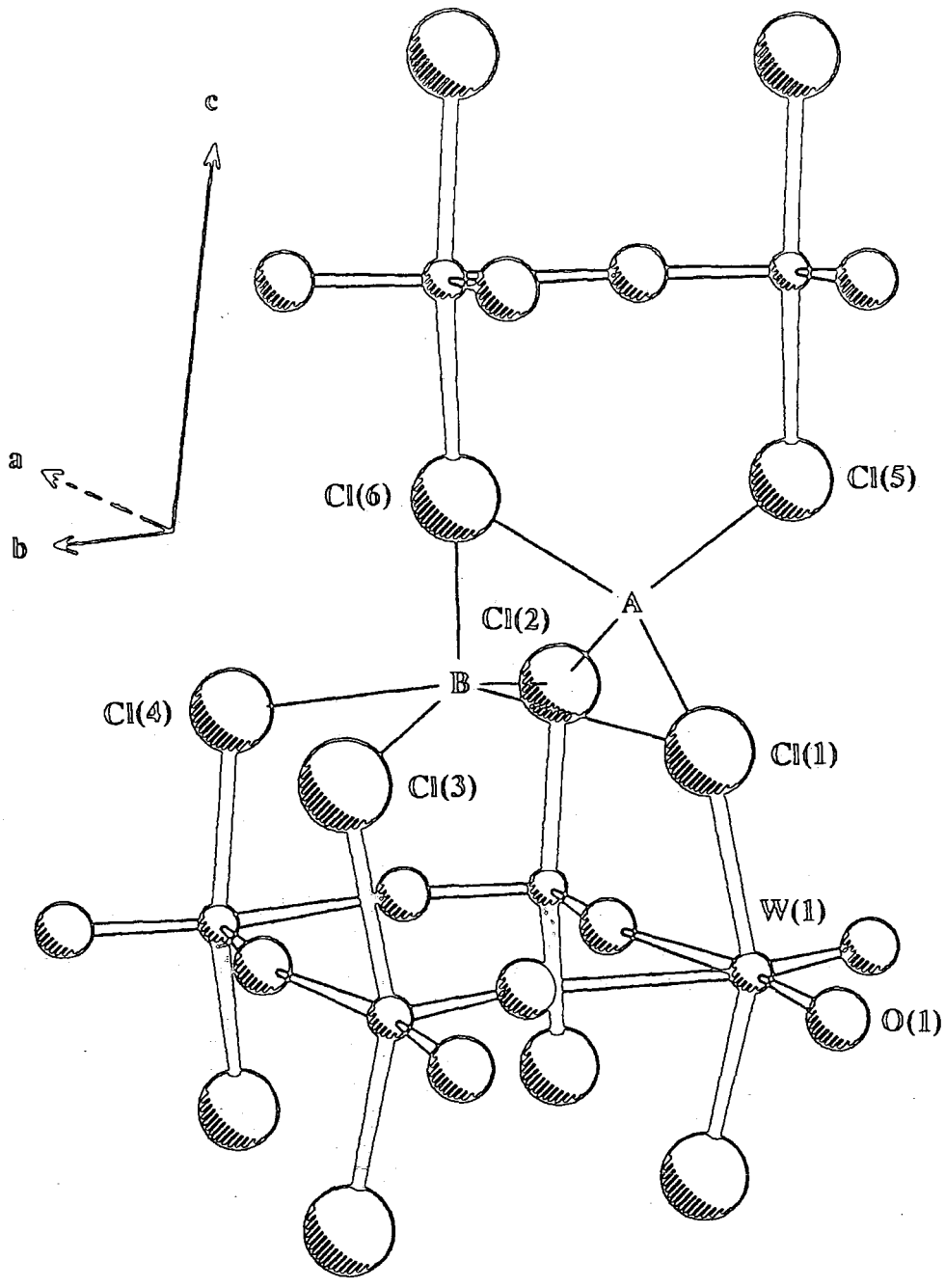

Figure 6.1, *A section of two layers of tungsten $W(O)_2Cl_2$ showing possible four (A) and five (B) coordinate intercalation sites.*

space between the adjacent van der Waals bonded layers reveals that two sets of sites are available for accommodating guest species. One square pyramidal site (B in Figure 6.1) and two tetrahedral sites (A in Figure 6.1) per tungsten atom may be identified. The two sets of sites share common faces providing a continuous pathway for the migration of guest species. $W(O)_2Cl_2$ is therefore an excellent candidate to act as a mixed anion intercalation host.

The following sections describe the preparation of a range of new 'Halide Bronze' materials and a preliminary investigation of their conductivity characteristics.

6.2 Reaction of $W(O)_2Cl_2$ with LiO-2,6-$Bu^t_2C_6H_3$:

Preparation of $W(O)_2Cl_2{\cdot}Li_x$ where $0 < x \leq 1$.

The reaction of $W(O)_2Cl_2$ with two equivalents of Li-O-2,6-$Bu^t_2C_6H_3$ was described briefly in chapter 3, section 3.4.1. It was found that the reaction proceeded quite differently to that of $Mo(O)_2Cl_2$ and LiOAr to give, in preference to metathetical exchange of chloride for aryloxide groups, an insoluble, dark, moisture sensitive, crystalline solid and a red-green dichroic supernatant solution according to equation 6.1.

$$W(O)_2Cl_2 + xLi(O\text{-}2,6\text{-}Bu^t_2C_6H_3) \xrightarrow{\text{tol.}} W(O)_2Cl_2.Li_x + \text{'organics'} \quad (6.1)$$
$$0 < x \leq 1$$

The supernatant solution was decanted from the solid which was collected, washed with petroleum ether and dried *in vacuo*.

The solid, which appears purple and displays a metallic lustre, was characterised as $W(O)_2Cl_2{\cdot}Li_{1.0}$ by elemental analysis (Chapter 7, section 7.6.1). Concentration of the supernatant solution gave a red crystalline solid. Analysis of this solid by ^1H NMR spectroscopy showed it to be a 50:50 mixture of the biphenol (1) and HO-2,6-$Bu^t_2C_6H_3$ (2). A pure sample of (1) was obtained as a white crystalline solid by

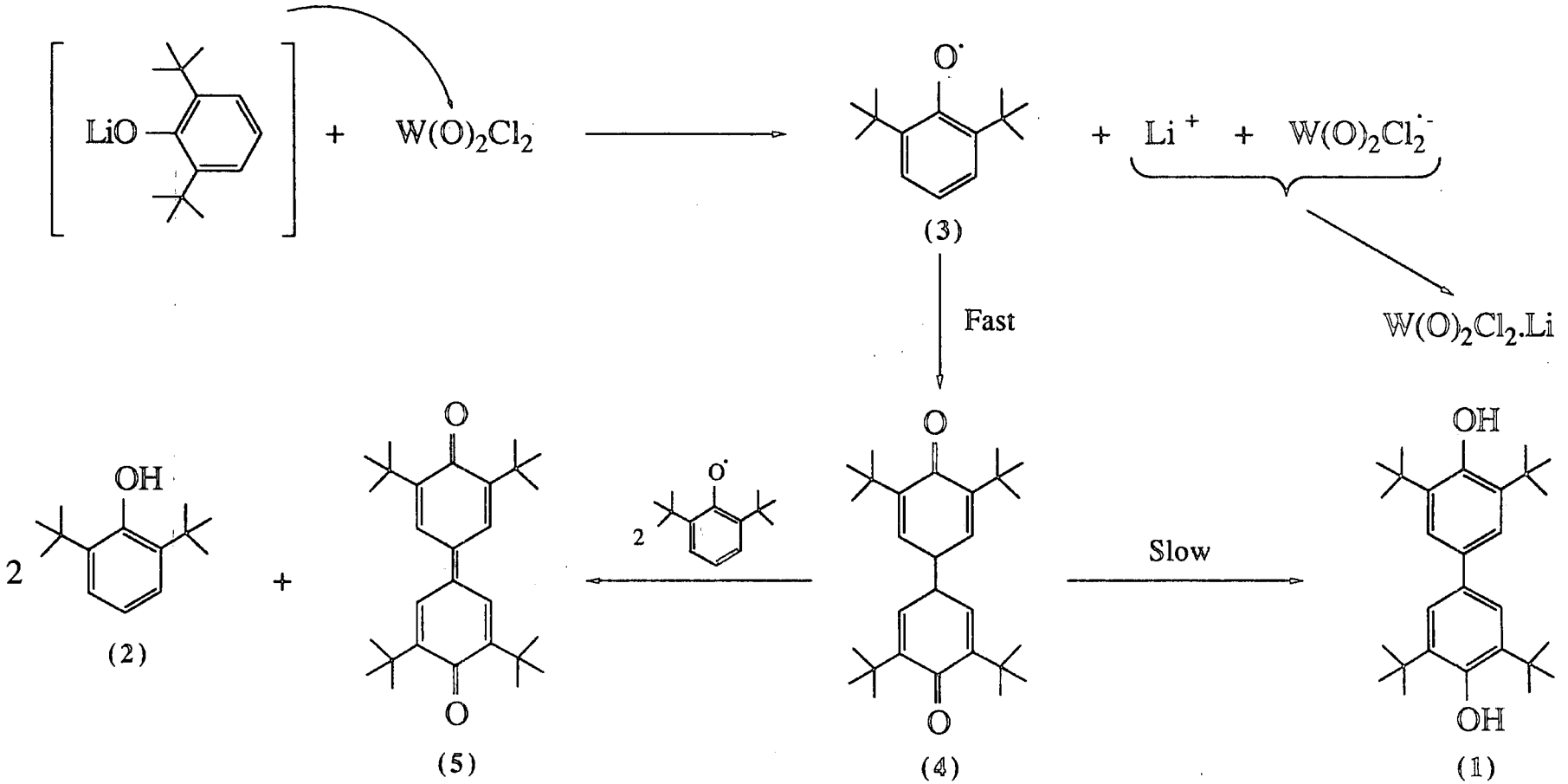

Scheme 6.1, *Proposed mechanism for the reaction between $W(O)_2Cl_2$ and Li-O-2,6-$Bu^tC_6H_3$*

sublimation of the phenolic mixture at 120°C, 10^{-5} Torr. (1) was subsequently characterised by elemental analysis, infrared, ^{1}H, ^{13}C and mass spectroscopies (Chapter 7, section 7.6.1).

The formation of (1) and (2) supports a mechanism involving an electron transfer from LiOAr to $W(O)_2Cl_2$ to give phenoxy radicals followed by migration of lithium metal ions into the $W(O)_2Cl_2$ lattice by a classical electrostatic intercalation mechanism (Scheme 6.1). The generation of phenoxy radicals in the oxidation of a variety of phenols under different conditions is well documented[12]. Thus, once atomic lithium is generated, para-para C–C coupling of the mesomeric phenoxy radical (3) takes place followed by enolisation of the resultant dimer (4). Evidence to support this and the reversibility of the coupling reaction comes from a study of the oxidation of HO-2,6-$Bu^t_2C_6H_3$ in benzene[12]. It has also been reported that the diketo-dimer (4), but not the biphenol (1), dissociates slowly in solution to the phenoxy radical (3) which in turn reacts with the diketo-dimer to give the diquinone (5) and the phenol (2). The observation of the diquinone (5) when the reaction is performed with 0.75 equivalents of LiOAr provides further support for the mechanism postulated in scheme 6.1.

With Li-O-2,6-$Bu^t_2C_6H_3$, the para-para C–C coupled product is selectively obtained as a result of the steric constraints placed on the dimer by the bulky Bu^t substituents. When a lithium aryloxide other than DTBP is used, e.g. Li-O-2,6-$Me_2C_6H_3$, Li-O-2,6-$Pr^i_2C_6H_3$, products arising by ortho-ortho and ortho-para C-C coupling are produced as shown in scheme 6.2.

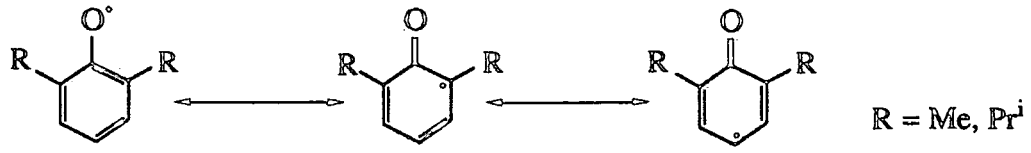

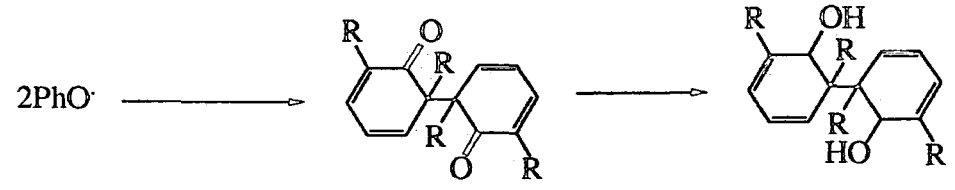

ortho-ortho C-C coupling

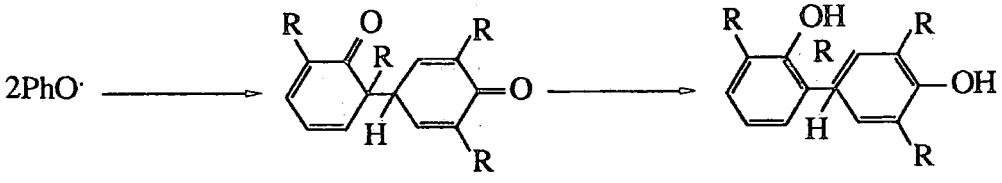

ortho-para C-C coupling

Scheme 6.2

The mechanism is therefore unaffected by the substituents on the phenyl ring, the only difference, resulting from a change in R, being a variation in the type of biphenol produced. It would appear, however, that only aryloxides possess the appropriate oxidation potentials to act in this manner since a mixture of $W(O)_2Cl_2$ and 2 equivalents of LiOBu^t do not react even at elevated temperatures. The possibility of proton transfer from the phenol to the $W(O)_2Cl_2$ lattice playing an important part in the mechanism was also investigated and the reaction between $W(O)_2Cl_2$ and LiOAr was repeated but in the presence of an excess of the proton acceptor NEt_3. Formation of $W(O)_2Cl_2{\cdot}Li_x$ proceeded normally according to equation 6.1 indicating that proton transfer is not an integral component of the mechanism outlined in scheme 6.1.

Interestingly, attempts to prepare $W(O)_2Cl_2 \cdot Li_x$,where $x > 1.0$, by the above route were unsuccessful, presumably because the electro-chemical reduction potential of $W(O)_2Cl_2 \cdot Li_{1.0}$ no longer matches the oxidation potential of LiOAr.

6.3 Reaction of $W(O)_2Cl_2$ with $LiBu^n$: *Preparation of $W(O)_2Cl_2 \cdot Li_x$ where $0 < x \leq 2$.*

Although materials with $x > 1$ are not accessible using the phenoxide reagent LiO-2,6-$Bu^tC_6H_3$, further intercalation is possible using n-butyl lithium which has proved an effective reagent for intercalating Li into a variety of layered host structures[13]. Indeed, preliminary studies of lithium intercalation into $W(O)_2Cl_2$ by the $LiBu^n$ method have been reported by Ackerman[14] during the course of the work described here.

Thus, treatment of finely divided toluene suspensions of $W(O)_2Cl_2$ maintained at *ca.* -78°C with solutions of $xLiBu^n$ in toluene under dry argon, rapidly afforded dark, moisture sensitive, crystalline solids according to equation 6.2.

$$W(O)_2Cl_2 \xrightarrow[\text{tol.}]{xLiBu^n} W(O)_2Cl_2.Li_x \qquad (6.2)$$
$$0 < x \leq 2$$

The solids were washed with petroleum ether, collected and subsequently characterised as $W(O)_2Cl_2 \cdot Li_x$ where $0 < x \leq 2$ (Chapter 7, section 7.6.1).

6.4 Characterisation of Halide Bronzes of the Type $W(O)_2Cl_2 \cdot Li_x$ where $0 < x \leq 2$.

A series of materials of formula $W(O)_2Cl_2 \cdot Li_x$ with x ranging from zero to two have been subjected to a detailed analysis by X-ray powder diffraction (Guinier Camera). The results are tabulated in table 6.1 for x = 0.1, 0.50, 0.7 and 1.63 and the X-ray traces are reproduced in figure 6.2.

Phase	a [Å]	b [Å]	c [Å]
$W(O)_2Cl_2$	3.8299	3.8649	13.8498
$W(O)_2Cl_2 \cdot Li_x$ $0.2 < x < 0.6$	11.5283	7.8522	14.5745
$W(O)_2Cl_2 \cdot Li_x$ $x > 0.7$	16.8630	16.8630	14.9990

Table 6.2, *Cell parameters for phases pre sent in* $W(O)_2Cl_2 \cdot Li_x$.

In the range $0 < x \leq 0.2$, the material shows X-ray lines characteristic for 'pure' $W(O)_2Cl_2$, with the cell parameters shown in table 6.2. For $0.2 < x < 0.6$, the material consists of two phases; $W(O)_2Cl_2$ and a new phase. The intensities of the peaks corresponding to the second phase increase relative to those of $W(O)_2Cl_2$ until at x = 0.6 lines corresponding to $W(O)_2Cl_2$ no longer remain. Between x = 0.6 and x = 0.7 a third phase appears corresponding to the composition $W(O)_2Cl_2 \cdot Li_{2.0}$.

As outlined in the introduction, the crystal structure of $W(O)_2Cl_2$ (Figure 6.1) consists of layers of $W(O)_2Cl_2$ octahedra which share corners via oxygen, leaving the apices occupied by chlorine. The layers are separated from one another by a 3.7 Å van der Waals region. Within this region there are 2 different sites (A and B) compatible with metal atom occupation. Whereas the type B sites are found to be occupied in the related oxohalide FeOCl[15], the interlayer expansion encountered in $W(O)_2Cl_2 \cdot Li_x$

	I	2ϑ(degrees)	d (Å)	(h,k,l)
$WO_2Cl_2 \cdot Li_{0.10}$	s	12.821	6.904	002
	s	23.795	3.740	
	s	24.019	3.705	
	m	25.710	3.465	
	w	30.136	2.965	
	m	32.765	2.733	
	m	35.321	2.541	
	w	36.908	2.435	
	s	38.893	2.316	
	s	39.985	2.255	
	w	42.049	1.757	
	w	46.774	1.942	
	w	47.296	1.922	
	w	48.689	1.870	
	w	49.211	1.852	
	s	51.743	1.766	
	m	52.686	1.737	
	w	53.206	1.722	
	w	53.529	1.712	
	w	54.596	1.681	
	vw	56.952	1.617	
$WO_2Cl_2 \cdot Li_{0.50}$	s	11.928	7.419	002
	s	12.202	7.253	
	s	12.750	6.943	
	s	23.454	3.793	
	m	23.902	3.723	
	s	24.200	3.778	
	s	24.648	3.612	
	m	25.719	3.464	
	vw	29.278	3.050	
	w	29.677	3.010	
	w	30.000	2.978	
	w	30.199	2.959	
	w	32.639	2.743	
	m	33.087	2.707	
	w	33.410	2.682	
	m	35.452	2.532	
	m	36.348	2.472	
	m	37.244	2.414	
	w	37.891	2.374	
	w	38.165	2.358	
	m	38.588	2.333	
	m	38.912	2.314	
	m	39.385	2.287	
	m	39.982	2.225	
	w	41.500	2.176	
	m	47.972	1.896	
	vw	48.943	1.861	
	w	49.267	1.849	
	w	50.337	1.813	
	w	50.611	1.803	
	s	51.781	1.765	
	w	52.752	1.735	
	w	53.050	1.726	
	vw	53.598	1.709	
	w	54.444	1.685	
	w	54.917	1.672	
	w	60.792	1.524	

Table 6.1

$WO_2Cl_2 \cdot Li_{0.70}$	s	11.948	7.407	002
	m	12.196	7.257	
	w	12.742	6.947	
	m	23.429	3.797	
	w	23.925	3.719	
	vs	27.197	3.678	
	m	24.594	3.619	
	vw	29.281	3.050	
	m	29.703	3.007	
	vw	30.149	2.964	
	vw	33.026	2.712	
	s	33.422	2.681	
	m	35.505	2.528	
	m	36.299	2.475	
	m	36.968	2.431	
	w	37.810	2.379	
	s	38.431	2.343	
	w	39.225	2.297	
	w	41.481	2.177	
	w	47.854	1.900	
	m	49.044	1.857	
	w	49.466	1.842	
	m	50.086	1.821	
	w	50.433	1.809	
	vw	51.673	1.769	
	vw	52.987	1.728	
	s	54.301	1.689	
	w	57.277	1.608	
	w	58.690	1.573	
	w	60.029	1.541	
	w	60.549	1.529	
	m	61.443	1.509	
	w	63.030	1.475	
	w	63.947	1.455	
	w	64.517	1.444	
$WO_2Cl_2 \cdot Li_{1.63}$	s	11.893	7.441	002
	vw	23.761	3.744	
	s	24.380	3.651	
	w	29.607	3.017	
	m	33.596	2.667	
	m	35.801	3.453	
	vw	37.065	2.425	
	m	38.304	2.349	
	vw	48.209	1.887	
	w	48.730	1.868	
	m	49.874	1.828	
	m	54.742	1.677	
	vw	57.647	1.599	
	vw	58.666	1.574	
	vw	61.518	1.507	
	vw	63.227	1.471	
	vw	64.020	1.454	
	vw	64.615	1.442	

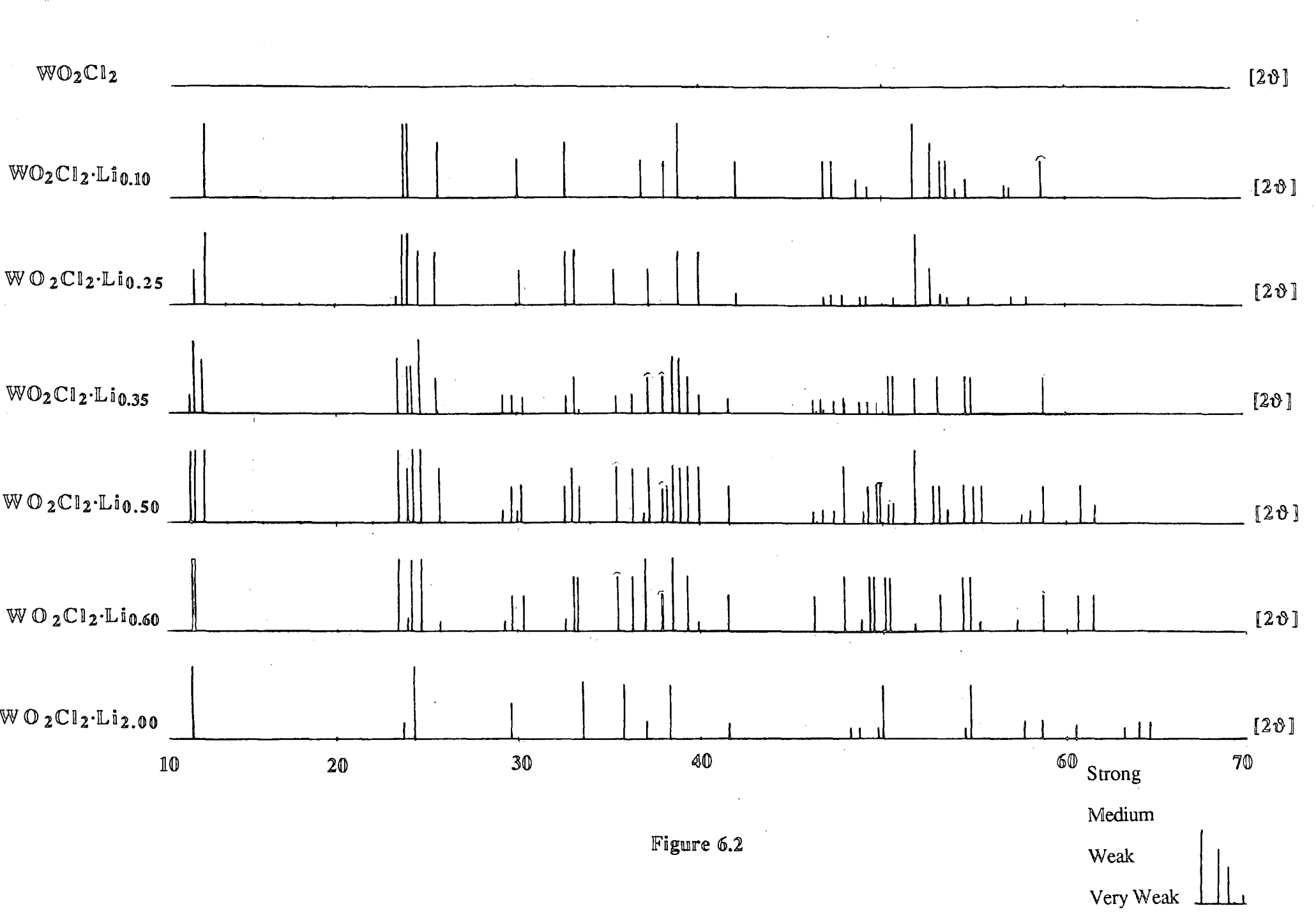
WO2Cl2
[2ϑ]
WO2Cl2·Li0.10
[2ϑ]
WO2Cl2·Li0.25
[2ϑ]
WO2Cl2·Li0.35
[2ϑ]
WO2Cl2·Li0.50
[2ϑ]
WO2Cl2·Li0.60
[2ϑ]
WO2Cl2·Li2.00
[2ϑ]
10
20
30
40
60
70
Strong
Medium
Weak
Very Weak

Figure 6.2

suggests that they are not occupied here. The sum of the covalent radii of Li and Cl is 2.40 Å[16]. Assuming that the site occupied by the lithium is equidistant from each of the surrounding chlorines, then the B site to chlorine distance of 2.73 Å, calculated on the available crystal data, is large enough to accommodate the small lithium atom without any expansion of the lattice. However, the A site to chlorine distances are 2.25 Å some 0.15 Å shorter than the sum of the covalent radii of Li and Cl. Therefore, occupation of these sites would result in layer expansion. Consistently, the observed interlayer expansion of 0.5746 Å ($c/2$) leads to a Li-Cl distance of 2.44 Å (calculated assuming an idealised geometry) which compares favourably with the sum of the covalent radii. An extended view of $W(O)_2Cl_2{\cdot}Li_{1.0}$ between the tungsten oxide layers with the lithium metal occupying one set of the tetrahedral sites is shown in figure 6.3.

6.5 Reaction of $W(O)_2Cl_2$ with MO-2,6-$Bu^t_2C_6H_3$ where M =Na and K: *Preparation of $W(O)_2Cl_2{\cdot}M_x$ where $0 < x \leq 1$.*

The ready intercalation of lithium into $W(O)_2Cl_2$ using aryloxide reagents suggested that it might prove possible to intercalate the larger alkali metal ions, Na and K by a similar method. MOAr (M = Na, K) do indeed react in an analogous manner with $W(O)_2Cl_2$ to afford, in each case, insoluble, dark, moisture sensitive, crystalline solids and a red-green dichroic supernatant solution according to equation 6.3.

$$W(O)_2Cl_2 + xM(O\text{-}2,6\text{-}Bu^t_2C_6H_3) \xrightarrow[M = Na, K]{tol.} W(O)_2Cl_2.M_x + \text{'organics'} \quad (6.3)$$
$$0 < x \leq 1$$

Characterisation of the product solids was provided by elemental analysis (Chapter 7, section 7.6.2-3) which indicated that up to one molar equivalent of sodium and potassium may be intercalated. ^1H NMR analysis of the organic components showed

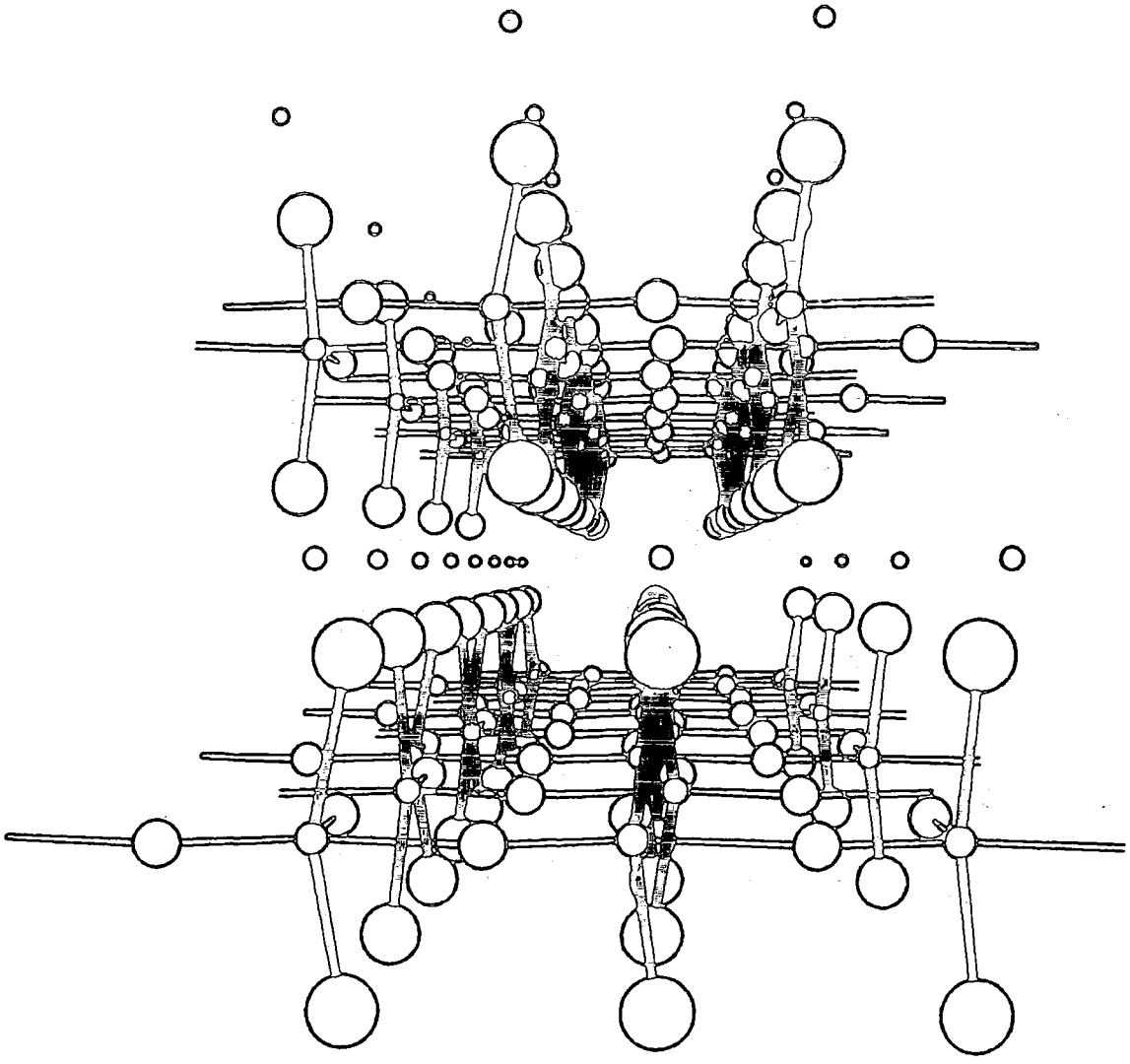

Figure 6.3 *An extended view between the tungsten oxide layers with the alkali metal occupying one set of tetrahedral sites.*

them to be a 50:50 mixture of the biphenol (1) and HO-2,6-$Bu^t_2C_6H_3$ (2) indicating that a similar mechanism to that shown in scheme 6.1 is operating.

6.6 Reaction of $W(O)_2Cl_2$ with $NaBu^n$:

Preparation of $W(O)_2Cl_2{\cdot}Na_x$ where $0 < x \leq 2$.

Since $LiBu^n$ results in incorporation of up to two molar equivalents of lithium, it was of interest to establish if additional sodium could be introduced using the analogous $NaBu^n$ reagent. To our knowledge, highly pyrophoric $NaBu^n$ has not been explored extensively as a sodium intercalation reagent, the preferred mediator being sodium napthalenide. When $W(O)_2Cl_2$ is treated with $NaBu^n$, a range of complexes of stoichiometry $W(O)_2Cl_2{\cdot}Na_x$ $0 < x \leq 2$ may be obtained in high yield according to equation 6.4.

$$W(O)_2Cl_2 \xrightarrow[\text{tol.}]{x NaBu^n} W(O)_2Cl_2.Na_x \quad (6.4)$$

$0 < x \leq 2$

Characterisation of the products was again provided by elemental analysis (Chapter 7, section 7.6.2).

6.7 Characterisation of Halide Bronzes of the Type $W(O)_2Cl_2{\cdot}M_x$

(M = Na) where $0 < x \leq 2$ and

$W(O)_2Cl_2{\cdot}M_x$ (M = K) where $0 < x \leq 1$.

A range of materials of formula $W(O)_2Cl_2{\cdot}M_x$ (M = Na, K) and x ranging from zero to two have been subjected to X-ray powder diffraction analysis (Debye Scherrer Camera). The results are tabulated in tables 6.3 and 6.4 for x = 0.25, 0.50, 0.75, 1.0 and 2.0.

	I	2ϑ(degrees)	d (Å)	(h,k,l)
$WO_2Cl_2 \cdot Na_{0.25}$	s	11.482	7.700	002
	s	23.810	3.734	
	s	24.305	3.656	
	m	26.200	3.398	
	m	33.990	2.635	
	w	44.545	2.032	
	m	49.475	1.841	
	w	55.090	1.666	
$WO_2Cl_2 \cdot Na_{0.50}$	s	11.375	7.772	002
	s	23.395	3.716	
	s	24.301	3.700	
	w	26.155	3.404	
	m	33.975	2.636	
	w	44.431	2.037	
	m	49.051	1.856	
	w	50.120	1.819	
	w	55.205	1.662	
$WO_2Cl_2 \cdot Na_{0.75}$	s	11.557	7.650	002
	s	23.750	3.743	
	s	24.305	3.659	
	vw	26.185	3.400	
	m	34.005	2.634	
	w	44.630	2.029	
	vw	49.600	1.836	
	w	54.785	1.674	
$WO_2Cl_2 \cdot Na_{1.00}$	s	11.370	7.782	002
	s	23.661	3.757	
	s	24.311	3.658	
	m	26.211	3.397	
	m	34.061	2.630	
	m	44.661	2.027	
	w	48.161	1.888	
	w	49.611	1.836	
	vw	54.461	1.683	
$WO_2Cl_2 \cdot Na_{2.00}$	s	11.649	7.590	002
	s	23.780	3.738	
	m	24.295	3.660	
	vw	26.175	3.402	
	w	33.950	2.638	
	m	45.010	2.012	
	w	49.555	1.838	
	w	54.965	1.669	

Table 6.3

	I	2ϑ(degrees)	d (Å)	(h,k,l)
$WO_2Cl_2 \cdot K_{0.25}$	s	10.894	8.115	002
	s	12.744	6.940	
	s	22.794	3.898	
	m	23.944	3.713	
	m	33.144	2.701	
	m	35.144	2.551	
	w	40.294	2.236	
	vw	49.044	1.856	
	w	54.001	1.697	
	m	55.205	1.662	
	w	59.150	1.561	
	w	64.255	1.448	
$WO_2Cl_2 \cdot K_{0.50}$	s	10.740	8.230	002
	s	12.765	6.929	
	s	22.670	3.919	
	m	24.105	3.689	
	m	33.741	2.654	
	m	35.141	2.551	
	w	40.29	2.237	
	m	49.050	1.856	
	vw	54.245	1.690	
	w	55.100	1.665	
	w	57.750	1.595	
	w	65.185	1.430	
$WO_2Cl_2 \cdot K_{0.75}$	s	10.780	8.200	002
	s	12.570	7.036	
	m	22.595	3.932	
	w	24.240	3.669	
	w	32.730	2.734	
	vw	37.211	2.414	
	w	40.350	2.233	
	w	47.265	1.922	
	m	55.375	1.658	
	w	55.095	1.666	
	w	58.245	1.583	
	m	64.951	1.434	
$WO_2Cl_2 \cdot K_{1.00}$	s	10.700	8.261	002
	w	21.951	4.050	
	s	23.450	3.790	
	s	25.850	3.437	
	s	33.400	2.680	
	s	40.655	2.218	
	w	47.600	1.909	
	w	53.750	1.704	
	m	55.151	1.664	
	vw	58.950	1.565	
	vw	64.450	1.444	

Table 6.4

The sum of the covalent radii of Na and Cl and K and Cl are 2.80 and 3.18 Å repectively[16]. Since the B site to chlorine distances, assuming an equidistant position from Cl(1-4) and Cl(6) (Figure 6.1), are 2.73 Å and the A site to chlorine distances, assuming an equidistant position from Cl(1-2) and Cl(5-6) (Figure 6.1) are 2.25 Å, occupancy of either sites A or B would lead to an interlayer expansion with sodium and potassium ions. The observed interlayer expansions for Na and K are illustrated graphically in figure 6.4.

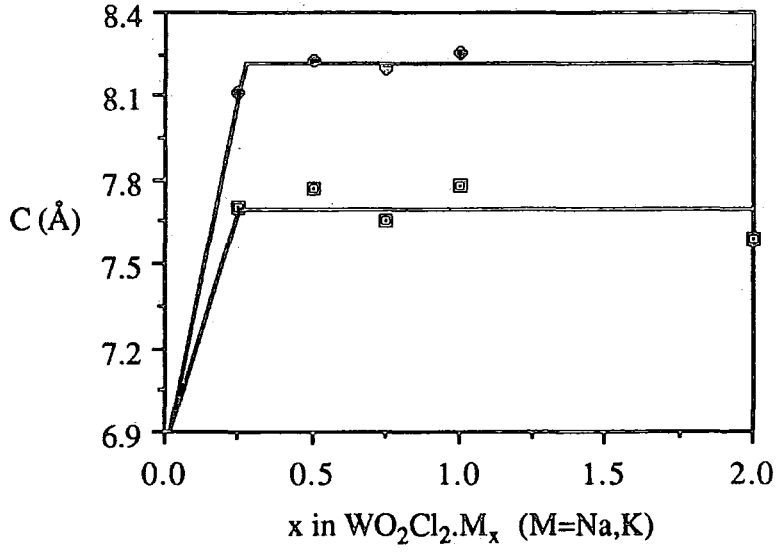

Figure 6.4

Occupancy of the 4-coordinate site would lead to an interlayer expansion of 1.69 Å for sodium which is far greater than the observed expansion of 0.77 Å (the latter is calculated by deducting the average value of d[Å] for the 002 reflection for $W(O)_2Cl_2{\cdot}Na_x$ (x = 0.25, 0.50, 0.75, 1.0 and 2.0) (Table 6.3) from the analogous value for $W(O)_2Cl_2$ (Table 6.2)). Similarly for K, occupancy of the A site would result in an expansion of 2.86 Å, considerably greater than the observed value of 1.28 Å. These inter-layer expansions are more consistent with sodium and potassium occupying the 5-coordinate sites in contrast to lithium which is believed to reside in the 4-coordinate site.

The Debye-Scherrer data also suggest that there is only one phase present for the Na and K chloride bronze materials, indeed the X-ray diffraction pattern giving only two sets of peaks at all doping levels, attributable to $W(O)_2Cl_2$ and a layer-expanded phase whose intensity increases with doping.

6.8 Conductivity/Resistivity Properties of Halide Bronzes of the Type $W(O)_2Cl_2 \cdot M_x$ (M = Li,Na) where $0 < x \leq 2$ and $W(O)_2Cl_2 \cdot M_x$ (M = K) where $0 < x \leq 1$.

Conductivity measurements carried out at room temperature inside an argon filled glove box on powdered samples (15 - 25 mg) compressed under ca. 0.2 GPa pressure into cylindrical pellets (3 mm diameter, 0.5 to 1.0 mm thickness) showed that resistivity, ρ decreases with increased doping to a minimum in the region of $x \cong 0.75$ after which ρ increases (dramatically for Li at $x > 1$) (Figure 6.5). The resistivity as a function of temperature was measured for $W(O)_2Cl_2 \cdot Li_{0.25}$ by the four-contact van der Pauw[17] method in a specially designed cell under argon atmosphere using gold paste (M8001, Degussa) to fabricate electrical contacts between four thin platinum leads (radially arranged at 90°) and the circumference of a pellet (3 mm diameter and 0,6 mm thickness). A good agreement was obtained for the room temperature resistivity value as measured by the former and the latter methods; $\ln\rho_{298} = 6.2$ and 5.8 Ω.cm respectively. A non-linear Arrhenius plot within the 213 to 373 K temperature range may be consistent with a mixed ionic-electronic conduction mechanism.

Some indirect evidence for lithium ion mobility is provided by the observation that Li is readily removed upon washing $W(O)_2Cl_2 \cdot Li_{2.0}$ with a polar solvent such as THF. Thus a sample of $W(O)_2Cl_2 \cdot Li_{2.0}$ (1.0g, 3.33 mmol.) washed several times with fresh THF (6 * 20 cm^3), resulted in the extraction of LiCl to yield a black solid of stoichiometry $W(O)_2Cl \cdot Li_{1.0}$ (Yield, 0.85g (99%)). Analysis of the product by X-ray powder diffraction indicated that removal of Li is accompanied by degradation of the $W(O)_2Cl_2 \cdot Li_{2.0}$ lattice presumably in favour of a new oxohalide matrix.

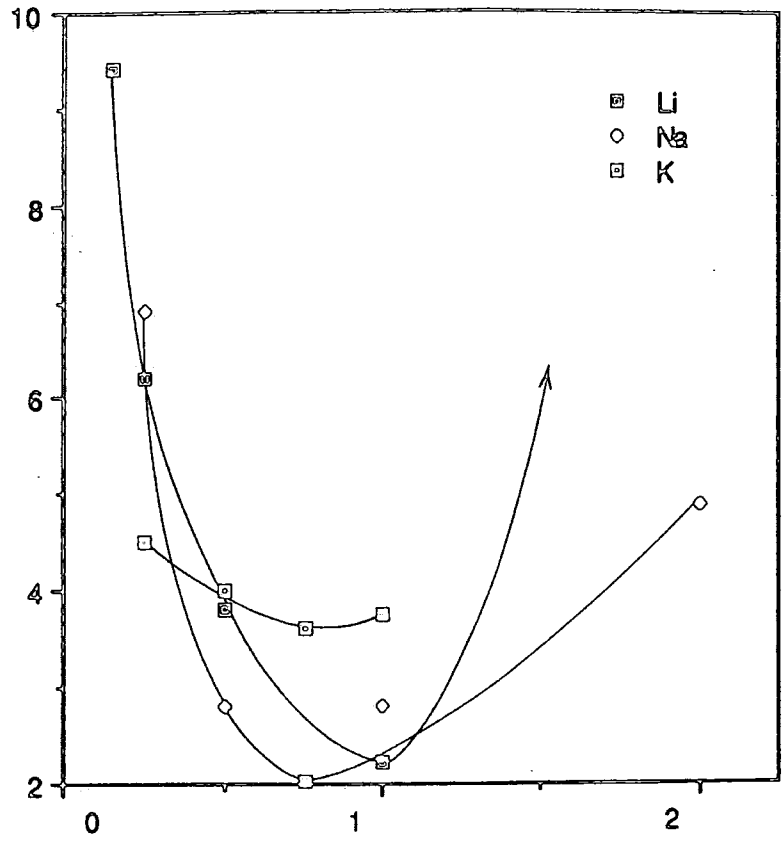

Ln ρ

x in $W(O)_2Cl_2 \cdot M_x$

Figure 6.5

6.9 Summary.

The convenient synthesis of $W(O)_2Cl_2$ by a low temperature, high yield route and the unexpected observation that alkali metal aryloxides may act as intercalating agents has led to the isolation of a series of tungsten 'halide bronzes' of general formula $W(O)_2Cl_2 \cdot M_x$. In general, the alkali metal aryloxides are suitable for the intercalation of one molar equivalent of the alkali metal ions Li, Na and K. However, up to two lithiums and sodiums may be introduced using MBu^n (M = Li, Na) reagents. The materials have been characterised by elemental analysis and X-ray powder diffraction. Much further work is required; neutron diffraction studies on the structures will be sought along with a more detailed assessment of conductivity properties. It will also be of considerable interest to establish whether other mixed anion species e.g. $W(O)_2Br_2$, $W(S)_2Cl_2$, $W(O)(S)Cl_2$ etc. prepared by the low temperature route described in chapter 2 can also act as intercalation hosts.

6.10 References.

1. F. Wöhler, *Ann. Chim. Phys.*, 1823, 43, 29.
2. See, for example 'Tungsten Bronzes, Vanadium Bronzes and Related Compounds', P. Hagenmüller in 'Comprehensive Inorganic Chemistry', Vol 4, pp. 541-605, Pergamon Press (1973).
3. M.M. Thackeray, W.I.F. David, P.G. Bruce and J.B. Goodenough, *Mat. Res. Bull.*, 1983, 18, 461.
4. J.B. Goodenough, M.M. Thackeray, W.I.F. David and P.G. Bruce, *Revue de Chimie Mineral*, 1984, 21, 435.
5. M.M. Thackeray, P.J. Johnson, L.A. de Picciotto, W.I.F. David, P.J. Bruce and J.B. Goodenough, *Mat. Res. Bull.*, 1984, 19, 179.
6. M.M. Thackeray, W.I.F. David and J.B. Goodenough, *Mat. Res. Bull.*, 1982, 17, 785.
7. J.A. Perri, E. Banks and B. Post, *J. Appl. Phys.*, 1957, 28, 1272.
8. A.P. Legrand and S. Flandrois, Chemical Physics of Intercalation; NATO ASI Series, Plenum Press (1989).

9. M.G.S.R. Thomas, P.G. Bruce and J.B. Goodenough, *Solid State Ionics*, 1985, 17, 13.

10. A.W. Sleight, *Inorg. Chem.*, 1969, 8, 1764.

11. O. Jarchow, *Z. Anorg. Allg. Chem.*, 1968, 363, 58.

12. D.C. Nonhebel and J.C. Walton, 'Free-radical Chemistry', pp 326-345, Cambridge University Press (1974).

13. M.S. Withington, Electrochem. Soc. Meeting, Dallas Texas (1975).

14. J.F. Ackerman, *Mat. Res. Bull.*, 1988, 23, 165.

15. L. Palvadeau, C. Rouxel and J. Portier, *Mat. Res. Bull.*, 1978, 13, 221.

16. W.W. Porterfield, "Inorganic Chemistry-A Unified Approach', Addison-Wesley, New York (1984).

17. L.J. van der Pauw, *Phillips Res. Rep.*, 1958, 13 1.

Chapter Seven

Experimental Details.

7.1 General.

All manipulations of air and/or moisture sensitive materials were performed on a conventional vacuum/inert atmosphere (nitrogen or argon) line using standard Schlenk and cannula techniques, or in an inert atmosphere (nitrogen or argon) filled glove box.

The following solvents were dried by prolonged reflux over a suitable drying agent, being freshly distilled and deoxygenated before use (drying agent in parentheses): toluene (sodium metal), petroleum ether (40-60°C and 100-120°C, lithium aluminium hydride), octane (lithiumaluminium hydride), tetrahydrofuran (sodium benzophenone ketyl), acetonitrile (calcium hydride), dichloromethane (calcium hydride), 1,2-dichloroethane (calcium hydride), carbon disulphide (4Å molecular sieves) and diethyl ether (lithium aluminium hydride).

The following NMR solvents were dried by vacuum distillation from a suitable drying agent (in parentheses) and stored over activated 4Å molecular sieves: d^6-benzene (phosphorus (V) oxide), d^8-toluene (phosphorus (V) oxide) and d-chloroform (phosphorus (V) oxide).

Elemental analyses were performed by the microanalyltical services of this department.

Infra red spectra were recorded on Perkin-Elmer 577 and 457 grating spectrophotometers using either KBr or CsI windows. Absorptions abbreviated as: s (strong), m (medium), w (weak), br (broad), sp (sharp), sh (shoulder).

Mass spectra were recorded on a VG 7070E Organic Mass Spectrometer.

NMR spectra were recorded on the following instruments, at the frequencies listed, unless stated otherwise: Brucker AC 250, ^1H (250.13 MHz), ^{13}C (62.90 MHz), ^{31}P (101.26 MHz); Varian EM 360L, ^1H (60 MHz); Hitachi Perkin Elmer R-24(B), ^1H (60 MHz). The following abbreviations have been used for band multiplicities: s (singlet), d (doublet), t (triplet), q (quartet), qnt (quintet), sxt (sextet), spt (septet), m (multiplet). Chemical shifts are quoted as δ in ppm with respect to the following references, unless stated otherwise: ^{31}P (dilute aq. H_3PO_4, 0 ppm); ^{13}C (C_6D_6, 128.0 ppm); ^1H (C_6D_6, 7.15 ppm and $CDCl_3$, 7.24 ppm).

X-ray (powder) diffraction data were recorded using either (a) a Debye Scherrer Camera or (b) a Guinier Camera. Line intensities abbreviated as:
vs (very strong) s (strong), m (medium), w (weak), vw (very weak).

The following chemicals were prepared by previously published procedures: $Mo(O)Cl_4$[1], $LiOAr$[2], PMe_3[3], $CpNbCl_4$[4], $CpTaCl_4$[4], Cp^*TaCl_4[5], $NaOAr$[6], C_4H_9Na[7], $KOAr$[6]. A new preparative procedure for $SPMe_3$ is described below.

The following chemicals were obtained commercially and used as recieved unless stated otherwise: molybdenum pentachloride (Aldrich), tungsten hexachloride (Aldrich), niobium pentachloride (Aldrich), tantalum pentachloride (Aldrich), tungsten trioxide (Aldrich), molybdenum trioxide (Aldrich), chlorotrimethylsilane (Aldrich), hexamethyldisiloxane (Aldrich, dried and stored over 4Å molecular sieves), hexamethyldisilathiane (Fluka, distilled, dried and stored over 4Å molecular sieves), 2,6-dimethylphenol (Aldrich), 2,4,6-trimethylphenol (Aldrich), 2,6-diisopropylphenol (Aldrich), 2,6-ditertiarybutyl phenol (Aldrich), 2,6-diphenylphenol (Aldrich), tertiarybutanol (Aldrich), n-butyl lithium (Aldrich), phosphorus pentachloride (Aldrich), triethylamine (Aldrich, dried and stored over 4Å molecular sieves).

7.1.1 Preparation of Trimethylphosphine Sulphide.

Trimethylphosphine (4.75g, 62.4 mmol.) was condensed onto a frozen mixture of elemental sulphur (1g, 31.2 mmol.) and toluene ($50cm^3$). The mixture was allowed to warm to room temperature and was stirred for 1h. to afford a clear solution. Filtration, followed by concentration to *ca.* 20 cm^3 and cooling to *ca.* -78°C afforded colouress crystals which were collected and dried *in vacuo*. Yield, 3.25g (96%).

Elemental analysis for C_3H_9SP Found (Required): %C, 33.30 (33.32), %H, 8.45 (8.39), %S, 30.00 (29.65).

Infrared data (Nujol, CsI, cm^{-1}): 2260(w), 2025(w), 1418(m), 1405(m), 1310(s,sh), 1304(s), 1292(s,sh), 1284(s), 1270(s,sh), 1122(m), 945(s,br), 861(s), 791(m), 740(s), 710(br,sh), 560(s), 288(s).

Mass spectral data (CI, isobutane carrier gas, m/z, ^{32}S): 108$[M]^+$, 93$[M-Me]^+$, 78$[M-Me_2]^+$, 63$[M-Me_3]^+$.

^{1}*H NMR data* (250MHz, d^6-benzene, 298K): 1.03 (d, $^2J_{(PH)}$ = 13.1 Hz, SP*Me*3).

7.2 Experimental Details To Chapter 2.

7.2.1 Synthesis of W(O)Cl4 (1).

A dichloromethane solution of $(Me_3Si)_2O$ (2.05g,12.6 mmol. in 15 cm^3 CH_2Cl_2) was added dropwise to a suspension of WCl_6 (5.0g, 12.6 mmol.) in dichloromethane (20 cm^3) at room temperature over a period of 15 min. An immediate reaction ensued leading to deposition of W(O)Cl4 in the form of red crystals. The mixture was stirred for a further 60 min. The supernatant liquor was then removed by filtration and the solid was collected, washed with petroleum ether (2 x 10 cm^3, b.p. 40-60°C) and dried *in vacuo*. Yield, 4.28g (99%).

Elemental analysis for Cl_4OW, Found, (Required): %W, 53.9 (53.8); %Cl, 41.2 (41.5).

Infra red data (Nujol,CsI, cm^{-1}): 880-900(s,br), 387(s,br), 368(m,sh), 355(m,sh), 334(s,sp), 329(m,sh), 320(m,sh), 308(w,sh), 285(w).

7.2.2 Synthesis of $W(O)_2Cl_2$ (2).

An octane solution of $(Me_3Si)_2O$ (2.38g, 14.7 mmol. in 15 cm^3 octane) was added to a stirred suspension of $W(O)Cl_4$ (5.0g, 14.6 mmol.) in octane (40 cm^3). The mixture was rapidly warmed to 80°C and stirred untill the orange colouration of the octane solution was discharged to leave a yellow solid and a colourless solution. After cooling to room temperature, the supernatant solution was decanted from the solid, which was collected, washed with petroleum ether (2 x 20 cm^3, b.p. 40-60 °C) and dried *in vacuo*. Yield, 3.99g (95%).

Elemental analysis for Cl_2O_2W, Found (Required): %W, 63.7, (64.1); %Cl, 24.4, (24.7).

Infra red data (Nujol, CsI, cm^{-1}): 800-830(s,br), 415(s), 395(s,sh), 385(s,sh), 347(s), 300(m,sh), 290(m,sh), 279(s), 260(m,sh).

7.2.3 Synthesis of $W(O)_2(Cl)_2(CH_3CN)_2$ (3).

An acetonitrile solution of $(Me_3Si)_2O$ (2.38g, 14.7 mmol. in 15 cm^3) was added dropwise to a stirred suspension of $W(O)Cl_4$ (5g, 14.6 mmol.) in acetonitrile (40 cm^3) at room temperature, over a period of 15 min. An immediate reaction ensued leading to a pale blue solution which was stirred for a further 2h. Filtration of the supernatant solution followed by concentration to half volume and cooling to *ca.* -45°C afforded colourless moisture sensitive $W(O)_2(Cl)_2(CH_3CN)_2$. The dark blue mother liquor was decanted from the solid which was collected, washed with petroleum ether (2 x 10 cm^3, b.p. 40-60°C) and dried *in vacuo*. Yield, 3.77g (70%).

Elemental analysis for $N_2C_4H_6Cl_2O_2W$, Found (Required): %W, 50.12, (49.84); %Cl, 19.25, (19.22); %H, 1.65, (1.64); %C, 13.02, (13.03); %N, 7.64 (7.59).

Infra red data (Nujol, CsI, cm^{-1}): 2320(s,sp), 2300(s,sp), 1409(m), 1367(s,sp), 1040(m,sp), 1031(m,sh), 980(s,sp), 971(m,sh), 946(s,sh), 932(s,sh), 927(s,sp), 920(s,sh), 379(s,sp), 394(s,br), 380(m,sh).

7.2.4 Synthesis of $W(O)_2Cl(OSiMe_3)$ (4).

A dichloromethane solution of $(Me_3Si)_2O$ (0.96g, 5.86 mmol. in 15 cm^3 CH_2Cl_2) was added dropwise to a stirred suspension of $W(O)Cl_4$ (1.0g, 2.93 mmol.) in dichloromethane (20 cm^3) at room temperature over a period of 15 min. The $W(O)Cl_4$ suspension was consumed during 2h. to give a blue solution. Filtration, followed by concentration to half volume and cooling to *ca.* -78°C, afforded blue crystals of $W(O)_2Cl(OSiMe_3)$. Yield, 0.7g (70%).

Elemental analysis for $C_3H_9SiClWO_3$, Found, (Required): %W, 55.9 (56.7); %Cl, 10.1 (10.9); %C, 10.2 (11.1); %H, 2.5 (2.8).

Infra red data (Nujol,CsI, cm^{-1}): 1255(s,sp), 1002(s,br), 700-900(s,br), 280-360(s,br).

^1H NMR data (250MHz, d-chloroform, 298K): 0.42 (s,Si*Me*$_3$).

7.2.5 Synthesis of $Mo(O)Cl_3$ (5).

A dichloromethane solution of $(Me_3Si)_2O$ (2.97g, 18.3 mmol. in 15 cm^3 CH_2Cl_2) was added dropwise at room temperature to a solution of $MoCl_5$ (5.0g, 18.3 mmol.) in dichloromethane (20 cm^3). The mixture was stirred at room temperature overnight to give a dark brown solid and a colourless solution. The supernatant solution was decanted from the solid, which was collected, washed with petroleum ether (2 x 20 cm^3, b.p. 40-60°C) and dried *in vacuo*. Yield 3.90g (97.5%).

Elemental analysis for Cl_3OMo, Found (Required): %Cl, 48.69 (48.72).

Infra red data (Nujol, CsI cm^{-1}): 1007(s,sp), 398(s), 352(s), 309(m) 295(m,sh).

Mass spectral data m/z (EI, 70eV, ^{96}Mo, ^{35}Cl,^{16}O): 201$[MoCl_3]^+$, 182$[MoOCl_2]^+$, 166$[MoCl_2]^+$, 148$[MoOCl]^+$, 131$[MoCl]^+$, 113$[MoO]^+$, 96$[Mo]^+$.

7.2.6 Synthesis of $Mo(O)_2Cl_2$ (6).

A dichloromethane solution of $(Me_3Si)_2O$ (3.2g, 19.7 mmol. in 15 cm^3 CH_2Cl_2) was added dropwise at room temperature to a stirring suspension of $Mo(O)Cl_4$ (5.0g, 19.7 mmol.) in dichloromethane (20 cm^3). The mixture was stirred at room temperature for 4h. to give a pale yellow solid suspended in a brown solution. The solid was isolated by cannular filtration, washed with light petroleum ether (2 x 20 cm^3, b.p. 40-60°C) and dried *in vacuo*. Yield 3.78g (97%).

Elemental analysis for Cl_2O_2Mo, Found (Required): %Cl, 35.7 (35.7).

Infra red data (Nujol, CsI, cm^{-1}): 800-830(s,br), 443(s,sp), 425(m,sh), 409(m,sh), 385(s,sp), 354(s,sp), 291(m,sp).

7.2.7 Synthesis of $W(S)Cl_4$ (7).

A suspension of WCl_6 (5.0g, 12.6 mmol.) in dichloromethane (20 cm^3) was cooled in a dry-ice/acetone slush bath and treated dropwise over a period of 15 min. with a chilled (*ca.* -30°C) solution of $(Me_3Si)_2S$ (2.25g, 12.6 mmol. in 15 cm^3 CH_2Cl_2). An immediate reaction ensued leading to a red solution and precipitation of a brown amorphous solid. The mixture was allowed to warm to room temperature and stirred for a further 30 min. Filtration of the supernatant solution followed by concentration and cooling to *ca.* -78°C afforded red moisture sensitive crystals of

$W(S)Cl_4$ (2.95g, 65%). A second extraction of the residue with CH_2Cl_2 (20cm^3) followed by crystallization resulted in a combined yield of 80% of analytically pure $W(S)Cl_4$.

Elemental analysis for Cl_4SW, Found (Required): %W, 51.5, (51.4); %Cl, 39.5, (39.6); %S, 9.0, (9.0).

Infrared data (Nujol,CsI,cm^{-1}): 560(s,sp), 392(m,sh), 355(s), 306(m,sh), 285(w).

Mass spectral data m/z (EI, 70eV, ^{184}W, ^{32}S, ^{35}Cl). 356 $[WSCl^4]^+$, 321 $[WSCl_3]^+$, 286 $[WSCl_2]^+$, 251 $[WSCl]^+$, 216 $[WS]^+$, 324 $[WCl_4]^+$, 289 $[WCl_3]^+$, 254 $[WCl_2]^+$, 219 $[WCl]^+$.

7.2.8 Synthesis of $W(S)_2Cl_2$ (8).

A solution of $WSCl_4$ (1.0g, 2.8 mmol.) in dichloromethane (20 cm^3) was cooled in a dry-ice/acetone slush bath and treated dropwise with a chilled (*ca.* -30°C) dichloromethane solution of $(Me_3Si)_2S$ (0.50g, 2.8 mmol. in 15 cm^3 CH_2Cl_2) over a period of 15 min. An immediate reaction ensued, which after 30 min. resulted in a colourless solution and a black amorphous solid. The mixture was allowed to warm to room temperature and stirred for a further 2 hours. The supernatant solution was decanted from the black solid, which was collected, washed with petroleum ether (2 x 10cm^3, b.p.40-60°C) and dried *in vacuo*. Yield, 0.72g (81%).

Elemental analysis for Cl_2S_2W, Found, (Required): %W,57.64 (57.66); %Cl, 21.69 (22.24); %S, 19.90 (20.11).

Infra red data (Nujol,CsI,cm-^{1}): 538(s,sp), 365(m,sh), 321(s,br), 287(m,sh).

Mass spectral data m/z (EI, 70eV, ^{184}W, ^{32}S, ^{35}Cl) 318 $[WS_2Cl_2]^+$, 286 $[WSCl_2]^+$, 251 $[WSCl]^+$, 216 $[WS]^+$, 184 $[W]^+$.

7.2.9 Synthesis of $Mo(S)Cl_3$ (9).

A solution of $MoCl_5$ (1.0g, 3.66 mmol.) in dichloromethane (20 cm^3) was cooled in a dry-ice/acetone slush bath and treated dropwise with a chilled (*ca.* -30°C) dichloromethane solution of $(Me_3Si)_2S$ (0.65g, 3.66 mmol. in 15 cm^3 CH_2Cl_2) over a period of 15 min. An immediate reaction ensued, which after 30 min. resulted in a colourless solution and an olive green, amorphous solid. The mixture was allowed to warm to room temperature and stirred overnight. The supernatant solution was decanted from the solid which was collected, washed with petroleum ether (2 x 20 cm^3, b.p. 40-60°C) and dried *in vacuo*. Yield 0.75g (87%).

Elemental analysis for Cl_3SMo, Found (Required): %S, 14.40 (13.68); %Cl, 45.25 (45.38).

Infra red data Nujol, CsI, cm^{-1}): 398(s,br); 375(m,sh), 354(m), 346(w,sh), 290(m,br).

Mass spectral data m/z (EI, 70eV, ^{96}Mo, ^{32}S, ^{35}Cl,^{16}O): 326$[Mo_2S_2Cl_2]^+$, 291$[Mo_2S_2Cl]^+$, 259$[Mo_2SCl]^+$, 233$[MoSCl_3]^+$, 198$[MoSCl_2]^+$, 163$[MoSCl]^+$, 128$[MoS]^+$.

7.2.10 Synthesis of $W(O)(S)Cl_2$ (10).

A chilled (ca. -30°C) dichloromethane solution of $(Me_3Si)_2S$ (0.52g, 2.93 mmol. in 15 cm^3 CH_2Cl_2) was added dropwise over a period of 15 min. to a stirred suspension of $W(O)Cl_4$ (1.0g, 2.93 mmol.) in dichloromethane (20 cm^3) cooled in a dry-ice/acetone slush bath. An immediate reaction ensued, which after 30 min. resulted

in a colourless solution and a light brown amorphous solid. The mixture was allowed to warm to room temperature and stirred for a further 2 hours. The supernatant solution was decanted from the light brown solid, which was collected, washed with petroleum ether (2 x 10 cm^3, b.p. 40-60°C) and dried *in vacuo*. Yield, 0.73g (82%).

Elemental analysis for Cl_2SOW, Found, (Required): %W, 60.09, (60.71); %S, 9.75, (10.59); %Cl, 22.83, (23.42).

Infra red data (Nujol, CsI, cm^{-1}): 815(s,br), 540(s,sp), 410(s), 372(m,br), 343(s,sp).

Mass spectral data m/z (EI, 70eV, ^{184}W, ^{32}S, ^{35}Cl, ^{16}O). 604 $[W_2O_2S_2Cl_4]^+$, 585 $[W_2S_2O_3Cl_3]^+$, 566 $[W_2S_4Cl_2]^+$, 318 $[WS_2Cl_2]^+$, 302 $[WOSCl_2]^+$.

7.2.11 Synthesis of $Mo(O)(S)Cl_2$ (11).

A chilled (ca. -30°C) carbon disulphide solution of $(Me_3Si)_2S$ (0.70g, 3.92 mmol. in 15 cm^3 CS_2) was added dropwise over a period of 15 min. to a stirred suspension of $Mo(O)Cl_4$ (1.0g, 3.92 mmol.) in carbon disulphide (20 cm^3) cooled in a dry-ice/acetone slush bath. An immediate reaction ensued, which after 30 min. resulted in a colourless solution and a light brown, amorphous solid. The mixture was allowed to warm to room temperature and stirred overnight. The supernatant solution was decanted from the solid, which was collected, washed with petroleum ether (2 x 20 cm^3, b.p. 40-60°C) and dried *in vacuo*. Yield 0.73g (86%).

Elemental analysis for Cl_2OSMo, Found, (Required): % S, 15.14 (14.92); % Cl, 32.75 (32.99).

Infra red data (Nujol, CsI, cm^{-1}): 982(s,sp), 851(w), 720(m), 473(s,sp), 378(s), 369(m,sh), 325(s,sp), 298(s,sh), 255(m).

Mass spectral data m/z (EI, 70eV, ^{96}Mo, ^{32}S, ^{35}Cl,^{16}O): 361 $[Mo_2O_2SCl_3]^+$, 342 $[Mo_2OS_2Cl_2]^+$, 326 $[Mo_2S_2Cl_2]^+$, 310 $[Mo_2OSCl_2]^+$, 214 $[MoOSCl_2]^+$, 198 $[MoSCl_2]^+$, 179 $[MoOSCl]^+$, 163 $[MoSCl]^+$, 147 $[MoOCl]^+$, 128 $[MoS]^+$, 112 $[MoO]^+$.

7.2.12 Synthesis of $Nb(O)Cl_3$ (12).

A 1,2-dichloroethane solution of $(Me_3Si)_2O$ (1.8g, 11.1 mmol. in 15 cm^3 $C_2H_4Cl_2$) was added to a suspension of $NbCl_5$ (3.0g, 11.1 mmol.) in 1,2-dichloromethane (20 cm^3) at room temperature. The mixture was swiftly warmed to 80°C with stirring, and maintained at this temperature for 4.5h. Dissolution of the yellow $NbCl_5$ was accompanied by formation of a white, granular precipitate. After cooling to room temperature, the supernatant solution was decanted from the white solid, which was collected, washed with petroleum ether (2 x 10 cm^3, b.p. 40-60°C) and dried *in vacuo*. Yield, 2.03g (75%).

Elemental analysis for Cl_3ONb, Found (Required): %Cl, 49.62 (49.41); %Nb,43.30 (43.16).

Infrared data (nujol, CsI, cm^{-1}): 1257(m), 940(m,sh), 780(s,br), 414(s,br), 295(s).

Mass spectral data (EI, 70eV, m/z, ^{93}Nb, ^{16}O, ^{35}Cl): 393$[Nb_2O_2Cl_5]^+$, 214$[NbOCl_3]^+$, 179$[NbOCl_2]^+$, 163$[NbCl_2]^+$, 144$[NbOCl]^+$, 128$[NbCl]^+$, 109$[NbO]^+$.

7.2.13 Synthesis of $Nb(O)Cl_3(CH_3CN)_2$ (13).

An acetonitrile solution of $(Me_3Si)_2O$ (1.8g, 11.1 mmol. in 15 cm^3 CH_3CN) was added dropwise at room temperature to a stirred suspension of $NbCl_5$ (3.0g, 11.1 mmol.) in acetonitrile (20 cm^3). The mixture was stirred at room temperature for 2h. to give a colourless solution which was filtered, concentrated to *ca.* 5 cm^3 and cooled to *ca.* -78°C. The resultant colourless, crystalline product was collected and dried *in vacuo*. Yield, 3.1g (95%).

Elemental analysis for $C_4H_6Cl_3N_2NbO$, Found (Required): %C, 15.94 (16.15); %H, 2.11 (2.02), %N, 9.41 (9.42).

Infrared data (Nujol, CsI, cm^{-1}): 2322(s), 2310(s), 2293(s), 2284(s), 1368(m), 1355(m), 1026(m), 960(s,br), 947(s), 935(s), 370(s,br), 333(s), 250(m).

7.2.14 Synthesis of $Nb(O)Cl_3(THF)_2$ (14) .

Tetrahydrofuran (30 cm^3) was added to $Nb(O)Cl_3(CH_3CN)_2$ (0.53g, 1.78 mmol.) at *ca.*-30°C. The mixture was warmed to room temperature with stirring to afford a colourless solution. After 15 min. the mixture was filtered, concentrated to *ca.* 5 cm^3 and cooled to *ca.* -78°C. Addition of cold petroleum ether (10 cm^3, b.p. 40-60°C, *ca.* -30°C) gave colourless crystals of $Nb(O)Cl_3(THF)_2$. Yield, 0.57g (90%).

Elemental analysis for $C_8H_{16}Cl_3NbO_3$, Found (Required): %C, 26.13 (26.70); %H, 4.42 (4.45); %Cl, 26.25 (26.10); %Nb, 22.80 (22.80).

Infrared data (Nujol, CsI, cm^{-1}): 1366(m), 1347(s), 1301(m), 1250(m), 1180(m), 1138(w), 1060(s), 1048(m), 1029(m), 1018(m), 1016(s), 996(m), 960(s), 861(s,br), 833(s,br), 676(m), 578(w), 365(s,br), 327(s), 250(m).

7.2.15 Synthesis of $Nb(O)Br_3$ (15).

The synthesis of yellow $Nb(O)Br_3$ is essentially analogous to that previously described for the synthesis of $Nb(O)Cl_3$. Yield, 3.54g (92%).

Elemental analysis for Br_3ONb, Found (Required): %Br, 69.17 (68.76); %Nb, 26.62 (26.65).

Infrared data (nujol, CsI, cm^{-1}): 750(s,br), 341(m), 309(m,br), 294(s), 269(m).

Mass spectral data (EI, 70eV, m/z, ^{93}Nb, ^{16}O, ^{80}Br): 349$[NbOBr_3]^+$, 333$[NbBr_3]^+$, 269$[NbOBr_2]^+$, 253$[NbBr_2]^+$, 189$[NbOBr]^+$, 173$[NbBr]^+$, 109$[NbO]^+$.

7.2.16 Synthesis of $Nb(O)Br_3(CH_3CN)_2$ (16).

An acetonitrile solution of $(Me_3Si)_2O$ (1.65g, 10.2 mmol. in 15 cm^3 CH_3CN) was added dropwise at room temperature to a stirred suspension of $NbBr_5$ (5.0g, 10.2 mmol.) in acetonitrile (20 cm^3). The mixture was stirred at room temperature for 2h. to give a red solution which was filtered, concentrated to *ca.* 5 cm^3 and cooled to *ca.*-78°C. The resultant yellow, crystalline product was collected and dried *in vacuo*. Yield, 4.4g (63%).

Elemental analysis for $C_4H_6Br_3N_2NbO$, Found (Required): %C, 11.17 (11.15); %H, 1.40 (1.40), %N, 6.52 (6.50).

Infrared data (Nujol, CsI, cm^{-1}): 2310(s), 2299(s), 2281(s), 2270(s), 1364(m), 1352(m), 1022(m), 953(s,sp), 942(s), 929(s), 311(s,sh), 295(s,sh), 275(s,br), 259(m,sh).

7.2.17 Synthesis of $Nb(O)Br_3(THF)_2$ (17).

The synthesis of yellow $Nb(O)Br_3(THF)_2$ is essentially analogous to that previously described for the synthesis of $Nb(O)Cl_3(THF)_2$. Yield, 0.32g (56%).

Elemental analysis for $C_8H_{16}Br_3NbO_3$, Found (Required): %C, 20.20 (19.50); %H, 3.34 (3.27); %Br, 46.56 (48.64); %Nb, 18.92 (18.85).

Infrared data (Nujol, CsI, cm^{-1}): 1368(m), 1347(s), 1300(m), 1250(m), 1190(m), 1170(m), 1135(w), 1036(s), 1009(s), 991(m), 960(s), 920(s), 852(s,br), 820(s,br), 270(s,br).

7.2.18 Synthesis of $Nb(S)Cl_3$ (18).

A chilled (*ca.* -30°C) carbon disulphide solution of $(Me_3Si)_2S$ (0.78g, 4.37 mmol. in 15 cm^3 CS_2) was added dropwise over a period of 15 min. to a stirred suspension of $NbCl_5$ (1.0g, 4.37 mmol.) in carbon disulphide (20 cm^3) cooled in a dry-ice/acetone slush bath. Dissolution of the $NbCl_5$ occured over the course of 30 min. to afford a clear yellow solution. The mixture was allowed to warm to room temperature and stirred overnight to give a brown solution. The solution was then filtered and the volatiles removed under reduced pressure to leave an amorphous grey solid which was washed with petroleum ether (2 x 20 cm^3, b.p. 40-60°C) and dried *in vacuo*. Yield 0.75g (87%).

Elemental analysis for Cl_3SNb, Found (Required): %Nb, 39.62 (40.16); %S, 14.11 (13.86); %Cl, 44.01 (45.98).

Infrared data (Nujol, CsI, cm^{-1}): 550(s,sp), 414(s,sh), 401(s,sh), 394(s,br), 355(m), 292(m).

Mass spectral data (EI, 70eV, m/z, ^{93}Nb, ^{32}S, ^{35}Cl) 425$[Nb_2S_2Cl_5]^+$, 390$[Nb_2S_2Cl_4]^+$, 230$[NbSCl_3]^+$, 195$[NbSCl_2]^+$.

7.2.19 Synthesis of $Nb_2Cl_8S(CH_2Cl_2)$ (19).

A chilled (*ca.* -30°C) dichoromethane solution of $(Me_3Si)_2S$ (0.66g, 3.70 mmol. in 15 cm^3 CH_2Cl_2) was added dropwise over a period of 15 min. to a stirred solution of $NbCl_5$ (1.0g, 3.70 mmol.) in dichloromethane (20 cm^3) cooled in a dry-ice/acetone slush bath. An immediate reaction ensued, which after 30 min. resulted in a red solution and a grey amorphous solid. The mixture was allowed to warm to room temperature and stirred for a further 2 hours. Filtration of the supernatant solution followed by concentration and cooling to *ca.* -78°C afforded grey moisture sensitive crystals of $Nb_2Cl_8S(CH_2Cl_2)$. Yield, 0.12g (11%).

Elemental analysis for $C_2H_2Cl_{10}SNb$, Found,(Required): %C,1.95 (2.05); %H, 0.34 (0.32); %Cl, 61.1 (60.5); %S, 5.4 (5.5); %Nb, 31.9 (31.7).

Infra red data (Nujol,CsI,cm^{-1}): 720(m,), 410(m,sh), 390(s,sp), 380(m,sh), 365(w,sh).

7.2.20 Synthesis of $Nb_3S_3Br_8$ (20).

A chilled (*ca.* -30°C) dichloromethane solution of $(Me_3Si)_2S$ (0.36g, 2.03 mmol. in 15 cm^3 CH_2Cl_2) was added dropwise over a period of 15 min. to a stirred suspension of $NbBr_5$ (1.0g, 2.03 mmol.) in dichloromethane (20 cm^3) cooled in a dry-ice/acetone slush bath. Dissolution of the $NbBr_5$ occured over the course of 30 min. to afford a clear purple solution. The mixture was allowed to warm to room temperature and stirred overnight to give a red solution. The solution was then filtered, concentrated to half volume and cooled to *ca.* -78°C to afford lilac moisture sensitive crystals of $Nb_3S_3Br_8$. Yield, 0.62g (90%).

Elemental analysis for $Br_8S_3Nb_3$, Found (Required): %Nb, 27.25 (27.48); %S, 10.07 (9.48); %Br, 62.67 (63.03).

Infrared data (Nujol, CsI, cm^{-1}): 310(m,sh), 298(m,sh), 280(s,br), 258(m,sh), 255(m,sh).

Mass spectral data (EI, 70eV, m/z, ^{93}Nb, ^{32}S, ^{80}Br) 682$[Nb_2S_3Br_5]^+$, 650$[Nb_2S_2Br_5]^+$, 586$[Nb_2Br_5]^+$, 445$[NbSBr_4]^+$, 429$[NbS_3Br_3]^+$, 413$[NbBr_4]^+$, 365$[NbSBr_3]^+$, 317$[NbS_2Br_2]^+$, 253$[NbBr_2]^+$, 237$[NbS_2Br]^+$.

7.2.21 Synthesis of $Nb(S)Cl_3(CH_3CN)_2$ (21).

A chilled (*ca.* -30°C) acetonitrile solution of $(Me_3Si)_2S$ (1.97g, 12.6 mmol. in 15 cm $^3CH_3CN$) was added dropwise to a stirred suspension of $NbCl_5$ (3.0g, 11.1 mmol.) in acetonitrile (20cm^3) at *ca.* -30°C. The mixture was warmed to room temperature with stirring to give a green solution which gradually turned yellow with stirring overnight. The volatile components were then removed under reduced pressure and the residue was dried *in vacuo* to give a 95% yield of crude $Nb(S)Cl_3(CH_3CN)_2$.

An analytically pure sample was obtained by re-extraction with CH_3CN (30 cm^3), followed by filtration, concentration to half volume and cooling to *ca.* -30°C to afford yellow crystals. Yield 2.26g (65%).

Elemental analysis for $C_4H_6Cl_3N_2SNb$, Found, (Required): %C, 15.1 (15.3); %H, 2.0 (1.9); %Cl, 32.9 (33.9); %N, 8.1 (8.9); %S, 10.1 (10.2); %Nb, 29.9 (29.7).

Infrared data (nujol, CsI, cm^{-1}): 2310(s,sp), 2280(s,sp), 1368(m), 1358(m), 1030(m), 523(s,sp), 379(m,sh), 370(m,sh), 354(s,sp), 334(s), 316(s,sp), 280(m).

7.2.22 Synthesis of $Nb(S)Br_3(CH_3CN)_2$ (22).

The synthesis of $Nb(S)Br_3(CH_3CN)_2$ is essentially analogous to that previously described for $Nb(S)Cl_3(CH_3CN)_2$. Yield, 0.85g (93%).

Elemental analysis for $C_4H_6Br_3N_2SNb$, Found, (Required): %C, 10.69 (10.75); %H, 1.37 (1.35); %Br, 54.17 (53.65); %N, 6.4 (6.3); %S, 7.6 (7.2); %Nb, 20.19 (20.79).

Infrared data (nujol, CsI, cm^{-1}): 2309(s,sp), 2280(s,sp), 1369(m), 1358(m), 1022(m), 527(s,sp), 351(m), 326(m), 260(s,br).

7.2.23 Synthesis of $Nb(S)Cl_3(THF)_2$ (23).

Tetrahydrofuran (30 cm^3) was added to $Nb(S)Cl_3(CH_3CN)_2$ (0.5g, 1.60 mmol.) at *ca.* -30°C. The mixture was warmed to room temperature with stirring to afford a colourless solution. After 15 min. the mixture was filtered, concentrated to *ca.*

5 cm^3 and cooled to *ca.* -78°C. Addition of cold petroleum ether (10 cm^3, b.p. 40-60°C, *ca.* -30°C) gave yellow crystals of $Nb(S)Cl_3(THF)_2$. Yield, 0.3g (50%).

Elemental analysis for $C_8H_{16}O_2Cl_3SNb$, Found (Required): %Nb, 24.96 (24.74) ; %S, 8.49 (8.54); %Cl, 28.35 (28.32); %H, 4.33 (4.29); %C, 25.54 (25.59).

Infrared data (Nujol, CsI, cm^{-1}): 1367(m), 1358(m), 1344(s), 1298(w), 1246m), 1171(m), 1040(s), 1010(s), 993(s), 958(s), 920(m), 830(s,br), 720(m), 670(m), 529(s,sp), 352(s,br), 319(s,sh).

7.2.24 Synthesis of $Ta(S)Cl_3$ (24).

A chilled (*ca.* -30°C) carbon disulphide solution of $(Me_3Si)_2S$ (0.5g, 2.80 mmol. in 15 cm^3 CS_2) was added dropwise over a period of 15 min. to a stirred suspension of $TaCl_5$ (1.0g, 2.80 mmol.) in carbon disulphide (20 cm^3) cooled in a dry-ice/acetone slush bath. Dissolution of the $TaCl_5$ occured over the course of 30 min. to afford a clear yellow solution. The mixture was allowed to warm to room temperature and stirred overnight to give a colourless solution and an orange, amorphous solid. The supernatant solution was decanted from the solid which was collected, washed with petroleum ether (2 x 20 cm^3, b.p. 40-60°C) and dried *in vacuo*. Yield 0.73g (82%).

Elemental analysis for Cl_3STa, Found (Required): %Ta, 56.67 (56.66); %S, 11.29 (10.04); %Cl, 31.09 (32.88).

Infrared data (Nujol, CsI, cm^{-1}): 460(s,sp), 413(m,sh), 380(s,br), 330(m,sh), 319(m), 279(m).

Mass spectral data m/z (EI, 70eV, ^{181}Ta, ^{32}S, ^{35}Cl): 601$[Ta_2S_2Cl_5]^+$, 566$[Ta_2S_2Cl_4]^+$, 318$[TaSCl_3]^+$, 283$[TaSCl_2]^+$, 248$[TaSCl]^+$, 216$[TaCl]^+$, 213$[TaS]^+$, 181$[Ta]^+$.

7.3 Experimental Details to Chapter 3.

7.3.1 Reaction of $W(O)Cl_4$ with Li-O-2,6-$Pr^i_2C_6H_3$: *Preparation of $W(O)(O\text{-}2,6\text{-}Pr^i_2C_6H_3)_4$ (1).*

Procedure (a). Toluene (40 cm^3) was added to a weighed mixture of $W(O)Cl_4$ (0.5g, 1.46 mmol.) and LiO-2,6-$Pr^i_2C_6H_3$ (1.08g, 5.85 mmol.) at room temperature. The mixture was stirred for 18h. at room temperature, during which time the solution adopted a dark red colouration. The solution was then filtered and the solvent removed under reduced pressure and the residue dried *in vacuo*. The solid was extracted with light petroleum ether (80 cm^3, b.p. 40-60°C) at room temperature to give a dark red solution which was concentrated to *ca.* 20 cm^3 and cooled to *ca.* -78°C to afford red moisture sensitive prisms. The crystals were collected, washed with cold (*ca.* -78°C) petroleum ether (2 x 5 cm^3, b.p. 40-60°C) and dried *in vacuo*. Yield of W(O)(DIPP)4 (1.05g, 79%).

Procedure (b). Triethylamine (0.59g, 5.85 mmol.) was condensed onto a weighed mixture of $W(O)Cl_4$ (0.50g, 1.46 mmol.) and HO-2,6-$Pr^i_2C_6H_3$ (1.04g, 5.85 mmol.) in a glass 'rotoflow' ampoule. Toluene (40 cm^3) was introduced by cannular addition under an atmosphere of dinitrogen, and the resultant red solution was stirred at room temperature for 18h. The solution was then filtered to remove $[Et_3NH]^+Cl^-$, and the volatile components were removed under reduced pressure. The residue was washed with cold (*ca.* -78°C) petroleum ether (2 x 10 cm^3, b.p. 40-60°C) to remove unreacted phenol and amine and dried *in vacuo*. Extraction of the dark sold with light petroleum ether (80 cm^3, b.p. 40-60°C) gave a red solution which was

concentrated to *ca.* 20 cm^3 and cooled at *ca.* -78°C to afford red crystals of $W(O)(DIPP)_4$ (0.69g, 52%).

Elemental analysis for $WC_{48}H_{68}O_5$ Found (Required): %W, 20.10 (20.23), %C, 63.65 (63.43), %H, 7.76 (7.54).

Infrared data (Nujol, CsI, cm^{-1}): 1439(m), 1367(m), 1328(m), 1251(m), 1190(s), 1111(w,sh), 1101(m), 1059(w), 1046(w), 970(s,sp), 907(s), 901(s,sh), 894(s,sh), 874(s), 796(m), 751(s,sp), 715(m), 608(m).

Mass spectral data (CI, isobutane carrier gas, m/z,^{184}W): 732 $[W(O)(DIPP)_3]^+$, 689 $[W(O)(DIPP)_3\text{-}CHMe_2]^+$, 571 $[W(O)_2(DIPP)_2]^+$, 555 $[W(O)(DIPP)_2]^+$, 512 $[W(O)(DIPP)_2\text{-}CHMe_2]^+$, 393 $[W(O)_2(DIPP)]^+$, 377 $[W(O)(DIPP)]^+$, 334 $[W(O)(DIPP)\text{-}CHMe_2]^+$.

^{1}H NMR data (250MHz, d^6-benzene, 298K): 1.22 (d, 48, J_{HH} = 6.8, $CHMe_2$), 3.72 (sept., 8, $^3J_{HH}$ = 6.8, $CHMe_2$), 6.83 (t, 4, $^3J_{HH}$ = 7.6, H_p), 6.98 (d, 8, $^3J_{HH}$ = 7.6, H_m). (250MHz, d-chloroform, 298K): 1.01 (d, 48, J_{HH} = 6.7, $CHMe_2$), 3.39 (sept., 8, $^3J_{HH}$ = 6.8, $CHMe_2$), 6.87 (t, 4, $^3J_{HH}$ = 7.1, H_p), 7.02 (d, 8, $^3J_{HH}$ = 7.5, H_m).

^{13}C NMR data (68MHz, d^6-benzene, 298K): 23.76 (q, J_{CH} = 125, $CHMe_2$), 27.53 (d, J_{CH} = 131, $CHMe_2$), 123.74 (d , J_{CH} = 152, ring C), 124.72 (d, J_{CH} = 159, ring C), 139.02 (s, ring C), 158.32 (s, ring C). (68MHz, d-chloroform, 298K): 23.60 (q, J_{CH} = 125, $CHMe_2$), 26.78 (d, J_{CH} = 131, $CHMe_2$), 123.27 (d , J_{CH} = 156, ring C), 124.17 (d, J_{CH} = 161, ring C), 138.98 (s, ring C), 158.16 (s, ring C).

7.3.2 Reaction of $W(O)Cl_4$ with Li-O-2,4,6-$Me_3C_6H_2$: *Preparation of* $W(O)(O\text{-}2,4,6\text{-}Me_3C_6H_2)_4$ *(2).*

Procedure (a). Toluene (40 cm^3) was added to a weighed mixture of $W(O)Cl_4$ (0.5g, 1.46 mmol.) and LiO-2,4,6-$Me_3C_6H_2$ (0.83g, 5.85 mmol.) at room temperature. The mixture was stirred for 18h. at room temperature, during which time the solution adopted a dark red colouration. The solution was then filtered and the solvent removed under reduced pressure and the residue dried *in vacuo*. The solid was extracted with light petroleum ether (80 cm^3, b.p. 40-60°C) at room temperature to give a dark red solution which was concentrated to *ca.* 20 cm^3 and cooled to *ca.* -78°C to afford red moisture sensitive prisms. The crystals were collected, washed with cold (*ca.* -78°C) petroleum ether (2 x 5 cm^3, b.p. 40-60°C) and dried *in vacuo*. Yield of $W(O)(TMP)_4$ (0.81g, 75%).

Procedure (b). Triethylamine (0.59g, 5.85 mmol.) was condensed onto a weighed mixture of $W(O)Cl_4$ (0.50g, 1.46 mmol.) and HO-2,4,6-$Me_3C_6H_2$ (0.80g, 5.85 mmol.) in a glass 'rotoflow' ampoule. Toluene (40 cm^3) was introduced by cannular addition under an atmosphere of dinitrogen, and the resultant red solution was stirred at room temperature for 18h. The solution was then filtered to remove $[Et_3NH]^+Cl^-$, and the volatile components were removed under reduced pressure. The residue was washed with cold (*ca.* -78°C) petroleum ether (2 x 10 cm^3, b.p. 40-60°C) to remove unreacted phenol and amine and dried *in vacuo*. Extraction with light petroleum ether (80 cm^3, b.p. 40-60°C) gave a red solution which was concentrated to *ca.* 20 cm^3 and cooled at *ca.* -78°C to afford red crystals of $W(O)(TMP)_4$ (0.62g, 57%).

Elemental analysis for $WC_{36}H_{44}O_5$ Found (Required): %W, 24.85 (24.82), %C, 58.60 (58.38), %H, 6.07 (5.99).

Infrared data (Nujol, CsI, cm^{-1}): 1416(m), 1364(m), 1262(m), 1232(w), 1202(s), 1160(w), 1095(m), 1078(m,sh), 964(s,sp), 898(s), 759(s,sp), 726(s,sp), 568(m).

Mass spectral data (CI, isobutane carrier gas, m/z, ^{184}W): 755 $[W(O)(TMP)_4+Me]^+$, 740 $[W(O)(TMP)_4]^+$, 725 $[W(O)(TMP)_4-Me]^+$, 651 $[W(O)_2(TMP)_3+2Me]^+$, 605 $[W(O)(TMP)_3]^+$, 501 $[W(O)_2(TMP)_2+Me]^+$.

^{1}*H NMR data* (250MHz, d^6-benzene, 298K): 2.03 (s, 12, p-Me), 2.40 (s, 24, o-Me), 6.55 (s, 8, aromatic). (250MHz, d-chloroform, 298K): 2.22 (s, 36, o-Me and p-Me), 6.67 (s, 8, aromatic).

^{13}*C NMR data* (68MHz, d^6-benzene, 298K): 17.38 (q, J_{CH} = 125, Me), 20.97 (q, J_{CH} = 125, Me), 128.77 (d , J_{CH} = 161, meta-ring C), 130.22 (s, ring C), 132.62 (s, ring C), 159.58 (s, ring C). (68MHz, d-chloroform, 298K): 16.72 (q, J_{CH} = 129, Me), 20.48 (q, J_{CH} = 127, Me), 127.93 (d , J_{CH} = 155, meta-ring C), 128.46 (s, ring C), 132.52 (s, ring C), 159.24 (s, ring C).

7.3.3 Reaction of $W(O)Cl_4$ with Li-O-2,6-$Me_2C_6H_3$:

Preparation of $W(O)(O\text{-}2,6\text{-}Me_2C_6H_3)_4$ (3).

Procedure (a). Toluene (40 cm^3) was added to a weighed mixture of $W(O)Cl_4$ (0.5g, 1.46 mmol.) and LiO-2,6-$Me_2C_6H_3$ (0.75g, 5.85 mmol.) at room temperature. The mixture was stirred for 18h. at room temperature, during which time the solution adopted a dark red colouration. The solution was then filtered and the solvent removed under reduced pressure and the residue dried *in vacuo*. The resulting solid was washed with cold (*ca.* -78°C) petroleum ether (2 x 5 cm^3, b.p. 40-60°C) and re-extracted with toluene (50 cm^3) to give a dark red solution. The solution was concentrated to *ca.* 20 cm^3 and cooled to *ca.* -78°C to afford red moisture sensitive crystals. The crystals were

collected, washed with cold (*ca.* -78°C) petroleum ether (2 x 5 cm^3, b.p. 40-60°C) and dried *in vacuo*. Yield of $W(O)(DMP)_4$ (0.77g, 77%).

Procedure (b). Triethylamine (0.59g, 5.85 mmol.) was condensed onto a weighed mixture of $W(O)Cl_4$ (0.50g, 1.46 mmol.) and HO-2,6-$Me_2C_6H_3$ (0.71g, 5.86 mmol.) in a glass 'rotoflow' ampoule. Toluene (40 cm^3) was introduced by cannular addition under an atmosphere of dinitrogen, and the resultant red solution was stirred at room temperature for 18h. The solution was then filtered to remove $[Et_3NH]^+Cl^-$, and the volatile components were removed under reduced pressure. The residue was washed with cold (*ca.* -78°C) petroleum ether (2 x 10 cm^3, b.p. 40-60°C) to remove unreacted phenol and amine and dried *in vacuo*. Extraction of the dark sold with toluene (80 cm^3) gave a red solution which was concentrated to *ca.* 20 cm^3 and cooled at *ca.* -78°C to afford red crystals of $W(O)(DMP)_4$ (0.60g, 60%).

Elemental analysis for $WC_{32}H_{36}O_5$ Found (Required): %W, 26.74 (26.86), %C, 56.12 (56.15), %H, 5.60 (5.30).

Infrared data (Nujol, CsI, cm^{-1}): 1414(m), 1311(m), 1250(w,sh), 1220(s), 1156(s), 1012(w), 961(s,sp), 871(s), 855(s,sh), 722(s,sp), 571(m), 561(m).

Mass spectral data (CI, isobutane carrier gas, m/z, ^{184}W): 742 $[W(O)(DMP)_4+Bu^t]^+$, 700$[W(O)(DMP)_4+Me]^+$, 685 $[W(O)(DMP)_4]^+$, 563 $[W(O)(DMP)_3]^+$, 488 $[W(O)(DMP)_2+2Me]^+$, 473 $[W(O)_2(DMP)_2+Me]^+$, 442 $[W(O)(DMP)_2]^+$, 336 $[W(O)(DMP)+Me]^+$.

^1H *NMR data* (250MHz, d^6-benzene, 298K): 2.34 (s, 24, Me), 6.57 (t, 4, $^3J_{HH}$ = 7.6, H_p), 6.74 (d, 8, $^3J_{HH}$ = 7.5, H_m). (250MHz, d-chloroform, 298K): 2.22 (s, 24, Me), 6.67 (t, 4, $^3J_{HH}$ = 7.6, H_p), 6.79 (d, 8, $^3J_{HH}$ = 7.5, H_m).

^{13}*C NMR data* (68MHz, d^6-benzene, 298K): 16.70 (q, J_{CH} = 127, Me), 123.81 (d , J_{CH} = 161, ring C), 128.36 (d, J_{CH} = 163, ring C), 128.55 (s, ring C), 161.09 (s, ring C). (68MHz, d-chloroform, 298K): 16.76 (q, J_{CH} = 127, Me), 123.39 (d , J_{CH} = 160, ring C), 128.04 (d, J_{CH} = 160, ring C), 128.33 (s, ring C),160.86 (s, ring C).

7.3.4 Reaction of $W(O)(O\text{-}2,6\text{-}Me_2C_6H_3)_4$ with PhOH:

Preparation of $W(O)(OPh)_4$ (4).

C_6H_5OH (0.41g, 4.36 mmol.) in toluene (15 cm^3) was added to a stirred solution of $W(O)(O\text{-}2,6\text{-}Pr^i{}_2C_6H_3)_4$ (1.0g, 1.10 mmol.) in toluene (25 cm^3) at room temperature. An immediate reaction ensued leading to deposition of a copious orange precipitate and a colourless supernatant solution. The solid was isolated by cannular filtration, washed with light petroleum ether (2 x 10 cm^3, b.p. 40-60°C) and dried *in vacuo* to afford 0.55g (87%) of $W(O)(OPh)_4$.

Elemental analysis for $WC_{24}H_{20}O_5$ Found (Required): %W, 32.45 (32.13), %C, 50.78 (50.37), %H, 3.80 (3.52).

Infrared data (Nujol, CsI, cm^{-1}): 3050(w), 1585(s), 1480(s), 1368(s), 1279(w), 1250(s,br), 1165(m,sp), 1071(w), 1021(w), 897(s), 755(s,sp), 725(s), 690(s,sh), 655(s,sp), 461(s).

Mass spectral data (CI, isobutane carrier gas, m/z, ^{184}W): 1160 $[\{W(O)(OPh)_4\}_2+Me]^+$, 1066$[\{W(O)(OPh)_4\}_2-OPh+Me]^+$, 666 $[W(O)(OPh)_5]^+$, 649 $[W(OPh)_5]^+$, 572 $[W(O)(OPh)_4]^+$.

7.3.5 Reaction of $W(O)Cl_4$ with Li-O-Bu^t:

Preparation of $W(O)(OBu^t)_4$ (5).

To a stirred suspension of $LiOBu^t$ (2.0g, 24.98 mmol.) in diethylether (40 cm^3) at *ca.* -78°C was added $W(O)Cl_4$ (2.13g, 6.23 mmol.) in diethylether (20 cm^3). As the mixture was allowed to warm to room temperature with stirring, the solution adopted first a yellow, followed by a blue, colouration. After 4h. at room temperature the solution had lightened to pale yellow and a precipitate of LiCl was in evidence. The solution was filtered and the solvent removed *in vacuo* to leave a yellow waxy solid. Sublimation at 50°C (5 x 10^{-2} Torr) afforded white crystalline $W(O)(OBu^t)_4$ (1.30g, 65%).

Elemental analysis for $WC_{16}H_{36}O_5$ Found (Required): %W, 37.58 (37.34), %C, 39.23 (39.04), %H, 6.99 (7.37).

Infrared data (Nujol, CsI, cm^{-1}): 1388(s), 1360(s), 1236(s), 1170(s), 1075(m), 1029(m), 940(s), 785(s,sp), 726(m), 673(w), 561(s), 522(s).

Mass spectral data (CI, isobutane carrier gas, m/z, ^{184}W): 549 $[W(O)(OBu^t)_4+Bu^t]^+$, 492 $[W(O)(OBu^t)_4]^+$, 419 $[W(O)(OBu^t)_3]^+$, 362 $[W(O)_2(OBu^t)_2]^+$.

^{1}*H NMR data* (250MHz, d^6-benzene, 298K): 1.46 (s, 36, CMe_3). (250MHz, d-chloroform, 298K): 1.42 (s, 36, CMe_3).

^{13}*C NMR data* (68MHz, d^6-benzene, 298K): 31.09 (q, J_{CH} = 125, $C(CH_3)_3$), 82.63 (s, $C(CH_3)_3$). (68MHz, d-chloroform, 298K): 31.17 (q, J_{CH} = 125, $C(CH_3)_3$), 82.57 (s, $C(CH_3)_3$).

7.3.6 Reaction of $Mo(O)Cl_4$ with Li-O-2,6-$Me_2C_6H_3$:

Preparation of $Mo(O)(O\text{-}2,6\text{-}Me_2C_6H_3)_4$ (6).

To a stirred suspension of LiO-2,6-$Me_2C_6H_3$ (2.02g, 15.76 mmol.) in diethylether (40 cm^3) at *ca.* -78°C was added $Mo(O)Cl_4$ (1.0g, 3.94 mmol.) in diethylether (20 cm^3). An immediate reaction ensued leading to dissolution of the starting oxo-halide and formation of a blue solution. After 18h. at room temperature the solution was filtered and the solvent removed under reduced pressure. The resulting solid was re-extracted with light petroleum ether (50 cm^3, b.p. 40-60°C) to give a blue solution which was concentrated to *ca.* 20 cm^3 and cooled to *ca.* -78°C to afford blue moisture sensitive crystals. The crystals were collected, washed with cold (*ca.* -78°C) petroleum ether (2 x 5 cm^3, b.p. 40-60°C) and dried *in vacuo*. Yield of $Mo(O)(DMP)_4$ (1.67g, 71%).

Elemental analysis for $MoC_{32}H_{36}O_5$ Found (Required): %C, 64.49 (64.43), %H, 6.07 (6.08).

Infrared data (Nujol, CsI, cm^{-1}): 1415(m), 1262(s), 1200(s), 1160(m), 1090(s), 1072(m), 1030(m), 1003(w), 982(s), 950(s), 888(s,br), 825(m,sh), 749(s,sp), 729(s,sp), 721(s,sh), 716(s,sh), 569(s,sp), 539(s,sh), 481(s,sp).

Mass spectral data (CI, m/z, ^{96}Mo): 611 $[Mo(OMe)(DMP)_4]^+$,490 $[Mo(OMe)(DMP)_3]^+$, 475 $[Mo(O)(DMP)_3]^+$, 370$[Mo(O)_2(DMP)_2]^+$, 354 $[Mo(O)(DMP)_2]^+$, 249 $[Mo(O)_2(DMP)]^+$.

^{1}*H NMR data* (250MHz, d^6-benzene, 298K): 2.35 (s, 24, Me), 6.55 (t, 4, $^3J_{HH}$ = 7.5, H_p), 6.69 (d, 8, $^3J_{HH}$ = 7.4, H_m). (250MHz, d-chloroform, 298K): 2.44 (s, 24, Me), 6.65 (t, 4, $^3J_{HH}$ = 7.6, H_p), 6.78 (d, 8, $^3J_{HH}$ = 7.5, H_m).

^{13}*C NMR data* (68MHz, d^6-benzene, 298K): 16.77 (q, J_{CH} = 127, Me), 123.81 (d , J_{CH} = 161, ring C), 128.42 (d, J_{CH} = 163, ring C), 128.57 (s, ring C), 163.10 (s, ring C). (68MHz, d-chloroform, 298K): 16.83 (q, J_{CH} = 127, Me), 124.45 (d , J_{CH} = 160, ring C), 127.87 (d, J_{CH} = 160, ring C), 128.39 (s, ring C),164.33 (s, ring C).

7.3.7 Reaction of $W(O)Cl_4$ with $Li\text{-}O\text{-}2,6\text{-}Me_2C_6H_3$:

Preparation of $W(O)Cl(O\text{-}2,6\text{-}Me_2C_6H_3)_3$ (7).

Toluene (40 cm^3) was added to a weighed mixture of $W(O)Cl_4$ (1.0g, 2.93 mmol.) and $LiO\text{-}2,6\text{-}Me_2C_6H_3$ (0.75g, 5.85 mmol.) at room temperature. The mixture was stirred for 18h. at room temperature, during which time the solution adopted a dark red colouration. The solution was then filtered and the solvent removed under reduced pressure and the residue dried *in vacuo*. The resulting solid was washed with cold (*ca.* -78°C) petroleum ether (2 x 5 cm^3, b.p. 40-60°C) and re-extracted with toluene (50 cm^3) to give a dark red solution. The solution was concentrated to *ca.* 20 cm^3 and cooled to *ca.* -78°C to afford red moisture sensitive crystals. The crystals were collected, washed with cold (*ca.* -78°C) petroleum ether (2 x 5 cm^3, b.p. 40-60°C) and dried *in vacuo*. Yield of $W(O)Cl(DMP)_3$ (0.55g, 49%).

Elemental analysis for $WC_{24}H_{27}O_4Cl$ Found (Required): %W, 29.66 (30.70), %C, 48.13 (48.14), %H, 4.48 (4.54), %Cl, 5.89 (5.92).

Infrared data (Nujol, CsI, cm^{-1}): 1420(m), 1368(m), 1300(w), 1268(w,sh), 1216(m,sh), 1200(s,sp), 1186(s,sp), 1168(m,sh), 1100(m,sp), 1089(m,sh), 1035(w), 988(s,sp), 920(m,sh), 902(s), 855(s), 779(s,sh), 776(s,sp), 735(s,sp), 728(s,sh), 720(w,sh), 589(w,sh), 580(m), 570(w,sh), 400(s,br).

Mass spectral data (CI, isobutane carrier gas, m/z, ^{184}W): 589 $[W(O)Cl(DMP)_3]^+$, 563$[W(O)(DMP)_3]^+$, 477 $[W(O)Cl(DMP)_2]^+$.

^{1}*H NMR data* (250MHz, d^6-benzene, 298K): 2.43 (s, 12, Me), 2.51 (s, 6, Me), 6.63 (t, 3, $^3J_{HH}$ = 7.3, H_p), 6.84 (d, 6, $^3J_{HH}$ = 7.5, H_m).

^{13}*C NMR data* (68MHz, d-chloroform, 298K): 16.77 (q, J_{CH} = 124, Me), 125.22 (d , J_{CH} = 161, ring C), 127.17 (d, J_{CH} = 160, ring C), 127.77 (s, ring C),164 (s, ring C),127.87 (d , J_{CH} = 162, ring C), 129.48 (d, ring C), 130.45 (s, ring C),157.92 (s, ring C), 162.46 (s, ring C).

7.3.8 Reaction of $Mo(O)_2Cl_2$ with Li-O-2,6-$Me_2C_6H_3$:

Preparation of $Mo_2(O)_2(\mu-O)(O\text{-}2,6\text{-}Me_2C_6H_3)_6$ (8).

Toluene (40 cm^3) was added to a weighed mixture of $Mo(O)_2Cl_2$ (1.0g, 5.0 mmol.) and LiO-2,6-$Me_2C_6H_3$ (1.93g, 15.1 mmol.) at room temperature. The mixture was stirred for 18h. at room temperature, during which time the solution adopted a dark blue colouration. The solution was then filtered and the solvent removed under reduced pressure and the residue dried *in vacuo*. The resulting solid was washed with cold (*ca.* -78°C) petroleum ether (2 x 5 cm^3, b.p. 40-60°C) and re-extracted with toluene (50 cm^3) to give a dark blue solution. The solution was concentrated to *ca.* 20 cm^3 and cooled to *ca.* -78°C to afford purple moisture sensitive crystals. The crystals were collected, washed with cold (*ca.* -78°C) petroleum ether (2 x 5 cm^3, b.p. 40-60°C) and dried *in vacuo*. Yield of $Mo_2(O)_2(\mu-O)(O\text{-}2,6\text{-}Me_2C_6H_3)_6$ (1.85g, 76%)

Elemental analysis for $MoC_{48}H_{54}O_9$ Found (Required): %Mo, 19.85 (19.85), %C, 60.33 (59.63), %H, 5.79 (5.63).

Infrared data (Nujol, CsI, cm^{-1}): 1410(w), 1254(m), 1207(s), 1198(s,sh), 1188(s,sh), 1161(m), 1090(m), 970(s,sp), 950(m,sh), 890(s), 871(s,sh), 775(s,sp), 751(s,sp), 730(s,sp), 722(m,sh), 716(m,sh), 579(m), 540(w).

Mass spectral data (CI, isobutane carrier gas, m/z, ^{96}Mo): 846 $[Mo_2(O)_3(DMP)_5]^+$, 709$[W_2(O)_2(DMP)_4]^+$, 581 $[Mo(DMP)_4]^+$, 475 $[Mo(O)(DMP)_3]^+$, 370 $[Mo(O)_2(DMP)_2]^+$.

^{1}*H NMR data* (250MHz, d^6-benzene, 298K): 2.35 (s, 36, Me), 6.55 (t, 6, $^3J_{HH}$ = 7.9, H_p), 6.69 (d, 12, $^3J_{HH}$ = 7.5, H_m).

^{13}*C NMR data* (68MHz, d-chloroform, 298K): 17.07 (q, J_{CH} = 132, Me), 123.79 (d , J_{CH} = 159, ring C), 127.95 (d, J_{CH} = 160, ring C), 128.70 (s, ring C),165.08 (s, ring C).

7.3.9 Reaction of $W(O)_2Cl_2(CH_3CN)_2$ with Li-O-2,6-$Me_2C_6H_3$:

Preparation of $W_2(O)_2(\mu-O)(O\text{-}2,6\text{-}Me_2C_6H_3)_6$ (9).

Toluene (40 cm^3) was added to a weighed mixture of $W(O)_2Cl_2(CH_3CN)_2$ (1.0g, 2.71 mmol.) and LiO-2,6-$Me_2C_6H_3$ (1.04g, 8.12 mmol.) at room temperature. The mixture was stirred for 18h. at room temperature, during which time the solution adopted a dark red colouration. The solution was then filtered and the solvent removed under reduced pressure and the residue dried *in vacuo*. The resulting solid was washed with cold (*ca.* -78°C) petroleum ether (2 x 5 cm^3, b.p. 40-60°C) and re-extracted with toluene (50 cm^3) to give a dark red solution. The solution was concentrated to *ca.* 20 cm^3 and cooled to *ca.*-78°C to afford red moisture sensitive crystals. The crystals were collected, washed with cold (*ca.* -78°C) petroleum ether (2 x 5 cm^3, b.p. 40-60°C) and dried *in vacuo*. Yield of $W_2(O)_2(\mu\text{-}O)(O\text{-}2,6\text{-}Me_2C_6H_3)_6$ (1.32g, 85%)

Elemental analysis for $WC_{48}H_{54}O_9$ Found (Required): %W, 31.90 (32.20), %C, 50.23 (50.50), %H, 4.85 (4.76).

Infrared data (Nujol, CsI, cm^{-1}): 1418(m), 1366(m), 1271(m,sh), 1266(s), 1258(m,sh), 1208(s,br), 1162(w), 1100(m), 1080(m), 1030(w), 985(w), 969(s,sp), 900(s,br), 765(s), 730(s,sp), 571(s,sp).

Mass spectral data (CI, isobutane carrier gas, m/z, ^{184}W: 1022 $[W_2(O)_3(DMP)_5]^+$, 779$[W_2(O)_3(DMP)_3]^+$, 731 $[W_2(DMP)_3]^+$, 684 $[W(O)(DMP)_4]^+$, 668 $[W(DMP)_4+]^+$, 563 $[W(O)(DMP)_3]^+$.

^{1}*H NMR data* (250MHz, d^6-benzene, 298K): 2.30 (s, 36, Me), 6.70 (t, 6, $^3J_{HH}$ = 7.4, H_p), 6.91 (d, 12, $^3J_{HH}$ = 7.6, H_m).

^{13}*C NMR data* (68MHz, d-chloroform, 298K): 16.77 (q, J_{CH} = 132, Me), 123.38 (d , J_{CH} = 159, ring C), 128.06 (d, J_{CH} = 160, ring C), 128.35 (s, ring C),160.85 (s, ring C).

7.3.10 Reaction of $Mo(O)_2Cl_2$ with Me_3SiO-2,6-$Me_2C_6H_3$:

Preparation of $Mo(O)Cl_2(O$-2,6-$Me_2C_6H_3)_2$ (10).

A toluene solution of Me_3SiO-2,6-$Me_2C_6H_3$ (0.98g, 5.04 mmol. in 20 cm^3 toluene) was added to a stirring suspension of $Mo(O)_2Cl_2$ in toluene (0.5g, 2.51 mmol. in 20 cm^3 toluene). An immediate reaction ensued leading to dissolution of the starting oxo-halide and formation of a dark blue solution. The mixture was stirred for 18h. at room temperature. The solution was then filtered and the solvent removed under reduced pressure and the residue dried *in vacuo*. The resulting solid was washed with cold (*ca.* -78°C) petroleum ether (2 x 5 cm^3, b.p. 40-60°C) and re-extracted with toluene (50 cm^3) to give a dark blue solution. The solution was

concentrated to *ca.* 20 cm^3 and cooled to *ca.* -78°C to afford purple moisture sensitive crystals. The crystals were collected, washed with cold (*ca.* -78°C) petroleum ether (2 x 5 cm^3, b.p. 40-60°C) and dried *in vacuo*. Yield of $Mo(O)Cl_2(O\text{-}2,6\text{-}Me_2C_6H_3)_2$ (0.77g, 72%)

Elemental analysis for $MoC_{16}H_{18}O_3Cl_2$ Found (Required): %Mo, (22.57), %C, 44.68 (45.20), %H, 4.27 (4.27), %Cl, 16.82 (16.68).

Infrared data (Nujol, CsI, cm^{-1}): 1436(m), 1200(s), 1209(m), 1191(m), 1162(m), 1028(m), 980(s,sp), 972(m,sh), 961(m,sh), 905(s), 780(m,sh), 770(s,sp), 720(s,sh), 535(m), 405(m,sh), 399(s,sh), 375(s,br), 338(m,sh), 255(m).

Mass spectral data (CI, isobutane carrier gas, m/z, ^{96}Mo): 510 $[Mo(O)Cl(DMP)_3]^+$, 475$[Mo(O)(DMP)_3]^+$, 424 $[Mo(O)Cl_2(DMP)_2]^+$, 389 $[Mo(O)Cl(DMP)_2]^+$, 373 $[MoCl(DMP)_2]^+$, 303 $[Mo(O)Cl(DMP)]^+$, 287 $[Mo(Cl)_2(DMP)]^+$, 268 $[Mo(O)Cl(DMP)]^+$.

^{1}*H NMR data* (250MHz, d^6-benzene, 298K): 2.35 (s, 12, Me), 6.58 (t, 6, $^3J_{HH}$ = 7.2, H_p), 6.68 (d, 12, $^3J_{HH}$ = 7.4, H_m).

^{13}*C NMR data* (68MHz, d-chloroform, 298K): 17.42 (q, J_{CH} = 132, Me), 128.33 (d , J_{CH} = 162, ring C), 129.35 (d, J_{CH} = 159, ring C), 132.54 (s, ring C),169.16 (s, ring C).

7.4 Experimental Details to Chapter 4.

The reactions described in this section all yield product mixtures of either one or two different isomers of the same compound. In each case, the ratio of isomers

formed, is found to be largely dependant on the starting material used. In light of this, each individual reaction is presented seperately.

7.4.1 Reaction of $Nb(O)Br_3$ with PMe_3:

Preparation of β-$Nb(O)Br_3(PMe_3)_3$ (2).

Trimethylphosphine (0.38g, 5.02 mmol.) was condensed onto a frozen mixture of $Nb(O)Br_3$ (0.5g, 1.43 mmol.) and dichloromethane (50 cm^3). The mixture was allowed to warm to room temperature and was stirred for 12h. to afford a clear orange solution. Filtration followed by concentration to *ca.* 20 cm^3 and cooling to *ca.* -78°C afforded orange crystals, which were collected and dried *in vacuo*. Yield, 0.56g (67%). Analysis indicated that the crystals were a mixture of α (40%)- and β (60%)-isomers. Recrystallisation from a saturated toluene solution at -35°C afforded the β-product as red cubes.

Characterising Data on β-$Nb(O)Br_3(PMe_3)_3$.

Elemental analysis for $C_9H_{27}Br_3NbOP_3$ Found (Required): %C, 31.94 (32.06), %H, 8.05 (8.07).

Infrared data (Nujol, CsI, cm^{-1}): 1423(m), 1415(m), 1299(m), 1295(m), 1279(s), 953(s,br), 871(s), 849(m,sh), 740(s), 669(s,sp), 351(s), 342(m,sh), 299(s,sh), 289(s), 271(s,sh), 255(m).

^{1}*H NMR data* (250MHz, d^6-benzene, 298K): 1.13 (s, br, $\Delta_{1/2}$ = 18 Hz, P*Me*3).

7.4.2 Reaction of $Nb(O)Br_3(CH_3CN)_2$ with PMe_3.

A procedure analogous to that described for $Nb(O)Br_3$ was used but with $Nb(O)Br_3(CH_3CN)_2$ starting material. Stirring at room temperature for 2 days afforded an orange suspension. Filtration, followed by removal of the volatiles under reduced pressure afforded an orange solid mixture of α (45%)- and β (55%)- isomers.

7.4.3 Reaction of $Nb(S)Cl_3$ with PMe_3:

Preparation of β-$Nb(S)Cl_3(PMe_3)_3$ (3).

Trimethylphosphine (0.58g, 7.56 mmol.) was condensed onto a frozen mixture of $Nb(S)Cl_3$ (0.5g, 2.16 mmol.) and dichloromethane (50 cm^3). The mixture was allowed to warm to room temperature and was stirred for 12h. to afford a clear red solution. Filtration followed by concentration to *ca.* 20 cm^3 and cooling to *ca.* -78°C afforded golden yellow crystals, which were collected and dried *in vacuo*. Yield, 0.55g (56%). Analysis indicated that the crystals were a mixture of α (20%)- and β (80%)- isomers. Recrystallisation from a saturated toluene solution at -35°C afforded the β-product as green cubes.

Characterising Data on β-$Nb(S)Cl_3(PMe_3)_3$.

Elemental analysis for $C_9H_{27}Cl_3NbSP_3$ Found (Required): %C, 23.30(23.52), %H, 5.90 (5.92).

Infrared data (Nujol, CsI, cm^{-1}): 1421(m), 1419(m), 1296(m), 1277(m), 950(s,br), 850(m), 732(s), 668(m), 489(s,sp), 346(m,sh), 335(s), 290(s,sh), 269(s,br), 249(s,sh).

Mass spectral data (CI, isobutane carrier gas, m/z, ^{35}Cl, ^{32}S): 458 $[M]^+$, 382 $[M\text{-}PMe_3]^+$.

^1H *NMR data* (250MHz, d^6-benzene, 298K): 1.33 (s, br, $\Delta_{1/2}$ = 13 Hz, P*Me*3). (250MHz, d-chloroform, 298K): 1.58 (s, br, $\Delta_{1/2}$ = 16 Hz, P*Me*3).

7.4.4 Reaction of $Nb(S)Cl_3(CH_3CN)_2$ with PMe_3:

Preparation of α-Nb(S)Cl3(PMe3)3 (3).

A procedure analogous to that described for $Nb(S)Cl_3$ was used but with $Nb(S)Cl_3(CH_3CN)_2$ starting material. Stirring at room temperature for 2 days afforded a clear red/brown solution. Filtration, followed by concentration to *ca.* 20 cm^3 and cooling to *ca.* -78°C afforded golden yellow crystals, which were collected and dried *in vacuo*. Yield, 0.35g (60%). Analysis indicated that the crystals were a mixture of α (45%)- and β (55%)- isomers. Recrystallisation from a saturated toluene solution at -35°C afforded the α-product as orange cubes.

Characterising Data on α-$Nb(S)Cl_3(PMe_3)_3$.

Elemental analysis for $C_9H_{27}Cl_3NbSP_3$ Found (Required): %C, 23.47 (23.52), %H, 5.95 (5.92).

Infrared data (Nujol, CsI, cm^{-1}): 1423(m), 1421(m), 1283(m), 1251(m), 950(s,br), 854(m), 735(s), 667(m), 455(s,sp), 347(m,sh), 335(s), 290(s,sh), 273(s,br), 248(s,sh).

Mass spectral data (CI, isobutane carrier gas, m/z, ^{35}Cl, ^{32}S): 458 $[M]^+$, 382 $[M\text{-}PMe_3]^+$.

^{1}*H NMR data* (250MHz, d^6-benzene, 298K): 1.41 (d, $^2J_{(PH)}$ = 8.9, P*Me*$_3$). (250MHz, d-chloroform, 298K): 1.77 (d, $^2J_{(PH)}$ = 8.8, P*Me*$_3$).

7.4.5 Reaction of $Nb(S)Cl_3(THF)_2$ with PMe_3.

A procedure analogous to that described for $Nb(S)Cl_3(CH_3CN)_2$ was used but with $Nb(S)Cl_3(THF)_2$ starting material. Yield, 0.34g (56%). Analysis indicated that the crystals were a mixture of α (15%)- and β (85%)- isomers.

7.4.6 Reaction of $Nb_3S_3Br_8$ with PMe_3:

Preparation of β-Nb(S)Br$_3$(PMe$_3$)$_3$ (4).

Trimethylphosphine (0.39g, 5.18 mmol.) was condensed onto a frozen mixture of $Nb_3S_3Br_8$ (0.5g, 0.49 mmol.) and dichloromethane (50 cm^3). The mixture was allowed to warm to room temperature and was stirred for 12h. to afford a yellow precipitate and a clear red solution. Filtration followed by concentration to *ca.* 20 cm^3 and cooling to *ca.* -78°C afforded red crystals, which were collected and dried *in vacuo.* Yield, 0.47g (54%). Analysis indicated that the crystals were pure β-$Nb(S)Br_3(PMe_3)_3$.

Characterising Data on β-$Nb(S)Br_3(PMe_3)_3$.

Elemental analysis for $C_9H_{27}Br_3NbSP_3$ Found (Required): %C, 18.00(18.23), %H, 4.34 (4.59).

Infrared data (Nujol, CsI, cm^{-1}): 1428(m), 1369(m), 1299(s,sp), 1284(s,sh), 1279(s,sp), 952(s, br), 731(s), 669(m), 489(s,sp), 328(m), 261(s).

^{1}*H NMR data* (250MHz, d^6-benzene, 298K): 1.42 (s, br, $\Delta_{1/2}$ = 18 Hz, P*Me*3).

7.4.7 Reaction of $Nb(S)Br_3(CH_3CN)_2$ with PMe_3.

A procedure analogous to that described for $Nb_3S_3Br_8$ was used but with $Nb(S)Br_3(CH_3CN)_2$ starting material. Stirring at room temperature for 2 days afforded a yellow precipitate and a clear red solution. Filtration, followed by concentration to *ca.* 20 cm^3) and cooling *ca.* -78°C afforded orange crystals, which were collected and dried *in vacuo*. Yield, 0.38g (57%). Analysis indicated that the crystals were a mixture of α (35%)- and β (30%)- and γ (35%)- isomers.

7.4.8 Reaction of $Ta(S)Cl_3$ with PMe_3:

Preparation of β-Ta(S)Cl3(PMe3)3 (5).

Trimethylphosphine (0.42g, 5.48 mmol.) was condensed onto a frozen mixture of $Ta(S)Cl_3$ (0.5g, 1.57 mmol.) and dichloromethane (50 cm^3). The mixture was allowed to warm to room temperature and was stirred for 12h. to afford a dark green solution. Filtration followed by concentration to *ca.* 20 cm^3 and cooling to *ca.* -78°C afforded yellow crystals, which were collected and dried *in vacuo*. Yield, 0.62g (72%). Analysis indicated that the crystals were a mixture of α (90%)- and β (10%)- isomers. Recrystallisation from a saturated toluene solution at -35°C afforded the β-product as orange cubes.

Characterising Data on β-$Ta(S)Cl_3(PMe_3)_3$.

Elemental analysis for $C_9H_{27}Cl_3TaSP_3$ Found (Required): %C, 19.39(19.74), %H, 4.98 (4.97).

Infrared data (Nujol, CsI, cm^{-1}): 1431(m), 1423(m), 1299(s,sp), 1280(s), 950(s,br), 853(s), 735(s), 670(s,sp), 470(s, sp), 392(s), 260(s,br).

Mass spectral data (CI, isobutane carrier gas, m/z, ^{181}Ta, ^{35}Cl, ^{32}S): 546 $[M]^+$, 470 $[M\text{-}PMe_3]^+$, 435 $[M\text{-}PMe_3,Cl]^+$, 400 $[M\text{-}PMe_3,2Cl]^+$.

^1H *NMR data* (250MHz, d^6-benzene, 298K): 1.40 (s, br, $\Delta_{1/2}$ = 18 Hz, P*Me*3).

7.5 Experimental Details to Chapter 5.

7.5.1 Reaction of $CpNbCl_4$ with $(Me_3Si)_2O$:

Synthesis of $(CpNbCl_3)_2(O)$ (1).

A dichloromethane solution of $(Me_3Si)_2O$ (0.54g, 3.34 mmol. in 15 cm^3 CH_2Cl_2) was added dropwise to a stirred suspension of $CpNbCl_4$ (1.0g, 3.34 mmol.) in dichloromethane (20 cm^3) at room temperature. The red $CpNbCl_4$ suspension was consumed overnight to give an orange amorphous solid and a colourless solution. The supernatant solution was decanted from the orange solid, which was collected, washed with petroleum ether (2 x 10 cm^3, b.p. 40-60°C) and dried *in vacuo*. Yield, 0.52g (64%).

Elemental analysis for $C_{10}H_{10}Cl_6Nb_2O$ Found (Required): %C, 22.07 (22.05), %H, 1.73 (1.85), %Cl, 39.08 (39.05), %Nb, 34.15 (34.11).

Infrared data (Nujol, CsI, cm^{-1}): 3110(s,sp), 1445(s), 1435(s), 1319(m), 1019(m,sp), 860(s), 660(s,br), 581(w), 561(m), 388(s,sp), 374(m,sh), 352(s,sh), 326(m,sh), 312(m,sh), 300(s,sp), 285(m,sh).

Mass spectral data (CI, Isobutane carrier gas, m/z, ^{35}Cl, ^{16}O): 526 $[Cp_2Nb_2Cl_6]^+$, 491 $[Cp_2Nb_2Cl_5]^+$, 472 $[Cp_2Nb_2OCl_4]^+$, 456 $[Cp_2Nb_2Cl_4]^+$,421 $[Cp_2Nb_2Cl_3]^+$, 279 $[CpNbOCl_3]^+$, 263 $[CpNbCl_3]^+$, 244 $[CpNbOCl_2]^+$, 228 $[CpNbCl_2]^+$.

7.5.2 Reaction of $CpTaCl_4$ with $(Me_3Si)_2O$:

Synthesis of [CpTaCl3]2[O] (2).

The synthesis of yellow $(CpTaCl_3)_2(O)$ is essentially analogous to that described for $(CpNbCl_3)_2(O)$. Yield, 0.81g (87%).

Elemental analysis for $C_{10}H_{10}Cl_6Ta_2O$ Found (Required): %C, 15.89 (16.66), %H, 1.42 (1.40), %Cl, 29.58 (29.52), %Ta, 48.89 (50.00).

Infrared data (Nujol, CsI, cm^{-1}): 3109(s), 1445(s), 1370(s), 1018(s), 878(s,sh), 862(s), 841(s,sh), 800(s), 695(s,br), 334(s,sh), 308(s,br), 288(s,sh).

Mass spectral data (CI, Isobutane carrier gas, m/z, ^{35}Cl, ^{181}Ta, ^{16}O): 386 $[CpTaCl_4]^+$, 351 $[CpTaCl_3]^+$, 332 $[CpTaOCl_2]^+$, 316 $[CpTaCl_2]^+$.

7.5.3 Reaction of Cp^*TaCl_4 with $(Me_3Si)_2O$.

Synthesis of $(Cp^*TaCl_3)_2(O)$ (3).

The synthesis of yellow $(Cp^*TaCl_3)_2(O)$ is essentially analogous to that previously described for $(CpNbCl_3)_2(O)$. Yield, 0.50g (53%).

Elemental analysis for $C_{20}H_{30}Cl_6OTa_2$, Found (Required): %C, 27.58 (27.89); %H, 3.69 (3.52); %Cl, 24.65 (24.70); %Ta, 42.01 (42.03).

Infrared data (nujol, CsI, cm^{-1}): 1485(m), 1436(m), 1073(w), 1023(m), 690(s,br), 610(w), 600(m), 429(w), 377(s), 337(s), 328(s), 314(s,sh), 296(s), 278(m).

Mass spectral data (CI, Isobutane carrier gas, m/z, ^{35}Cl, ^{181}Ta, ^{16}O): 859 $[M_2+H]^+$, 823 $[M_2-Cl]^+$, 420 $[Cp^*TaCl_3-H]^+$, 402 $[Cp^*Ta(O)Cl_2]^+$.

^1H NMR data (250MHz, d^6-benzene, 298K): 2.07 (s,C_5Me_5); (250MHz, $CDCl_3$, 298K) 2.39 (s, C_5Me_5).

7.5.4 Thermolysis of $(Cp^*TaCl_2)_2(O)_2$ (6) in Toluene:

Synthesis and Characterisation of $Cp^*_3Ta_3O_4Cl_4$ (7).

A toluene solution of $(Cp^*TaCl_2)_2(O)_2$ (0.25g, 3.10mmol. in 40 cm^3 toluene) was stirred at 90°C over a period of 1 week to yield a pale yellow solution and a yellow amorphous precipitate. Filtration of the supernatant solution followed by concentration to *ca.* 10 cm^3 and cooling to -35°C afforded pale yellow crystals of $(Cp^*_3Ta_3O_4Cl_4 \cdot C_7H_8)$ which were collected and dried *in vacuo*. Yield, 0.072g (50%).

Elemental analysis for $C_{37}H_{53}Cl_4O_4Ta_3$, Found (Required): %C, 35.53 (35.65); %H, 4.14 (4.29); %Cl, 11.42 (11.38); %Ta, 43.52 (43.55).

Infrared data (nujol, CsI, cm^{-1}): 1370(s), 1345(m), 1025(m), 957(m), 689(s), 622(s), 595(s,sh), 525(w,sh), 518(w), 478(w), 398(w,sh), 356(s), 352(m,sh), 312(s,sh), 308(s), 298(s,sh).

Mass spectral data (CI, Isobutane carrier gas, m/z, ^{35}Cl, ^{181}Ta, ^{16}O): 772 $[Cp^*_2Ta_2Cl_4]$, 402 $[Cp^*TaOCl_2]^+$, 386 $[Cp^*TaCl_4]$.

^{1}*H NMR data* (250MHz, d^6-benzene, 298K): 2.15 (s, C_5Me_5); (250MHz, $CDCl_3$, 298K): 2.21 (s, $2C_5Me_5$), 2.19 (s, C_5Me_5).

7.6 Experimental Details to Chapter 6.

7.6.1 Preparation of $W(O)_2Cl_2 \cdot Li_x$ where $0 < x \leq 2$.

Procedure (a). Using xLiO-2,6-$Bu^t_2C_6H_3$ where $0 < x \leq 1$.

Toluene (40 cm^3) was added to a weighed mixture of $W(O)_2Cl_2$ (1g, 3.49 mmol.) and x equivalents of LiO-2,6-$Bu^t_2C_6H_3$ (x=0.25, 0.18g, 0.87 mmol; x=0.50, 0.37g, 1.74 mmol; x=0.75, 0.55g, 2.62 mmol; x=1.00, 0.74g, 3.49 mmol) at room temperature. The mixture was stirred for 72h. at room temperature, to give a dark solid and a red-green dichroic solution. The solution was decanted from the solid, which was collected, washed with petroleum ether (2 x 20 cm^3, b.p. 40-60 °C) and dried *in vacuo*. Characterising data for $W(O)_2Cl_2 \cdot Li_x$ are presented in table 7.1.

xLi	Yield (%)	Product Colour	Analysis (%)					
			W		Cl		Li	
			Calc.	Found	Calc.	Found	Calc.	Found
0.25	88	Lt. Blue	63.73	64.05	24.58	24.47	0.60	0.65
0.50	88	Blue	63.35	63.65	24.43	24.40	1.20	1.24
0.75	87	Dk. Blue	62.97	62.89	24.29	23.43	1.78	1.86
1.00	86	Purple	62.60	62.79	24.14	24.30	2.36	2.36
2.00	84	Black	61.15	62.19	23.59	24.00	4.62	4.70

Table 7.1

The supernatant solution was filtered and the volatiles removed *in vacuo* to give a red crystalline sold. Sublimation of the solid at 120°C, 10^{-5} Torr yielded a white crystalline solid which was collected. Yield, 0.2g (49%).

Elemental analysis for $C_{28}H_{42}O_2$ Found (Required): %C, 81.96 (81.90), %H, 10.12 (10.31).

Infrared data (Nujol, CsI, cm^{-1}): 3630(s,sp), 3070(w), 1458(s), 1389(s), 1359(s), 1316(m,sh), 1301(s), 1260(w,sh), 1246(m,sh), 1228(s), 1200(m,sh), 1137(s), 1118(m,sh), 1104(s), 1020(w), 883(m,sh), 873(s,sp), 804(s,sp), 769(s,sp), 620(s,sp), 529(m).

Mass spectral data (CI, isobutane carrier gas, m/z): 410 $[M]^+$, 408 $[M - 2H]^+$, 380 $[M - C,O,2H]^+$, 205 $[M/2]^+$, 204 $[M/2 - H]^+$, 176 $[M/2 - C,O,H]^+$.

^{1}*H NMR data* (250MHz, d^6-benzene, 298K): 1.43 (s, 36), 4.94 (s, 2), 7.59 (s, 4).

^{13}*C NMR data* (68MHz, d-chloroform, 298K): 30.36 (q, J_{CH} = 125, C(*Me*)3), 34.46 (s, *C*(Me)3), 124.07 (d , J_{CH} = 155, ring C), 133.93 (s, ring C), 135.90 (s, ring C), 152.80 (s, ring C).

Procedure (b). Using xC_4H_9Li where $0 < x \leq 2$.

A stirred solution of x equivalents of C_4H_9Li (x = 0.25, 0.06g, 0.87 mmol; x=0.50, 0.11g, 1.74 mmol; x=0.75, 0.17g 2.62 mmol; x=1.00, 0.22g, 3.49 mmol; x=2.0, 0.45g, 6.97 mmol) in toluene (20 cm^3) was added to a suspension of $W(O)_2Cl_2$ (1g, 3.49 mmol.) in toluene (20 cm^3) maintained at *ca.* -78°C. The $W(O)_2Cl_2$ rapidly developed a blue colouration which darkened during the course of the addition. After the addition was complete (30 min.) the mixture was allowed to warm to room temperature and stirred for 24h. to give a colourless solution and a dark

solid. The solution was decanted from the solid, which was collected, washed with petroleum ether (2 x 20 cm^3, b.p. 40-60 °C) and dried *in vacuo*.

7.6.2 Preparation of $W(O)_2Cl_2 \cdot Na_x$ where $0 < x \leq 2$.

The synthesis of $W(O)_2Cl_2 \cdot Na_x$ where $0 < x \leq 2$ is essentially analogous to that described for $W(O)_2Cl_2 \cdot Li_x$ where $0 < x \leq 2$ {procedures (a) & (b)}.

Characterising data for $W(O)_2Cl_2 \cdot Na_x$ is presented in table 7.2.

xNa	Yield (%)	Product Colour	Analysis (%)					
			W		Cl		Na	
			Calc.	Found	Calc.	Found	Calc.	Found
0.25	86	Lt. Blue	62.85	63.01	24.24	24.62	1.96	1.84
0.50	87	Blue	61.64	62.25	23.77	24.15	3.85	3.39
0.75	86	Dk. Blue	60.48	61.00	23.32	23.68	5.67	5.30
1.00	85	Purple	59.36	60.04	22.89	22.95	7.42	7.08
2.00	82	Black	55.25	56.35	21.31	21.60	13.82	13.21

Table 7.2

7.6.3 Preparation of $W(O)_2Cl_2 \cdot K_x$ where $0 < x \leq 1$.

The synthesis of $W(O)_2Cl_2 \cdot K_x$ where $0 < x \leq 1$ is essentially analogous to that described for $W(O)_2Cl_2 \cdot Li_x$ where $0 < x \leq 1$ {procedure (a)}.

Characterising data for $W(O)_2Cl_2 \cdot K_x$ are presented in table 7.3.

xK	Yield (%)	Product Colour	Analysis (%)					
			W		Cl		K	
			Calc.	Found	Calc.	Found	Calc.	Found
0.25	82	Lt. Blue	62.00	62.41	23.91	24.05	3.30	3.02
0.50	85	Blue	60.02	60.76	23.15	23.45	6.38	6.08
0.75	84	Dk. Blue	58.17	59.21	22.43	22.67	9.28	9.41
1.00	84	Purple	56.42	57.00	21.76	22.00	12.00	11.80

Table 7.3

7.7 References.

1. A.J. Nielson, *Inorg. Synth.*, 1985, 23, 195.

2. T.V. Lubben, P.T. Wolczanski and G.D. Van Duyne, *Organometallics*, 1984, 3, 7, 982.

3. W. Wolfsberger and H. Schmidbaur, *Synth. React. Inorg. Metal. -Org. Chem.*, 1974, 4, 149.

4. M.J. Bunker, A. De Cian, M.L.H. Green, J.J.E. Moreau and N. Siganporia, *J. Chem. Soc. Dalton Trans.*, 1980, 2155.

5. V.C. Gibson, J.E. Bercaw, W.J. Bruton Jr. and R.D. Sanner, *Organometallics*, 1986, 5, 976.

6. A. Rodrique, J.W. Bovenkamp, B.V. Lacroix, R.A.B. Bannard and G.W. Buchanan, *Can. J. Chem.*, 1986, 64, 808.

7. C. Schade, W. Bauer and P. von Rague Schleyer, *J. Organomet. Chem.*, 1985, 295, C25.

Appendices

Crystal Data, Colloquia and Lectures.

Appendix 1A: Crystal Data for $NbCl_5(OEt_2)$.

$C_4H_{10}Cl_5ONb$: 344.29

Crystal System: Orthorhombic

Space Group: Pnma

Cell Dimensions: a = 14.085

b = 11.003

c = 7.674

U = 1189.30 $Å^3$

Z = 4

D_c = 1.923 g cm^{-3}

Final R-value: 0.0525 (wR = 0.0583)

Appendix 1B: Crystal Data for $[NbCl_4(OMe)]_2$.

$C_2H_{16}Cl_8O_2Nb_2$: 531.50

Crystal System: Monoclinic

Space Group: P21/n

Cell Dimensions: a = 13.389

b = 12.077

c = 9.475

U = 1463.39 $Å^3$

Z = 4

D_c = 1.792 g cm^{-3}

Final R-value: 0.0415 (wR = 0.0417)

Appendix 1C: Crystal Data for W(O)(O-2,6-$Pr^iC_6H_3$)$_4$.

$C_{48}H_{76}O_5W$: 908.86

Crystal System: Monoclinic

Space Group: $P_{21/c}$

Cell Dimensions: a = 22.667

b = 11.663

c = 18.700

U = 4574.22 Å^3

Z = 4

D_c = 2.412 g cm^{-3}

Final R-value: 0.0534 (wR = 0.0515)

Appendix 1D: Crystal Data for Mo(O)(O-2,6-$Me_2C_6H_3$).

$C_{32}H_{36}O_5Mo$: 596.53

Crystal System: Tetragonal

Space Group: P4/n

Cell Dimensions: a = 14.130

b = 14.130

c = 7.420

U = 1481.45 Å^3

Z = 2

D_c = 1.337 g cm^{-1}

Final R-value: 0.0565 (wR = 0.0515)

Appendix 1E: Crystal Data for α-$Nb(S)Cl_3(PMe_3)_3$.

$C_9H_{27}Cl_3NbSP_3$: 459.56

Crystal System: Monoclinic

Space Group: $P2_1/c$

Cell Dimensions: a = 15.190

b = 11.415

c = 11.690

U = 2042.78 $Å^3$

Z = 4

D_c = 1.494 g cm^{-3}

Final R-value: 0.0434 (wR = 0.0450)

Appendix 1F: Crystal Data for β-$Nb(S)Cl_3(PMe_3)_3$.

$C_9H_{27}Cl_3NbSP_3$: 459.56

Crystal System: Monoclinic

Space Group: $P2_1/c$

Cell Dimensions: a = 15.151

b = 11.565

c = 11.668

U = 2024.63 $Å^3$

Z = 4

D_c = 1.508 g cm^{-3}

Final R-value: 0.0567 (wR = 0.0591)

Appendix 1G: Crystal Data for α-$Ta(S)Cl_3(PMe_2)_3$.

$C_9H_{27}Cl_3TaSP_3$: 547.60

Crystal System: Monoclinic

Space Group: $P2_1/C$

Cell Dimensions: a = 15.131

b = 11.471

c = 11.710

U = 2029.98 $Å^3$

Z = 4

D_c = 1.792 g cm^{-3}

Final R-value: 0.0357 (wR = 0.0378)

Appendix 1H: Crystal Data for $Cp^*_3Ta_3O_4Cl_4$.

$C_{30}H_{45}Cl_4O_4Ta_3$: 1246.5

Crystal System: Triclinic

Space Group: PT

Cell Dimensions: a = 9.310

b = 11.854

c = 19.294

U = 2048.3 $Å^3$

Z = 2

D_c = 2.021 g cm^{-3}

Final R-value: 0.0440 (wR = 0.0421)

Appendix 2

First Year Induction Courses: October 1986

The course consists of a series of one hour lectures on the services available in the department.

1. Departmental Organisation
2. Safety Matters
3. Electrical appliances and infrared spectroscopy
4. Chromatography and Microanalysis
5. Atomic absorption and inorganic analysis
6. Library facilities
7. Mass spectroscopy
8. Nuclear Magnetic Resonance
9. Glass blowing techniques

Research Colloquia, Seminars and Lectures Organised By the Department of Chemistry

* - Indicates Colloquia attended by the author

During the Period: 1986-1987

* ALLEN, Prof. Sir G. (Unilever Research) Biotechnology and the Future of the Chemical Industry	13th November 1986
BARTSCH, Dr. R. (University of Sussex) Low Co-ordinated Phosphorus Compounds	6th May 1987
BLACKBURN, Dr. M. (University of Sheffield) Phosphonates as Analogues of Biological Phosphate Esters	27th May 1987
BORDWELL, Prof. F.G. (Northeastern University, U.S.A.)	9th March 1987

Carbon Anions, Radicals, Radical Anions and Radical Cations

* CANNING, Dr. N.D.S. (University of Durham) Surface Adsorption Studies of Relevance to Heterogeneous Ammonia Synthesis	26th November 1986
CANNON, Dr. R.D. (University of East Anglia) Electron Transfer in Polynuclear Copmplexes	11th March 1987
* CLEGG, Dr. W. (University of Newcastle-upon-Tyne) Carboxylate Complexes of Zinc; Charting a Structural Jungle	28th January 1987
DOPP, Prof. D. (University of Duisburg) Cyclo-additions and Cyclo-reversions Involving Captodative Alkenes	5th Novenber 1986
DORFMULLER, Prof. T. (University of Bielefeld) Rotational Dynamics in Liquids and Polymers	8th December 1986
GOODGER, Dr. E.M. (Cranfield Institute of Technology) Alternative Fuels for Transport	12th March 1987
* GREENWOOD, Prof. N.N. (University of Leeds) Glorius Gaffes in Chemistry	16th October 1986
* HARMER, Dr. M. (I.C.I. Chemicals & Polymers Group) The Role of Organometallics in Advanced Materials	7th May 1987
HUBBERSTEY, Dr. P. (University of Nottingham) Demonstration Lecture on Various Aspects of Alkali Metal Chemistry	5th February 1987
* HUDSON, Prof. R.F. (University of Kent) Aspects of Organophosphorus Chemistry	17th March 1987
HUDSON, Prof. R.F. (University of Kent) Homolytic Rearrangements of Free Radical Stability	18th March 1987
JARMAN, Dr. M. (Institute of Cancer Research) The Design of Anti Cancer Drugs	19th February 1987
KRESPAN, Dr. C. (E.I. Dupont de Nemours) Nickel (0) and Iron (0) as Reagents in Organofluorine Chemistry	26th June 1987
* KROTO, Prof. H.W. (University of Sussex) Chemistry in Stars, between Stars and in the laboratory	23rd October 1986
LEY, Prof. S.V. (Imperial College) Fact and Fantasy in Organic Synthesis	5th March 1987
MILLER, Dr. J.(Dupont Central Research U.S.A.) Molecular Ferromagnets; Chemistry and Physical Properties	3rd December 1986
MILNE/CHRISTIE, Dr. A./Mr. S. (International Paints)	20th November 1986

Chemical Serendipity - A Real Life Case Study

NEWMAN, Dr. R. (University of Oxford) 4th March 1987
Change and Decay: A Carbon-13 CP/MAS NMR Study of Humification and Coalification Processes

OTTEWILL, Prof. R.H. (University of Bristol) 22nd January 1987
Colloid Science a Challenging Subject

* PASYNKIEWICZ, Prof. S. (Technical University, Warsaw) 11th May 1987
Thermal Decomposition of Methyl Coppor and its Reaction with Trialkylaluminium

ROBERTS, Prof. S.M. (University of Exeter) 24th June 1987
Synthesis of Novel Antiviral Agents

RODJERS, Dr. P.J. (I.C.I. Billingham) 12th February 1987
Industrial Polymers from Bacteria

SCROWSTON, Dr. R.M. (University of Hull) 6th November 1986
From Myth and Magic to Modern Medicine

SHEPHERD, Dr. T. (University of Durham) 11th February 1987
Pteridine Natural Products; Synthesis and Use in Chemotherapy

THOMSON, Prof. A. (University of East Anglia) 4th February 1987
Metalloproteins and Magnetooptics

* WILLIAMS, Prof. R.L. (Metropolitan Police Forensic Science) 27th November1987
Science and Crime

* WONG, Prof. E.H. (University of New Hampshire U.S.A.) 29th October 1986
Coordination Chemistry of P-O-P Ligands

WONG, Prof. E.H. (University of New Hampshire U.S.A.) 17th February 1987
Symmetrical Shapes from Molecules to Art and Nature

During the Period: 1987-1988

BIRCHALL, Prof. D. (I.C.I. Advanced Materials) 25th April 1988
Enviromental Chemistry of Aluminium

* BORER, Dr. K.(University of Durham Industrial Research Labs.) 18thFebruary1988
The Brighton Bomb- A Forensic Science View

BOSSONS, L. (Durham Chemistry Teacher's Centre) 16th March 1988
GCSE Practical Assessment

* BUTLER, Dr. A.R. (University of St. Andrews) 5th November 1987
Chinese Alchemy

CAIRNS-SMITH, Dr. A. (Glasgow University) 28th January 1988
Clay Minerals and the Origin of Life

DAVIDSON, Dr. J. (Herriot-Watt University) November 1987

Metal Promoted Oligomerisation of Alkynes

* GRADUATE CHEMISTS (Northeast Polytechnics and Universities) 19th April 1988
R.S.C. Graduate Symposium

* GRAHAM, Prof. W.A.G. (University of Alberta, Canada) 3rd March 1988
Rhodium and Iridium Complexes in the Activation of Carbon-Hydrogen Bonds

* GRAY, Prof. G.W. (University of Hull) 22nd October 1987
Liguid Crystals and their Applications

HARTSHORN, Prof. M.P. (University of Canterbury, New-Zealand) 7th April 1988
Aspects of Ipso-Nitration

HOWARD, Dr. J. (I.C.I. Wilton) 3rd December 1987
Chemistry of Non-Equilibrium Processess

* LUDMAN, Dr. C.J. (University of Durham) 10th December 1987
Explosives

McDONALD, Dr. W.A. (I.C.I. Wilton) 11th May 1988
Liguid Crystal Polymers

MAJORAL, Prof. J.-P. (Universite' Paul Sabatier) 8th June 1988
Stabilisation by Complexation of Short-Lived Phosphorus Species

MAPLETOFT, Mrs. M. (Durham Chemistry Teacher's Centre) 4th November 1987
Salter's Chemistry

NIETO DE CASTRO, Prof. C.A. (University of Lisbon) 18th April 1988
Transport Properties of Non-Polar Fluids

OLAH, Prof. G.A. (University of Southern California) 29th June 1988
New Aspects of Hydrocarbon Chemistry

PALMER, Dr. F. (University of Nottingham) 21st January 1988
Luminescence (Demonstration Lecture)

* PINES, Prof. A. (University of California, Berkeley, U.S.A.) 28th April 1988
Some Magnetic Moments

RICHARDSON, Dr. R. (University of Bristol) 27th April 1988
X-Ray Diffraction from Spread Monolayers

ROBERTS, Mrs. E. (SATRO Officer for Sunderland) 13th April 1988
Talk-Durham Chemistry Teacher's Centre - "Links Between Industry and Schools

ROBINSON, Dr. J.A. (University of Southampton) 27th April 1988
Aspects of Antibiotic BioSynthesis

* ROSE van Mrs. S. (Geological Museum) 29th October 1987
Chemistry of Volcanoes

SAMMES, Prof. P.G. (Smith, Kline and French) 19th December 1987
Chemical Aspects of Drug Development

SEEBACH, Prof. D. (E.T.H. Zurich) — 12th November 1987
From Synthetic Methods to Mechanistic Insight

SODEAU, Dr. J. (University of East Anglia) — 11th May 1988
Durham Chemistry Teacher's Centre Lecture: "Spray Cans, Smog and Society"

SWART, Mr. R. M. (I.C.I.) — 16th December 1987
The Interaction of Chemicals with Lipid Bilayers

* TURNER, Prof. J.J. (University of Nottingham) — 11th February 1988
Catching Organometallic Intermediates

UNDERHILL, Prof. A. (University of Bangor) — 25th February 1988
Molecular Electronics

WILLIAMS, Dr. D.H. (University of Cambridge) — 26th November 1987
Molecular Recognition

* WINTER, Dr. M.J. (University of Sheffield) — 15th October 1987
Pyrotechnics (Demonstration Lecture)

During the Period: 1988-1989

ASHMAN, Mr. A. (Durham Chemistry Teacher's Centre) — 3rd May 1989
The Chemical Aspects of the National Curriculum

* AVEYARD, Dr. R. (University of Hull) — 15th March 1989
Surfactants at your Surface

AYLETT, Prof. B.J. (Queen Mary College, London) — 16th February 1989
Silicon-Based Chips: - The Chemist's Contribution

* BALDWIN, Prof. J.E. (University of Oxford) — 9th February 1989
Recent Advances in the Bioorganic Chemistry of Penicillin Biosynthesis

* BALDWIN & WALKER, Drs. R.R. & R.W. (Hull University) — 24thNovember 1988
Combustion: Some Burning Problems

BOLLEN, Mr. F. (Durham Chemistry Teacher's Centre) — 18th October 1988
Lecture about the use of SATIS in the classroom

BUTLER, Dr. A.R. (St. Andrews University) — 15th February 1989
Cancer in Linxiam: The Chemical Dimension

* CADOGEN, Prof. J.I.G. (British Petroleum) — 10th November 1988
From Pure Science to Profit

CASEY, Dr. M. (University of Salford) — 20th April 1989
Sulphoxides in Stereoselective Synthesis

WATERS & CRESSEY, Mr. D. & T. (Durham Chemistry Teacher's Centre) — 1st February 1989
GCSE Chemistry 1988: "A Coroners Report"

CRICH, Dr. D. (University College London) — 27th April 1989
Some Novel Uses of Free Radicals in Organic Synthesis

DINGWALL, Dr. J. (Ciba Geigy) — 18th October 1988
Phosphorus-containing Amino Acids: Biologically Active Natural and Unnatural Products

* ERRINGTON, Dr. R.J. (University of Newcastle-upon-Tyne) — 1st March 1989
Polymetalate Assembly in Organic Solvents

FREY, Dr. J. (Southampton University) — 11th May 1989
Spectroscopy of the Reaction Path: Photodissociation Raman Spectra of NOCl

HALL, Prof. L.D. (Addenbrooke's Hospital Cambridge) — 2nd February 1989
NMR - A Window to the Human Body

HARDGROVE, Dr. G. (St. Olaf College U.S.A.) — December 1988
Polymers in the Physical Chemistry Laboratory

HARWOOD, Dr. L.(Oxford University) — 25th January 1988
Synthetic Approaches to Phorbols Via Intramolecular Furan Diels-Alder Reactions: Chemistry under Pressure

JAGER, Dr. C. (Friedrich-Schiller University GDR) — 9th December 1988
NMR Investigations of Fast Ion Conductors of the NASICON Type

* JENNINGS, Prof. R.R. (Warwick University) — 26th January 1989
Chemistry of the Masses

JOHNSON, Dr. B.F.G. (Cambridge University) — 23rd February 1989
The Binary Carbonyls

JONES, Dr. M.E. (Durham Chemistry Teacher's Centre) — 14th June 1989
Discussion Session on the National Curriculum

JONES, Dr. M.E. (Durham Chemistry Teacher's Centre) — 28th June 1989
GCSE and A Level Chemistry 1989

* LUDMAN, Dr. C.J. (Durham University) — 18th October 1988
The Energetics of Explosives

MACDOUGALL, Dr. G. (Edingburgh University) — 22nd February 1989
Vibrational Spectroscopy of Model Catalytic Systems

* MARKO, Dr. I. (Sheffield University) — 9th March 1989
Catalytic Asymmetric Osmylation of Olefins

McLAUCHLAN, Dr. K.A. (University of Oxford) — 16th November 1988
The Effect of Magnetic Fields on Chemical Reactions

MOODY, Dr. C.J. (Imperial College) — 17th May 1989
Reactive Intermediates in Heterocyclic Synthesis

* MORTIMER, Dr. C. (Durham Chemistry Teacher's Centre) — 14th December 1988
The Hindenberg Disaster - an Excuse for Some Experiments

* NICHOLLS, Dr. D. (Durham Chemistry Teacher's Centre) 11th July 1989
Demo. "Liquid Air"

PAETZOLD, Prof. P. (Aachen) 23rd May 1989
Iminoboranes XB=NR: Inorganic Acetylenes

PAGE, Dr. P.C.B. (University of Liverpool) 3rd May 1989
Stereocontrol of Organic Reactions Using 1,3-dithiane-1-oxides

POLA, Prof. J. (Czechoslovak Academy of Science) 15th June 1989
Carbon Dioxide Laser Induced Chemical Reactions
New Pathwats in Gas-Phase Chemistry

REES, Prof. C.W. (Imperial College London) 27th October 1988
Some Very Heterocyclic Compounds

REVELL, Mr. P. (Durham Chemistry Teacher's Centre) 14th March 1989
Implementing Broad and Balanced Science 11-16

SCHMUTZLER, Prof. R. (Technische Universitat Braunschweig) 6th October 1988
Fluorophosphines Revisited - New Contributions to an Old Theme

* SCHROCK, Prof. R.R. (M.I.T.) 13th February 1989
Recent Advances in Living Metathesis

SINGH, Dr. G. (Teesside Polytechnic) 9th November 1988
Towards Third Generation Anti-Leukaemics

* SNAITH, Dr. R. (Cambridge University) 1st December 1988
Egyptian Mummies: What, Where, Why and How

STIBR, Dr. R. (Czechoslovak Academy of Sciences) 16th May 1989
Recent Developments in the Chemistry of Intermediate-Sited Carboranes

VON RAGUÉ SCHLEYER, Prof. P. (Universitat Erlangen Nurnberg) 21st October 1988
The Fruitful Interplay Between Calculational and Experimental Chemistry

* WELLS, Prof. P.B. (Hull University) 10th May 1989
Catalyst Characterisation and Reactivity

Conferences and Symposia Attended

(*denotes paper presentation)
(°denotes poster presentation)

1. "*Third International Conference on the Chemistry of the Platinum Group Metals*", University of Sheffield, 13th-17th July, 1986.

2. * "*Twenty-third University of Stathclyde Inorganic Chemistry Conference*", 27th-28th June, 1988.

3. * "*Durham University Graduate Symposium*", University of Durham, 12th April, 1989.

Publications

1. New, Improved Syntheses of the Group 6 Oxohalides, $W(O)Cl_4$, $W(O)_2Cl_2$ and $Mo(O)_2Cl_2$, Vernon C. Gibson, Terence P. Kee and Alan Shaw, *Polyhedron*, 1988, 7, 579.

2. Convenient, High Yield Syntheses of $[Nb(O)Cl_3]$, $[Nb(O)Cl_3(CH_3CN)]_2$ and $[Nb(O)Cl_3(THF)_2]$. Formation and Decomposition of Intermediate Alkoxo (and Siloxo) Derivatives of General Formula $[NbCl_4(OR)]_2$ (R = Me, Et, $SiMe_3$), Vernon C. Gibson, Terence P. Kee and Alan Shaw, *Polyhedron*,1988, 7, 2217.

3. The Use of Hexamethyldisilthiane in the Synthesis of Transition Metal Sulphidohalides, Vernon C. Gibson, Alan Shaw and David N. Williams, *Polyhedron*, 1988, 8, 549.